UNIVERSITY OF OKLAHOMA

GRADUATE COLLEGE

Iron Uptake in Gram-negative and Gram-positive Bacteria

A Dissertation

SUBMITTED TO THE GRADUATE FACULTY

In partial fulfillment of the requirements for the

degree of

Doctor of Philosophy

By
Bo Jin
Norman, Oklahoma
2005

Downloaded from SHAREOK. Persistent Handle URL: https://hdl.handle.net/11244/1003

UMI Number: 3207595

INFORMATION TO USERS

The quality of this reproduction is dependent upon the quality of the copy submitted. Broken or indistinct print, colored or poor quality illustrations and photographs, print bleed-through, substandard margins, and improper alignment can adversely affect reproduction.

In the unlikely event that the author did not send a complete manuscript and there are missing pages, these will be noted. Also, if unauthorized copyright material had to be removed, a note will indicate the deletion.

UMI®

UMI Microform 3207595

Copyright 2006 by ProQuest Information and Learning Company.

All rights reserved. This microform edition is protected against unauthorized copying under Title 17, United States Code.

ProQuest Information and Learning Company
300 North Zeeb Road
P.O. Box 1346
Ann Arbor, MI 48106-1346

Iron Uptake in Gram-negative and Gram-positive Bacteria

A Dissertation APPROVED FOR THE

DEPARTMENT OF CHEMISTRY AND BIOCHEMISTRY

BY

_____Phillip E Klebba_____

_____Elena I Zgurskaya_____

_____Ann H West_____

_____George B Richter-Addo_____

_____John S downard_____

© Copyright by Bo Jin 2005

All Rights Reserved.

Acknowledgements

I would first like to thank my advisor, Dr. Phillip E Klebba, for giving me the opportunity to join his laboratory. His guidance, support, patience, and ideas have helped me to finish this work. His passion and knowledge of bacterial membrane biochemistry will surely serve as a great inspiration in developing my career goals. I would also like to thank Dr. Salete MC Newton who has been giving me an extraordinary source of advice, training, and discussion.

I would like to thank all the members of my doctoral committee, Dr. Elena I Zgurskaya, Dr. Ann H West, Dr. George B Richter-Addo, and Dr. John S Downard, for their great advices and supports throughout my graduate studies.

I would like to extend my thanks to all the previous and current members in Dr. Klebba's lab, who have become my colleagues, confidants, and friends over the years. They are Wallace Kaserer, Zhenghua Cao, Zengbiao Qi, Paul Warfel, Matt Bauler, Xiaoxu Jiang, Yi Shao, Li Ma, and Marj Montague. I thoroughly enjoyed working with all of them and I am grateful for all the suggestions and the discussions from them. I want to give special thanks to Rajasekaran Annamalai, who has been working and helping with me since I joined this lab, and become one of my best friends.

Last but not least, I would like to thank my dad, my mom, my brother for their support, encouragement, and eternal love.

This is for my dearest wife: Qingwei Luo

Table of Contents

List of Tables.....ix

List of Illustrations.....x

Abstract.....xv

Chapter 1. Introduction.....1

1.1 Varieties of Bacterial Transport Systems.....2

1.2 Significance of Iron Uptake for Bacterial Growth.....6

1.3 Iron Transport Systems.....6

1.4 Siderophores: FeEnt, FeCrn, and Fc.....9

1.5 FepA: The Outer Membrane Porin for Ferric Enterobactin.....14

1.6 Protein Toxins and Bacteriophages that Utilize Siderophore Receptors.....17

1.7 TonB Dependence of Transport.....17

1.8 Siderophore Transport Mechanisms.....18

1.9 Cross-Linking of Cell Membrane Proteins.....19

1.10 Surface Topology of FepA.....20

1.11 Gram-positive Bacteria.....21

Chapter 2. Materials and Methods.....29

2.1 Bacterial Strains and Plasmids.....30

2.2 Growth Media.....32

2.3 Preparation of Siderophores.....34

2.4 Plasmids: pITS449 and pITS23.....35

2.5 Preparation of Competent Cells.....36

2.6 Site-Directed Mutagenesis.....37

2.7 Siderophore Nutrition Assays.....42

2.8 Colicin Sensitivities.....43

2.9 Binding Assays.....43

2.10 Transport Assays.....45

2.11 Expression of FepA.....46
2.12 Purification of Outer Membrane Proteins (FepA and FhuA).....47
2.13 Sarkosyl Extraction of Outer Membrane.....48
2.14 Sucrose Density Gradient Fractionation of cell envelopes.....49
2.15 Sulfo-EGS Cross-Linking.....50
2.16 Construction of TEV Protease Sites.....50
2.17 Purification of IgG.....50
2.18 Purification of Fab Fragment.....51
2.19 ELISA.....52
2.20 *In vivo* Reconstitution of Cell Envelopes.....52
2.21 Periplasm Extraction of *E. coli*.....53
2.22 Site-Directed Chromosomal Deletion.....53

Chapter 3. Aromaticity of the Surface Loops of FepA.....55

3.1 Experimental Strategies.....56
3.2 Candidates of the Aromatic Component.....56
3.3 Site-Directed Mutagenesis.....60
3.4 Protein Expression and Localization.....60
3.5 Nutrition Tests.....63
3.6 Colicin Killing Assays.....65
3.7 Quantitative Assays.....66
3.8 N-domain Loop Deletions.....70
3.9 X-Linking.....72
3.10 Competition between FeEnt and Other Siderophores.....76
3.11 Discussion.....79

Chapter 4. Accessibility of N domain from the Periplasmic Side.....90

4.1 Experimental Strategies.....90
4.2 Disulfide Bond Mutations.....90
4.3 Osmotic Shock of MAb (1).....113

4.4 Osmotic Shock of MAb (2).....134
4.5 Osmotic Shock of Fab.....156
4.6 Transport in the Periplasm only.....180
4.7 Examine Residue 2-12 of FepA.....184

Chapter 5. Gram-positive Bacteria Uptake.....188

5.1 *Listeria monocytogenes*.....188
5.2 *Bacillus subtilis*.....219

Chapter 6. Discussion.....232

References.....240

List of Tables

Table 2.1 Strains and plasmids used in this study.....30
Table 2.2 Media used in this study.....33

Table 3.1 Effects of mutagenesis on FeEnt uptake.....74

Table 4.2.1 Colicin B and D killing of disulfide bond mutants.....94
Table 4.2.2 Siderophore nutrition tests of disulfide bond mutants.....100
Table 4.2.3 Quantitative ^{59}FeEnt uptake assay of disulfide bond mutants.....103
Table 4.2.4 Nutrition tests of OKN3 and OKN13 strains and their derivatives.....105
Table 4.4.1 ELISA of anti FepA N-domain antibodies.....137
Table 4.4.2 Nutrition tests of bacteria after osmotic shock with MAb1.....150
Table 4.7.1 Phenotypes of residue 2-12 deletion mutant of FepA protein.....185

Table 5.1.1 Siderophore nutrition tests and mouse infection experiments with EGD-e and its mutant derivatives.....193
Table 5.1.2 Transport properties of EGD-e and its derivatives.....207
Table 5.2.1 Summary of siderophore binding and uptake by *B. subtilis*.....228

List of Illustrations

Fig. 1.1 Cell envelopes of Gram (-) and Gram (+) bacteria.....5
Fig. 1.2 A pictorial scheme that shows the transmembrane topology of the FeEnt uptake proteins and how they function.....8
Fig. 1.3 Ferric enterobactin, a prototypical catechol-type siderophore.....11
Fig. 1.4 The chemical structures of the two trilactone siderophores: enterobactin and corynebactin.....12
Fig. 1.5 Structure of apoferrichrome.....13
Fig. 1.6 The crystal structure of FepA.....16
Fig. 1.7 Iron uptake systems in Gram (+) bacteria.....28

Fig. 2.1 Quikchange mutagenesis.....41

Fig. 3.1 Candidates of site-directed FepA mutations.....58
Fig. 3.2 Genetic map of pHSG575 plasmid.....59
Fig. 3.3 Expression and localization in the OM.....62
Fig. 3.4 Siderophore nutrition tests.....64
Fig. 3.5 ^{59}FeEnt binding by Ala substitution mutants.....67
Fig. 3.6 ^{59}FeEnt transport by Ala substitution mutants.....69
Fig. 3.7 A backbone model of FepA.....71
Fig. 3.8 Cross-linking of bacteria with SulfoEGS.....73
Fig. 3.9 FeEnt binding and transport by Ala mutants and competition with FeTrn and FeCrn.....78
Fig. 3.10 Crystal structure of FepA.....80
Fig. 3.11 Model of FeEnt transport through FepA.....88

Fig. 4.2.1 Construction of five disulfide bonds mutants within FepA.....92
Fig. 4.2.2 0.07% bis-acrylamide SDS-PAGE followed by ^{125}I Immunoblot of KDF541/pITS23 and KDF541/pITS23/I14CG300C.....97
Fig. 4.2.3 Determination of concentration of DTT which is high enough to reduce all the disulfide bonds formed in cells with I14G300C FepA.....97

Fig. 4.2.4 Determination of concentration of BME which is high enough to reduce all the disulfide bonds formed in cells with T51N608C and G54T585C FepA.....98
Fig. 4.2.5 Immunoblot of cell lysates including KDF541, wild type and all the disulfide bond mutants in KDF541 growing with or without 5mM BME.....98
Fig. 4.2.6 Siderophore nutrition tests of the wild type and its disulfide bond mutants of FepA.....101
Fig. 4.2.7 Nutrition tests pictures of OKN3 strain, and its derivatives.....106
Fig. 4.2.8 Nutrition tests pictures OKN13 strain and its derivatives. 106
Fig. 4.2.9 Crystal structures of FepA and FhuA.....110
Fig. 4.3.1 Diagram of how antibodies bind the N domain in the PP.....114
Fig. 4.3.2 ELISA of cell samples after osmotic shock with MAb4 in Ca^{2+}-sucrose reconstitution buffer and French-Press.....116
Fig. 4.3.3 ELISA of cell fluids after osmotic shock with or without glycerol in Tris/$CaCl_2$ buffer.....118
Fig. 4.3.4 Examine the effect of benzamidine in the procedure of osmotic shock with Tris/$CaCl_2$ buffer.....119
Fig. 4.3.5 ELISA of cell fluids after bacteria were shocked with MAb1, 4, 27, or 41, followed by incubation at 37°C with or without 10 μM FeEnt.....121
Fig. 4.3.6 ELISA of cell fluid after bacteria were shocked with MAb2, 26, or 29, followed by incubation at 37°C with or without 10 μM FeEnt.....122
Fig. 4.3.7 ^{59}FeEnt uptake of KDF541/pITS23 cells and cells that were shocked without or with MAb1 ascites fluids.....124
Fig. 4.3.8 ELISA of KDF541/pITS23 cells that were shocked with MAb4 ascites fluids and then incubated at 37°C either with or without the presence of FeEnt.....125
Fig. 4.3.9 ^{59}FeEnt 10-second uptake of KDF541/pITS23 cells and cells that were shocked with or without MAb4 ascites fluids. 126
Fig. 4.3.10 ^{59}FeEnt two-hour uptake of KDF541/pITS23 cells and cells that were shocked with or without MAb4 ascites fluids.....127
Fig. 4.3.11 KDF541 and KDF541/pITS23 samples or denatured samples incubated with serial dilutions of MAb1 ascites fluids at pH2.5 or 6.5.....130

Fig. 4.3.12 KDF541 and KDF541/pITS23 samples or denatured samples incubated with serial dilutions of MAb45 ascites fluids at pH2.5 or 6.5.....131
Fig. 4.3.13 KDF541 and KDF541/pITS23 samples or denatured samples incubated with serial dilutions of MAb1 ascites fluids at pH2.5, 3.5, 5.5 or 7.5.....132
Fig. 4.4.1 Spot Immunoblot to test the reactivity of anti FepA N-domain antibodies to goat-anti-mouse or rabbit-anti-mouse with I^{125}-proteinA.....135
Fig. 4.4.2 10% SDS-PAGE of KDF541 and KDF541/pITS23 cell fluid after osmotic shock for 30 minutes.....138
Fig. 4.4.3 ELISA of samples that were the same as in Fig. 4.4.2.....139
Fig. 4.4.4 10% SDS-PAGE of KDF541 and KDF541/pITS23 cell fluid after osmotic shock for two hours.....140
Fig. 4.4.5 ^{59}FeEnt uptake of KDF541/pITS23 after osmotic shock.....141
Fig. 4.4.6 SDS-PAGE and Western blot of KDF541/pITS23 cells after osmotic shock with different concentrations of Tris.....143
Fig. 4.4.7 ^{59}FeEnt uptake of cells same as in Fig. 4.4.6.....144
Fig. 4.4.8 SDS-PAGE of KDF541/pITS23 shocked with MAb4 for 5 min, 15 min, 30 min and 2 hours.....146
Fig. 4.4.9 SDS-PAGE of KDF541/pITS23 shocked with MAb4 or TEV protease as control.....147
Fig. 4.4.10 Osmotic shock of KDF541/pITS23 with MAb1.....149
Fig. 4.4.11 Osmotic shock of KDF541/pITS23 with increased amount of MAb1.....151
Fig. 4.4.12 SDS-PAGE and ELISA of KDF541/pITS23 shocked with MAb1 followed by incubation with or without FeEnt at 37°C.....152
Fig. 4.4.13 SDS-PAGE of OKN3/pITS23 shocked with MAb4.....153
Fig. 4.5.1 Schematic drawing of an IgG molecule interacted with the antigens.....158
Fig. 4.5.2 Protein concentration was determined by UV absorbance at 280nm for the DE-52 fractions of ascites fluids of MAb2.....159
Fig. 4.5.3 SDS-PAGE of DE-52 fractions of ascites fluids of MAb2.....160
Fig. 4.5.4 Western blot of DE-52 fractions.....161
Fig. 4.5.5 ELISA of DE-52 column fractions.....162
Fig. 4.5.6 Western blot of papain digestion of IgG.....164

Fig. 4.5.7 Western blot of papain digestion reaction for longer period.....165
Fig. 4.5.8 Western blot of large scale papain digestion of MAb2.....167
Fig. 4.5.9 Western blot of ascites fluid, IgG, and F_{ab} of MAb2.....168
Fig. 4.5.10 Western blot of samples of IgG after papain digestion and DE52 column, and DE52 column fractions containing F_{ab} fragment stored at -20°C for a few days.....170
Fig. 4.5.11 ELISA of DE52 column fractions that contain F_{ab} fragment.....171
Fig. 4.5.12 Western blot of the samples after osmotic shock with F_{ab} fragment (1).....173
Fig. 4.5.13 Western blot of the samples after osmotic shock with F_{ab} fragment (2).....174
Fig. 4.5.14 ^{59}FeEnt transport assay of KDF541/pITS23 cells after osmotic shock with F_{ab} fragment. 177
Fig. 4.6.1 One hour ^{59}FeEnt uptake of TJB1 and TJB1 *fepC*- strains.....182
Fig. 4.6.2 One hour ^{59}FeEnt uptake of UT5600 and UT2300 (*fepC*-) strains.....183

Fig. 5.1.1 Target operons that may be involved in the iron utilization and nutrition tests of EGD-e strain and its derivatives.....190
Fig. 5.1.2 Cloning of deletion mutation in pKSV7.....191
Fig. 5.1.3 Agarose gels showing the complete cloning process.....192
Fig. 5.1.4 Binding and transport of ^{59}FeCrn by EGD-e.....197
Fig. 5.1.5 Binding and transport of ^{59}FeEnt by EGD-e.....199
Fig. 5.1.6 Binding and transport of ^{59}Fc by EGD-e.....200
Fig. 5.1.7 ^{59}Fc and ^{59}FeCrn uptake of Δ*lmo1959*.....204
Fig. 5.1.8 ^{59}Fc uptake of *Δlmo2429*, *Δlmo1959*, *Δlmo1960*, *Δlmo1961*, *Δlmo2183*, and *Δfri*.....205
Fig. 5.1.9 Binding and transport of ^{59}FeCrn by *Δfri* compared to EGD-e.....206
Fig. 5.1.10 ^{59}FeCrn uptake of EGD-e, *Δlmo1961*, *ΔfeoB*, *and Δfri*.....208
Fig. 5.1.11 ^{59}FeCrn uptake of *Δfur*, *Δfri*, *and Δlmo1959*.....209
Fig. 5.1.12 SDS-PAGE of *L. monocytogenes* EGD-e strain cell envelope in the absence or presence of iron in MOPS minimum medium.....210
Fig. 5.1.13 Protein sequence alignment of *lmo1960*, *lmo2429* with other closely related proteins.....218
Fig. 5.2.1 Predicted regulon that may be involved in the utilization of Fc in *B. subtilis*.220

Fig. 5.2.2 Nutrition test of *B. subtilis168* strain.....222
Fig. 5.2.3 ^{59}FeCrn uptake of *B. subtilis*.....225
Fig. 5.2.4 ^{59}FeEnt uptake of *B. subtilis*.....226
Fig. 5.2.5 ^{59}Fc binding and uptake of *B. subtilis*.....227
Fig. 5.2.6 Growth curve of *B. subtilis* in MOPS minimum media.....230

ABSTRACT

Bacteria, including both Gram-positive and Gram-negative bacteria, utilize iron sources from the environment. Iron uptake systems in Gram-negative bacteria are well studied. *Escherichia coli* FepA transports certain catecholate ferric siderophores, but not others (Annamalai *et al.*, 2004), nor noncatecholate compounds (Annamalai *et al.*, 2004). Direct binding and competition experiments demonstrated that this selectivity originates during the adsorption stage. The synthetic tricatecholate Fe-TRENCAM bound to FepA with 50- to 100-fold-lower affinity than Fe-enterobactin (FeEnt), despite an identical metal center and Fe-corynebactin only bound at much higher concentrations. Neither Fe-agrobactin nor ferrichrome bound at all, even at concentrations 10^6-fold above the K_d. Thus, FepA only adsorbs catecholate iron complexes and it selects FeEnt among even its close homologs. I used alanine scanning mutagenesis to study the contributions of surface aromatic residues to FeEnt recognition. Although not apparent from crystallography, aromatic residues in L3, L5, L7, L8, and L10 affected the interaction between FepA and FeEnt. Among 10 substitutions that eliminated aromatic residues, K_d increased as much as 20-fold (Y481A and Y638A) and K_m increased as much as 400-fold (Y478A), showing the importance of aromaticity around the pore entrance. Although many mutations equally reduced binding and transport, others caused greater deficiencies in the latter. Y638A and Y478A increased K_m 10- and 200-fold more, respectively, than K_d. The N-domain loop deletions created the same phenotype: Δ60-67 (in NL1) and Δ98-105 (in NL2) increased K_d 10- to 20-fold but raised K_m 500- to 700-fold. W101A (in NL2) had little effect on K_d but increased K_m 1,000-fold. These data suggested that the primary role of the N terminus is in ligand uptake. Fluorescence and radioisotopic experiments showed

biphasic release of FeEnt from FepA. In spectroscopic determinations, k_{off1} was 0.03/s and k_{off2} was 0.003/s. However, FepAY272AF329A did not manifest the rapid dissociation phase, corroborating the role of aromatic residues in the initial binding of FeEnt. Thus, the β-barrel loops contain the principal ligand recognition determinants and the N-domain loops perform a role in ligand transport.

The genome of *Listeria monocytogenes* encodes several potential cell envelope iron uptake systems. I tested their ability to transport iron complexed by siderophores and mammalian proteins. Nutrition assays showed that *L. monocytogenes* acquires iron from ferrichrome, ferrichrome A, ferrioxamine B, ferric citrate, ferric enterobactin, ferric corynebactin, and the eukaryotic iron-binding proteins transferrin, lactoferrin, ferritin, and hemoglobin. ^{59}Fe uptake experiments showed that *Listeria* has 10 - 100-fold lower affinity for ferric siderophores ($K_m \approx$ 1 - 10 nM) than *Escherichia coli* has for the same compounds. The uptake rate for [^{59}Fe]-enterobactin (V_{max} = 0.15 pMol/10^9 cells/min) was 400-fold lower than that of *E. coli*. The rate of [^{59}Fe]-corynebactin uptake was also slow (V_{max} = 1.2 pMol/10^9 cells/min), but *L. monocytogenes* transported [^{59}Fe]-ferrichrome 20-fold faster (V_{max} = 24 pMol/10^9 cells/min), at a rate equivalent to Gram-negative bacterial ferrichrome transport systems. These transporters provided sufficient iron for growth in defined media. Sequence homologies and iron regulation identified 4 possible iron transporters in the *L. monocytogenes* chromosome: at 2.031 Mb (the *fur* region), 2.184 Mb (the *feo* region), 2.27 Mb (the *srtB* region) and at 2.499 Mb (which we designated the *hupDGC* region). We generated chromosomal deletions of genes in each of these loci, but only mutations in the *fur* and *hupDGC* regions diminished iron uptake, from ferric hydroxamates and hemin/hemoglobin, respectively. In the former locus, deletion of *fhuD*

(*lmo1959)*) or *fhuC* (*lmo1960*), the putative binding protein and membrane permease of an ABC-transporter, severely reduced ferrichrome, ferrichrome A and ferrioxamine B uptake. Hemin, hemoglobin, ferric transferrin, and ferritin uptake were not affected in these strains. Deletion of *hupC* (*lmo2429*), a putative membrane permease in a second ABC transporter locus, eliminated the uptake of hemin and hemoglobin, without affecting transport of ferric hydroxamates, ferric transferrin, or ferritin. The deletion of genes in the *srtB* locus, including *lmo2185, lmo2186, lmo2183* (a putative permease in an ABC-transport system) and *srtB* itself, did not impair the transport of iron from any ferric siderophores or eukaryotic iron-binding protein. Similarly, Δ*srtA*, Δ*srtAB*, Δ*fur* and Δ*feoB* mutations had no discernable effects on iron uptake. Deletion of the bacterioferritin structural gene, *fri* (*lmo943;* 0.97 Mb), diminished growth in defined media, but not in iron-replete brain-heart infusion broth. The rate of [^{59}Fe]-corynebactin transport tripled in this strain, whereas the rate of ^{59}Fe-ferrichrome decreased 20-fold. In summary, the experiments identified multiple cell envelope iron transport systems in *Listeria*, and defined the structural genes for transporters of ferric hydroxamates and heme/hemoglobin. The elimination of the latter system, in strain EGD-e Δ*hupC*, decreased the virulence of *L. monocytogenes* 50-fold in the mouse model system.

I also studied iron uptake systems in another Gram-positive bacterium, *Bacillus subtilis*. Nutrition assays showed that *Bacillus subtilis* acquires iron from ferrichrome, ferric enterobactin, ferric corynebactin, and the eukaryotic iron-binding proteins ferritin, heme, and hemoglobin. ^{59}Fe uptake experiments showed that *Bacillus* has 10 - 200-fold lower affinity for ferric siderophores ($K_m \approx 1$ - 20 nM) than *Escherichia coli* has for the same compounds. The uptake rate for [^{59}Fe]-enterobactin (V_{max} = 3.35 pMol/10^9

cells/min) was 20-fold lower than that of *E. coli*. The rate of [^{59}Fe]-corynebactin uptake was also slow (V_{max} = 1.34 pMol/10^9 cells/min), but *Bacillus subtilis* transported [^{59}Fe]-ferrichrome 10- to 30-fold faster (V_{max} = 43.8 pMol/10^9 cells/min), at a rate almost equivalent to Gram-negative bacterial ferrichrome transport systems. Sequence homologies identified several possible iron transporters in the *Bacillus subtilis* chromosome: at 3.378 Mb (the *yusV* region), 0.82 Mb (the *yfm* operon), 3.41 Mb (the *fhu* operon), 0.92 Mb (the *yfi* operon), 0.18 Mb (the *feu* operon), 3.40 Mb (the *yvr* operon), and at 4.06 Mb (the *yxe* operon). I specifically chose the *yfm* operon to study the iron uptake because of it high homology to the *E. coli.* iron uptake systems. I generated chromosomal deletions of genes in this locus. Nutrition test with Fc showed that deletion of *yfmE* did not affect the growth of *Bacillus subtilis.* More deletion mutants need to be constructed in the future in order to identify the genes involved in ferrichrome uptake.

Chapter 1

Introduction

1.12 Varieties of Bacterial Transport Systems

1.13 Significance of Iron Uptake for Bacterial Growth

1.14 Iron Transport Systems

1.15 Siderophores: FeEnt, FeCrn, and Fc

1.16 FepA: The Outer Membrane Porin for Ferric Enterobactin

1.17 Protein Toxins and Bacteriophages that Utilize Siderophore Receptors

1.18 TonB Dependence of Transport

1.19 Siderophore Transport Mechanisms

1.20 Cross-Linking of Cell Membrane Proteins

1.21 Surface Topology of FepA

1.22 Gram-positive Bacteria

1.1 Varieties of Bacterial Transport Systems

Bacteria are classified into two categories by grain staining: Gram-negative bacteria and Gram-positive bacteria, because their cell envelopes (Fig. 1.1) are different from each other. The Gram-negative bacteria envelopes contain an outer membrane (OM), periplasmic space (PP), peptidoglycan (PG), and an inner membrane (IM, or cytoplasmic membrane). However, cell envelopes of Gram (+) bacteria are composed of only a cytoplasmic membrane (CM) and PG. In Gram (-) bacteria, the PG layer is very thin, around a few angstroms. But in Gram (+) bacteria, the PG layer is very thick, up to 50-100 angstroms.

In Gram-negative bacteria, the outer membrane functions as a permeability barrier to toxic molecules, such as detergents, bacterial toxins, and chemicals, and prevents all of them from entering the cell from the environment. This barrier protects the bacteria from the detergent action of bile salts and degradation by degradative enzymes they encounter within the intestinal tract of their hosts. It also provides the bacteria with the resistance to antibiotics that are effective against Gram (+) bacteria (Nikaido and Nakae, 1979). Meanwhile, this efficient barrier blocks the entrance of nutrients and the exit of wastes. To solve these problems, the bacteria utilize very sophisticated systems in cell envelopes.

The outer membrane of Gram (-) bacteria is an asymmetric bilayer, consisting of an inner leaflet composed of typical phospholipids and an outer leaflet composed of lipopolysaccharide (LPS). This lipid bilayer allows the diffusion of hydrophilic molecules smaller than 600 Da (Nikaido and Vaara, 1985). Bacteria utilize varieties of outer membrane uptake systems to acquire molecules larger than 600 Da. The first type of system is 8-Stranded OM proteins. A typical example is the outer membrane protein A

(OmpA). OmpA, an outer membrane monomer (Sugawara and Nikaido, 1992), provides structural integrity to the bacterial cell surface. It is composed of an N-terminal 8-stranded β-transmembrane segment of 170 amino acids and a C-terminal domain that extends into the periplasmic space. The crystal structure of the N-terminal domain of OmpA has been solved (Pautsch and Schulz, 1998). The size of the pore formed by the transmembrane domain indicates that OmpA does not function as a non-specific diffusion channel, because the diameter of the pore is smaller than the diameter of a molecule as small as water. On the other hand, the C-terminal domain is anchored to the outer membrane by the N-terminal domain, and Sonntag *et al.* (1978) suggested it to interact with peptidoglycan layer supported by the OmpA mutations.

The second type of system is 16-stranded general porins. OmpF and PhoE (Cowan *et al.*, 1992) are examples of this type of general porins. They provide permeability without possessing specificity to hydrophilic molecules with molecular weight smaller than 600 Da. They function as general diffusion channels, and their diffusion rate is proportional to the concentration of the substrate (Nikaido, 1992). However, OmpF shows a preference for diffusion of cations (Cowan *et al.*, 1992), and PhoE displays a preference for diffusion of anions (Cowan *et al.*, 1992).

The third type of system is 18-stranded specific porins. Maltoporin (LamB) stands for this category. LamB facilitates the diffusion of maltodextrins across the outer membrane of *E. coli* (Szmelcman and Hofnung, 1975; Benz *et al.*, 1992; Klebba and Newton, 1998). LamB also has a specific activity toward the lambda phage (Szmelcman and Hofnung, 1975; Randall and Schwartz, 1973). The crystal structure of LamB complexed with maltose and malto-saccharide derivatives has been solved (Schirmer *et al.*, 1995; Forst *et*

al., 1998). The structural basis for the specificity of the channel has been investigated (Charbit *et al.*, 1998; Andersen *et al.*, 1999; Shirmer, 1997; Schmid K. *et al.*, 1999). The mechanism of the binding and transport process has also been studied (Benz *et al.*, 2002; Klebba and Hofnung *et al.*, 1997; Orlik and Benz, 2002 (1) and (2)). Greasy slide (Schimer *et al.*, 1996; Van Gelder *et al.*, 2002; Charbit, 2003) has been suggested to facilitate diffusion of maltose and to lower the energy barriers in the binding site. Polar track (Dumas *et al.*, 2000) reveals a strong cooperative effect of hydrogen bond formation and affects both on and off rates in sugar transport by being involved in facilitating movement of the sugar molecule.

The last type, which is also my main interest, is 22-stranded energy-dependent, ligand-gated porins. These proteins are usually TonB-dependent, energy-dependent, ligand-gated porins (LGP) functioning differently from the general and substrate-specific porins. FepA and FhuA are examples of this class. FepA (Buchanan *et al.*, 1999) and FhuA (Locher *et al.*, 1998; Ferguson *et al.*, 1998 and 2000; Braun *et al.*, 2000) transport ferric-enterobactin and ferrichrome, respectively (McIntosh *et al.*, 1979; Wayne *et al.*, 1976). They also serve as the receptors for bacterial phages, toxins, and for some antibiotics. Both of them have C-terminal transmembrane β-barrel structure, with the N-terminal domain functioning as plugs. The transport of substrates across the outer membrane requires proton motive force (Pugsley and Reeves, 1977; Bradbeer, 1993) as the energy source from the cytoplasmic membrane involving the participation of a TonB, ExbB, and ExbD complex (Postle *et al.*, 1995, 2002; Higgs and Postle 2002; Braun, 1995).

Gram-positive bacterial system will be discussed later in this introduction.

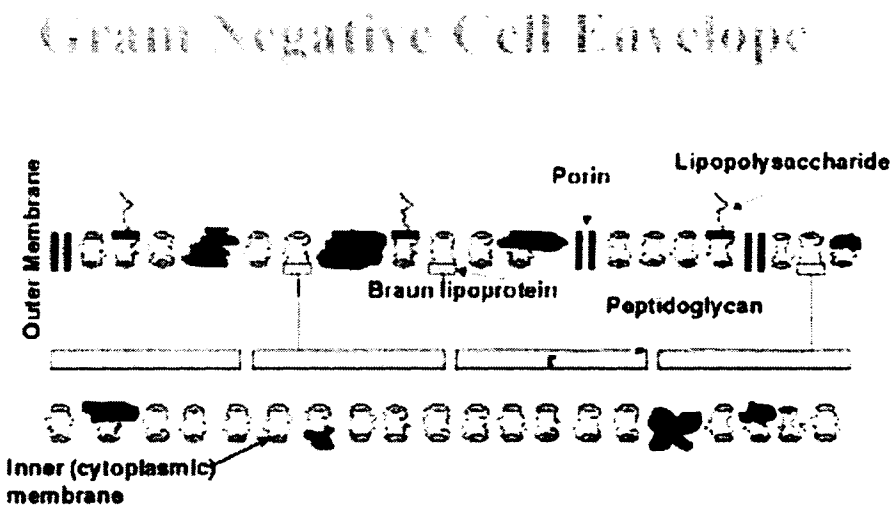

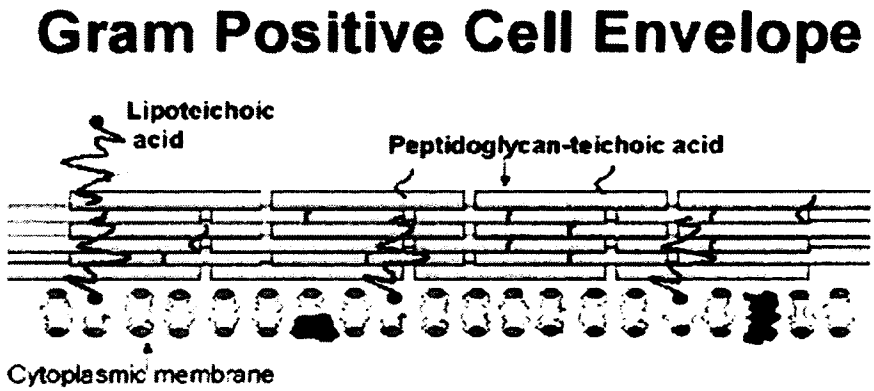

Fig. 1.1 Cell envelopes of Gram (-) and Gram (+) bacteria (http://pathmicro.med.sc.edu/fox/cell_envelope.htm).

1.2 Significance of Iron Uptake for Bacterial Growth

Most bacteria require iron for a wide range of metabolic and signaling functions. However, despite its abundance on earth, and the micromolar concentrations (Klebba *et al.*, 1982) required for cell growth, it is biologically unavailable (10^{-38} M; Neilands, 1974) in most environment due to formation of $Fe(OH)_n$. To protect themselves, animals also synthesize proteins (such as ferritin and transferrin) that can store free irons in fluids to keep iron concentration very low (~10^{-18} M; Neilands *et al.*, 1980) that is not sufficient to support the growth of bacteria or other parasites (Klebba, 1982; Neilands, 1974). In order to capture iron from such environments, bacteria developed different mechanisms. Some bacteria synthesize and secrete high-affinity iron chelators, called siderophores (Neilands, 1981). Once siderophores are bound by irons in their environments, bacteria adopt complicated systems to transport iron-siderophore complexes back into cells, and then get iron out of the complexes by either degradation of siderophores or reduction of Fe^{3+} to Fe^{2+}. Other bacteria directly acquire iron from eukaryotic iron containing proteins (Konopka and Neilands, 1984b). Iron acquisition has also been shown by most studies to be strongly related to bacterial virulence (Bullen, 1974; Cornelissen and Sparling, 1994 a and b; Fernandez-Beros *et al.*, 1989; Furman *et al.*, 1994; Bearden *et al.*, 1998; Stork *et al.*, 2004; Braun, 2005; and Renauld-Mongenie *et al.*, 2004). Briefly, iron uptake is very important for the growth of bacteria, especially pathogenic bacteria during their invasion.

1.3 Iron Transport Systems

In Gram (-) bacteria, common transport systems contains an OM iron transporter, a periplasmic iron binding protein, and an ABC type of transport system in the IM

including an inner membrane permease, ATPase or other proteins that supply energy sources, and other auxiliary proteins. For example, in *E. coli* (Fig. 1.2), the OM protein FepA transports FeEnt from the extracellular environment into the periplasm. This process requires proton motive force (pmf) and the supply of this energy involves the IM TonB-ExbB-ExbD complex that connects the OM and the IM. FepB as the periplasmic binding protein binds FeEnt in PP and transfers it to the IM ABC system: FepDGC. FepC is an ATPase. FepD and FepG are both permeases. FepDGC along with other auxiliary proteins will transport FeEnt into the cytoplasm. Once FeEnt is in the cytoplasm, it will be degraded and reduced by ferric esterase (Fes). In Gram (+) bacteria, although not much information is known so far, a common transport system is considered to contain a binding lipoprotein, a cytoplasmic permease, and an ATP binding protein. This will also be discussed later in this introduction.

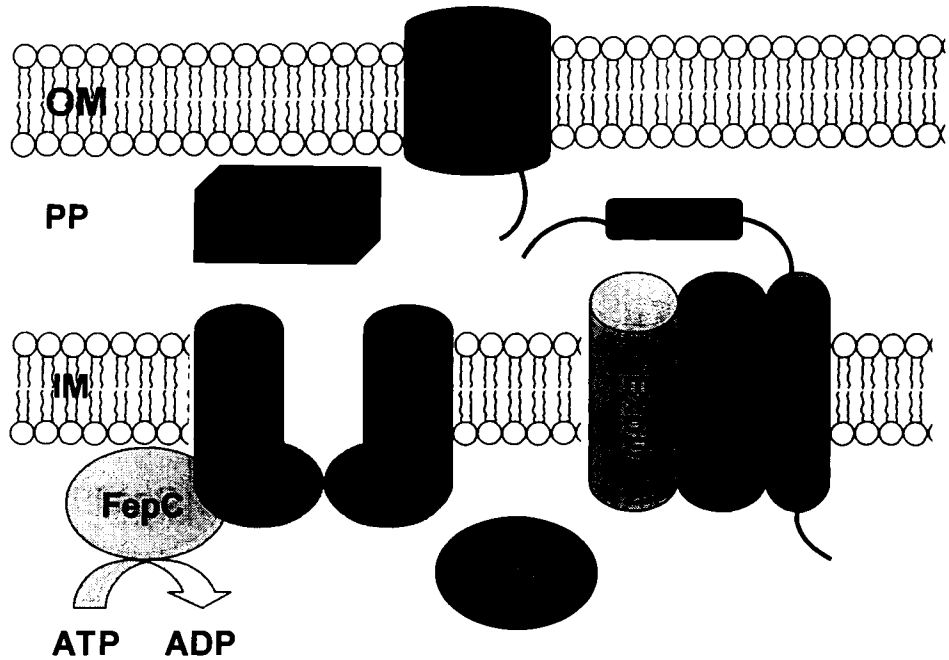

Fig. 1.2 A pictorial scheme shows the transmembrane topology of the FeEnt uptake proteins and how they function. In an iron-deficient state, iron receptors proliferate among the outer membrane (OM) proteins. FepA is a channel protein composed of a β-barrel and an N-terminal gate protein (Fig. 1.6). The FepA receptor is highly specific and recognizes the iron binding domain and amide linkage domains of FeEnt. The gating movement of FepA is transduced by the complex TonB-ExbB-ExbD, which is anchored in the cytoplasmic membrane (CM). FepB delivers FeEnt to the cytoplasmic pores formed by FepD and FepG. It appears that the cytoplasmic ATPase, FepC, provides energy to assist the uptake through the inner membrane. FeEnt esterase, which is encoded by the *fes* gene, catalyzes hydrolytic cleavage of the backbone, leading to the intracellular release of iron (Raymond *et al.*, 2003).

1.4 Siderophores: FeEnt, FeCrn, and Fc

Bacteria have elegant transport systems to obtain iron from their environments. Siderophores (Neilands, 1995) are organic, iron-chelating molecules synthesized and secreted by bacteria or fungi. They usually have a very high affinity toward iron; for example, enterobactin has a formation constant of 10^{52} M^{-1} for iron (Raymond and Carrano, 1979). Siderophores are classified into three categories by their chemical structures: catecholate-type, hydroxamate-type, and mixed. Ferric iron is bound by a siderophore and form a hexa-coordinate octahedral complex. The weak affinity of ferrous iron towards siderophores provides an efficient way to release siderophores inside of the cells after being reduced.

Enterobactin (Neilands, 1973; Hantke, 1990; Fig. 1.3 and 1.4) is the native siderophore of *E. coli*. The synthesis of enterobactin is completed by seven enzymes coded by the genes *entA-G*. Enterobactin is composed of three dihydroxybenzoylserine groups (dhbs) that are esterified to form a trilactone backbone. The three catechol rings form a hexa-coordinate octahedral around iron to give a net charge of -3. Enterobactin's ability to form hexa-coordination with iron ensures that enterobactin has much higher affinity for iron than any other chemical compounds. The chirality of the iron center in enterobactin is Δ (Karpishin and Raymond, 1993; Stack and Raymond, 1993), and this chirality (Thulasiraman *et al.*, 1998) does not originate at the stage of binding between the ferric siderophore and FepA, but probably reside in a subsequent stage of the uptake process, likely after transport through FepA. The mirror image enantioenterobactin-iron complex does not promote microbial growth (Neilands, 1981).

Corynebactin (Fig. 1.4) is synthesized in Gram (+) bacteria, *Corynebacterium glutamicum* (Budzikiewicz, 1997) and *Bacillus subtilis* (Marahiel, 2001). It is a catecholate siderophore (Raymond *et al.*, 2003). It is based on a trilactone backbone, consisting of L-threonine units. Each side chain also contains one glycine spacer. Most importantly, corynebactin has a Λ chirality, which is opposite to the chirality of the enterobactin (Δ).

Ferrichrome (Fig. 1.5), on the other hand, is a hydroxamate-type of siderophore. It is synthesized by fungus, *Ustilago sphaerogena*. The biosynthesis of ferrichrome was strongly but not completely repressed by iron (Emery, 1982). Ferrichrome is based on a cyclohexapeptide backbone (D. van der Helm *et al.*, 1980). It has the Λ configuration. The central iron atom is coordinated octahedrally by six oxygen donor atoms of the hydroxamic acid moieties of three ornithine residues, which, with the three glycine residues, make up the peptide backbone.

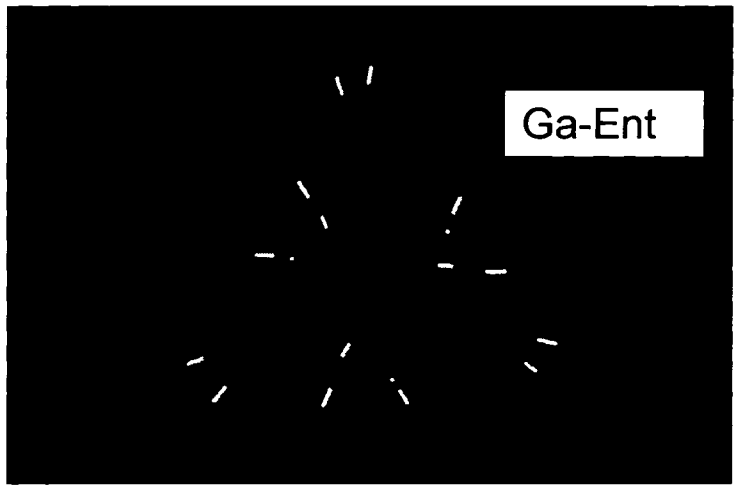

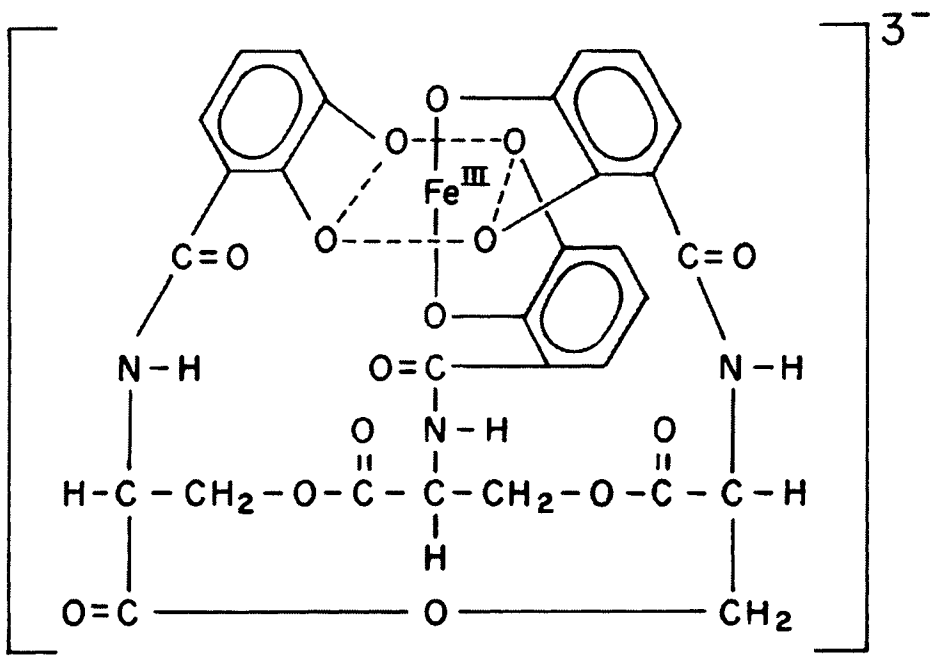

Fig. 1.3 Ferric enterobactin, a prototypical catechol-type siderophore. The three catechol rings wrap around the Fe (III) to afford a right-handed (Δ) coordination propeller with the highest known binding constant for ferric ion. Enterobactin is produced generally by enteric bacteria (Neilands, 1995).

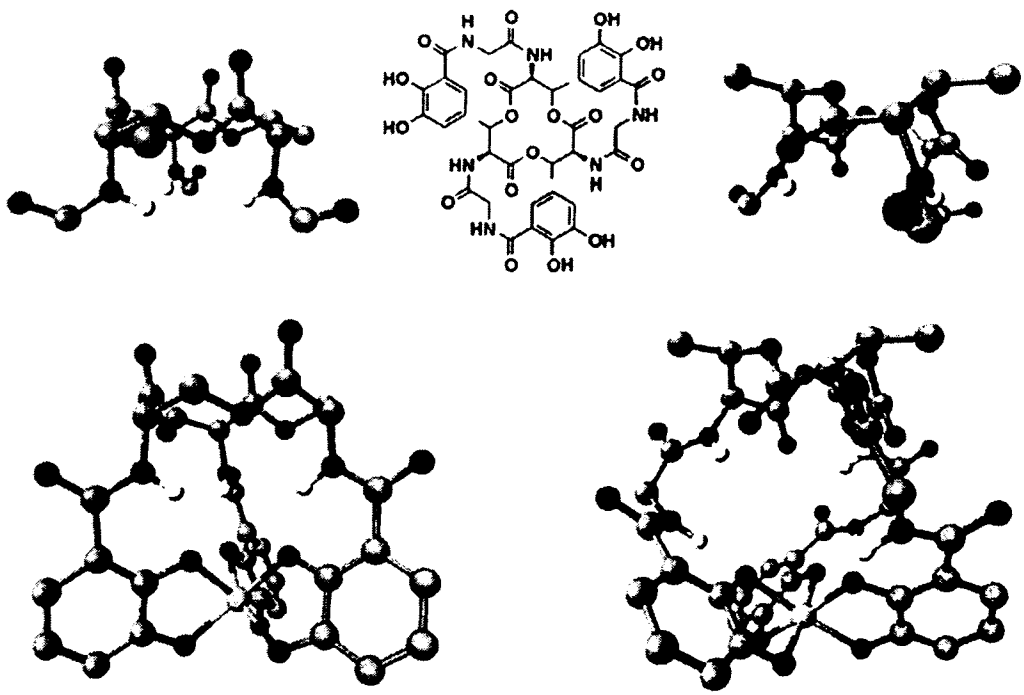

Fig. 1.4 The structures of the two trilactone siderophores: enterobactin (Left) and corynebactin (Right). The chemical structure of corynebactin (Center), which has a glycine spacer between the catechol ligands and the trilactone ring, is shown (that for enterobactin is in Fig. 1.3). The conformation for the 12-membered triserine ring of enterobactin places both the lactone carbonyl and the exocyclic amine groups in axial positions. The conformation for the trithreonine ring of corynebactin is inverted, with ester carbonyls planar. The consequence is that, while the ferric enterobactin complex (Lower Left) is Δ, the ferric corynebactin complex (Lower Right) is Λ (Raymond *et al.*, 2003).

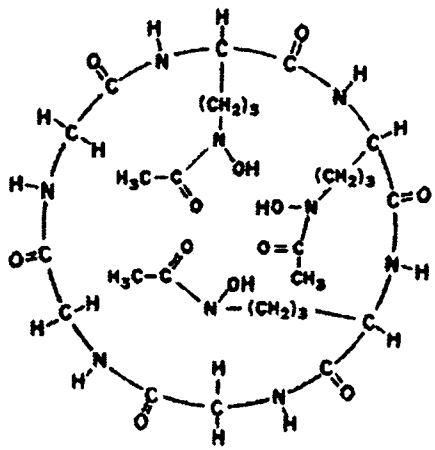

Fig. 1.5 Structure of apoferrichrome (Annamalai *et al.*, 2004).

1.5 FepA: The Outer Membrane Receptor for Ferric Enterobactin

FepA is the focus of the Gram (-) part of this study. Ferric enterobactin, with a molecular weight of 714 Da, is too large to penetrate the outer membrane of the Gram (-) bacteria by diffusion. As a result, FepA is utilized as the outer membrane transporter that transports Ferric enterobactin across the outer membrane. FepA is iron regulated by a repressor protein Fur (Hantke, 1984; Pettis *et al.*, 1988). Under the condition of iron depletion, FepA will be well expressed because the Fur protein is not able to bind to the promoter region of FepA, which is called the "Fur box." However, under the condition of iron repletion, the iron-Fur complex will bind to the promoter region of FepA, and stop the mRNA transcription (Pettis *et al.*, 1988; Hunt *et al.*, 1994) and then the translation.

Looking at the crystal structure of FepA (Fig. 1.6) carefully, a few structural features appear. First, aromatic residues of the β-barrel are located at the interface of membrane bilayer, forming an "aromatic girdle." Second, eleven large loops are hanging on the extracelluar surface toward the environment. Cross-linking experiments suggest that the loops of FepA undergo conformational changes *in vivo*, with an approximate magnitude of 15 Å, from a ligand-free open state to a ligand-bound closed state (Scott *et al.*, 2002). Aromatic residues on these surface loops are involved in the binding process of the ligand (Annamalai *et al.*, 2004). Third, the anti-parallel β-sheets are connected by large loops on the extracellular surface and short turns at the periplasmic face. Finally, the transmembrane β-barrel is plugged by the entire N-terminal domain. As a result, upon binding of the ligand, the N-terminal domain either has to undergo a conformational change, or exit the barrel and enter the periplasmic space, in order to make a channel for the ligand to pass through.

Although the crystal structure of FepA (Buchanan *et al.*, 1999) is solved, the mechanism of the binding and transport processes remains a mystery. Because the iron-siderophore complex cannot be co-crystallized with FepA, we do not know which residues of the protein are involved in the binding of the ligand. However, due to the aromatic property of the enterobactin, and the -3 charge of the ferric enterobactin, both aromatic residues and positively charged residues could participate in the binding process. The potential candidates of positively charged residues have been studied (Newton *et al.*, 1997). Results showed that Arg-286 and Arg-316 participated in the binding and transport. Also, seven aromatic residues were mutated to alanine (Cao *et al.*, 2000). Among single mutants, Y260A and F329A were most detrimental, reducing the affinity between FepA and ferric enterobactin 100- and 10-fold respectively. Double substitutions involving Y260, Y272 and F329 impaired (100- to 2500-fold) adsorption of the iron chelate more strongly. For Y260A and Y272A, the drop in adsorption affinity caused commensurate decreases in transport efficiency, suggesting that the target residues primarily act in ligand binding. F329A, like R316A, showed greater impairment of transport than binding, intimating mechanistic involvement during ligand internalization.

In the crystal structure of the FepA, there are lots of other aromatic and positive charged residues on the 11 surface loops and the two N-terminal loops. However, when the iron transporters from several different species were aligned, aromatic residues were found to be the most dominant residues that were conserved. Therefore, aromatic residues on the surface loop extremities and on the top of the N-terminal loops become excellent candidates for studying the binding process.

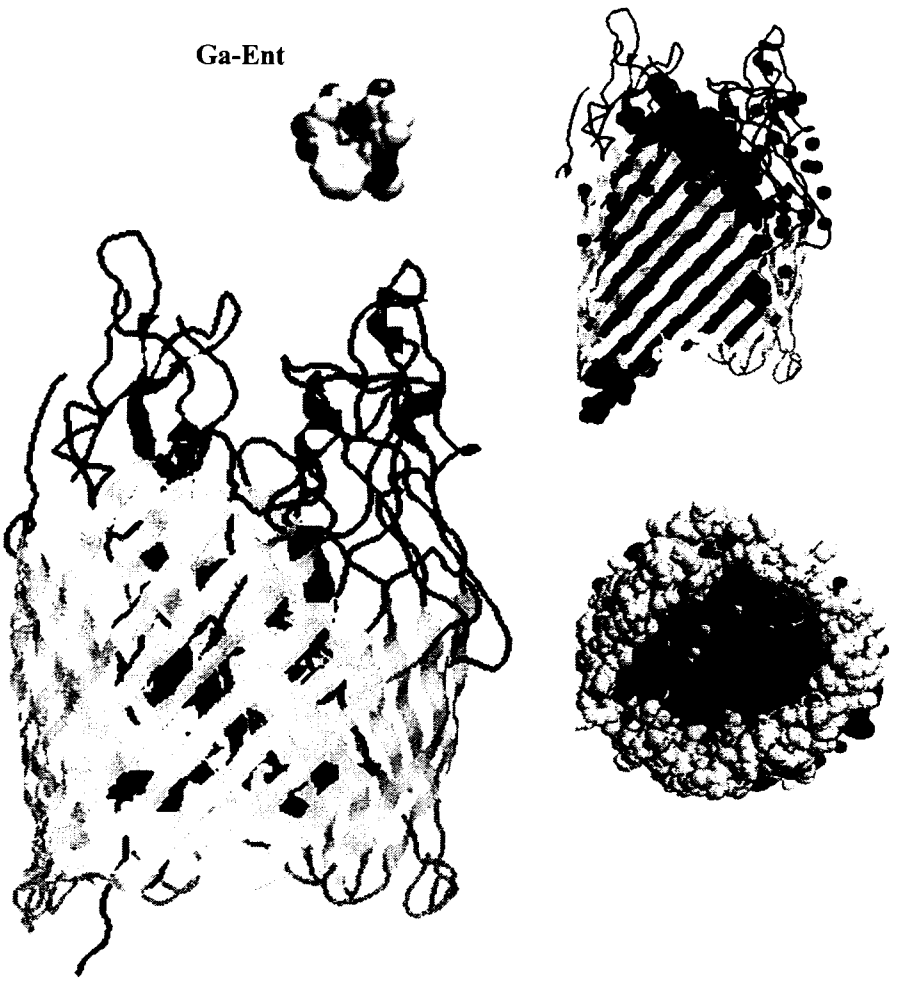

Fig. 1.6 The crystal structure of FepA, surface loops in green; β-barrel is in yellow; N-terminal domain is in red.

1.6 Protein Toxins and Bacteriophages that Utilize Siderophore Receptors

In Gram (-) bacteria, FepA also serves as the receptor for bacterial toxins colicin B and D (Guterman, 1971; Buterman, 1973; Davies and Reebes, 1975; Wayne *et al.*, 1976; Pugsley and Reeves, 1976). Colicins penetrate the outer membrane and kill the cells by different mechanisms. Colicin B kills cells by forming pores within the inner membrane (Schramm *et al.*, 1987; Gouaux, 1997; Lazdunski *et al.*, 1998, Hilsenbeck *et al.*, 2004), and colicin D kills cells by its activity of ribonuclease. The competition for binding between colicin B and ferric enterobactin suggested that the binding sites for them overlap (Wayne *et al.*, 1976), which was also proved by the fact that residues involved in the binding of ferric enterobactin were shown to take part in the recognition of colicin B by FepA (Newton *et al.*, 1997; Newton *et al.*, 1999; Cao *et al.*, 2000; Barnhard *et al.*, 2001). However, because colicins are much larger than siderophores, FepA is believed to have a much more complicated binding site for colicins. So far little is known about phage recognition by FepA, except the newly identified phage H8 (communication in our lab).

1.7 TonB Dependence of Transport

FeEnt transport by FepA is TonB-dependent. However, the mechanism of TonB function remains unclear. TonB is a 239 amino acid small protein that contains three domains: N-terminal transmembrane domain (Postle and Skare, 1988; Skare *et al.*, 1989), a central "rigid rod" domain (Evans *et al.*, 1996), and a C-terminal domain. TonB associates with two additional inner membrane proteins, ExbB and ExbD, forming a functional complex (Karrlson *et al.*, 1993; Ahmer *et al.*, 1995; Held *et al.*, 2002).

TonB's N-terminal domain appears to be involved in the interaction with ExbB and ExbD (Higgs *et al.*, 1998; Larsen *et al.*, 1999). Function of TonB is abolished when this domain is replaced (Karlsson *et al.*, 1999). The crystal structure of the C-terminal domain was solved at 1.55Å (Chang *et al.*, 2001). The structure shows a novel architecture that has no structural homologs among any known proteins. The dimer of the C-terminal domain of TonB is cylinder-shaped with a length of 65 angstroms and a diameter of 25 angstroms. Each monomer contains three beta strands and a single alpha helix. On the other hand, TonB still functions when the central "rigid rod" is removed (Larsen *et al.*, 1993). Because of its unique structure, it was proposed that the C-terminal dimer could spin like a propeller in the periplasmic space or function to transduce energy by shuttling between the outer membrane and the inner membrane (Letain *et al.*, 1997; Larsen *et al.*, 1997; Larsen *et al.*, 2003). However, recent study from our lab suggested when the GFP is attached to the N-terminus of the TonB, the fusion protein is localized in the inner membrane and is fluorescent. Also the fusion protein still functions to supply energy to the transport of FeEnt so that in the nutrition test FeEnt can still stimulate the growth of *E. coli* with the fusion protein expressed (data not shown). These data suggests that during the transport of FeEnt, TonB protein does not interact with the OM by leaving the IM.

1.8 Siderophore Transport Mechanisms

Although the mechanism of siderophore transport is not yet clear, a lot of information is available. Without FeEnt bound, surface loops of FepA are in an open state (Scott *et al.*, 2002) and in a closed state upon the binding of siderophores (Scott *et al.*, 2002). Aromatic residues on the surface loops are the primary residues that are involved in the

initial recognition and binding of FeEnt (Annamalai *et al.*, 2004). TonB-box was proposed to interact with TonB, and TonB/ExbB/ExbD may be involved in the energy transduction between the outer membrane and the inner membrane (Postle, 1993 a and b). Ligand passes through the C-domain channel via outer membrane transporters. Another set of proteins, FepBDGC, function in delivering siderophores into the cytoplasm although this mechanism is unknown. The N domain became the center of recent research in our lab because the N domain that sits inside of the β-barrel completely blocks the channel that siderophores enter. Either the N domain dislodges from the channel (Klebba, 2003), or the N domain has to undergo certain conformational changes to produce a channel inside of the β-barrel and facilitate ligand transport. But both possibilities are not fully substantiated. After transport the receptor reassembles, either by reinsertion of the N domain into the β-barrel, or by structural changes *in situ* within the pore. The protein needs to recover the original protein structure and conformation, which is another potential phase for the input of energy by TonB. Lastly, the loops reopen to a state of maximum receptivity toward ligands.

1.9 Cross-Linking of Cell Membrane Proteins in *E. coli*

In the presence of formaldehyde, FepA cross-links to another cell envelope protein, TonB (Klebba *et al.*, 1998). I used the bifunctional, cleavable cross-linking agent SulfoEGS that selectively reacts with primary amines and is too large (661 kDa) to pass through the aqueous channels of the OM, restricting its chemical action to lysine residues on the membrane surface. When applied to live bacteria or purified *Escherichia coli* outer membranes, SulfoEGS generated two prominent protein complexes that included FepA,

of approximate molecular masses 100 kDa (band 1) and 120 kDa (band 2) (Scott *et al.*, 2001). The identity of the cross-linked protein(s) in the 100-kDa complex is currently unknown. When cleaved, the 120-kDa product yielded, in addition to FepA, the major OM proteins OmpF/C and OmpA (Scott *et al.*, 2001), as determined by Edman degradations of their N-terminal 15 residues. Because the molecular mass of FepA (81 kDa) is almost three fold higher than those of OmpF/C or OmpA, in SDS-PAGE of a (dissociated) 1:1 complex of FepA·OmpA, for example, a nearly three-fold lower intensity is expected for the OmpA band. Two conditions influenced the cross-linking reaction between FepA and the major OM proteins (Scott *et al.*, 2001). First, both *in vivo* and *in vitro* the binding of FeEnt to FepA eliminated band 2, and drastically reduced the level of band 1. The removal of the N domain, in Fepβ, produced analogous results, reducing the levels of the 100- and 120-kDa products to barely detectable levels.

1.10 Surface Topology of FepA

The surface of FepA contains eleven large loops except that loops 1 and 6 are very small. Sulfo-EGS cross-linking experiments of wild-type FepA and K483A with or without ferric enterobactin added to the reactions (Scott *et al.*, 2002) suggested that FepA L7 undergoes conformational changes in the presence or absence of the ferric siderophore with an approximate magnitude of 15 Å, from a ligand-free open state to a ligand-bound closed state. The crystal structure of FepA did not reveal the residues in contact with the ligand within the two binding sites, B1 and B2. However, the binding sites showed the aromatic residues that encircle the mouth of the FepA vestibule probably involved in the binding process by hydrophobic bonds and/or ring stacking interactions in B1. One

aromatic residue on one of the loops of the N-terminal domain, W101, is visible from the extracellular side of the outer membrane in the spacefill model of the protein and is probably in contact with the ligand when the ligand comes in.

1.11 Gram-positive Bacteria

Gram-positive bacterial uptake is another important part of my thesis. *Bacillus subtilis* and *Listeria monocytogenes* belong to the same order of bacteria: *bacillales*. Under this order, *Bacillus subtilis* belongs to the bacillus genus of the *bacillaceae* family, and *Listeria monocytogenes* belongs to the *listeria* genus of the *listeriaceae* family. They are very close to each other in the taxonomy. *Bacillus subtilis* is a rod-shaped and endospore-forming aerobic bacterium. It is found in soil and rotting plant material and is non-pathogenic. However, in the same genus of bacillus, another species, *Bacillus anthracis*, is attracting all the attention around the world because of its pathogenicity. So it is very significant to study *bacillus subtilis* as well. In addition, we do not have to handle with pathogenic bacteria by studying *Bacillus subtilis*. *Listeria monocytogenes* is also rod-shaped and widespread in nature and has been isolated from soil, vegetation, marine sediments, and water. *Listeria monocytogenes* is a food-borne pathogen. During last decade, this species is of particular concern to the food industry and public health agencies because of its ability to grow at refrigeration temperatures (4°C) and widespread in the environment (Brackett, 1988). Only 25-30% of patients can survive listeriosis despite of antibiotic therapy. The fact that *Listeria monocytogenes* can infect a variety of cells and tissues suggests that it may have developed various iron uptake systems that are

useful in different environments. So the iron acquisition of *Listeria monocytogenes* is particularly strongly related to its pathogenesis.

Also, *Listeria monocytogenes* is consistently associated with human illness (Hitchins, 1998). More recently, it has been identified as the cause of listeriosis in humans. Victims of severe listeriosis are usually immunocompromised. Those at highest risk include cancer patients, individuals taking drugs that affect the body's immune system, alcoholics, pregnant women, persons with low stomach acidity, and individuals with AIDS. Severe listeriosis can cause meningitis, abortions, septicemia, and a number of other maladies, some of which may lead to death. Because iron acquisition is crucial to the pathogenesis of Gram-negative bacteria, including *Salmonella*, *Neisseria*, *Yersinia*, *Vibrio*, and *Hemophilus* (Fernandez-Beros *et al.*, 1989; Furman *et al.*, 1994; Cornelissen *et al.*, 1998; Zhu *et al.*, 2000; Bearden *et al.*, 1999; Occhino *et al.*, 1998; Cope *et al.*, 2000), it may be very important to study the iron transport system in Gram-positive bacteria in order to study the pathogenicity of Gram-positive bacteria. However, the iron uptake systems, especially in *Listeria monocytogenes* and *Bacillus subtilis,* have not been well studied. Below are some of the known iron utilization systems.

Staphylococcus aureus produces at least three different siderophores, staphyloferrin A (Konetschny-Rapp *et al.*, 1990; Meiwes *et al.*, 1990), staphyloferrin B (Drechsel *et al.*, 1993; Haag *et al.*, 1994), and aureochelin (Courcol *et al.*, 1997), and staphylobactin (Dale *et al.*, 2004). Also the *SirABC* operon (Heinrich *et al.*, 1999; Dale *et al.*, 2004) is identified as an ABC type transport system that is involved in the import of staphylobactin but not other iron complexes, such as FeEnt, ferric hydroxamate, or ferric citrate. Inactivation of SirA and SirB results in *S. aureus* defective in staphylobactin

transporter but not staphylobactin biosynthesis, which is regulated by *sbn* operon (Dale *et al.*, 2004). Also the expression of SirA is regulated by Fur (Dale *et al.*, 2004a; Xiong *et al.*, 2000). *S. aureus* was also shown to transport iron complexed to a variety of hydroxamate type siderophores, including ferrichrome (Sebulsky, 2000; 2001; 2003; 2004), aerobactin, and desferrioxamine. Especially for ferrichrome, extensive study is present on the ferric hydroxamate uptake (*fhu*) system. This operon contains *fhuC* (ATP-binding protein), *fhuB* and *fhuG* (membrane permease), and *fhuD1* and *fhuD2* (lipoprotein), which represents a classic ABC type transporter system. An *fhuB* knockout mutant shows impaired uptake of iron ferrichrome complex. Recently, *fhuD2* is shown to code for a posttranslationally modified lipoprotein FhuD2 (Sebulsky *et al.*, 2001) that is anchored in the cytoplasmic membrane. Insertional inactivation shows that FhuD1 is involved in the transport of iron complexed with ferrichrome, ferrioxamine B, aerobacin, and coprogen. FhuD2, shares 41% identity and 56% total similarity with FhuD1. *fhuD1* (Sebulsky *et al.*, 2004) is shown to be a gene duplicate for *fhuD2*. FhuD1 is only expressed under conditions of iron limitation through the regulatory activity of Fur. FhuD1 fractions with the cell membrane and binds iron hydroxamate complexes but with lower affinity than FhuD2, indicating that FhuD1 is redundant to FhuD2 and plays a minor role in hydroxamate transport. In addition, *S. aureus* is known to be capable of utilizing transferring-bound iron, via transferring-binding protein-mediated iron-acquisition systems besides the iron-siderophore uptake systems. Whole *isd* (iron-regulated surface determinant) operon (*isdA* to *isdG*) (Mazmanian *et al.*, 2003; Skaar *et al.*, 2004) is identified and shown to encode factors responsible for hemoglobin binding

and passage of heme-iron to the cytoplasm. However, study shows that this *isd* system only plays an ancillary role (Park *et al.*, 2005) in the uptake of iron transferrin.

Another Gram-positive bacterium, *Streptococcus pyogenes*, is a human pathogen (Bates *et al.*, 2003). It can produce a diverse array of skin and mucus membrane infections, as well as aggressive deep tissue diseases and streptococcal toxic shock syndrome. Most iron in humans is located intracellularly in complexes with proteins such as hemoglobin, myoglobin, other heme-containing proteins, ferritin, and non-heme iron-containing proteins. This pathogen can use a variety of heme compounds as an iron source. Although it could be most crucial for the pathogenesis of this bacterium, iron acquisition is not well studied so far. Only Heme uptake has been investigated recently. The 10-gene operon, from *spy1787* to *spy1798* (not including *spy1792* and *spy1997*), is identified to be related to iron. Two proteins, encoded by *spy1796* (*shp*; Lei *et al.*, 2002) and *spy1798* (*shr*; Bates *et al.*, 2003), are defined as novel classes of proteins. Shp is identified by the conserved pentapeptide sequence (LPXTG). It is cloned and overexpressed in *E. coli* and purified to homogeneity. Shp does not have significant homologues in public microbial genome databases. Purified Shp protein associates with heme in a 1:1 stoichiometry observed by UV-visible absorbance spectrum. Shp is not a lipoprotein, so it is defined as the first member of a new class of heme-associated proteins. On the other hand, Shr encodes a large hydrophilic protein (140 kDa) that has no significant homologues in other bacteria either, but shares partial homology with eukaryotic receptors such as Toll and G-protein-dependent receptors. However, a heme-binding motif is identified. Shr is also cloned, expressed, and purified. It is susceptible in intake cells to protease digestion, indicating it is associated with the cell surface. Besides

these two proteins, proteins encoded by *spy1793*, *spy1794* and *spy1795* are designated by two groups with different names, SiaABC (Bates *et al.*, 2003) and HtsABC (Lei *et al.*, 2003; 2005). Purified SiaA protein (encoded by *spy1795*) binds hemoglobin in a solid-phase binding assay (Bates *et al.*, 2003). Inactivation of this gene and *shr* will give bacteria 40% reduction in hemoglobin binding, indicating the *sia* operon contributes to the *in vivo* binding of hemoglobin, but additional proteins are likely to be involved. Another group also finds that HtsA (encoded by *spy1795*) binds heme in 1:1 stoichiometry. Further investigation is needed to study this huge operon.

Streptococcus pneumoniae also can utilize heme and hemoglobin as an iron source (Tai *et al.*, 1993). A surface heme-binding protein (Tai *et al.*, 1997), as well as two operons *piu* and *pia*, encoding ABC transporters, are identified (Brown *et al.*, 2001 a and b).

Corynebacterium diphtheriae is the causative agent of diphtheria, a severe respiratory disease in humans. The principal and best-characterized virulence factor, diphtheria toxin (DT), is negatively regulated at the transcriptional level by iron and the DT repressor protein, DtxR. *C. diphtheriae* produces its native siderophore, corynebactin (Russell *et al.*, 1984). It also uses hemin (Drazek *et al.*, 2000; Schmitt *et al.*, 1998) and hemoglobin (Schmitt *et al.*, 1997; 1999), transferrin (Schmitt *et al.*, 1997) as essential sources of iron during growth in iron-depleted media. More, it can also utilize aerobactin (Russell *et al.*, 1984) from *Shigella flexneri* and another siderophore from *Corynebacterium glutamicum*, also called corynebactin. Two operons were identified. A three-gene operon, *hmuTUV*, is identified as hemin utilization system (Drazek *et al.*, 2000) in this bacterium as well as *Corynebacterium ulcerans* (Schmitt *et al.*, 2001). Another

operon, *irp6ABC*, is identified as corynebactin uptake system. Both of them are ABC transport systems. Furthermore, a heme oxygenase (Schmitt *et al.*, 1997 and 1998), encoded by *hmuO* gene, is identified to release iron from heme.

In *Bacillus subtilis,* very little information about iron transport is available. Fur, the iron regulator, has been studied. Fur protein (Bsat *et al.*, 1999) is overexpressed and purified. It is shown to interact with the operator region controlling the expression of the dihydroxybenzoate siderophore biosynthesis (*dhb*) operon with high affinity and selectivity. Besides Fur protein, only a lipoprotein (Schneider *et al.*, 1993) is identified as part of an iron-hydroxamate uptake system. FhuD protein shows significant homology to the binding proteins FepB, FecB and FhuD of *Escherichia coli*, which are all components of binding protein-dependent, ferric siderophore transport systems. It is able to complement a mutant defective in ferrichrome uptake.

In *Listeria monocytogenes*, similarly, the regulators, Fur and PerR, are shown to play a significant role in virulence (Rea *et al.*, 2004). Although *Listeria monocytogenes* does not produce siderophores for iron acquisition (Simon *et al.*, 1985), a number of microbial siderophores and natural iron-binding compounds, including ferrioxamine B, ferric pyoverdin, rhodotorulic acid, ferric catechin, ferric esculetin, ferric quercetin, caffeic acid, chlorogenic acid, ferric norepinephrine, ferric DOPA, and several more, are able to promote the growth of iron-starved *Listeria monocytogenes*. The siderophores and iron-binding proteins I studied, except for ferrioxamine B and ferrichrome, are different from above compounds. However, Simon (1985) also shows that *Listeria monocytogenes* does not utilize ferric ferrichrome, which conflicts with what I find in my study. There are probably two ways (Fig. 1.7) that ferric iron can be utilized. One is that putative

extracellular iron reductases (Coulanges *et al.*, 1997; Cowart, 2002) are capable of immobilizing the extracellular iron. The other is by siderophores. The only study is recent and from our lab. Dr. Newton (Newton *et al.*, 2005) shows that *svpA* transcription and SvpA production markedly increases, 80-fold and 10-fold respectively, in response to iron deprivation, indicating *svpA-srtB* locus is regulated by iron availability through Fur protein. SvpA is also shown to attach to the cell wall through SrtB-mediated covalent linkage. However, site-directed in-frame chromosomal deletions of these structural genes do not impair hemin, hemoglobin, or ferrichrome utilization in nutrition tests, although SvpA bears homology to IsdC, a hemin-binding protein of *Staphylococcus aureus*, and also SvpA binds heme in solution. Further more, the *svpA-srtB* mutants show no significant attenuation of virulence in an intravenous mouse model system, but the mutations do reduce the persistence of *L. monocytogenes* in murine liver, spleen, and intestines after oral administration.

In summary, no iron transport systems involved in any type of iron complexes, except a lipoprotein named FhuD identified in *Bacillus subtilis* in 1993, are known today. In this study, four iron regulated operons are studied, and a ferrichrome uptake system as well as a hemin/hemoglobin uptake system is identified.

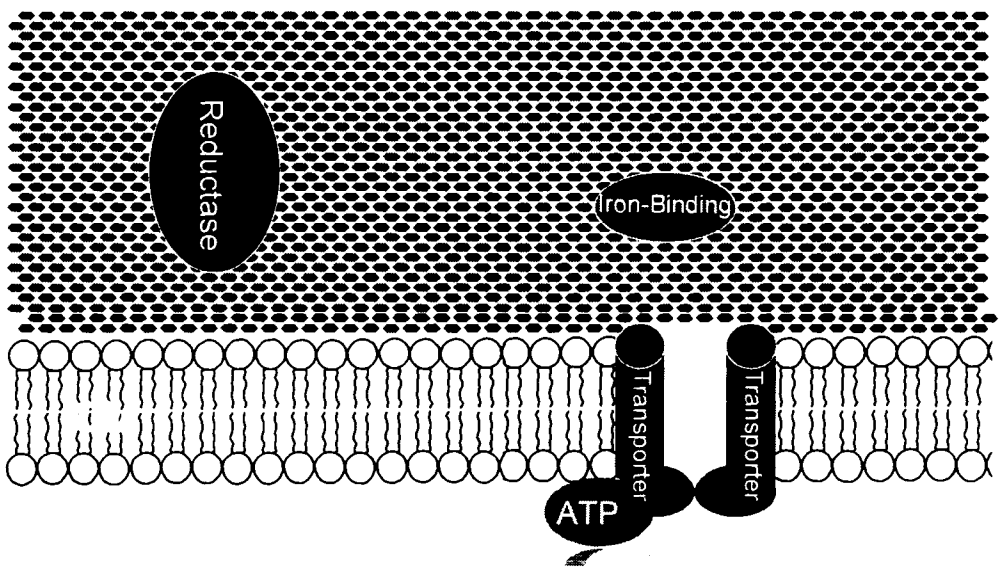

Fig. 1.7 Iron uptake systems in Gram (+) bacteria.

Chapter 2 Materials and Methods

2.1 Bacterial Strains and Plasmids

2.2 Growth Media

2.3 Siderophores Preparation

2.4 Plasmids: pITS449 and pITS23

2.5 Preparation of Competent Cells

2.6 Site-Directed Mutagenesis

2.7 Siderophore Nutrition Assays

2.8 Colicin Sensitivities

2.9 Binding Assays

2.10 Transport Assays

2.11 Expression of FepA

2.12 Purification of Outer Membrane Proteins (FepA and FhuA)

2.13 Sarkosyl Extraction of the Outer Membrane

2.14 Sucrose Density Gradient Fractionation of Cell Envelopes

2.15 Sulfo-EGS Cross-Linking

2.16 Construction of TEV Protease Sites

2.17 Purification of IgG

2.18 Purification of Fab Fragment

2.19 ELISA

2.20 *In vivo* Reconstitution of Cell Envelopes

2.21 Periplasm Extraction of *E. coli*

2.22 Site-Directed Chromosomal Deletion

2.1 Bacterial Strains and Plasmids

All bacterial strains used in these studies are derivatives of *E. coli* K-12, listed in Table 2.1 with their genotypes and references. AN102 was used for purification of enterobactin; JM101 and CJ236 were used for purification of uracylated templates for mutagenesis. Phage m13mp18 was used for mutagenesis. UT5600 was used as inner membrane component deficient strain for outer membrane transport study. KDF541 was used for phenotypic characterization of FepA and its derivatives. SF120 was used as a protease deficient strain. BN1071 was used as a chromosomal control of FepA function. Plasmids used in the studies are listed in Table 2.1 along with their genotypes.

Table 2.1 Strains and plasmids used in this study.

Strains, plasmids	Genotype	References
Strains		
E. coli		
AN102	*thi trp fep proC leu tonA*	Yeowell and White, 1982
CJ236	*dut1 ung1 thi-1 relA1/pCJ105(cam^{r}F')*	Kunkel *et al.*, 1987
JM101	*supE this Δ(lac-proAB) F' [traD36 proAB+ lacI lacZ Δ M15]*	Messing, 1979
BN1071	*F$^-$ thi, entA, pro, trp, rpsL*	Klebba *et al.*, 1982
KDF541	BN1071 *recA, fepA, fhuA, cir*	Rutz *et al.*, 1992
UT5600	F$^-$*ara-14 leuB6 azi-6 lacY1 proC14 tsx67 Δ(ompT-fepC266) entA403 trpE38 rfbD1 rpsL109 xyl-5 mtl-1 thi-1*	McIntosh et al., 1979
UT2300	*F − ara-14 leuB6 azi6 lacY1 proC14 tsx-67 entA403 trpE38 rfbD1 rpsL109 xyl-5 mtl-1 thi1*	McIntosh *et al.*, 1979
TJB1	F- *thi trp- pro leu lacY mtl xyl RpsL azi tsx SupA-, Δfiu::cat, entA-*	From Dr. McIntosh
RW193	*entA403 purE$^-$ fhuA$^-$*	Leong&Neilands, 1976
SF120	KS272 *depP ptr ompT*	Meerman *et al.*, 1994
DH5α	*supE44 ΔlacU169(Φ80lacZ ΔM15) hsdR17 recA1 endA1 gyrA96 thi-1 relA1*	Hanahan, 1983
OKN3	*fepA* derivative of BN1071	In this lab
OKN13	*fepA tonB* derivative of BN1071	In this lab
L. monocytogenes		
EGD-e	Wild type	Bierne *et al.*, 2004
B. subtilis		
168	Wild type	Dr. JD Ballard at OU
Fungus		
Ustilago Sphaerogena	-	Emery 1971
Plamids		
pITS449	*fepA$^-$* on pUC18	Rutz *et al.*, 1992
pHSG575	Low copy	Hashimoto-Gotoh *et al.*, 1981
pITS23	pHSG575 *fepA+*	Scott *et al.*, 2001
pHK232	*fhuA$^-$*	Hoffmann *et al.*, 1986
pKSV7	Thermosentitive vector	Smith and Youndman, 1992
pRZ540	*tonB+*	Postle *et al.*, 1983

2.2 Growth Media

Table 2.2 lists the growth media used to culture bacterial strains for this study. Luria-Bertani Broth (LB) was used as rich media for the growth of *E. coli* and *Bacillus subtilis*. T media and Mops media were used as iron-deficient media for protein expression in *E. coli*. 2xYT media and Nutrient Broth were used for site-directed mutagenesis and nutrition assays, respectively.

Table 2.2 Media used in this study.

Media	**References**
Luria-Bertani Broth	Miller *et al.*, 1972
T-media	Klebba *et al.*, 1982
MOPS media	Neidhardt *et al.*, 1974
Nutrient Broth	Sigma
RPMI1640	Sigma
KRM	Newton *et al.*, 2005
BHI	Difco
GE	Tarek *et al.*, 1998

2.3 Preparation of Siderophores

Siderophores and iron-binding proteins. Ferrichrome (Fc) and ferrichrome A (FcA) were purified from cultures of *Ustilago sphaerogena* (Emery, 1971). Enterobactin and corynebactin, the native siderophores of Gram-negative and Gram-positive bacteria, were purified from *E. coli* and *B. subtilis*, respectively; their iron complexes (FeEnt and FeCrn; (Annamalai *et al.*, 2004) were purified by passage over Sephadex LH20 (Annamalai *et al.*, 2004; Wayne *et al.*, 1975). Ferrioxamine B (FxB) was a gift from J. B. Neilands. We purchased purified hemin (Hn), bovine hemoglobin (Hb), bovine holotransferrin (HTf; approximately 80% saturated with Fe^{+++}) equine ferritin (Ftn), ferric citrate (FeCit) and ferrous sulfate ($FeSO_4$) from Sigma-Aldrich (St. Louis, Mo).

2.3.1 Preparation of ferric enterobactin

Enterobactin was purified from the supernatant of AN102 cultures grown to late exponential phase (Wayne *et. al.*, 1976), Ferric enterobactin was prepared by dissolving 1mg of enterobactin in 0.5 ml of methanol, and 0.5 ml of 4 mM $FeSO_4$ in dilute HCl was added, and incubated at room temperature for 1.5 hours to allow for complex formation, Then NaH_2PO_4, pH6.9, 500 mM, was added to make the final buffer concentration of 10mM. The mixture was loaded onto a Sephadex LH20 column equilibrated with 10mM NaH_2PO_4, pH6.9 and eluted with the same buffer. The concentration of ferric enterobactin was determined by measuring the absorbance at 495 nm (ε_{mM} = 5.6; Pollack *et al.*, 1970) on a DU Bechman 640 spectrophotometer. The purity of ferric enterobactin was determined by ratio of absorbance between 393 nm and 495 nm (optimum: 0.666). Ferric enterobactin was stored on ice and repurified after 2 days by running through the

Sephadex LH20 column. To prepare ^{59}ferric enterobactin, 0.05 mCi of $^{59}FeCl_3$ was mixed with $FeSO_4$ prior to the addition of enterobactin.

2.3.2 Preparation of ferrichrome

Ustilago Spherogena (Emery, 1971) was grown in one liter LB for at least one week. To one liter of culture supernatant, pH was dropped by concentrated HCl to around 2.5, and then solid ammonium sulfate was added to the supernatant until reaching "incipient turbidity". This supernatant was extracted with 20 mL aliquots of benzyl alcohol three times, and then shaken in a separatory funnel. Benzyl alcohol layer was drawn, combined, and centrifuged at 3000 rpm for 20 minutes. The supernatant after centrifugation was separated again in a separatory funnel to acquire the orange benzyl alcohol layer that contains ferrichrome. Approximately one liter of ethyl ether was added to the separatory funnel and then the supernatant was back-extracted with 20 mL of water twice. Last, combined water extracts were washed with ethyl ether to remove benzyl alcohol. Extracted ferrichrome was kept at 4°C.

2.4 Plasmids: pITS449 and pITS23

The pUC derived plasmid pITS449 contains *fep*A cloned via PstI and SacI restriction sites (Rutz *et al.*, 1992). *fep*A with full promoter, constructed from BN1071 genome, was transferred onto the low copy vector pHSG575 (Hashimoto-Gotoh *et al.*, 1981) using two mutual restriction sites EcoRI and HindIII, and named pITS23.

2.5 Preparation of Competent Cells

2.5.1 Gram-negative bacteria

A 1ml overnight LB culture of the strain to be rendered competent was subcultured (1/100) into 100 ml LB broth containing the appropriate antibiotics. The culture was chilled on ice for 15 minutes when it reached an $O.D._{600}\approx 0.5$. Bacteria were pelleted and washed with 100 ml and 50 ml ice cold dH_2O, 10 ml ice cold dH_2O plus 10% glycerol, respectively. Finally, the pellets were resuspended in 200 µl dH_2O plus 10% glycerol, aliquot (40 µl), and frozen at -80°C.

2.5.2 *Listeria monocytogenes* (Park *et al.*, 1990)

Overnight BHI culture of EGD-e was subcultured into 500 mL BHI (1% inoculum). Penicillin G was added to 0.12 µg/mL when the OD_{600} reached 0.3. Two more hours later, when OD_{600} was around 0.8-0.9, culture was spun down in GSA rotor at 8000 rpm for 20 minutes. Pellet was washed with 1mM Hepes/500 mM sucrose 100 mL once, 50 mL once, and then 25 mL three times. Finally pellet was resuspended in 500 µL Hepes/sucrose with 15% glycerol.

2.5.3 *Bacillus subtilis* (Tarek *et al.*, 1998)

Overnight LB culture of *Bacillus subtilis* at RT was subcultured in 20 mL of LB to OD~0.1 and shaken at 37°C until OD reached 1. Bacteria then were diluted 1:20 in GE minimal media. When bacteria entered stationary phase in 4-5 hours, 500 µL or 1 mL of culture was mixed with DNA to final 1 µg/mL, and shaken for 30 minutes at 37°C. Then 1 mL of LB was added, and shaking continues for another one hour. Culture was then plated out on LB plates containing proper antibiotics. Plates were incubated at 37°C overnight.

2.6 Site-Directed Mutagenesis

2.6.1 Sequence comparisons

The amino acid sequences of *Escherichia coli* FepA (Lundrigan *et al.*, 1986), *Salmonella typhimurium* (Tumumuru *et al.*, 1990), and amino acid sequences of *M. catarrahalis* CopB, *N. gonorrohoea* FetA, *B. pertussis* BfeA, *P. aeruginosa* PfeA, *Salmonella typhimurium* IronN, and *Escherichia coli Cir, FecA, BtuB, IutA, FhuA FhuE,* were compared by a PILEUP program (Genetics Computer Group, Madison, WI). The conserved residues were then chosen for the site-directed mutagenesis.

2.6.2 Site-directed mutagenesis using M13 method

Using the M13 method (Messing, 1983; Kunkel, 1985; Newton *et al.*, 1997), *fepAY472A, -Y478A, -Y481A, -Y488A, -Y495A, -Y553A,* and *-Y638A* on pITS449 (a pUC18 derivative) (Armstrong *et al.*, 1990; Cao *et al.*, 2000) in *fepA* were produced. These alleles were transferred to pITS23 by restriction fragment exchange with KpnI and SstI.

Using PstI and SacI sites, fepA structural gene from pITS449 was subcloned into the multiple cloning site of M13 mp19. The primers used in the in vitro mutagenesis reactions are listed in Table 2.2. The mutant fepA gene was then cloned back into the pITS449 fepA structural gene using the same cloning sites. The whole structural gene was sequenced to rule out any random errors in the mutagenesis.

Preparation of uracylated template for mutagenesis

A single M13mp19 plague carrying fepA allele was obtained from a LB plate of JM101 transformed with the phage DNA. The plague was then resuspended in 1 ml 2x YT media, incubated at 60°C for 5 minutes to kill JM101 host cells, vortexed to release

the phage, and centrifuged to get the supernatant containing the phage for uracylation. 25 µl of the above supernatant was then added to 50 ml 2xYT media containing

Phosphorylation of mutagenesis primers

Primers were diluted to 10 pmol/µL. 20 µL of the diluted primers was mixed with 3 µL of 10X kinasing buffer, 1.5 µL 10 mM ATP, 5 µL of water, and 0.5 µL T4 polynuclotide kinase (10 units/µL). The mixture was incubated at 37°C for 45 minutes and then the enzyme was inactivated by incubating at 65°C for 10 minutes.

In vitro mutagenesis reaction

First step, 200 ng of uracylated DNA template was mixed with 6 pmoles phosphorylated oligo nucleotides, 1 µL of 10X annealing buffer, and double distilled water to get the final volume of 10 µL. The mixture was incubated at 70°C for 2 minutes, then allowed to cool in a dish of 70°C water on the bench for 30 minutes till temperature below 30°C. Second step, the above hybridization mixture was set on ice, and 1 µL of 10X synthesis buffer, 1 µL of T4 DNA ligase and 1 µL of T7 DNA polymerase was added. The mixture was spun briefly, and then incubated on ice for 5 minutes, at 25°C for 5 minutes, and at 45°C for 45 minutes. 90 µL of stop solution was added after incubation. Last step, 1 µL of the mutagenesis reaction was electro-transformed into 40 µL JM101 competent cells. After adding 175 µL of chilled SOC medium (a medium that is used to enhance the growth of *E. coli* competent cells after transformation reaction due to the presence of glucose), it was transferred to test tubes, and incubated at 37°C for 10 minutes. 1 µL, 10 µL and the rest were plated out on tryptone plates along with 70 µL JM101 overnight culture and 3 mL melted tryptone top agar. Incubate at 37°C overnight.

Mutant selection

Several colonies were picked and then grown in LB overnight. DNA was extracted and sequenced to select mutants.

Transformation of the mutant DNA into the expression vector

M13 mutants were digested with SacI and PstI, purified by gene clean and then ligated to pITS449 vector, that was also cut with SacI and PstI and purified by GeneClean.

2.6.3 Site-directed mutagenesis using the QuikChange kit

We directly engineered *fepAW101A*, *-Y217A*, and *-Y540A* on pITS23 and *fepA*Δ *60-67* and *fepA* Δ *98-105* on pITS449 by using the QuikChange kit (Stratagene). Mutagenesis reactions contained 90 ng of template DNA, 125 ng of mutagenic primers, 10 μM dNTPs. 1X Reaction buffer (Stratagene), and 2.5 units of pfu turbo DNA polymerase in a 50 μl reaction volume. Temperature cycling was performed with the following parameters: 1 cycle of denaturation at 98°C for 2 minutes, followed by 18 cycles of denaturation (98°C for 30 seconds), annealing (55°C for 1 minute.), and extension (68°C 2 min/kb of target). A final extension step was incorporated after the eighteen cycles to ensure complete synthesis. An aliquot from the reaction was removed (10 μl) and electrophoresed on a 1% agarose gel to visualize the efficiency of the cycling process. The remaining reaction, 1 μl of the restriction enzyme DpnI was added and incubated for one hour at 37°C. The reaction then was adjusted to 100 μl by adding dH_2O, ethanol precipitated and resuspended in 20 μl of dH_2O. 2 μl of this solution was transformed into KDF541 by electroporation (*E. coli* pulser; Bio-Rad) and selected by plating on LB-agar plates containing chloramphenicol at 20 μg/ml.

We verified the mutations by DNA sequence analysis with an Alf Express sequencer (Amersham-Pharmacia) and appropriate CY-5-labeled oligonucleotide primers.

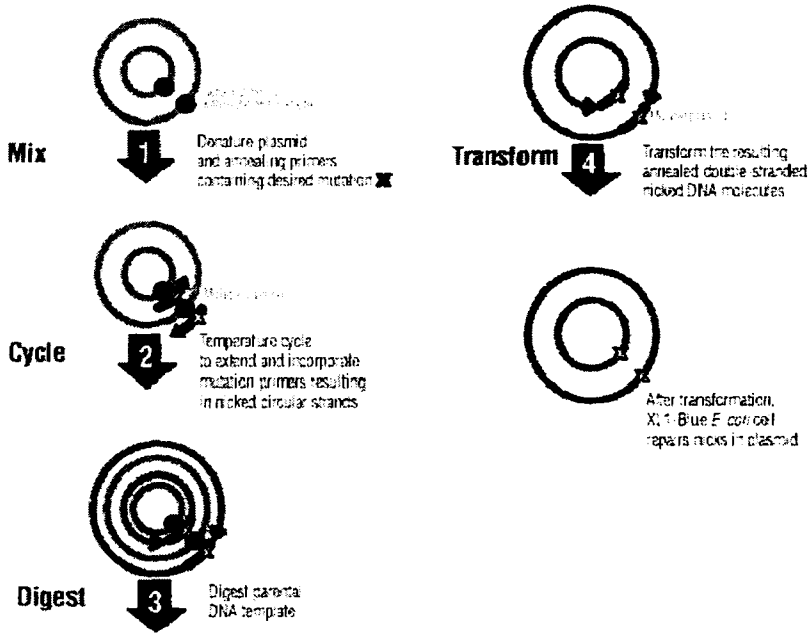

Fig. 2.1 Quikchange mutagenesis.

2.7 Siderophore Nutrition Assays

2.7.1 Gram (-) Bacteria

Siderophore nutrition tests (Cafiso *et al.*, 1982; Newton *et al.*, 1999; Scott *et al.*, 2001; Wayne *et al.*, 1976) provided qualitative determinations of FeEnt transport capability. Bacterial strains harboring wild type or mutant derivatives were inoculated from frozen permanents into LB media containing the appropriate antibiotic(s) for the strain and plasmid (100 μg/ml streptomycin, 100 μg/ml ampicillin, 20 μg/ml chloramphenicol, 50 μg/ml kanamycin). Cultures were grown overnight at 37°C and subcultured 1/100 into MOPS and allowed to reach mid-log growth ($O.D._{600}\approx 0.5$-0.6). 100 μl of the bacterial culture was plated in a six well culture cluster (Corning Incorporated) with 3 ml of nutrient top agar, 30 μl of 10 mM apo-ferrichrome A, and antibiotics with the same concentrations used in bacterial growth. The agar was allowed to solidify and a 1/4' diameter sterile paper filter disk (Becton Dickinson Microbiology Systems, MD) was placed on top of the agar. 10 μl of a 50 μM ferric-enterobactin solution was dispensed onto the disk and incubated for at least 8 hours at 37°C. Results are expressed as the diameter of the observed growth halo in millimeters.

2.7.2 Gram (+) Bacteria (*Listeria monocytogenes*)

Bacteria were grown in BHI and exposed to BP at 0.1 mM, as discussed above, and 2 x 10^7cells were plated in BHI agar containing 0.1 mM BP. Paper discs were applied to the surface of the agar, 10 μL aliquots of sterile solutions of ferric siderophores or iron-binding proteins were applied to the discs, and the plates were incubated overnight at 37° C, and the diameters of the resulting growth halos were measured.

2.8 Colicin Sensitivities

Colicin killing assays were used to assess the efficiency of protein toxin and bacteriophage sensitivity of FepA and its derivatives. Strains were grown overnight in LB at 37°C. 100μl of the bacterial culture was added to LB plates with tryptone top agar containing antibiotics. Serial dilutions of colicins B, D were prepared in 96-well microtiter plates. Approximately 5 μl volumes were transferred to the plate using a Clonemaster (Immusine Corp., San Leandro, CA), and the plates incubated overnight at 37°C. Results were expressed as the reciprocal of the highest dilution that still resulted in clearing of the bacterial lawn.

2.9 Binding Assays

Binding assays were utilized to investigate siderophore binding affinity and capacity of FepA and its derivatives. The adsorption of ^{59}Fe complexes of Ent, Trn, and Crn (specific activity, 150 to 1,000 cpm/pmol) were determined with bacteria KDF541 harboring wild-type FepA or its mutants on pITS23. Bacteria were grown in LB broth with streptomycin (100 μg/ml) and chloramphenicol (20 μg/ml) at 37°C for 16 hours, then they were subcultured into MOPS minimal media with streptomycin (100 μg/ml) and chloramphenicol (20 μg/ml) for 5.5~6.0 hours at 37°C with vigorous aeration until $O.D._{600}$ reached about 0.5. The assay was performed as described (Newton *et al.*, 1999) with some modifications to optimize the binding of each specific mutant. Above culture was incubated on ice for at least 30 minutes before the assay. Culture was diluted to $2*10^8$ cells per milliliter in MOPS media, 100ul of this solution containing $2*10^7$ cells was added into a 50ml pre-cooled tube on ice. Appropriate amounts of fresh purified ice-

cold ^{59}Fe-siderophore in 10ml MOPS was poured into the tube containing $2*10^7$ cells. Tubes were incubated on ice for varieties length of time (1 minute for wild type, longer time for mutants). Then the solution was filtered through a 25mm nitrocellulose filter (Schleicher & Schuell, NH), and the filters were washed with 10 mL 0.9% ice-cold lithium chloride, and counted in a Cobra counter (Packard). Triplicate was done for each sample. For each assay, cell density for each culture was determined by visible spectroscopy at 600 nm, and FepA protein expression was examined by Western immunoblot KDF541 providing negative control data that I subtracted from those of the test strains to eliminate nonspecifically adsorbed radioactivity. The K_d and capacity of ^{59}FeEnt binding were determined by using the bound-versus-total equation of Grafit 5.09 (Erithacus, Ltd., Middlesex, United Kingdom)

$$\text{Bound} = \frac{b - \sqrt{b^2 - 4 * \text{total} * \text{capacity}}}{2} \quad (2\text{-}1)$$

Where b= K_d + total + capacity; total is the amount of substrate added to the assay, and K_d and capacity are the two parameters determined by the least squared fitting using GraFit 5.09.

Equation (2-1) is derived as below:

$$\text{FepA} + \text{FeEnt} \underset{}{\overset{K_d}{\Longleftrightarrow}} \text{FepA*FeEnt} \quad (1)$$

$$K_d = \frac{[\text{FepA}] * [\text{FeEnt}]}{[\text{FepA*FeEnt}]} \quad (2)$$

$$K_d = \frac{(Cap - Bound) * (Total - Bound)}{Bound} \quad (3)$$

$$Bound^2 - (Cap + K_d) * Bound + Cap * Total = 0 \quad (4)$$

$$Bound = \frac{B - \sqrt{b^2 - 4 * Total * Cap}}{2} \quad (5)$$

where $b = K_d + total + Cap$

2.10 Transport Assays

This assay was designed to investigate the iron uptake ability of bacteria carrying FepA. Bacteria were grown and quantitated in the same way as the binding assay, and the uptake of ^{59}Fe-siderophore was measured at 37°C. Series of ^{59}FeEnt at different concentrations at 37°C MOPS media was poured into the assay tubes containing $2*10^7$ cells at 37°C, After incubation for different length of time, the uptake was quenched with a 100-fold excess of nonradioactive FeEnt. Reactions at high concentrations of ^{59}FeEnt (>100 nM) were not quenched because of the large amount of FeEnt required to achieve a 100-fold excess. We made measurements in triplicate for each concentration of FeEnt and determined the level of FepA expression for the strains under investigation. Transport K_m and V_{max} values were calculated with the enzyme kinetics equation of Grafit 5.09.

$$v = \frac{V_{max}}{1 + K_m / [S]} \quad (2\text{-}2)$$

Where [S] is the substrate concentration, and K_m and V_{max} are the parameters determined by the least squared fitting using GraFit5.09.

2.11 Expression of FepA

For measurements of protein expression, 5 x 10^8 bacteria were collected by centrifugation, resuspended in 100 µl of sample buffer (0.5 M Tris (pH 6.8), 30% glycerol, 3% sodium dodecyl sulfate (SDS)), and boiled for 3 minutes. After a brief centrifugation to pellet debris, we subjected 20 µl aliquots of the lysates to SDS-polyacrylamide gel electrophoresis (PAGE) in 10% slabs transferred the resolved proteins to nitrocellulose membranes, and performed Western immunoblots with anti FepA monoclonal antibody (MAb) 45 and ^{125}I-protein A. After overnight exposure to an imaging screen, radioactivity was quantitated on a STORMSCAN PhosphorImager (Molecular Dynamics). In other experiments we measured the concentration of FepA or mutant FepA proteins by immunoblots of purified OM fractions. We also used the OM fractions for determination of mutant protein localization. We prepared the OM fraction by Sarkosyl extraction, resolved the protein components by SDS-PAGE, and stained the protein components with Coomassie blue. Western blot was also done with goat anti mouse IgG conjugated with Alkaline Phosphatase, developed with p-Nitrophenyl Phosphate (Sigma, ST. LOUIS, MO).

The following was the recipe of 0.07% bis SDS-PAGE. 20 mL of running buffer contains 9 mL of 22% acrylamide/0.15% bis, 5 mL of LT buffer, 5.9 mL of distilled water, 100 µL of 10% APS, and 20 µL of TEMED. 5 mL of stacking buffer contains 0.83 mL of 30% acrylamide/0.3% bis, 1.25 mL of UT buffer, 2.91 mL of distilled water, 45 µL of 10% APS, and 15 µL of TEMED.

2.12 Purification of Outer Membrane Proteins (FepA and FhuA)

For FhuA, KDF541 carrying plasmid pHK232 was grown in 25 ml LB with 50 μg/ml neomycin at room temperature until O.D. $_{578nm}$ ≈0.2. It was transferred to 37°C to grow until O.D.$_{578nm}$ >1.0. Subculture it 1/100 into 1 L LB media with 50 μg/ml neomycin, allow them to grow at room temperature until O.D.$_{578nm}$ ≈0.16, then remove to 37°C for overnight. When O.D.$_{578}$ reached 1.4, cells were pelleted at 4000 rpm for 45 minutes with JS4.2 rotor and Backman J6-HC centrifuge at 4°C. All the following steps were done on ice. Cell pellet was resuspended in 100 ml 10 mM Tris-HCl, pH8, spun at 7000 rpm for 15 minutes with JA-14 rotor and Bechman J2 21M/E centrifuge. Cell pellet then was resuspended in 25 ml 100 mM Tris-HCl, pH8, and French Pressed twice at 20000 lb/in^2. Pellet was discarded after centrifuge at 3000 rpm for 15 minutes. The supernatant was spun at 31000 rpm for 45 minutes with 70Ti rotor and Beckman L8-70M ultracentrifuge. The pellet was the cell envelopes. The membranes were washed with 20 ml 10 mM Tris-HCl, 10 mM $MgCl_2$, pH8, and spun at 31000 rpm 45 minutes. This step was done twice. Then pellet was resuspended in 40 ml Tris-HCl, $MgCl_2$, 2% Triton X-100 buffer, centrifuged at 31000 rpm for 30 minutes after being shaken at room temperature for 20 minutes. This step was also repeated once. Pellet was washed with 10 mM Tris-HCl, and then 40 ml 10 mM Tris, 5 mM EDTA, 2% Triton X-100, pH8, shaken at room temperature for 20 minutes, then the supernatant contained outer membrane after centrifuge at 31000 rpm for 30 minutes. The above step was repeated, and the supernatants were combined.

Outer membrane was passed through DE-52 column equilibrated with TTE buffer (100 mM Tris, 10 mM EDTA, 4% Triton X-100, pH7.2), and fractions were collected when being eluted with 0-0.15 M NaCl in 1X TTE.

A colicin M affinity column was also used to further purify the protein. 5-10 ml Sepharose 6B was washed with dH_2O, and the pH was adjusted to 11 while stirring. 2 g CNBr dissolved in 3 ml DMF was added drop by drop into the resin and 2 N NaOH was used to maintain pH above 11. When pH was stable, the resin was filtered in a Hirsch funnel after ice was added. The resin then was washed with 1 L cold dH_2O, 1 L cold 0.2 M $NaHCO_3$ before it was transferred to a beaker. ColM (12.5 ml 50 μg/ml ColM in 50 ml 0.2 M $NaHCO_3$) was poured into the resin, stirred slowly @4°C overnight. The resin was then washed with 2 L cold dH_2O, 1 L cold 1 M Acetic acid, 2 L cold dH_2O, and 300 ml cold 1X TTE, and then resuspended in 1X TTE. After it was settled down at 4°c. supernatant was removed. And 1X TTE was added to the resin before it was loaded onto the column.

15 ml of 0.22 mg/ml FhuA was dialyzed in 1X TTE overnight twice before it was loaded onto the ColM-Sepharose 6B column. The column was washed with 150 ml 1X TTE and then with 0-2 M NaCl (in 1X TTE) gradient. Fractions were collected.

2.13 Sarkosyl Extraction of Outer Membrane

A total of 10^{10} cells were resuspended in 10 mL of Tris-buffered saline (TBS) with trace amounts of DNase and RNase and lysed by passage through a French pressure cell at 14,000 lb/in^2. Unbroken cells were removed by centrifugation at 5000*g for 10 minutes. The supernatant was centrifuged at 100,000*g for one hour to separate the

supernatant, which contained the inner membrane, and the pellet which was the outer membrane. The pellet was then resuspended in 1 mL of TBS containing 0.5% sodium sarcosinate and incubated for 30 minutes at room temperature. The extract was spun for 45 minutes at 20,000*g, and the pellet was the outer membrane.

2.14 Sucrose Density Gradient Fractionation of Cell Envelopes

15 mL overnight LB culture of *E. coli* K-12 was subcultured in 1.5 L at 0.1% and grown to mid log (OD_{600} 0.5-0.9). Cells were pelleted by centrifugation at 4°C in a pre-cooled rotor at 5000*g for 20 minutes. Pellets may be frozen at this stage (Overlay with 10 mM HEPES pH7.4 and freeze at -70°C). Frozen pellet was thawed, and washed with 200 mL 10 mM HEPES, pH7.4 (pre-cooled). Pellet then was resuspended in 28 mL of the same buffer in a 30 mL Corex tube. Trace amount of DNase and RNase was added. The suspension was passed through French Press twice at 14,000lb/in^2. The cell lysate was centrifuged at 3000*g for 5 minutes to remove debris. Then the supernatant was spun in an ultracentrifuge at 15000*g for 1 hour. Pellet was then resuspended in 10 mL HEPES to have a final volume of 7.5 mL with syringe and needles (#18 and #23). Finally, the membrane suspension was laid onto two sucrose gradients and spun in the SW27 rotor for 16 hours at 26,000 rpm and 4°C. The sucrose gradient had three layers: 4.8 mL of 2.03 M sucrose on the bottom, 16.8 mL of 1.44 M sucrose in the middle, and 13 mL of 0.77 M sucrose on the top. After 16 hours, the membrane portions were collected with a gradient collector and washed with 10 mM HEPES pH7.4.

2.15 Sulfo-EGS Cross-Linking

Bacteria grown in morpholinepropanesulfonic acid (MOPS) minimal medium or sucrose gradient-purified outer membrane fractions were suspended in phosphate-buffered saline (PBS) at 10^9 cells/ml or 10 mg/ml, respectively. Sulfo-EGS (Pierce) was added to 4 mM, and the samples were incubated for 2 hours at 0°C. Reactions were quenched by incubation with 50 mM Tris-Cl (pH 7.4) for 15 minutes, and cells or outer membrane proteins were pelleted by centrifugation, solubilized in sample buffer, subjected to SDS-PAGE, and then stained with Coomassie blue or transferred to nitrocellulose and stained with α-FepA MAb 45 and ^{125}I-labeled protein A. When indicated, 5 μM FeEnt was added to the cells prior to exposure to Sulfo-EGS.

2.16 Construction of TEV sites

Using site-directed mutagenesis, residues 94 to 100 was replaced with TEV recognition sequence "ENSYRQG"; residues 89 to 95, 96-102, and 126-132 were replaced with "ENLYFQS".

2.17 Purification of IgG

25 mL of ascites fluid was precipitated with ammonia sulfate to final concentration of 60%. The reaction was stirred in a cold room for at least two hours while ammonia sulfate was added slowly. The reaction was then centrifuged at 10,000 *g for ten minutes. The supernatant was removed. The precipitate was solubilized in a small amount of 50 mM Tris at pH8.0, and then dialyzed against two liters of the same buffer overnight. The solution after dialysis was loaded to a DE-52 column at RT. Column was

first washed with 50mM Tris at pH8.0, and then eluted with a 0-0.3 M of NaCl gradient in the same Tris buffer. All fractions in the washing and eluting steps were collected. Fractions were tested with Western blot and ELISA. Then fractions that contained IgG were pooled and stored in the cold room.

2.18 Purification of Fab Fragment

Once IgG was obtained, 20 mL of the solution was dialyzed against four liters of digestion sample buffer (20 mM NaH2PO4, 10 mM EDTA, pH7.0) overnight. The dialyzed solution was concentrated by Amicon Ultra-15 (10MWCO). Before the digestion of IgG with papain, the immobilized papain needs to be activated. 4 mL of digestion buffer (20 mM Cysteine-HCl in the digestion sample buffer) was added to 0.5 mL of 50% papain slurry (about 250 μg papain per mL of settled gel). After the solution was equilibrated, it was spun at 6000 rpm for four minutes. This activation process was repeated before the papain was resuspended in 0.5 mL of digestion buffer. The digestion reaction contained 0.5 mL of activated papain, IgG solution, digestion buffer (same volume as IgG solution). The enzyme to substrate ratio was about 1:160. This reaction was shaken at 250 rpm in a 37°C shaker for about 20-24 hours. At the end of shaking, 3 ml 10 mM Tris at pH7.5 was added to the digestion reaction to stop the reaction. The mixture was then centrifuged at 8000 rpm for three minutes, and the supernatant was collected. Another 3 mL of 10 mM Tris at pH7.5 was added to the pellet. Mixture was spun again at the same condition. The supernatant from two steps was than combined and dialyzed against two liters of 20 mM Tris, pH7.8 in a cold room overnight. This digestion

solution was then concentrated and loaded to a DE-52 column. The column was washed with 20 mM Tris, pH7.8. The flow through and the washing fractions (presumably Fab fragment) were collected. Then the column was eluted with 0-0.1 M NaCl gradient in the same Tris buffer. Fractions (presumably Fc fragment and undigested IgG) were collected as well. Solutions were then aliquot and frozen at -20°C.

2.19 ELISA

On a 96 well microtiter plates, 50 μL of serial dilutions of antigens, either proteins (2-10 μg/mL) or cell lysates (10^7/mL), was dried overnight in a 37°C incubator. Next day, the microtiter plate was incubated with 100 μL of blocking buffer (TBS/ 2% BSA) for 30 minutes. The plate was then washed three times with washing buffer (borate buffered saline, pH 8.5 (BBS)), coated with first antibody, incubated in a cold room for one hour. The plate was then washed for three times, coated with 1:1000 dilution of Goat-anti-Mouse IgG conjugated with Alkaline Phosphatase (AP) in blocking buffer (1% BSA in BBS) and incubated at room temperature for one hour. Finally, the plate was coated with 1 mg/mL of sigma104 in diethanolamine buffer which is the substrate of AP. Absorbance at 405 nm was measured when the reaction showed a visible bright yellow color.

2.20 *In vivo* Reconstitution of Cell Envelopes

10^9 cells were spun down. The pellet was washed once with either ice-cold 100 mM Tris-HCl pH7.2 containing 10 mM glycerol and 250 mM $CaCl_2$ or with ice-cold 50 mM Tris, followed by 100 mM $KHPO_4$ and 50 mM Tris containing 300 mM $CaCl_2$. Cells

were then resuspended at 0°C in 50 μL of the same Tris buffer with $KHPO_4$ and $CaCl_2$ containing antibody or Fab fragment of antibody in a test tube. The test tube was shaken on ice gently for 30 minutes. Cells were then washed with 1 mL of room temperature 0.9% sodium chloride for a few times until cells looked normal.

2.21 Periplasm Extraction of *E. coli*

To extract periplasm from *E. coli* (Ames *et al.*, 1984), 2 mL of overnight culture was spun at 1,100*g for ten minutes. Cell pellet was then resupsended by brief vortexing in the residual medium. After 20 μL of chloroform was added, the mixture was vortexed briefly and incubated at room temperature for 15 minutes. Finally, 0.2 ml of 0.01 M Tris HCl at pH 8.0 was added before the reaction was spun at 6,000*g for 20 minutes. The supernatant that contained the periplasm was frozen at -20°C.

2.22 Site-Directed chromosome deletions in Gram (+) Bacteria

Site-directed chromosomal deletion in wild-type *Listeria monocytogenes* strain EGD-e was done by *in vivo* recombination (Portnoy *et al.*, 1992; Bergmann *et al.*, 2002; Kreft *et al.*, 2002; Vazquez-Boland *et al.*, 2001; Domann *et al.*, 1992; Cossart *et al.*, 1989; Raveneau *et al.*, 1992; Bierne *et al.*, 2002; 2000; Lety *et al.*, 2001). Two chromosomal sequences, upstream and downstream of my target gene, were amplified by PCR with appropriate restriction digestion sites engineered on both sides of the sequences. They were then digested by restriction endonucleases and joined by ligation. The ligation product, with the elimination of my target gene, was cloned in a thermosensitive vector pKSV7. The construct was then transformed by electroporation into EGD-e (Poyart *et al.*,

1997). Transformant was grown at 30°C with 5 μg/mL of chloramphenicol and screened by colony PCR. Transformant was then subcultured and grown at 37°C with 5 μg/mL of chloramphenicol. At 37°C, the construction was integrated into the chromosome by homologous recombination with DNA flanking the target gene. The integrant was again subcultured at 37°C but without chloramphenicol. After several generations (at least six times of subculture), the integrant underwent a second recombination event excising my target gene on the chromosome. Each mutant of EGD-e was verified by colony PCR with appropriate primers designed to show the size of the deletion. Mutants were also sequenced.

pKSV7 is a thermo-sensitive vector. It replicates at 30°C, but not at 37°C or higher. It also has ampicillin resistance in *E. coli* and chloramphenicol resistance in Gram-positive bacteria.

Chapter 3 Aromaticity of the Surface Loops of FepA

3.1 Experimental Strategies

3.2 Candidates of the Aromatic Component

3.3 Site-Directed Mutagenesis

3.4 Protein Expression and Localization

3.5 Nutrition Assays

3.6 Colicin Killing Assays

3.7 Quantitative Assays

3.8 N-loop Deletions

3.9 X-Linking

3.10 Competition between FeEnt and Other Siderophores

3.11 Discussion

3.1 Experimental Strategies

A previous study (Newton *et al.*, 1997) indicated that the interaction between FepA and its ligand was multi-component. Aromatic residues are good candidate residues for the initial interaction between FepA and its ligand, ferric enterobactin, not only due to the aromatic property of ferric enterobactin, which can be extracted by ethyl acetate, but also due to the fact that most conserved residues between ferric enterobactin transporters in different bacteria are aromatic residues. In the crystal structure of FepA, the external loops of FepA together form the mouth of the pore vestibule. Hydrophobic amino acids predominate on the exterior surfaces of the vestibule mouth, whose interior contains aromatic residues that distribute in two regions proposed to participate in ligand binding (B1 and B2). The purpose of this chapter is to find the role and the importance of those aromatic residues on the surface loops of FepA and another interesting residue, W101, which is on the very top of the second loop of the N domain (NL2) and is at least 70% conserved among different proteins. This chapter also investigates two N-domain loop (NL1 and NL2) deletion mutants (*fepA_60-67* and *fepA_98-105)*.

3.2 Candidates

In the crystal structure of FepA, the external loops coalesce to form the mouth of the pore vestibule. Hydrophobic amino acids predominate on the exterior surfaces of the vestibule mouth, but its interior contains aromatic residues that distribute in two regions (B1 and B2) proposed to participate in ligand binding. The function of the most exterior aromatic amino acids of B1 in ferric siderophore recognition seemed interesting, and the sequences of FeEnt transporters from several Gram-negative bacteria (*E. coli*, *Salmonella*

enterica serovar Typhimurium, *Bordetella pertussis*, *Neisseria gonorrhoeae*, and *Xanthomonas citri*) and the *E. coli* metal transporters (Cir, FecA, IutA, BtuB, FhuA, and FhuE) were aligned using PILEUP (Genetics Computer Group, Madison, Wis.). They were also compared to the crystal structures of FepA, FhuA, and FecA (Ferguson *et al.*, 2002). Most of the conserved residues among these proteins turn out to be aromatic residues, although FeEnt is also negatively charged in addition to its aromaticity. The alignments identified four aromatic residues (Fig. 3.1) in the extremities of the surface loop 7 (tyrosine 472, 478, 481, 488 and 495) and one residue (W101, Fig. 1) in the second loop of the N domain (NL2) that were at least 70% conserved among the different proteins. Less-conserved, but well-exposed, tyrosine 217 (L2), 488 (L7), 540 (L8), 553 (L8), and 638 (L10) (Fig. 3.1) were also found. For each of these targets, I generated alanine substitutions either on pITS449 (Armstrong *et al.*, 1990; Cao *et al.*, 2000) and then transferred onto pITS23, or directly on pITS23, a low-copy-number vector derived from pHSG575 (Fig. 3.2; Hashimoto-Gotoh *et al.*, 1981) that carries *fepA* under the control of its natural promoter.

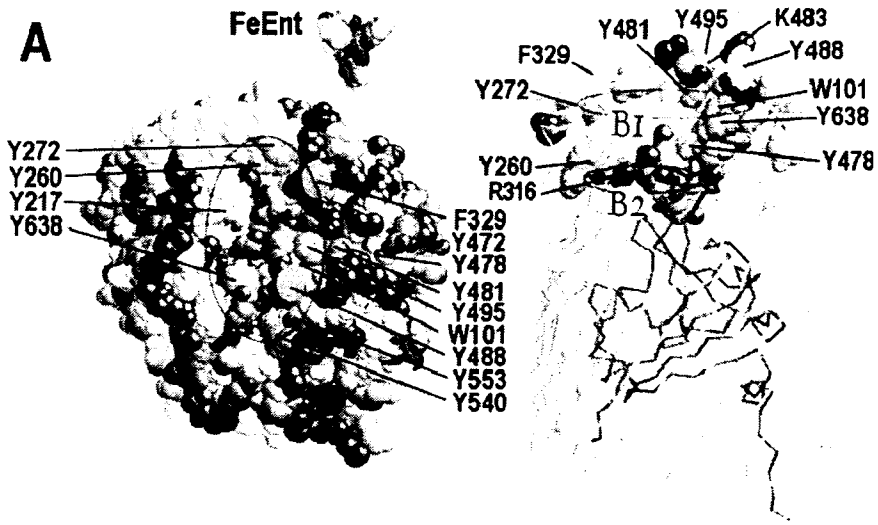

Fig. 3.1 Candidates of Site-directed FepA mutations (Annamalai et al., 2004). The model of FepA (Cafiso *et al.,* 1983) depicts aromatic residues (yellow) that we changed to alanine, in space filling format viewed from the top (left). Hydrophobic residues (L, I, V, M, and A) are colored green. The locations of residues F329 and Y488 are not known (Buchanan *et al.* 1999), but the last solved residues in L4 (red) flank the approximate location of the former (yellow oval), and the last solved residues in L7 (light green) flank the approximate location of the latter residue (yellow oval). Basic residues are shown in CPK format. Residues of interest are also shown in space-filling format on a backbone representation viewed from the side (right), with the same color scheme.

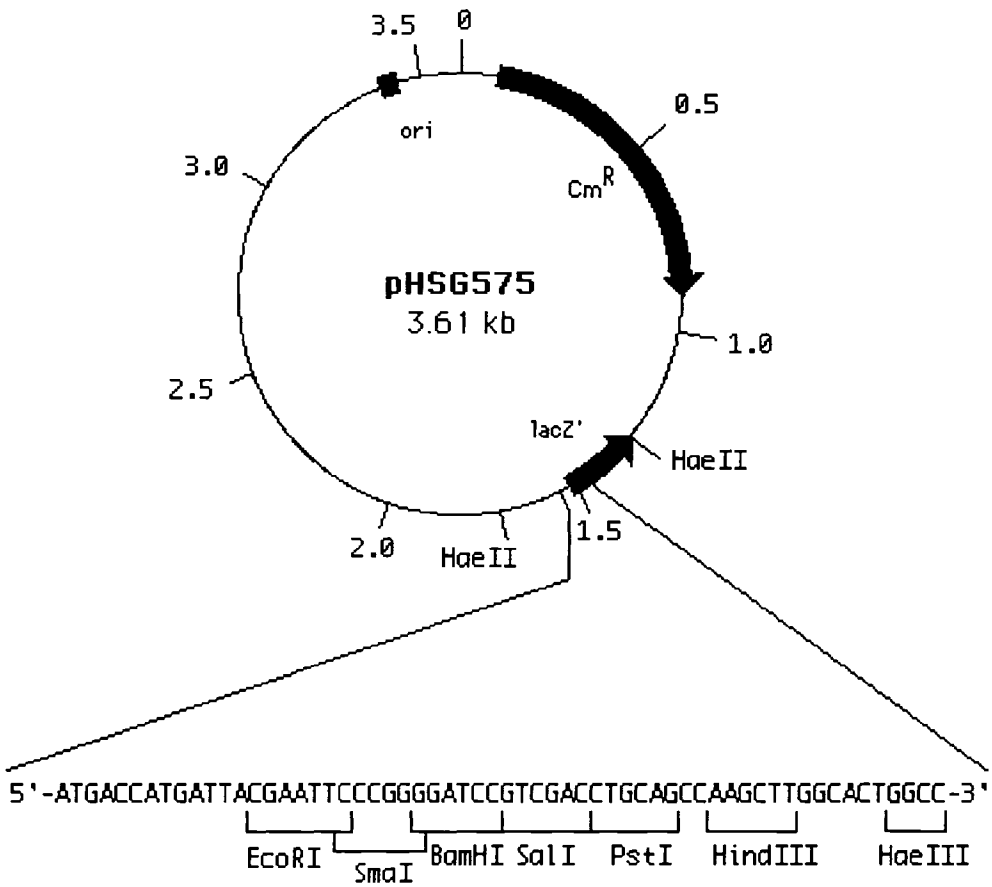

Fig. 3.2 Genetic map of pHSG575 plasmid (Hashimoto-Gotoh *et al.*, 1981).

3.3 Site-Directed Mutagenesis

Using either the M13 method (Newton *et al.,* 1997) or QuikChange (Stratagene, San Diego, CA; Scott *et al.,* 2002), I produced site-directed substitution mutations in *fepA*. The former method gave rise to *fepAY472A, -Y478A, -Y481A, -Y488A, -Y495A, -Y553A*, and *-Y638A* on pITS449 (a pUC18 derivative; Armstrong *et al.,* 1990; Cao *et al.,* 2000). I transferred these alleles to pITS23 (Fig. 3.2) by restriction fragment exchange with KpnI and SstI. I directly engineered *fepAW101A, -Y217A*, and *-Y540A* on pITS23 and *fepA_60-67* and *fepA_98-105* on pITS449 (Newton *et al.,* 1999) by using the QuikChange kit. I then verified the mutations by DNA sequence analysis with an Alf Express sequencer (Amersham-Pharmacia) and appropriate CY-5-labeled oligonucleotide primers.

3.4 Protein Expression and Localization

The levels of mutant FepA protein expression (Fig. 1.3), monitored by SDS-PAGE and by anti-FepA (MAb 45) immunoblots, developed with ^{125}I-protein A, showed few variations. *E. coli* k-12 strain KDF541 (FepA-) expressed all of the mutant proteins at levels similar to that of the wild-type FepA, and the immunoblot quantitation showed reasonable concentration of FepA proteins that accounts for the binding capacity of the amount of the bacteria used in the binding assay. Immunoblot provided the most accurate determination of the concentration of functional FepA proteins in the OM (Table 3.1). In addition, flow cytometric analyses (Table 3.1) indicated that KDF541 properly expressed all of the mutant FepA proteins. They were assembled in the OM such that surface epitopes on L4 and in L5 were accessible to binding by MAb 45 (residue 290 to 339 on

L4; Murphy *et al.*, 1990) and MAb24 (residues 382 to 400 on L5; Murphy *et al.*, 1990), respectively. All the mutant FepA proteins were recognized at levels that were comparable to the recognition to the wild-type FepA. These localization results, together with the capacity and expression measurements, showed that the mutations did not globally disrupt the structure of FepA such that it was poorly expressed, improperly targeted, or misfolded into an aberrant conformation. The data indicated that the substitution mutations created local perturbations of structures and phenotypes that we could compare to each other and to that of the wild-type FepA.

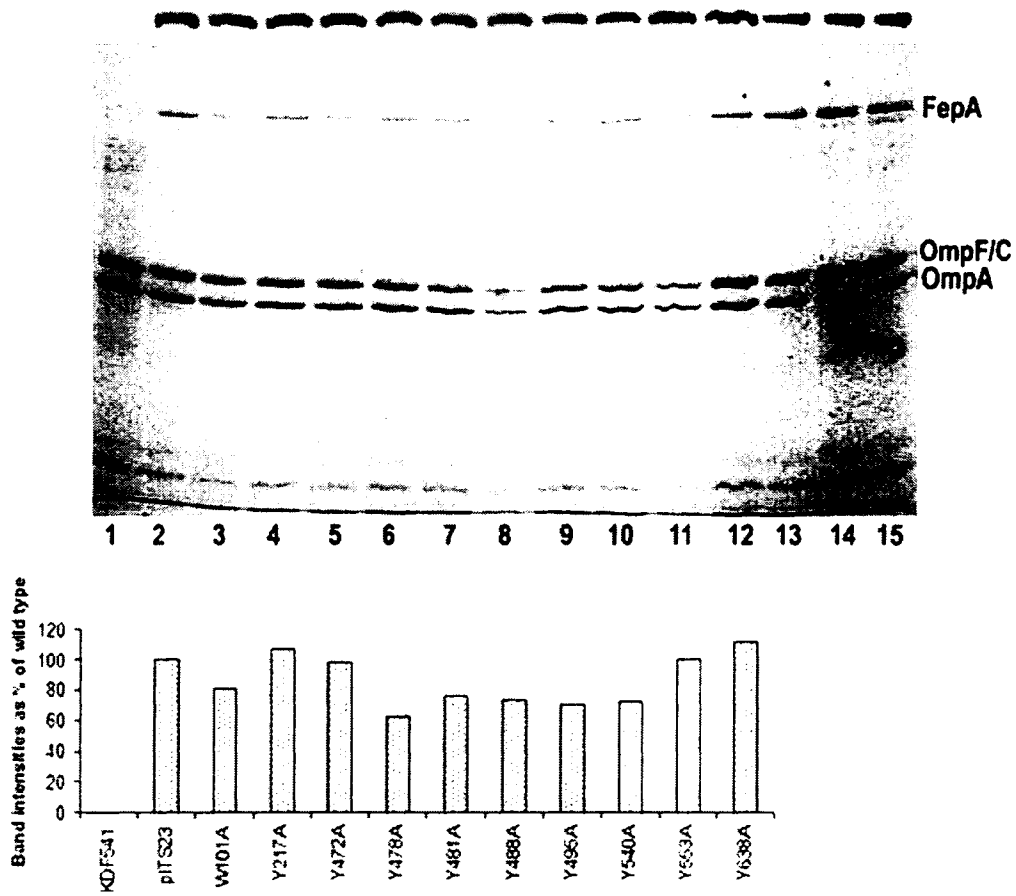

Fig. 3.3 Expression and localization in the OM. Cell lysates (top) or OM fractions (bottom) (Rutz *et al.*, 1991) from *E. coli* expressing wild-type FepA or its mutant derivatives were resolved by SDS-PAGE and either subjected to immunoblot analysis with anti-FepA MAb 45 and ^{125}I-protein and then quantitated except clones in pUC19. A (top) or stained with Coomassie blue (bottom). The expression levels of the mutant proteins and their localization to the OM were related to those of OmpF and OmpA and found to be comparable to that of wild-type FepA carried on the same plasmid. Lane 1 contains a sample from KDF541, and lanes 2 to 12 contain samples from KDF51 harboring pHSG575 carrying the *fepA* alleles *fepA*$^+$, *W101A*, *Y271A*, *Y472A*, *Y478A*, *Y481A*, *Y488A*, *Y495A*, *Y540A*, *Y553A*, and *Y638A*. Lanes 13 to 15 contains samples from KDF541 harboring pUC19 carrying the *fepA* alleles *fepA*$^+$, *ΔNL1*, and *ΔNL2*, respectively.

3.5 Nutrition Assays

In nutrition tests (Fig. 3.4), the negative control, KDF541, never gave a growth halo in the tests. Wild-type FepA consistently gave a dense zone of growth with sharp borders and a size of 18.5mm. The mutants produced several other types of growth halos, which reflected their transport properties. The growth zones of KDF541 harboring Y217A, Y472A, and Y488A were comparable to that conferred by pITS23 (*fepA*$^+$), which agreed with the near wild-type binding and transport properties acquired from the quantitative assays later on. The halos created by Y481A and Y553A had sharp margins like those of the wild-type FepA, but they were larger in diameters (about 21mm). This increase reflected their increased Km on transport. Mutants Y478A, Y495A, Y540A, and Y638A produced fainter, larger halos with diffuse borders that indicated more impairment of transport. The N-domain loop deletions created more different appearances in the tests. They have the same large halos as Y540A, Y495A, Y638A, and Y478A, but they have more diffuse margins. Quantitative uptake determinations showed that more impaired transport resulted in larger and more diffusing growth halos. Mutant W101A is different from others. Its halo was only slightly larger than that of the wild type, but it had a diffuse border comparable to the N-domain loop deletion mutants and a "bull's-eye" or "target" appearance that has not been seen in any other mutants before. This nutrition test offered plenty of information that are necessary for me to predict what is going to occur in the quantitative binding and transport assays.

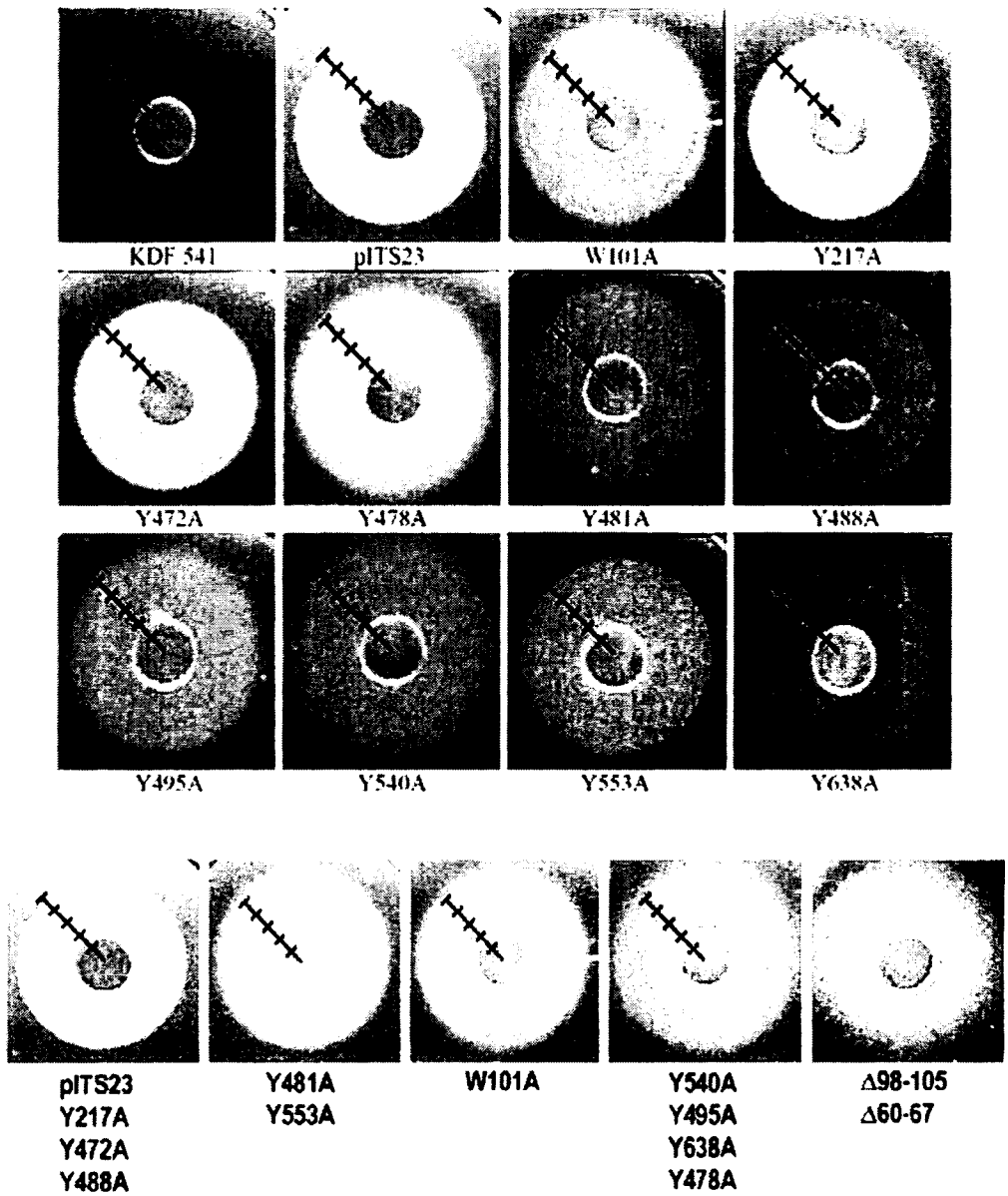

Fig. 3.4 Siderophore nutrition tests. The site-directed mutations created several different effects in qualitative uptake assays. Picture below is the summary and comparison of the halos of all mutants and the wild type.

3.6 Colicin Killing Assays

All of the constructs retained susceptibility to both ColB and ColD (Table 3.1), reiterating that neither the Ala substitution mutations nor the small N-domain loop deletions prevented proper folding and assembly of FepA in the OM. Most mutations decreased colicin sensitivity 2- to 10-fold. However, W101A and Y553A reduced ColB susceptibility 40-fold, which is consistent with the larger halos observed in the nutrition test, although different binding sites exist for siderophores and colicins. W101A also showed us much compromised binding and transport ability (Table 3.1) in the ^{59}FeEnt assays. But Y553A only had slightly increased Km (5 fold higher), which is not comparable to the effects produced in the nutrition test and the colicin killing test. On the other hand, W101A, Y481A, and Y638A created the opposite effect: for example, Y638A yielded only a twofold decrease in colicin sensitivity but almost 80 fold increase of Km in FeEnt uptake. The N-loop deletion mutants were similar in that their loss of colicin sensitivity (10-fold) which was much less than their effects on FeEnt transport (K_m increased 500- to 800-fold). This discrepancy reiterated that the effects of mutagenesis on FeEnt utilization and colicin susceptibility were usually not the same (Payne *et al.*, 1997) because residues that recognize FeEnt in the binding and transport are different from the residues that are involved in the invasion of the colicins. Finally, killing by the two toxins involves similar recognition and uptake determinants, because the mutations in FepA usually caused comparable reductions in susceptibility to both toxins. The sole exception was Y472A, which caused a 10-fold decrease in ColB killing but did not diminish sensitivity to ColD.

3.7 Quantitative Assays

Binding

Adsorption of ^{59}FeEnt to cells expressing the aromatic substitution mutant proteins revealed several affinity effects (K_d; Fig. 5 and Table 1). Y217A, Y488A, and Y553A had near-wild-type binding capabilities ($K_d \leq 0.5$ nM), whereas other mutations caused three- to five-fold lower affinity ($K_d \approx 1.5$ nM) in the following order of impairment: Y472 > Y540 > W101> Y495 > Y478. Substitutions Y481A and Y638A engendered greater reductions in affinity (>10- fold; $K_d \approx 5$ nM), as did the deletions in NL1 and NL2 ($K_d \approx 7.3$ and 11.7 nM, respectively).

With the exception of W101A and Y638A, the mutations did not affect the maximum amount of ^{59}FeEnt bound per cell (binding capacity), which concurred with the normal expression and localization of the mutant FepA proteins (Fig. 3.3). The capacity of bacteria expressing FepAW101A and FepAY638A was lower (20% and 5% of the wild type capacity), even though they were expressed at normal levels and localized in the OM (Fig. 3.3). Thus, their decreased capacities derived from specific detrimental effects of the Ala substitutions on FeEnt binding.

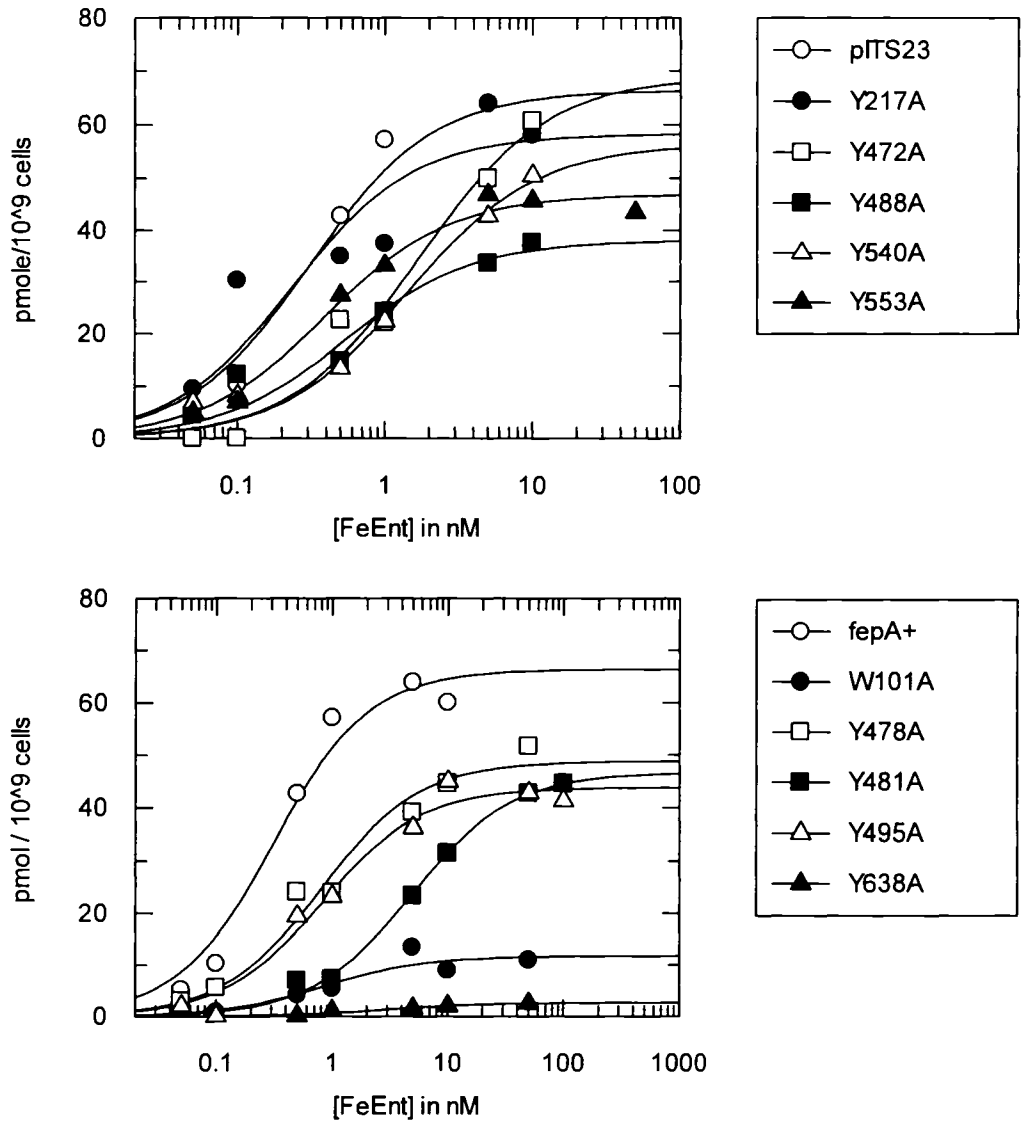

Fig. 3.5 ^{59}FeEnt binding by Ala substitution mutants. We determined the concentration dependence of ^{59}FeEnt binding by *E. coli* strain KDF541 expressing FepA substitution mutant proteins carried on the low-copy plasmid pHSG575 at six concentrations near K_d, with each point collected in triplicate and averaged. We analyzed the binding data, and plotted curves by using the bound-versus-total equation of Grafit 5.09. The concentration of ^{59}FeEnt is logarithmically plotted to demonstrate the decreases in affinity that some of the mutations caused. (Top) Mutants with near wild type binding properties. *fepA*$^+$, open circles; *Y217A*, closed circles; and *Y72A*, open squares; *Y488A*, close squares; *Y540A*, open triangles; *Y553A*, closed triangles. (Bottom) Mutants with impaired binding properties. *fepA*$^-$, open circles; *W101A* closed circles; *Y478A*, open squares; *Y481A*, closed squares; *Y495A*, open triangles; *Y638A*, closed triangles.

Transport

The mutants had different levels of deficiency in ^{59}FeEnt uptake (Table 3.1). They were classified into three categories by the properties of ^{59}FeEnt uptake together with binding. The decreased binding affinities created by Y472A, Y488A, Y540A, and Y481A were commensurate with their decreased uptake affinities (class I). Among these, Y481A caused the most impairment (a 17-fold increase in K_d and an 18-fold increase in K_m); its V_{max} was about 50% of that of the wild type. None of the other class I mutations significantly changed V_{max}. Class II mutants had more severe transport defects than binding deficiencies. Y478A had a more than 400-fold increase for K_m and a slightly higher Vmax compared to wild type. W101A created such large increases in transport K_m compared to their binding abilities that the transport was not even saturatable, and the Km and Vmax values could not be accurately determined even though I used ^{59}FeEnt concentrations as high as 500 nM (2,000-fold that of the wild-type K_m). This finding indicated that W101 plays a more important role in the internalization than the binding process. Y217A, Y553A, and Y638A also increased K_m but at lower magnitudes (K_m values 5- to 10-fold more than the K_d). Y638A had reduced binding capacity (5%), but its V_{max} was comparable to that of wild type (93 pmol/10^9 cells/min). Class III only has one mutant, that is, Y495A. Y495 was different because it has normal affinity for FeEnt (normal K_d or K_m), but a loss of transport velocity (fivefold drop in V_{max}) that resulted from a low turnover number (k_8 = 0.4/min).

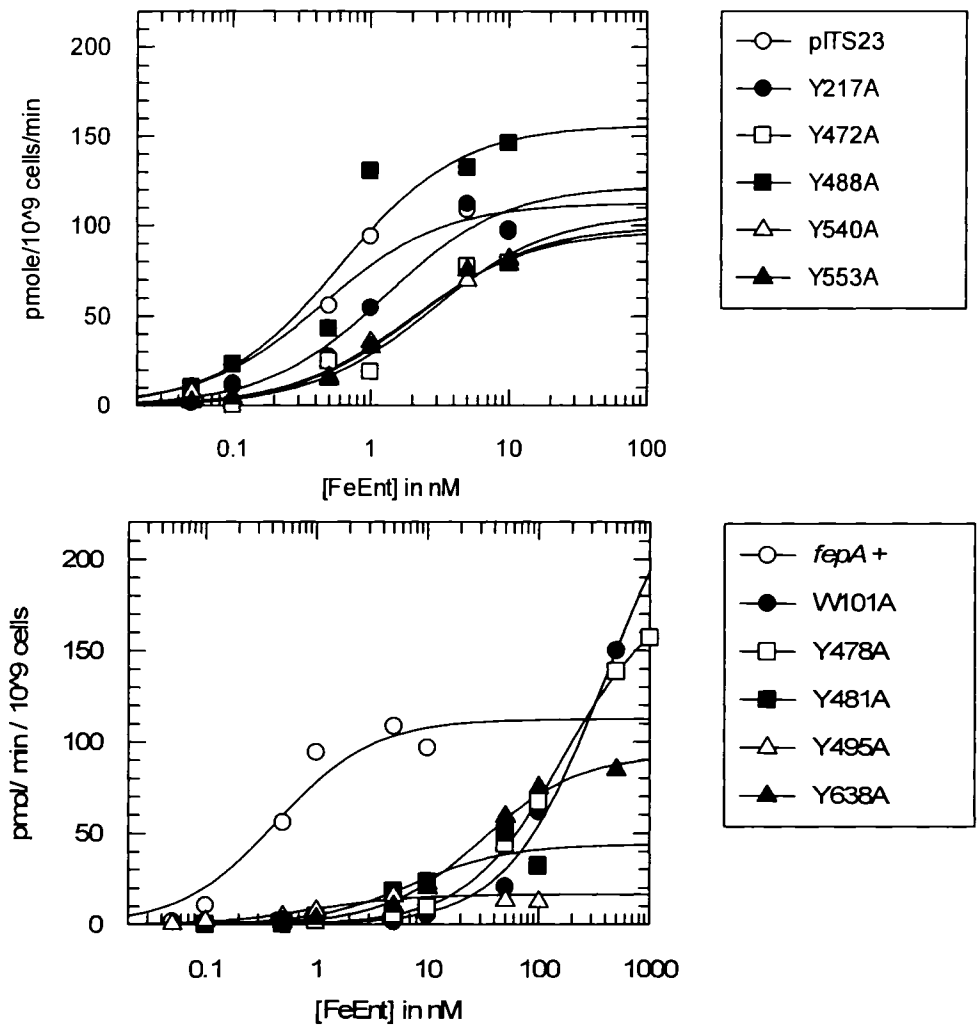

Fig. 3.6 ^{59}FeEnt transport by Ala substitution mutants. We determined the concentration dependence of ^{59}FeEnt binding by *E. coli* strain KDF541 expressing FepA substitution mutant proteins carried on the low-copy plasmid pHSG575 at six concentrations near K_M, with each point collected in triplicate and averaged. The transport data were analyzed, and curves were plotted by using the enzyme kinetics equation of Grafit 5.09. The concentration of ^{59}FeEnt is logarithmically plotted to demonstrate the decreases in affinity that some of the mutations caused. (Top) Mutants with near wild type transport properties. *fepA*$^+$, open circles; *Y217A*, closed circles; and *Y472A*, open squares; *Y488A*, close squares; *Y540A*, open triangles; *Y553A*, closed triangles. (Bottom) Mutants with impaired binding properties. *fepA*$^+$, open circles; *W101A* closed circles; *Y478A*, open squares; *Y481A*, closed squares; *Y495A*, open triangles; *Y638A*, closed triangles.

3.8 N-domain Loop Deletions

Experiments with the N-loop deletion mutations (Fig. 3.7) showed the importance of the N-domain in FeEnt uptake. The Δ60-67 and Δ98-105 deletions impaired binding (18- and 28-fold increases in K_d, respectively), but they decreased the affinity of FeEnt uptake much more (500- and 700-fold increases in K_m, respectively) (Table 3.1 and Fig. 3.6). It is very obvious that these two mutants dropped majority of their uptake abilities without even impairing much of the binding properties, which could be observed with Y481A and Y638A (10 to 20 fold increase of K_d). Similar phenomenon was also observed with W101A. The different level of effects between binding and transport of the N-domain loop deletion suggested that they are more predominantly involved in internalization than binding.

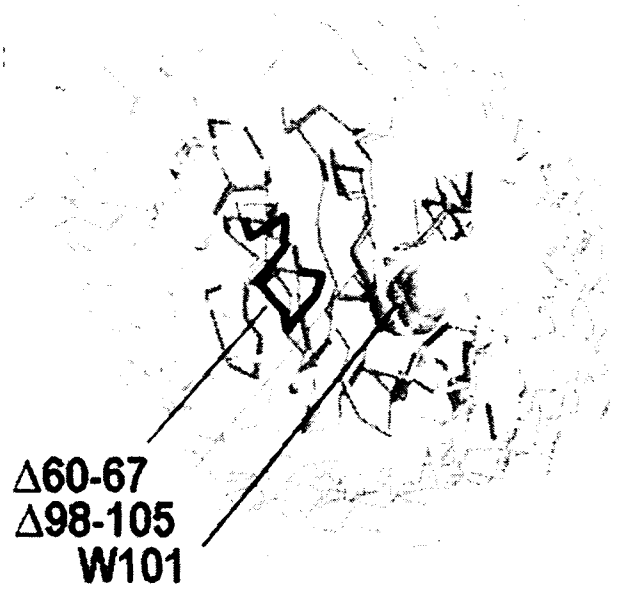

Fig. 3.7 A backbone model of FepA (Annamalai, *et al.*, 2004), viewed from the top, shows the location of two site-directed deletions, Δ60-67 (red; in NL1) and Δ98-105 (orange; in NL2); NL2 contains residue W101 (yellow, in space-filling format).

3.9 X-linking

I used Sulfo-EGS (Scott *et al.*, 2002) as the X-linker for FepA proteins. Without FeEnt, KDF541/pITS23 had two X-linking products, band 1 and band 2 (Fig. 3.8, top, red and green arrow, respectively). Band 2 is FepA X-linked to OmpF/C and OmpA. Band 1 is internal X-linked FepA (Scott *et al.*, 2002) between K332 and K483. In the presence of FeEnt, both band 1 and band 2 disappeared (Fig. 3.8, top, pITS23, lane c). Four mutants were chosen for X-linking. The same pattern as that of the wild type happened with W101A and Y495A. But in the presence of FeEnt, Y481A andY638A still had a small amount of band 2 (Fig. 3.8, top, yellow arrows).

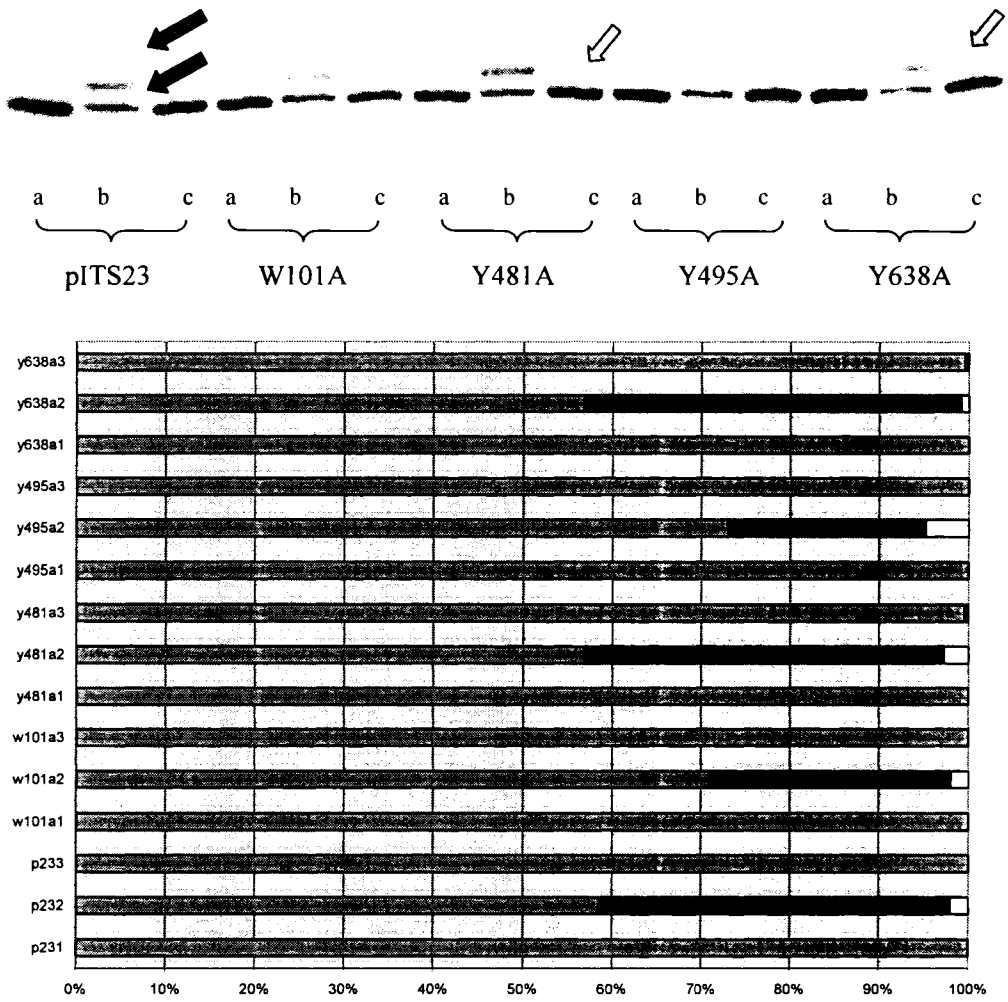

Fig. 3.8 Cross-linking of bacteria with SulfoEGS. Top, live cells of KDF541 harboring pITS23, W101A, Y481A, Y495A, and Y638A from left to right. Each strain has three lanes: Lane a, cells without X-linker; Lane b, cells with X-linker; Lane c, cells with X-linker and 5uM FeEnt. Cell lysates were transferred to nitrocellulose and analyzed by immunoblot with anti-FepA MAb 45, developed with ^{125}I-protein A. In lane b, three bands are designated from bottom to top to band 0, band 1, and band 2, respectively. Bottom, quantization of top immunoblot. Blue represents band 0, which is the cells treated without X-linker, as 100% for KDF541/pITS23; Purple represents band 1, which is the cells treated with X-linker; Yellow represents band 2, which is the cells treated with X-linker and FeEnt.

Table 3.1 Effects of mutagenesis on FeEnt uptake.

Group and alleles[a]	Loop	Ferric enterobactin									
		Binding[b]		Transport[c]				Colicin[e]		Flow cytometry[f]	
		K_d (nM)	Cap.	K_m (nM)	V_{max}	Nutr.	k_8[d]	B	D	MAb24	MAb45
fepA											
fepA	NA							R	R	0.14(97)	0.15 (99)
fepA$^+$	NA	0.27	67	0.4	113	18.5	1.7	100	100	4.2 (82)	45.2 (84)
fepA^{+g}	NA	0.41	150	0.24	123	18	0.8	100	100	4.1 (80)	11.7 (90)
Class I											
Y272A[g,h]	3	0.1	103	0.3	150	19	1.5	50	100	ND	ND
Y472A	7	1.5	68	2.6	105	19.5	1.5	10	100	8.34(89)	42.4 (84)
Y481A	7	4.8	47	7.2	44	21	0.9	10	25	11.3(84)	42.6 (78)
Y488A	7	0.5	38	0.6	156	19.5	4.1	25	50	3.5 (82)	38.5 (86)
Y540A	8	1.4	56	2	98	23	1.8	10	10	10.1(90)	45.9 (78)
Class II											
Δ60-67[g]	NL1	7.3	119	119	99	25	0.8	10	10	6.2 (91)	11.5 (93)
Δ98-105[g]	NL2	11.7	107	163	88	25	0.8	10	10	6.57(91)	12.6 (88)
W101A	NL1	0.85	12	393[i]	269[i]	20.5	ND	2.5	5	8.8 (92)	54.6 (86)
Y217A	2	0.2	58	1.3	122	18.5	2.1	20	50	3.5 (81)	44.1 (89)
F329A[g,h]	4	0.2	100	5.5	135	19	1.4	50	100	ND	ND
Y478A	7	0.76	49	167	184	21	3.8	10	10	14.2(90)	34.8 (88)
Y553A	8	0.4	46	2.1	100	20.5	2.2	2.5	5	7.2 (84)	47.3 (84)
Y638A	10	2.9	3	31	93	22	31	40	25	4.1 (79)	38.5 (86)
Y272AF329A[g,h]	3/4	7.8	76	23	128	23	1.7	50	100	ND	ND
Class III											
Y495A	7	0.79	44	0.9	17	21.5	0.4	20	10	8.8 (87)	39.1 (77)

[a] Class I, comparable increases in binding K_d and transport K_m; class II, disproportionate increase in transport K_m; class III, reduction in transport rate.

[b] K_d and capacity (Cap.: pmol bound/10^9 cells) were determined from the concentration dependence of FeEnt binding by analyzing the mean values from independent experiments with GRAFIT 5.09 by using the bound versus total equation. The average percent errors of the K_d and capacity determinations were 32 and 7%, respectively.

[c] K_m and V_{max} (pmol/10^9 cells/min) of uptake were determined from the concentration dependence of FeEnt transport by using GRAFIT 5.09 by using the enzyme kinetics equation. Nutrition (Nutr.) test results show the diameters of the growth halos in millimeters. The average percent errors of the K_m and V_{max} determinations were 34 and 10%, respectively.

[d] The kinetic constant k_8 is an expression of turnover number, relating the FeEnt transport rate to the amount bound: $k_8 = V_{max}$/capacity. It is equivalent to k_3 molecules/FepA protein/min.

[e] Colicin killing was determined by measuring the susceptibility of KDF541 harboring pHSG575 or pUC18 derivatives expressing the mutant FepA proteins to limiting dilutions of colicins B and D. Results are expressed as a percentage of the killing observed for KDF541/pITS23 (wild type FepA). R, complete resistance.

[f] We cytofluorimetrically monitored the localization of FepA in the OM and its normal overall folding with anti-FepA MAbs 45 and 24, which recognize cell surface determinants in L4 and L5, respectively. The tabulated value is the mean fluorescence intensity of 10^4 bacteria stained with the antibodies and fluoresceinated goat-anti-mouse immunoglobulin G. The parenthetic value is the percentage of the population within one standard deviation of the mean.

[g] The structural gene was carried on the pUC derivative pITS449.

[h] The mutant was previously described, and the data are reproduced here from Cao *et al.*

[i] We did not observe saturable transport of FeEnt through FepAW101A; K_m and V_{max} values were estimated. Without determination of saturation velocity, it was not possible to calculate k_8 NA, not applicable; ND, no data.

3.10 Competition between FeEnt and other Siderophores

In this part, I did direct [^{59}Fe]-siderophore binding experiments to characterize the binding properties of several other radioactive ferric siderophores by FepA. I also determined the ability of the nonradioactive ferric siderophores to inhibit ^{59}FeEnt adsorption using the competition experiments. Results showed the FepA prefer FeEnt, which is the native *E. coli* siderophore. Direct binding experiments showed that the K_d of ^{59}FeTrn (a synthetic analog of FeEnt) adsorption was 17 nM, ~50-fold higher than that of ^{59}FeEnt, 0.36 nM (Fig. 3.9). ^{59}FeCrn, another catecholate compound that is the native siderohpore of Gram-positive bacteria Corynebacterium, did not adsorb to FepA at concentrations as high as 1 μM (Fig. 3.9). Siderophore nutrition tests (Wayne *et al.*, 1976) and uptake reactions with [^{59}Fe] complexes (Fig. 3.9) reiterated the preference of FepA for FeEnt (K_m = 0.25 nM) over FeTrn (K_m = 4.5 nM) and the inability of FeCrn to supply iron to *E. coli*.

In competition reactions with FeTrn, FeCrn, ferric agrobactin, and ferrichrome, aside from the identity reaction with FeEnt, only FeTrn and FeCrn, whose structures are most similar to that of FeEnt, slightly inhibited the adsorption of ^{59}FeEnt. On the other hand, ferrichrome, a hydroxamate siderophore secreted by fungus, did not block the binding of ^{59}FeEnt, even at concentrations as high as 50 μM (Fig. 3.9). Ferric agrobactin, a dicatecholate siderophore, failed to inhibit FeEnt adsorption as well. The identity competition showed that nonradioactive FeEnt inhibited 50% of ^{59}FeEnt adsorption (IC_{50}) at 0.67 *n*M, whereas the IC_{50} of FeTrn was 120 nM, which is about 180-fold higher. Although FeCrn competed with 59FeEnt a little bit, its IC_{50} was only estimated to be 1 μM (Fig. 3.9), because FeCrn was not able to completely inhibit the adsorption of

^{59}FeEnt. This indicated that the affinity of FepA towards FeCrn was about 4000-fold lower than FeEnt.

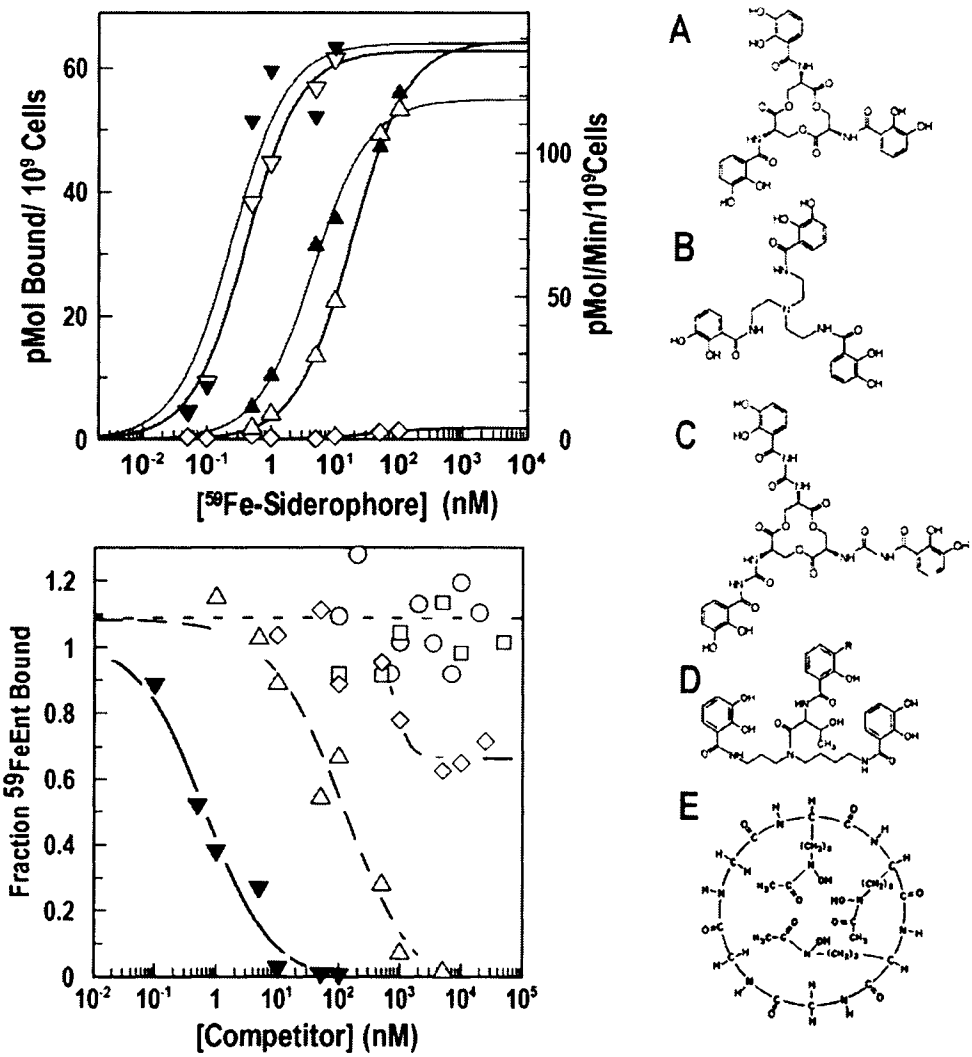

Fig. 3.9 (Top) Binding and transport. I compared the binding (open symbols) and transport (solid symbols) of ^{59}FeEnt (inverted triangles), ^{59}FeTrn (triangles), and FeCrn (diamonds) by *E. coli* strain KDF541/pITS23. (Bottom) Competition of ^{59}FeEnt binding to FepA by catecholate siderophores. We determined the abilities of ferrichrome (□), ferric agrobactin (O), FeTrn (△), FeCrn (◊), and FeEnt (▼) to inhibit the binding of ^{59}FeEnt to *E. coli* strain KDF541/pITS23 (*fepA*$^-$). The data were analyzed and plotted by the IC50-4 Parameter Logistic of Grafit 5.09. The right panel shows the structures of Ent (A), Trn (B), Crn (C), agrobactin A (D), and apoferrichrome (E).

3.11 Discussion

FepA has eleven surface loops (Fig. 3.10). Among them, loops 1 and 6 are very small. As we can see in Fig. 3.10, all the loops form a vestibule mouth where FeEnt comes in and binds. Especially, loops 7 and 9 (purple) and loops 2, 10 and 11 (blue), are pointing towards the center of the vestibule mouth. Individual loop deletions (Newton *et al.*, 1999) for other loops beside loops 1 and 6 were constructed on pITS449 and transformed into KDF541. All the loop deletions significantly decreased the affinity of FepA for FeEnt because of the much higher binding K_d and transport K_m observed in the assays. A more interesting finding was that loop 7 and loop 8 deletion mutants had no ability to bind or transport FeEnt even when cytofluorimetry showed that both mutants displayed similar surface topology to that of wild-type FepA, which indicated that the mutant proteins were expressed and folded properly. Although the crystal structure of FepA with the ligand is not available yet, aromatic residues on the extremities of the external loops could be the main residues that are involved in the initial binding of FeEnt, due to the above facts and the aromaticity of FeEnt. FeEnt carries a charge of -3. As a result, positively charged residues, Lys, Arg, and His, probably also participate in the initial binding. I chose aromatic residues to study.

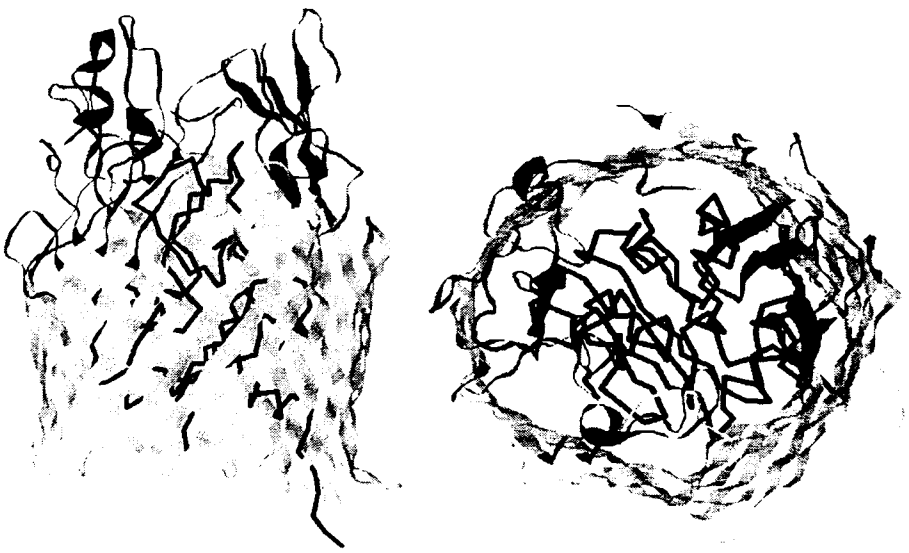

Fig. 3.10 Crystal structure of FepA. Left, side view. Right, top view. Loops 1 and 6 are red; Loops 2, 10, and 11 are blue; Loops 3, 4, 5, and 9 are green; Loops 7 and 8 are purple.

During ligand binding, FepA undergoes two stages of motion that imply the existence of B1 and B2 (Fig. 3.1) (Cao *et al.*, 2000). Appropriate contact with FeEnt (or colicins) presumably initiates conformational changes, driven by multiple noncovalent bonds that close the loops around the ligand, maximizing its retention on the cell surface (Klebba, 2003). As mentioned above, loop 7 deletion mutant does not bind and transport FeEnt. Among the aromatic candidates for single amino acid mutations, five residues are on loop 7, including Y472, Y478, Y481, Y488, and Y495. All the five residues are in the proposed B1 site. It is not surprising to see Y472A and Y481A has increased binding K_d. This decreased binding affinity also leads to the decrease of transport Km for these two mutants, even though the decreased affinity is not significant and the binding capacity and transport Vmax remain the same. Y488A did not show any phenotype, indicating it is not crucial in either binding or transport processes. This is actually surprising to me. Y488 is on the very top of L8, at an even higher position than Y481 and Y495. Also, Y488 is not visible in the crystal structure of FepA, probably because this very top region of L7 is very flexible. I could imagine such a residue as Y488 would look for ligands in the extracellular environment making use of its flexibility. However, data of Y488A do not support my view.

It is very interesting to compare Y478A and W101A. Y478 is on L7, and W101 is on the top of one of the N-domain loops. Both of them sit at the same level in the membrane. They are very close to each other (about 8 angstroms). Their benzene rings also face each other. Both of them have slightly decreased binding affinity (2-3 folds), although W101A has more decreased binding capacity (20% of wild type), and Y478A has more than 70% of capacity compared to wild type. However, they both show severely

impaired transport ability, although W101A is not even saturatable. These results suggest both of these two residues are more involved in the internalization of FeEnt than the binding process. Also W101 plays more important role than Y478A during the transition of FeEnt from B1 and B2 sites to the internalization process, because of the low binding capacity of W101A.

Y495A (class III) is particular interesting. It has almost wild-type binding properties (2-fold increase of K_d, close to wild type capacity), just like Y478A. However, completely different from Y478A that was not yet saturated in 1 μM range, Y495A has near wild-type transport Km (3-fold increase), and the maximum uptake rate is only 15% of the Vmax of the wild type. This is unlike any of the other mutants. Although Y495 is at even high position than Y478 in the crystal structure, the mutation to alanine does not impair binding, which is also very surprising. In addition, the Km is not impaired severely either. These suggest that Y495 is probably significantly involved in the transfer of B2-FeEnt complex to the transport competent state of the same complex (Fig. 3.11).

Another interesting fact to look at is how W101A has different impact on the FeEnt uptake of FepA compared to ΔN 98-105. FepA ΔN 98-105 has a normal capacity and a 40-fold decreased K_d in the binding process. It also has a normal Vmax and a 400-fold decreased Km. Because W101 is one of the eight residues that are deleted in FepA ΔN 98-105 mutant, I expected W101A to display similar effect on FeEnt binding and uptake. However, the data do not agree with it. Instead, W101A shows a normal Kd and an almost 6-fold decreased capacity. I am not able to acquire accurate Km and Vmax due to the insaturatability of iron. Why does FepA ΔN 98-105 have such a high K_d but a normal capacity? One possible explanation is that W101 is one of the residues that sits in

B2 site and participate in the binding process. So when W101 is mutated to alanine, the binding affinity will slightly decrease, concurrent with the increasing K_{off} and decreasing capacity. Km and Vmax of the uptake process then increases, and uptake becomes not saturatable, probably because the binding is compromised, and W101 plays a more important role in the following internalization process than the binding process, although this internalization process is still a mystery. When residue 98 to 105 is deleted, as expected, the binding affinity decreases more, probably because more residues from 98 to 105 besides W101 are involved in binding. However, because 8 residues are deleted, at least part of the B2 site is open. So it is possible that FeEnt will be released into the small pocket created by the deletion of the 8 residues, instead of being released to the B1 site, and then to the extracellular environment in probably an equilibrium process. Of course, when this process is not controlled by the residues that normally take part in the process, the internalization will become slower and have a very high K_m. And because of the pocket created, probably FeEnt will be available for the internalization, which accounts for the normal V_{max} of uptake.

Siderophore receptors exhibit different degrees of specificity in the reception of iron siderophore complexes. For example, FhuA displays a wild specificity towards several kinds of ferric hydroxamates, including ferrichrome, ferricrocin, ferrichrysin, ferrirubin, ferrirhodin, and albomycin (Luckey *et al.*, 1972), although it does not transport ferric catecholates. However, my results showed that FepA had a narrow specificity. FepA did not recognize hydroxamate compounds such as ferrichrome and dicatecholate compounds such as ferric agrobactin. FepA recognizes but differently the three catecholate compounds I tested: FeEnt, FeTrn, and FeCrn. Although the mechanism of

the specificity displayed by FepA is not yet clear, the binding and competition experiments suggest some possibilities. One possibility is that FepA initially adsorbs (hydrophobic) iron complexes by nonspecific interactions with the hydrophobic loop residues and then rejects inappropriate metal chelates as the binding equilibrium progresses further. However, the complete inability of ferrichrome and ferric agrobactin to inhibit ^{59}FeEnt adsorption contradicts to this possibility. FeEnt is a tricatecholate siderophore, readily extracted with ethyl acetate, aromatic and negatively charged. Fc is a nonpolar molecule that could have many types of interactions with FhuA protein. So the fact that FepA does not recognize Fc suggests that the initial interaction is not nonspecific and not related to nonpolar interactions; it is related to aromaticity, the charges, or other interaction, such as hydrogen bonds. However, the result that FepA does not recognize a dicatecholate compound, agrobactin, makes the specificity more complicated. ^{59}FeEnt binding is only impaired by ferric catecholate complexes that are structurally similar to FeEnt, Ent itself, Trn, and Crn. This indicates that the specificity may come from the structural differences of these three catecholate compounds. Ent, Trn, and Crn form tricatecholate, hexadentate, octahedral complexes with iron (III), respectively, but they differ in size and in the organic platforms from which their ligands arise. Unlike FeEnt, which has a trilactone backbone, the synthetic compound FeTrn contains three alkyl chains linked to a central amine that connect by amide bonds to its dihydroxybenzoic acid groups. The backbone of FeTrn (604 Da) is smaller than that of FeEnt, and with a pK_a of 5 its central amine is essentially nearly unprotonated at neutrality (Hay *et al.*, 2001). The 50-fold reduction in the affinity of FeTrn binding, and 20-fold reduction in the affinity of its transport indicate that the face of its iron center, which is identical to that of FeEnt, is

not the only determinant of its recognition by FepA. The structural alterations behind the iron center impair its binding, relative to that of FeEnt. The six oxygens of the natural siderophore's lactone ring provide many potential H-bond acceptors that are absent in FeTrn, suggesting a reason for its lower affinity. These data concur with the model in which the receptor's loops enwrap the ferric siderophore at binding equilibrium and thereby interact with the backbone.

FeCrn, the native siderophore of the Gram-positive bacterium *Bacillus subtilis*, is not recognized by FepA, although their structures are so close that the only difference seems to be glycine spacer groups between the cyclic ester backbone formed by serine for Ent and threonine for Crn, and the 6 hydroxyl chelating groups. The molecular mass of Crn is about 30% larger relative to FeEnt (933 Da versus 719 Da). Besides its greater mass, the metal center of FeCrn has opposite chirality (Λ) to that of FeEnt (Δ) and FeTrn (Δ) (Raymond *et al.*, 2003). However, although FepA recognizes the iron center of ferric siderophores (Ecker *et al.*, 1986; Heidinger *et al.*, 1983), chirality does not govern the receptor-ligand interaction: (Λ) ferric enantio-Ent with comparable affinity as FeEnt (Thulasiraman *et al.*, 1998). Thus, the rejection of ^{59}FeCrn was surprising and implied that its increased dimensions preclude productive adsorption to the receptor. The partial inhibition of ^{59}FeEnt binding by FeCrn and the nonretention of ^{59}FeCrn by cells expressing FepA suggest that the Gram-positive siderophore begins to bind but does not reach a stable equilibrium, supporting the idea that its larger size prevents loop closure and hence its passage from B1 to B2.

The aromatic mutations further showed that replacement of aromatic residues by alanine did impair the binding affinity. The special arrangement of the catecholate

groups of FeEnt seemed to be essential for the specific interactions between FepA and FeEnt. Also 5 of the aromatic residues which I mutated were on loop 7, indicating L7 may be essential for initial binding. This is also consistent with the finding with the L7 deletion mutant (Newton *et al.,* 1999). When loop 7 was deleted, the mutant protein was not able to bind or transport FeEnt any more. Unfortunately, the mutations of other aromatic residues (Y540 and Y553 in L8, Y217 in L2) did not reiterate this point, indicating that interactions of FeEnt with FepA involve multiple determinants. As discussed earlier, because of the negative 3 charge of FeEnt, ionic interactions with the acidic ferric siderophore may be another component that determines the binding specificity. Some evidence was present with K483 (Scott *et al.,* 2002) and R316 (Newton *et al.,* 1997). Looking at the crystal structure of FepA, the N-domain has two loops. W101 is on one loop, and it has been shown to be important for binding and more critical for internalization of FeEnt. There is also a positively charged residue, R66, on the other loop that sits in the deep center of the vestibule mouth together with W101. Mutation of this residue could provide more detail about the direction that FeEnt enters, besides merely that FeEnt enters the top of the vestibule mouth with the iron center facing the barrel. Likewise, Y495A created the class III phenotype: normal affinity for FeEnt, but a much reduced transport rate. In this case again, a surface loop mutation changed the efficiency of ligand uptake.

The mechanism of how FepA binds and internalizes FeEnt through the β-barrel and into the periplasm before it is bound by FepB protein is not yet clear. But considering all the information available so far, we proposed a possibility for the mechanism (Fig. 3.11). Briefly, surface loops contain the initial binding site for FeEnt. Before binding,

they are in an open state (Scott *et al.*, 2002). Upon binding, loops close and FeEnt is bound at the B1 site, where all the aromatic residues are involved. This initial binding process is reversible. Then FeEnt is transferred from the B1 site to the B2 site by unknown mechanism, where other aromatic residues and perhaps also positively charged residues are involved in the intermediate equilibrium between the FepA B2-FeEnt complex and the transport-competent state of this complex. This is also why W101 is so important to this state, and the replacement of W101 by alanine severely impairs this process. Then FeEnt will be internalized through the barrel and into the periplasm with an unknown mechanism before it is bound by the periplasmic binding protein FepB. TonB and energy are required upon the binding of FeEnt and the closure of loops with unknown mechanism. In this scheme, the movement of the N-domain still seems to be the critical part which I will discuss in the next chapter.

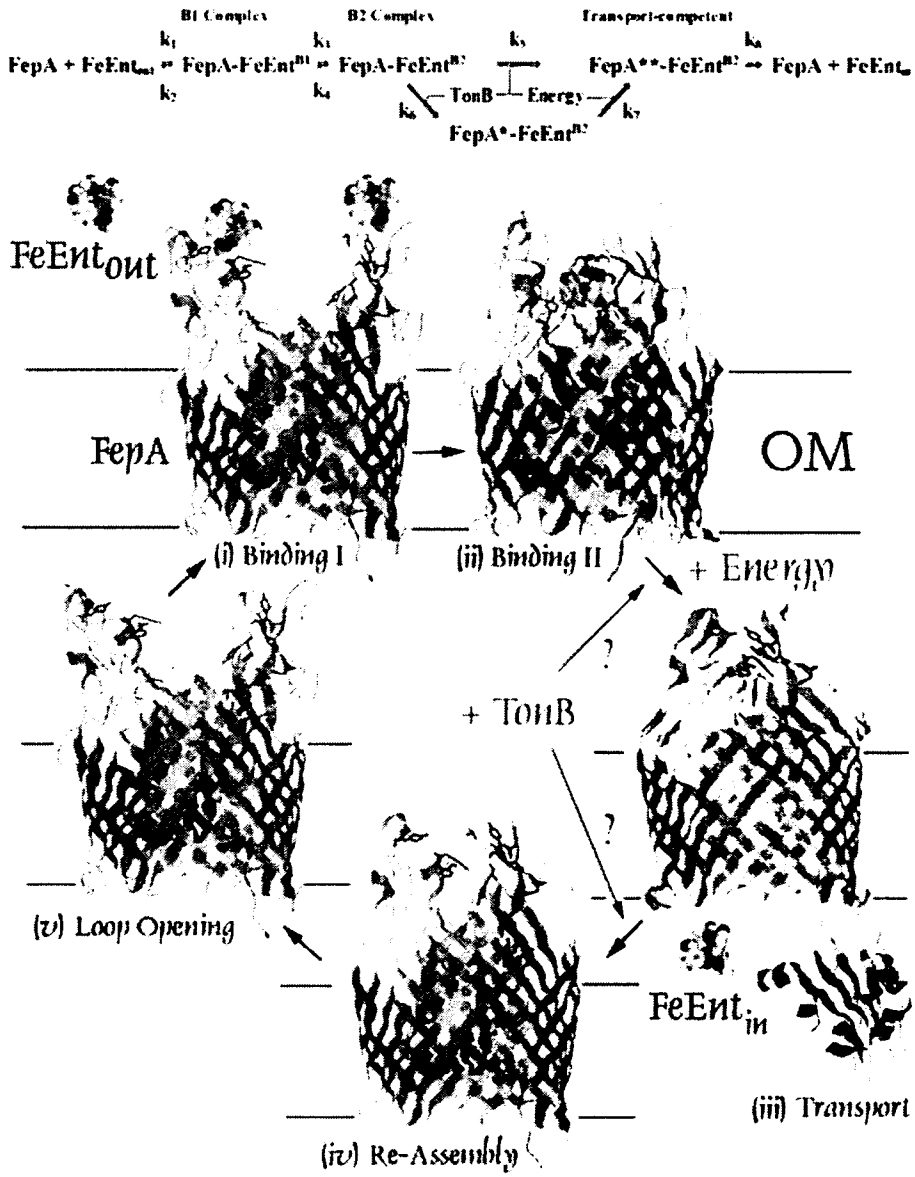

Fig. 3.11 Model of FeEnt transport through FepA (Annamalai *et al.*, 2004). (Top) Formal representation of the FepA transport process. Constants *k*1 to *k*4 are experimentally defined: fluors attached to L3 reflect both the first and second binding stages (*k*1 0.02/s and *k*3 0.005/s) (Payne *et al.*, 1997), which are both reversible (*k*2 0.03/s and *k*4 0.003/s (the present study)). (Bottom) The FepA transport cycle is depicted as a series of conformational stages (Cao *et al.*, 2003; Klebba, 2003; Scott *et al.*, 2001) that

result in binding and internalization of FeEnt. The representations of FepA originated from its crystal structure, but they are postulated forms that were not crystallographically demonstrated. By analogy to FhuA and FecA, FeEnt binding may relocate the TonB-box region of FepA away from the • •barrel wall. Such movement may signal receptor occupancy to TonB (Braun, 1999; 1989; 1997; 1980; 1996; 1991; 1994; Cadieux *et al.*, 2000; Cafiso *et al.*, 1983; 1982, Chimento *et al.*, 2003; Ferguson *et al.*, 2002a; 2002b; 1998; Locher *et al.*, 1998; Postle, 1993a; 1993b), but another view is that TonB-box movement away from the barrel wall frees the N-domain to dislodge from the channel. Next, the ligand passes through the C-domain channel (Transport). Theory and experiment suggest, but so far do not explicitly prove, that the input of energy is required at this stage. Similarly, TonB may or may not function during this phase of the transport reaction. A variety of findings raise the possibility that the N domain exits the pore during ligand uptake (Klebba, 2003), but this idea is not fully substantiated: structural changes that facilitate ligand transport may take place in the N domain while it is resident in the channel. After transport the receptor reassembles, either by reinsertion of the N domain into the • •barrel, or by structural changes in situ within the pore, another potential phase for the input of energy and/or TonB. Lastly, the loops reopen to a state of maximum receptivity toward ligands.

Chapter 4 Accessibility of the N domain from the Periplasmic Side

4.1 Experimental Strategies

FepA, the ferric enterobactin receptor, contains a transmembrane channel formed by amphiphilic β-strands that project to the cell surface as large loops (Buchanan *et al.*, 1999; Locher *et al.*, 1998; Furguson *et al.*, 1998). It also contains a globular N-terminus that resides within the transmembrane channel. When ligands are bound by the receptors, it triggers unknown processes that induce their internalization into the cells (Liu *et al.*, 1994; Moeck *et al.*, 1996; Letellier *et al.*, 1997). Since the N domain completely occupies the channel and leaves no discernible pore through which FeEnt might pass, structural changes must occur during transport. One possibility is that the N domain undergoes conformational changes upon the binding of the ligands, so that a pore with minimum diameter of 15Å is created inside of the channel to allow the ligands pass through. Another possibility is that the whole N domain exits the β-barrel and leaves a completely vacant channel. To study the conformation and function of the N-domain during transport, I tried a few different types of experiments to detect the motion of the N domain during the transport process.

4.2 Disulfide Bond Mutant Construction

Wild-type FepA protein has two native cysteine residues (C487 and C494). Although C487 is invisible in the crystal structure of FepA, their relative distance between these two cysteines is very short and they form a disulfide bond. However, these two cysteine residues are on the extremity of the surface loop, and not expected to affect the movement of the N domain directly. So it can be a valid strategy to study FepA by

constructing new disulfide bonds inside of the barrel. Considering the distance (usually no more than 4 angstroms) and direction (a pair of residues should face each other in sticks mode of Rasmol Molecular Graphics^{R}) of the candidates in the crystal structure of FepA (Buchanan *et al.,* 1999), five double mutations are constructed individually in FepA, including I14CG300C, A42N162C, G149T180C, T51N608C, and G54T585C. In each pair of residues, one residue is in the N-domain, and the other residue is on the β-barrel of the C-domain. The two residues in the five pairs are 4.4Å, 4Å, 4.5Å, 3.2Å, and 2.7Å away from each other, respectively. Mutants are transformed into *E. coli* strain KDF541 (*fepA*-) for further experiments. Because the N-domain resides in the β-barrel, it completely blocks the way that siderophores come in. In order to make a pathway for siderophores, the N-domain has to either exit the β-barrel and enter the periplasm, or undergo certain conformational changes to produce a space that is big enough for siderophores to pass through. So when a disulfide bond exists between the globular N-domain and the β-barrel of the C domain, during the uptake, the N-domain may be locked inside of the barrel, or undergo abnormal conformational change. Five double mutants (Fig. 4.2.1) were constructed in a low copy number plasmid pITS23 and confirmed by sequencing.

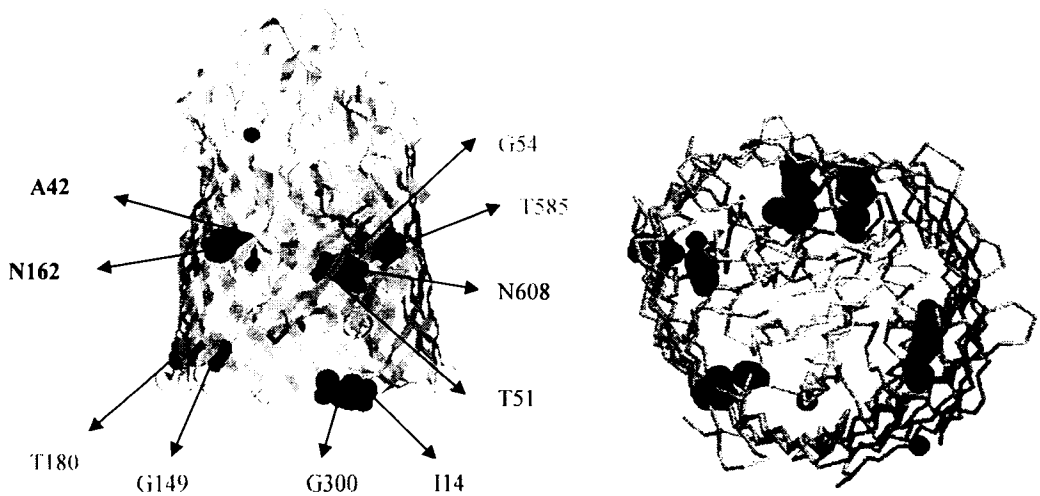

Fig. 4.2.1 Construction of five disulfide bonds mutants within FepA. The two residues in the same color are expected to form a disulfide bond *in vivo*. Left: side view. Right: periplasmic view.

Results

Colicin killing assay. Sensitivity to colicin killing is usually an indicator of the proper assembly and functionality of the mutant proteins (Table 4.2.1). However, it is not the same case concerning disulfide bond mutations, because the mutations may impair the substrate internalization process. Even when the global structure of the mutants remains the same, it is still possible that mutants are not sensitive to colicins. Results showed that sensitivity of FepA I14G300C to both colicin B and D decrease 200-fold relative to the wild-type FepA. Sensitivity of FepA T51N608C and G54T585C to both colicin B and D decrease 5-fold relative to the wild-type FepA. However, both A42N162C and G149T180C displayed near wild-type sensitivity to both colicins. These results suggest that two mutants, A42N162C and G149T180C, either do not form a disulfide bond *in vivo* as desired, or the disulfide bond formed do not affect the colicin recognition and internalization processes. However, for the other three mutants, I cannot conclude if the native conformation of the mutated FepA protein is changed or not without further investigation.

Table 4.2.1 Colicin B and D killing of disulfide bond mutants.

Strain	ColB	ColD
KDF541	-	-
KDF541/pITS23	100	100
I14G300C	0.5	0.5
A42N162C	100	100
G149T180C	100	100
T51N608C	20	20
G54T585C	20	20

Results are expressed as a percentage of the killing observed for KDF541/pITS23 (wild-type FepA).

Disulfide bond formation detected by immunoblot. I monitored the expression and the formation of the disulfide bonds by 10% acrylamide slabs with 0.07% bisacrylamide stacking gel (Murphy *et al.*, 1990; Grossman *et al.*, 1983; Hancock *et al.*, 1976) without BME in the sample buffer to disrupt the disulfide bond, followed by anti-FepA immunoblots (Murphy *et al.*, 1990), developed with ^{125}I-protein A (Kronvall *et al.*, 1970; Cao *et al.*, 2000). After overnight exposure to an imaging screen, radioactivity was quantitated on a STORMSCAN PhosphorImager (Molecular Dynamics). All the mutants were growing in nutrient broth without or with reducing reagents.

Without reducing reagents, about 90% FepA I14G300C protein forms disulfide *in vivo* (Fig 4.2.2) and the size of mutant proteins appears smaller than that of the wild type FepA on the blot. When 5mM BME is added during the growth of the cells, majority of the disulfide bonds are reduced. Dithiothreitol (DTT) is a more powerful reducing reagent than BME since 5 mM or 10 mM DTT is able to reduce almost 100% of the disulfide bonds (Fig. 4.2.3). Because disulfide bonds are formed in most of the FepA I14G300C proteins, oxidized DTT does not show that more disulfide bonds are formed when it is added. For FepA I14CG300C, a special 0.07% bis-acrylamide stacking SDS-PAGE is used because it gives better band separation than regular SDS-PAGE. FepA A42N162C and G149T180C show a size exactly like wild type FepA in western blot (Fig. 4.2.5). The other two mutants, T51N608C and G54T585C show a different pattern in immunoblot (Fig. 4.2.4). Their mutant proteins appear larger than wild-type FepA. Disulfide bonds are formed in about 50% of the protein. 20 mM and 5 mM of BME are high enough to reduce most of the disulfide bonds of T51N608C and G54T585C, respectively. Also, regular 10% SDS-PAGE gives better band separation for these two

mutants. An immunoblot is also done for wild type and all mutants together with or without 5 mM BME (Fig. 4.2.5).

So among the five disulfide bond mutants (Fig. 4.2.5) constructed, I14G300C seems to be most useful for further study.



1 2 3 4 5 6 7 8

Fig. 4.2.2 0.07% bis-acrylamide SDS-PAGE followed by ^{125}I Immunoblot of KDF541/pITS23 and KDF541/pITS23/I14CG300C. Lane 1 to 4 is KDF541/pITS23 without reagent, with 5 mM BME, 10 mM DTT, and 10 mM oxidized DTT, respectively. Lane 5 to 8 is KDF541/pITS23/I14CG300C cell lysates, same order as KDF541/pITS23.



1 2 3 4 5 6 7 8 9 10 11 12

Fig. 4.2.3 Determination of concentration of DTT which is high enough to reduce all the disulfide bonds formed in cells with I14G300C FepA. Lane 1 to 6 is wild type with 0, 0.1, 0.5, 1, 5, and 10mM DTT, respectively. Lane 7 to 12 is I14G300C with same concentrations of DTT.

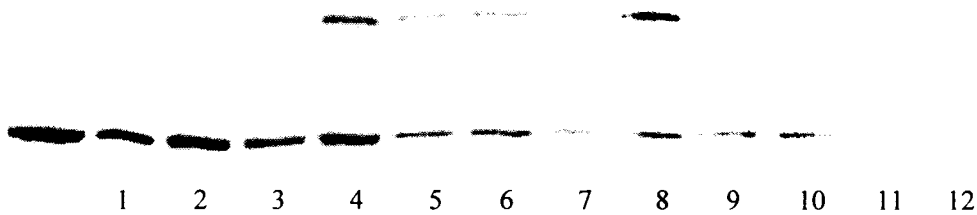

Fig. 4.2.4 Determination of concentration of BME which is high enough to reduce all the disulfide bonds formed in cells with T51N608C and G54T585C FepA. Lane 1 to 4 is KDF541/pITS23 without BME, with 5 mM BME, 10 mM BME, and 20 mM BME, respectively. Lane 5 to 8 is KDF541/pITS23/T51N608C with same order. Lane 9 to 12 is KDF541/pITS23/G54CT585C with same order.

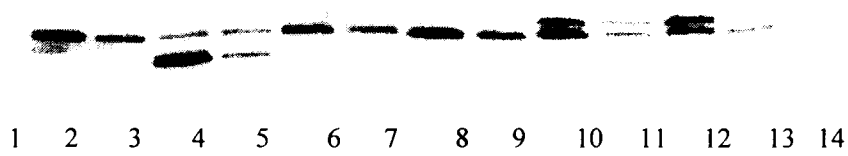

Fig. 4.2.5 Immunoblot of cell lysates including KDF541, wild type and all the disulfide bond mutants in KDF541 growing with (odd numbered lanes) or without 5mM BME (even numbered lanes). Lane 1 and 2 is KDF541; lane 3 and 4 is KDF541/pITS23; lane 5 and 6 is KDF541/pITS23/I14CG300C; lane 7 and 8 is pITS23/A42CN162C; lane 9 and 10 is pITS/G149CT180C; lane 11 and 12 is pITS/T51CN608C; lane 13 and 14 is pITS23/G54CT585C.

Qualitative assays of FeEnt uptake. Siderophore nutrition tests are employed to measure the overall FeEnt uptake capabilities of the mutant proteins. The diameter and the appearance of the growth zone (halo) reflect the functionality of mutant proteins. Wild type FepA consistently gives a dense zone of growth with sharp borders around discs containing 50 μM FeEnt. Three classes of siderophore nutrition halos are found (Table 4.2.2; Fig. 4.2.6). I14G300C gives no halo when sub-cultured in NB without any reducing reagent. When it grows in NB with 5mM BME and a nutrition test is done with addition of 0.5mM BME in the plate, I14G300C gives a sharp halo that is similar to that of the wild type. Second class includes A42N162C and G149T180C. They show no difference from wild type in siderophore nutrition tests. Last class includes T51N608C and G54T585C. They both give larger halos than wild type without BME added. However, T51N608C gives a smaller halo when BME is added, and G54T585C gives a larger halo when BME is added.

Table 4.2.2 Siderophore nutrition tests and measurement of the nutrition halos.

Strain	Halo (mm)	Appearance
KDF541	-	-
KDF541+BME*	-	-
KDF541/pITS23	18.5	Sharp
KDF541/pITS23+BME*	18	Sharp
I14G300C	-	-
I14G300C +BME*	20	Sharp
A42N162C	18.5	Sharp
A42N162C +BME*	18	Sharp
G149T180C	19.5	Sharp
G149T180C +BME*	19	Sharp
T51N608C	24	Sharp
T51N608C +BME*	21.5	Sharp
G54T585C	23.5	A little faint
G54T585C +BME*	28	A little faint

*Overnight LB culture is sub-cultured in 10 mL NB with 5 mM BME, and nutrition tests are done with 0.5 mM BME in the plates.

- no halo.

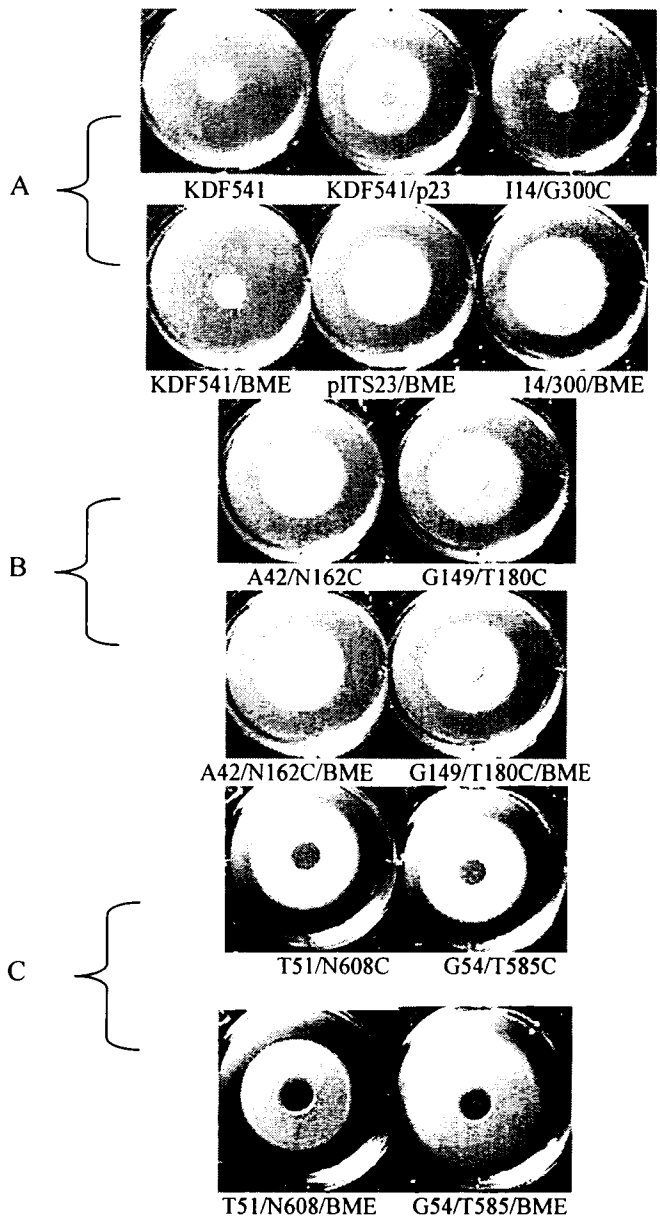

Fig. 4.2.6 Siderophore nutrition tests of wild type and disulfide bond mutants of FepA. A. (Top) Siderophore nutrition tests are performed for KDF541, KDF541/pITS and KDF541/pITS23/I14CG300C with NB culture, 20 μg/ml of chloramphenicol, and 10 μl of 50 μM FeEnt on the center paper discs. (Bottom) Bacteria are sub-cultured in NB with 5 mM BME and nutrition test are done with 0.5 mM BME in the plates. Strains are KDF541 (*fepA*-), KDF541/pITS23 (*fepA*+), and KDF541/pITS23/I14CG300C. B. KDf541/pITS23/A42CN162C and KDF541/pITS23/G149CT180C. C. KDF541/pITS23/T51CN608C and KDF541/pITS23/G54CT585C.

^{59}FeEnt binding and transport assays.

Quantitative ^{59}FeEnt uptake experiments (Table 4.2.3) were performed to determine the kinetic parameters of the uptake process. ^{59}FeEnt binding retains the same K_d and Capacity (data not shown). When BME added, the K_m of pITS23 is not changed, but the V_{max} is decreased by 20%. 14/300C does not transport FeEnt without the presence of BME. When cells are treated with BME, the bacteria start the uptake process, and the K_d is 1.3 nM, V_{max} is 20 pmole/10^9/min, indicating the active formation and deformation of the disulfide bonds *in vivo*. This result is consistent with what I observed in the nutrition tests. Binding and transport assays were not done for other disulfide mutants.

Table 4.2.3 Quantitative ^{59}FeEnt uptake assay.

Strains*	K_m (nM)	V_{max} (pmole/10^9/min)
KDF541/pITS23	0.33	58.5
KDF541/pITS23/BME	0.28	45
KDF541/pITS23/I14CG300C	-	-
KDF541/pITS23/I14CG300C/BME	1.3	20

* Bacteria were treated with 0.5 mM BME for 30 minutes, cells centrifuged, resuspended in NB with apoferrichrome at 37°C for 10 minutes before uptake experiment.

OKN strains and their derivatives. Because of the presence of the N-domain fragment detected in KDF541 strain, I transformed pITS23 and pITS23/I14G300C plasmids into OKN3 and OKN13 strains. OKN strains were recently constructed from BN1071, which is a wild-type *fepA+ E. coli* strain. OKN3 is *fepA-* and OKN13 is *fepA- tonB-*. I also transformed another plasmid, pRZ540 (*tonB+*) to OKN13 to compliment its tonB marker and recover the transport of FeEnt by FepA. I first did nutrition tests and I obtained similar results (Table 4.2.4; Fig. 4.2.7) as with KDF541. With or without BME or DTT, OKN3/pITS23/I14G300C only grew in the presence of FeEnt when 5mM or 10mM BME or 10mM DTT was present as well. OKN13/pITS23/I14G300C did not grow because of the absence of TonB. When pRZ540 complimented TonB, the OKN13/pITS23/I14G300C/pRZ540 displayed the same result as OKN3/pITS23/I14G300C, except that DTT did not work at this time. These data suggested that the I14G300C mutation formed an active disulfide bond *in vivo*. In the future, western blot needs to be done to show the presence of the disulfide bond. ^{59}FeEnt uptake experiment also needs to be performed to show that the formation of the disulfide bond affects the transport process.

Table 4.2.4 Nutrition tests of OKN13 strain and its derivatives.

Strains	Halo (mm)	Appearance
OKN3	-	-
OKN3/5mM BME+0.5mMBME*	-	-
OKN3/10mM BME+0.5mMBME*	-	-
OKN3/10mM DTT	-	-
OKN3/10mM O-DTT	ND	ND
OKN3/pITS23	ND	ND
OKN3/pITS23/5mM BME+0.5mMBME*	ND	ND
OKN3/pITS23/10mM BME+0.5mMBME*	ND	ND
OKN3/pITS23/10mM DTT	ND	ND
OKN3/pITS23/10mM O-DTT	ND	ND
OKN3/pITS23/I14G300C	-	-
OKN3/pITS23/I14G300C/5mM BME+0.5mMBME*	15.5	Sharp
OKN3/pITS23/I14G300C/10mM BME+0.5mMBME*	16	Sharp
OKN3/pITS23/I14G300C/10mM DTT	21	Sharp
OKN3/pITS23/I14G300C/10mM O-DTT	-	-
OKN13	-	-
OKN13/5mM BME+0.5mMBME*	-	-
OKN13/10mM BME+0.5mMBME*	-	-
OKN13/10mM DTT	-	-
OKN13/10mM O-DTT	-	-
OKN13/pITS23	-	-
OKN13/pITS23/5mM BME+0.5mMBME*	-	-
OKN13/pITS23/10mM BME+0.5mMBME*	-	-
OKN13/pITS23/10mM DTT	-	-
OKN13/pITS23/10mM O-DTT	-	-
OKN13/pITS23/I14G300C	-	-
OKN13/pITS23/I14G300C/5mM BME+0.5mMBME*	-	-
OKN13/pITS23/I14G300C/10mM BME+0.5mMBME*	-	-
OKN13/pITS23/I14G300C/10mM DTT	-	-
OKN13/pITS23/I14G300C/10mM O-DTT	-	-
OKN13/pITS23/I14G300C/pRZ540	-	-
OKN13/pITS23/I14G300C/pRZ540/5mM BME+0.5mMBME*	16	Sharp
OKN13/pITS23/I14G300C/pRZ540/10mM BME+0.5mMBME*	16	Sharp
OKN13/pITS23/I14G300C/pRZ540/10mM DTT	-	-
OKN13/pITS23/I14G300C/pRZ540/10mM O-DTT	-	-

ND: No Data; -: no halo.



Fig. 4.2.7 Nutrition tests pictures of OKN3/pITS23/I14G300C. From left to right, bacteria used in the nutrition tests were grown in nutrient broth without reducing or oxidizing reagents, with 5 mM BME, 10 mM BME, 5 mM DTT, 10 mM DTT, and 10 mM oxidized DTT, respectively.



Fig. 4.2.8 Nutrition tests pictures OKN13/pITS23/I14G300C and OKN13/pITS23/I14G300C/pRZ540. OKN13/pITS23/I14G300C (picture on the left) did not grow not matter BME or DTT was present or absent. OKN13/pITS23/I14G300C/pRZ540 (picture on the left) did not grow when reducing reagent was not present. OKN13/pITS23/I14G300C/pRZ540 grew when 5 mM BME (picture in the middle) or 10 mM BME (picture on the right) was present during its growth in the nutrient broth.

Discussion

Recently, a similar experiment (Coulton *et al.,* 2005) described a disulfide bond construction in FhuA protein. The hydroxamate siderophore receptor FhuA is a TonB-dependent outer membrane protein of *E. coli*. It is composed of a C-terminal 22-stranded β-barrel occluded by an N-terminal globular domain. Therefore, the structure of FhuA is very similar to that of FepA. During siderophore transport into the periplasm, the FhuA plug has also been proposed to either undergo conformational changes or be displaced from the barrel. Site-directed cysteine mutants in the N-domain, L109C and Q112C, and in the barrel, S356C and M383C, were created. Molecular modeling (SSBOND) predicted that the double cysteine mutants L109C/S356C and Q112C/M383C would form disulfide bonds, which was predicted to tether the N-domain and barrel domain. Although only a very small amount of the FhuA protein forms disulfide bonds *in vivo*, the author used oxidants, copper (II) phenanthroline (CuP) or copper sulfate, to increase the formation of disulfide bonds. With CuP, 99% and 90% of the proteins are observed to form disulfide bonds in L109C/S356C and Q112c/M383C, respectively. With $CuSO_4$, 99% and 83% of the proteins are observed to form disulfide bonds L109C/S356C and Q112C/M383C, respectively. Next, ^{55}Fe-Ferricrocin uptake experiments showed that both double cysteine mutants were proficient for transport of ferricrocin at levels of 93% and 99%, respectively, compared with non-oxidized double cysteine FhuA mutants. Then it was concluded that engineered disulfide bonds obstructing the putative siderophore transport pathway did not prevent ferricrocin transport through FhuA.

All these data seemed to suggest that the N domain does not exit the barrel, which contradict the data in our lab. There are a few explanations for the discrepancy. First of

all, the FhuA proteins with disulfide bonds migrated slower, which is similar to T51N608C and G54T585C mutants of FepA. Slightly less than 50% of the T51N608C mutant proteins and slightly more than 50% of the G54T585C mutant proteins (Fig. 4.2.4) formed disulfide bonds. However, the mutant I concentrated on, I14G300C migrated faster (Fig. 4.2.2). Also, around 90% of I14G300C FepA proteins have disulfide bonds formed *in vivo*, which made oxidant unnecessary, although I did try oxidized DTT and did not observe any improvement of disulfide bond formation. Even though I did not understand the structural difference of I14G300C FepA and L109C/S356C and Q112C/M383C FhuA, which made the different migration patterns, I do not think the data between FepA I14G300C and FhuA mutants are comparable. FepA I14G300C was shown to have an active disulfide bond *in vivo*. This disulfide bond did affect the transport of FeEnt and the reduction of the disulfide bond recovered the transport. I think FhuA L109C/S356C and Q112C/M383C mutants did not contain the perfectly "active" disulfide bonds that were observed in FepA I14G300C. It may be worthwhile to further study T51N608C and G54T585C mutants of FepA and compare them with L109C/S356C and Q112C/M383C FhuA in the future. Secondly, L109 and Q112 are at very high position in the crystal structure. They are about 30-35 Å away from the extracellular and the periplasmic sides of the outer membrane, which could be spanned by about 10 amino acids. Looking at the crystal structure of FhuA, residues 90 to 150 of the N domain is enough to block the channel disregarding conformational change due to the missing residues. However, removing residues 1-100 will create a channel (Fig. 4.2.9) that is large enough (15-25 Å) for Fc to pass through. This suggests to me that it is quite possible that N-domain exits the barrel only partially during transport. As a result of

partial displacement, L109C/S356C and Q112C/M383C FhuA will not show functional difference to the wild type FepA in the ^{55}Fe uptake experiments. Last, in uptake experiments, although iron uptake media with 100 μM nitrilotriacetate was used, bacteria were grown in TY media, which is rich and contains Fe. Intracellular iron stored by ferritin may affect the iron uptake. Also, expression of FhuA protein is not maximized in TY medium.

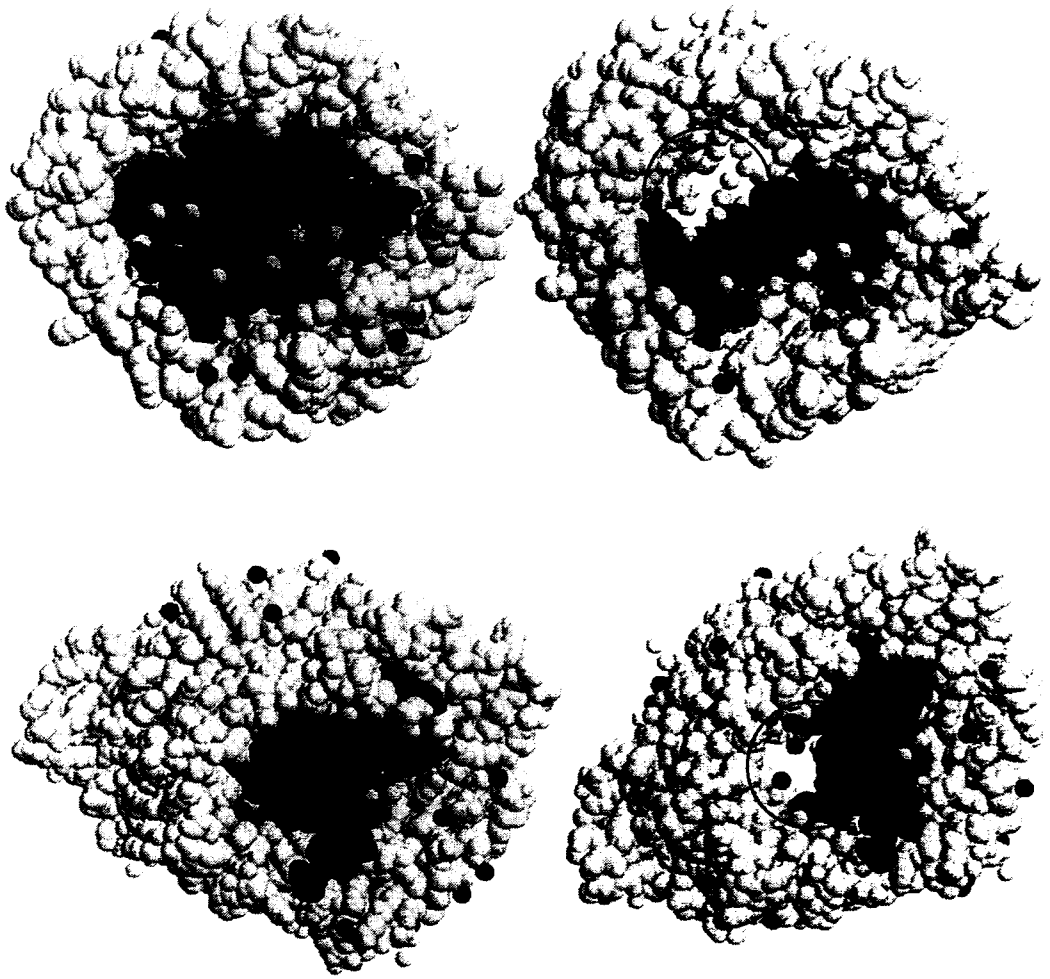

Fig. 4.2.9 FepA (top) and FhuA (bottom). Red is N domain. Yellow is C domain. Blue is L109 in FhuA. Left is full protein. Right is Δ1-100 of FepA and FhuA.

Whether the N domain exits or undergoes conformational change, the disulfide bonds constructed could affect the movement of the N domain. Although these experiments could not clearly close one of the possibilities, they did suggest that the disulfide bond limited the movement of the N domain during the active transport process of FeEnt. In addition, since FepA with I14G300C forming disulfide bond *in vivo* completely lost function, conformational change is less likely to be completely disabled by the disulfide bond so that FepA is fully not functional *in vivo*.

In KDF541 strain, although a small portion of the N domain was found to complement the Fepβ mutant, it should not affect the full-length FepA protein. Among the five disulfide bond mutants constructed, A42CN162C and G149CT180C did not actually form disulfide bonds *in vivo* suggested by the nutrition tests and immunoblots. The remaining three mutants showed two different patterns. Around 90% of the I14G300C fepA protein forms disulfide bond *in vivo*. The mutant protein migrates at the same speed as the wild-type protein when the disulfide bond was reduced by BME. However, when the disulfide bond was formed, the mutant proteins migrated faster than normal protein. The other two mutants, T51CN608C and G54CT585C, also form disulfide bonds in vivo. However, only about 50% of the mutant proteins form disulfide bonds *in vivo*. In the presence of BME, some of the disulfide bonds are reduced, and then the proteins migrate more slowly than the wild type protein. 5mM of BME is not enough to reduce the disulfide bonds of T51N608C, but a higher concentration of BME would be lethal to the bacteria. 5 mM of BME is good for G54T585C. However, due to the low percentage of disulfide bonds formed in these two mutants, I chose I14G300C for further study.

The nutrition tests clearly show that the disulfide bonds did affect the uptake process by showing no growth halo for the mutant. More convincingly, when BME is added in the media to reduce the disulfide bonds, the bacteria turned normal in the tests. This indicates that the disulfide bond formation is reversible and active in the uptake process. The quantitative ^{59}FeEnt binding and uptake experiments agree with the nutrition tests.

Although the N-domain fragment should not affect the experiment, I transformed I14G300C mutant into OKN strain to repeat the experiments. OKN3 is in-frame chromosomal *fepA* deletion derivative of BN1071. OKN13 is *fepA* and *tonB* deletion derivative. I then transformed I14G300C into both strains. I then reintroduced tonB back into OKN13/pITS23/I14G300C by transforming pRZ540 (*tonB*+). As expected, OKN3 and OKN13 showed no growth in nutrition tests as negative control. OKN3/pITS23/I14G300C only grew with FeEnt with BME added. Without the presence of TonB protein, OKN13/pITS23/I14G300C did not grow with FeEnt, with or without BME added. However, when TonB protein was expressed by the plasmid pRZ540, OKN13/pITS23/I14G300C grew with FeEnt when BME was added, but did not grow when BME was absent. This result showed that this process is TonB-dependent. Only when TonB protein is expressed in cells, will the transport of FeEnt happen, and the existence of the disulfide bond will affect the transport process.

In summary, this study shows that disulfide bonds can be engineered in FepA protein in vivo. They are active and affecting the functionality of FepA. The result of I14G300C suggests that the N domain is more likely displaced from the β-barrel into the periplasm during the transport of FeEnt.

4.3 Osmotic Shock of MAb ascites fluids and ELISA (1)

I tried different procedures of osmotic shock and used ELISA to detect the presence of MAb in the cells. My goal here was to introduce anti N-domain antibodies into the periplasmic space of *E. coli*. When FeEnt is added, the bacteria will bind and transport. During transport process, if the N domain exits the barrel upon binding, then the antibodies (Fig. 4.3.1) may have a chance to interact with the N domain. As a result, the N domain will not be able to go back to the β-barrel any more due to the large size of the antibodies (150 kDa). Because some antibodies will be stuck with the N domain instead of staying in the periplasm, the amount of the antibodies in the periplasm will decrease. I used ELISA to detect the decrease of the antibodies in the periplasm. It is also possible to detect the increase of the amount of antibodies associated with the cell envelopes. However, the antibodies in the PP probably will also nonspecifically bind to the periplasmic side of the OM. This will surely increase the background reaction in ELISA, and this background "noise" may be larger than the positive signal that I will observe when the antibodies bind to the N domain because of the relatively small amount of FepA present in the cells. The bacteria strain used here was KDF541/pITS23, which expressed FepA protein on a low copy plasmid. KDF541 strain was the negative control. Another way to detect the interaction between the antibodies and the N domain was to measure the transport of the bacteria that contained the antibodies in their PP. When the N domain is bound by the antibodies in the PP, the surface loops will be in a "closed" conformation (Scott *et al.*, 2002) at this stage. As a result, there is probably no signal that will be triggered to "open" the surface loops for next molecule of FeEnt. So the transport of FeEnt will cease, and I will be able to observe a different pattern of transport of FeEnt.

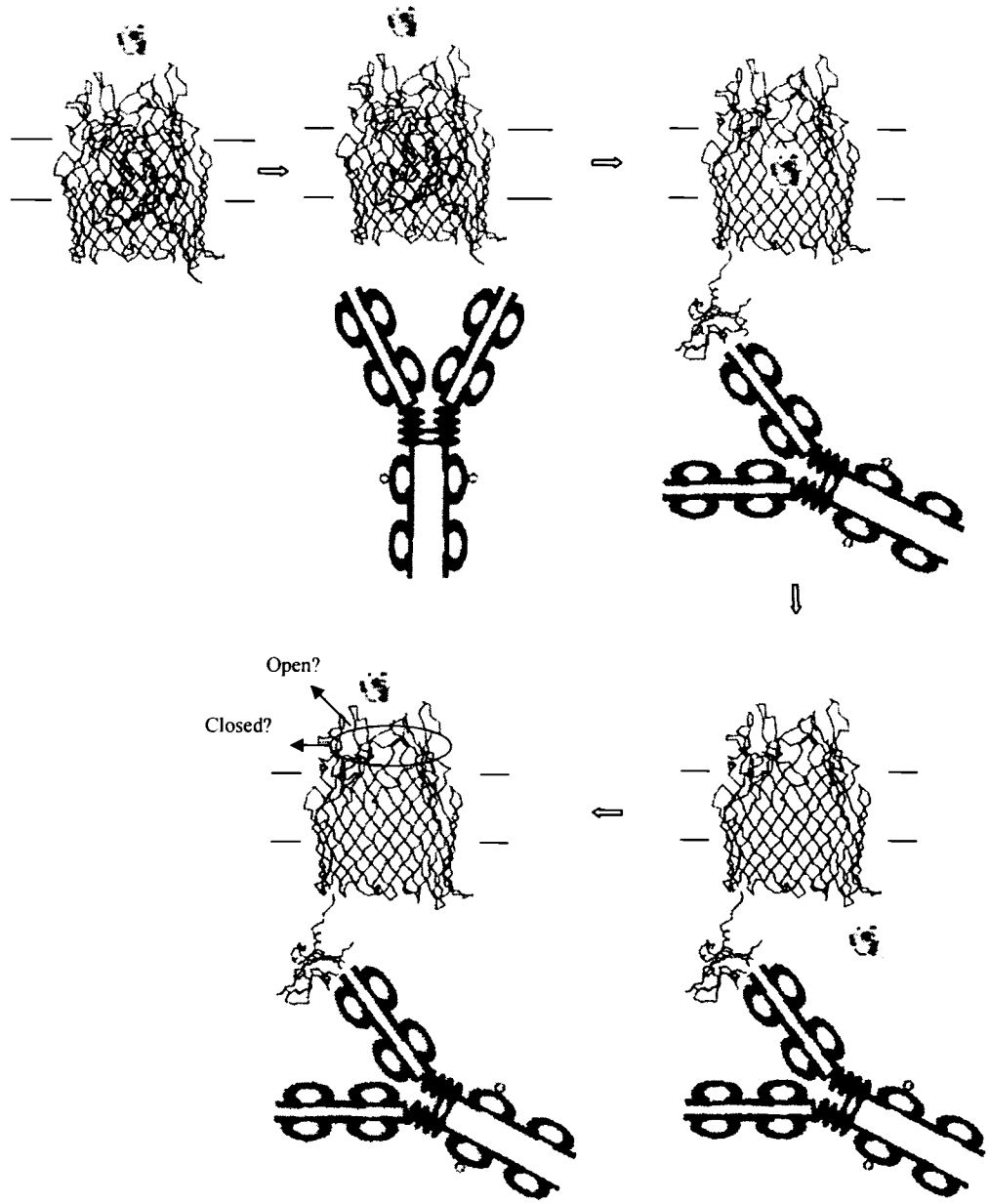

Fig. 4.3.1 Diagram of how antibodies bind the N domain in the PP.

First, I used the Ca^{2+}-sucrose shocking procedure (Zgurskaya *et al.*, 1999), which was effective with proteins smaller than 30 kDa. In this experiment, I denatured the purified FepA protein (0.23 μg/μl) by boiling with 1% SDS for 10 minutes. Then denatured protein was acetone precipitated, resuspended in the coating buffer (10 mM ammonium acetate and 10 mM ammonium carbonate, pH8.3), and applied to a 96-well microtiter plate. When the protein solutions dried at 37°C, I coated the plate with the samples from the osmotic shock experiment, including the supernatant after spinning down osmotic shocked bacteria, cell fluid and cell envelopes after French-Press. However, I was not able to see any positive reaction (data not shown here) with the cell fluid (periplasmic and cytoplasmic fluid). Then I replaced sucrose with dextran in the reconstitution buffer, and repeated the same procedure. I only observed positive reaction (Fig. 4.3.2) when undiluted fluid of cells that was shocked with MAb4 was coated to the plate. I could not see any positive reaction any more when the sample was diluted 10 times. Most of the MAb 4 ascites fluid still stayed in the supernatant after the shock.

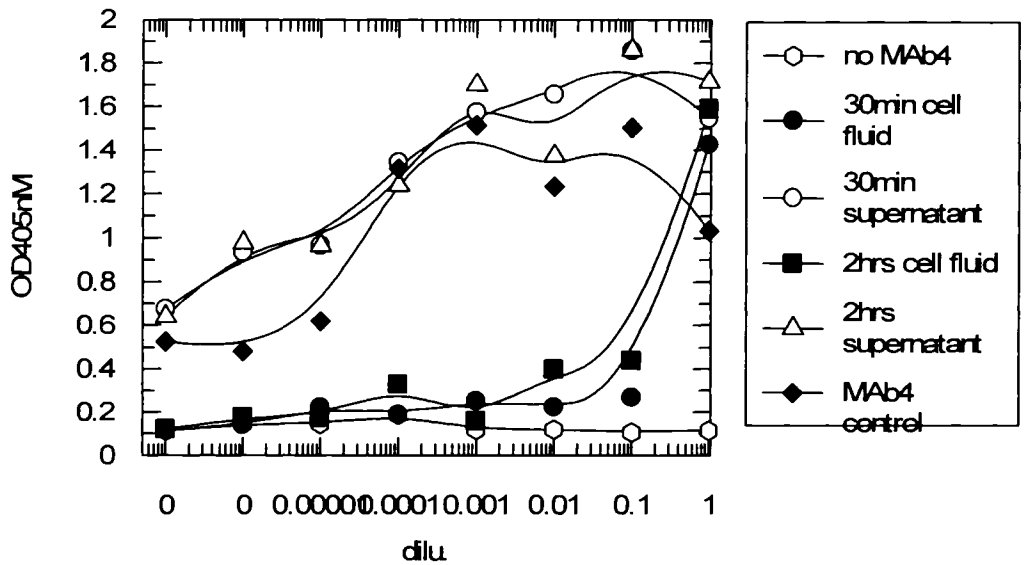

Fig. 4.3.2 Bacteria were treated with osmotic shock procedure using dextran reconstitution buffer. Samples were collected as described in the text above. Samples were dried in a 96-well microtiter plate. The plate was coated with the Goat-anti-Mouse IgG coupled with alkaline phosphatase (AP). The plate was then developed with the phosphatase substrate sigma 104 (p-Nitrophenyl Phosphate). ELISA procedures were the same for the data shown in all the other figures below. Each sample was labeled as seen in the figures.

In order to get more antibodies into the cells, I tried another method (Brass, 1986). I washed 10^9 cells with either ice-cold 0.1 M Tris buffer (pH7.5) and 0.1 M K_2HPO_4 (pH7.5), or ice-cold 0.1 M Tris/0.3 M $CaCl_2$ (pH7.5). Then I resuspended cells in ice-cold 0.1 M Tris/0.3 M $CaCl_2$ (pH7.5) with or without MAb4 ascites fluid. Solutions were incubated on ice for 30 minutes or 2 hours before French-Press. However, results (Fig. 4.3.3 bottom) showed that there was very limited increase in the amount of MAb4 in cell fluid after shock for two hours. I also tried 10 mM glycerol (Fig. 4.3.3 top) in the shocking buffer. But it did not improve at all. In all trials, majority of MAb4 added still remained in the supernatant.

I repeated the exact same experiment a few times, and the results (Fig. 4.3.4 top) were consistently not good. To test if some of the antibodies that were shocked into the cells were digested by proteases, I added the protease inhibitor, benzamidine, into the reconsititution buffer during osmotic shock. It turned out to be same tiny amount of MAb 4 existing in the cells (Fig. 4.3.4 bottom).

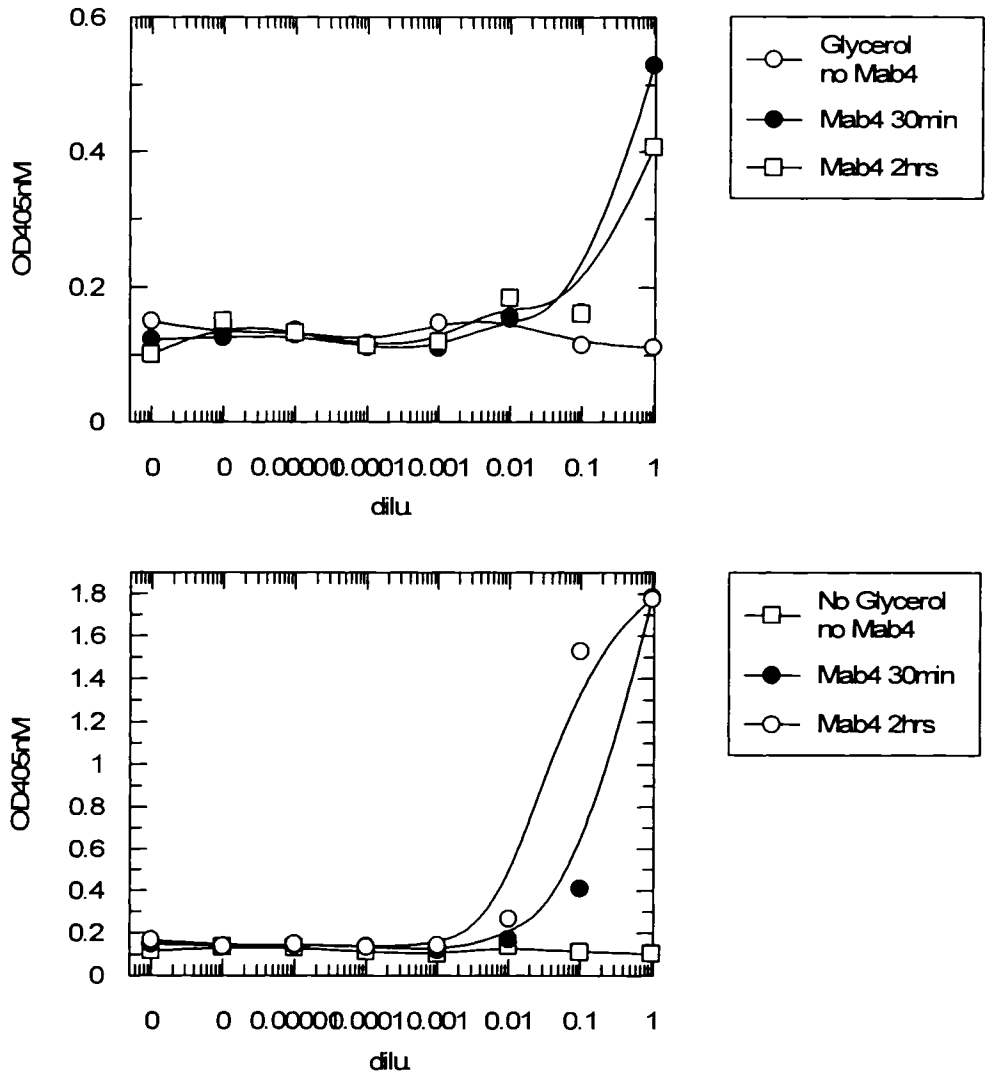

Fig. 4.3.3 ELISA of cell fluids after osmotic shock with or without glycerol in Tris/$CaCl_2$ buffer for either 30 minutes or 2 hours. Samples were dried in a 96-well microtiter plate. The plate was coated with the Goat-anti-Mouse IgG coupled with alkaline phosphatase (AP). The plate was then developed with the phosphatase substrate sigma 104 (p-Nitrophenyl Phosphate).

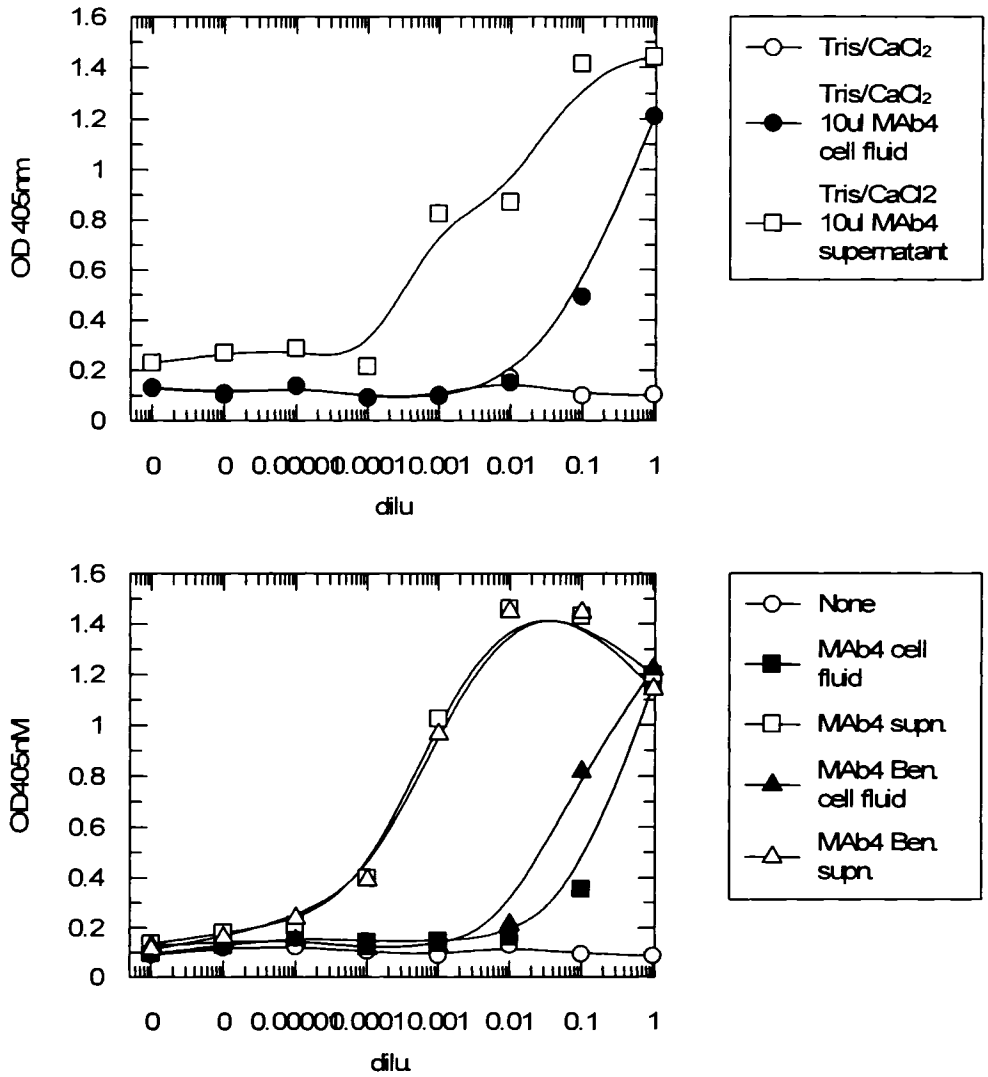

Fig. 4.3.4 Examine the effect of benzamidine in the osmotic shock with Tris/$CaCl_2$ buffer. Samples were dried in a 96-well microtiter plate. The plate was coated with the Goat-anti-Mouse IgG coupled with alkaline phosphatase (AP). The plate was then developed with the phosphatase substrate sigma 104 (p-Nitrophenyl Phosphate).

Although I cannot get most of the MAb4 into the cells, the optimized condition so far was with Tris/$CaCl_2$ buffer and two hours shocking with 10 μL of MAb4 ascites fluid. Next, I went ahead to try the same experiment with or without incubation with FeEnt at 37°C. After osmotic shock and wash, I resuspended cells in MOPS media, and shook the bacteria at 37°C for two hours either without or with 10 μM FeEnt. Then I broke cells by French-Press and collected cell fluid and the membrane envelopes. ELISA (Fig. 4.3.5 A) did not show much difference between cells incubated without FeEnt and cells incubated with FeEnt. I repeated the same experiment for MAb1 (Fig. 4.3.5B), MAb27 (Fig. 4.3.5C), and MAb41 (Fig. 4.3.5D). Results did not excite me at all, except that cell fluid of the bacteria with MAb27 inside of periplasm showed a little less reactivity to FepA in the presence of FeEnt during 37°C incubation. However, the inconsistency was between a few experiments and I explained it as a standard error.

I then tried to do the same experiment for MAb2, 26, and 29. However, I was not able to observe any amount of antibodies present in the cell fluid (Fig. 4.3.6).

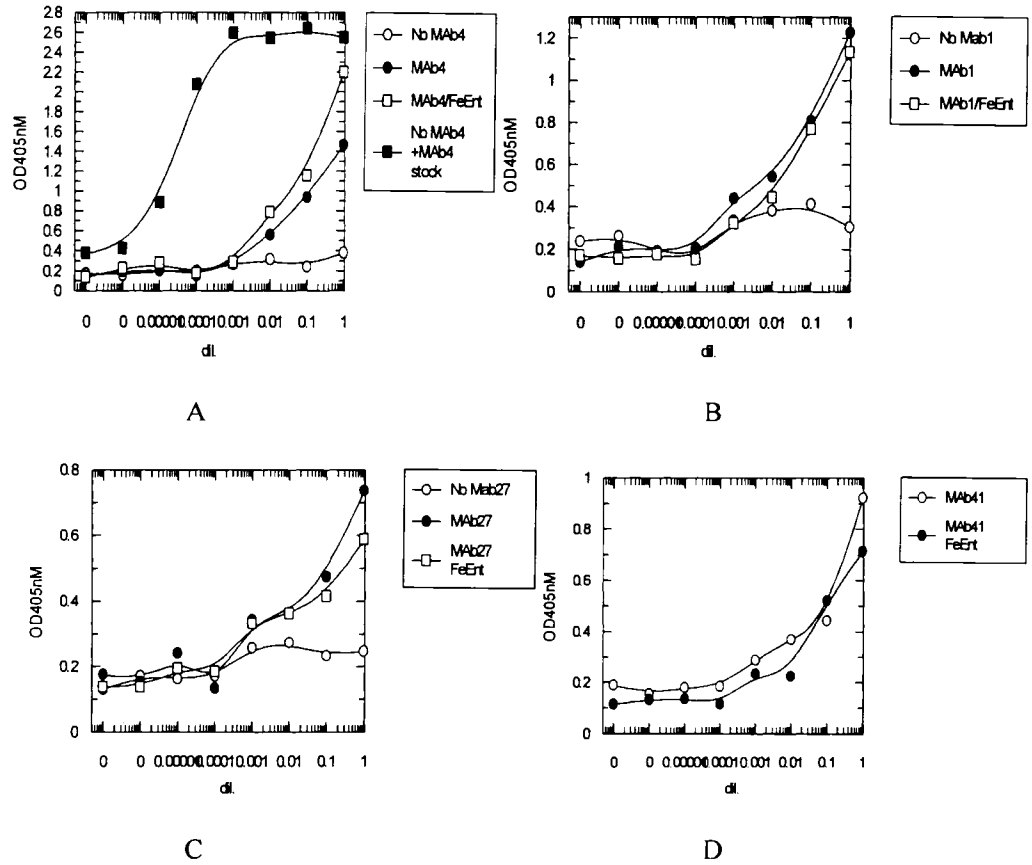

Fig. 4.3.5 ELISA of cell fluids after bacteria were shocked with MAb1, 4, 27, or 41, followed by incubation at 37°C with or without 10 μM FeEnt. Samples were dried in a 96-well microtiter plate. The plate was coated with the Goat-anti-Mouse IgG coupled with alkaline phosphatase (AP). The plate was then developed with the phosphatase substrate sigma 104 (p-Nitrophenyl Phosphate).

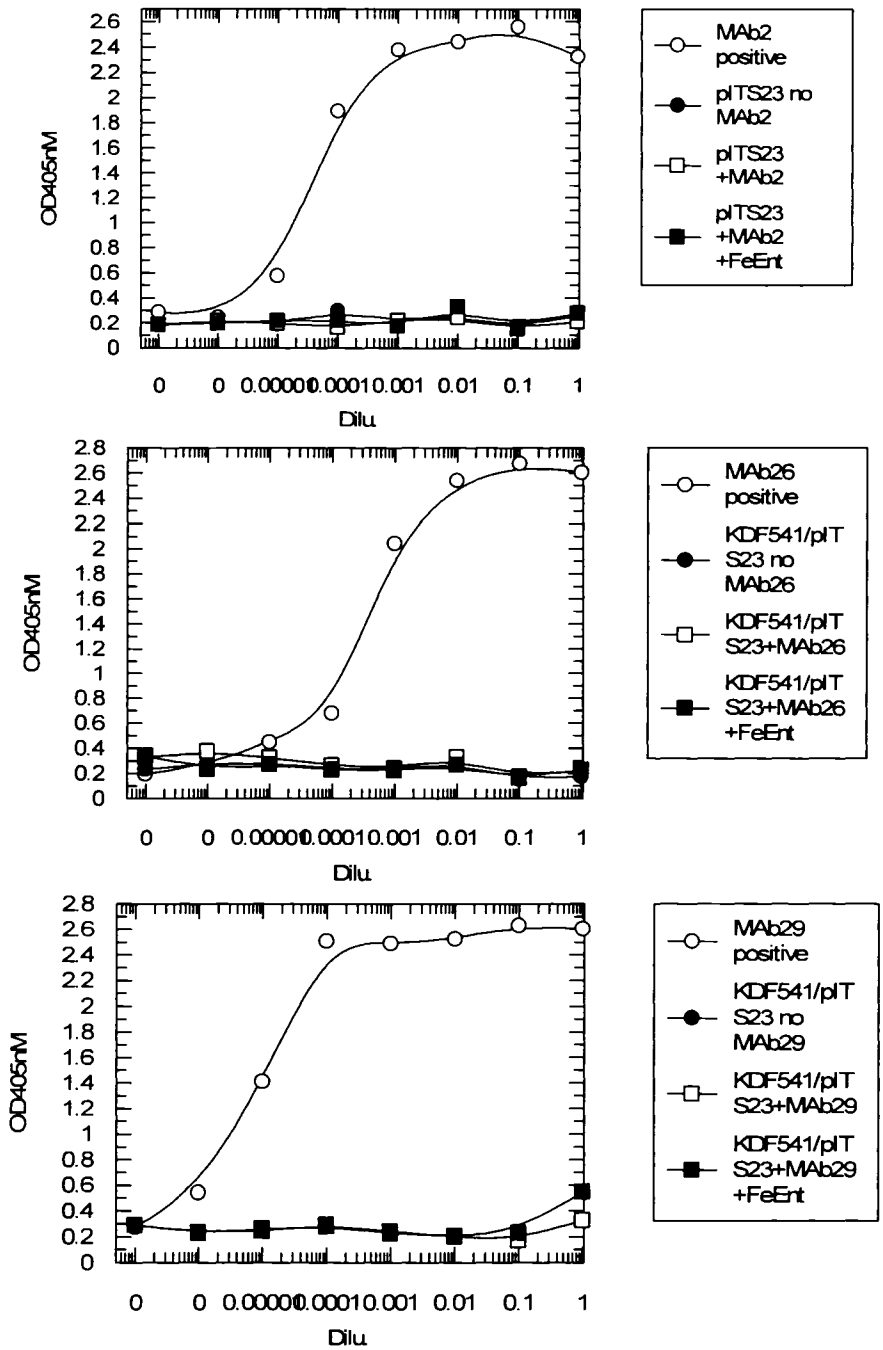

Fig. 4.3.6 ELISA of cell fluid after bacteria were shocked with MAb2, 26, or 29, followed by incubation at 37°C with or without 10 μM FeEnt. Samples were dried in a 96-well microtiter plate. The plate was coated with the Goat-anti-Mouse IgG coupled with alkaline phosphatase (AP). The plate was then developed with the phosphatase substrate sigma 104 (p-Nitrophenyl Phosphate).

Since the bacterial viability was always high (data not shown), I did ^{59}FeEnt uptake experiment to look at the functionality of FepA.

I used MAb1 first. Results (Fig. 4.3.7) did show decreased V_{max} when cells were osmotically shocked with MAb1 compared to cells shocked without MAb1. Although this decrease could come from the small amount of antibody present in the periplasm, this small difference is not significant enough to reach a conclusion.

I then tried Mab4. ELISA (Fig. 4.3.8) showed no difference between osmotically shocked cells incubated with or without FeEnt. The same cells were applied to ^{59}FeEnt uptake experiments. A 30-minute uptake experiment showed that V_{max} decreased when the cells went through osmotic shock procedure. However, when I compare bacteria shocked with MAb4 and bacteria shocked without MAb4, V_{max} and K_m (Fig. 4.3.9) are very close. When I did a two-hour uptake experiment, the same results were seen after comparison. However, there is one interesting finding. Normal cells (Fig. 4.3.10) showed a linear increasing pattern during two-hour uptake, as I also observed in other experiments. But the cells after osmotic shock showed saturation. This suggests that the osmotic shock procedure affects some functionality of the bacteria. One possibility is that during osmotic shock, the periplasmic binding protein FepB is partially lost.

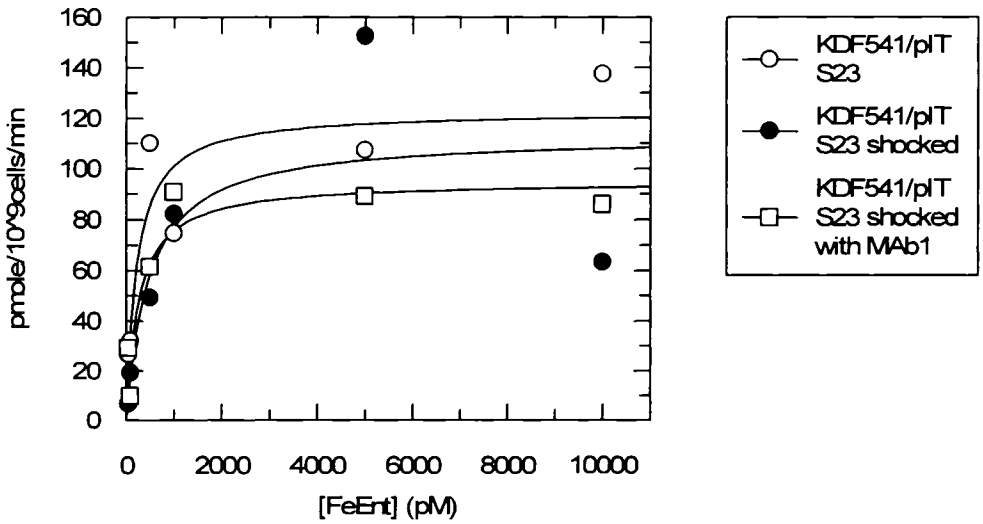

Parameter	Value	Std. Error
Vmax	122.6590	15.1867
Km	212.8485	126.8429

Parameter	Value	Std. Error
Vmax	112.8629	29.1705
Km	461.9069	479.2720

Parameter	Value	Std. Error
Vmax	94.8655	10.2382
Km	251.9108	124.2215

Fig. 4.3.7 ^{59}FeEnt uptake of KDF541/pITS23 cells and cells that were shocked without or with MAb1 ascites fluids.

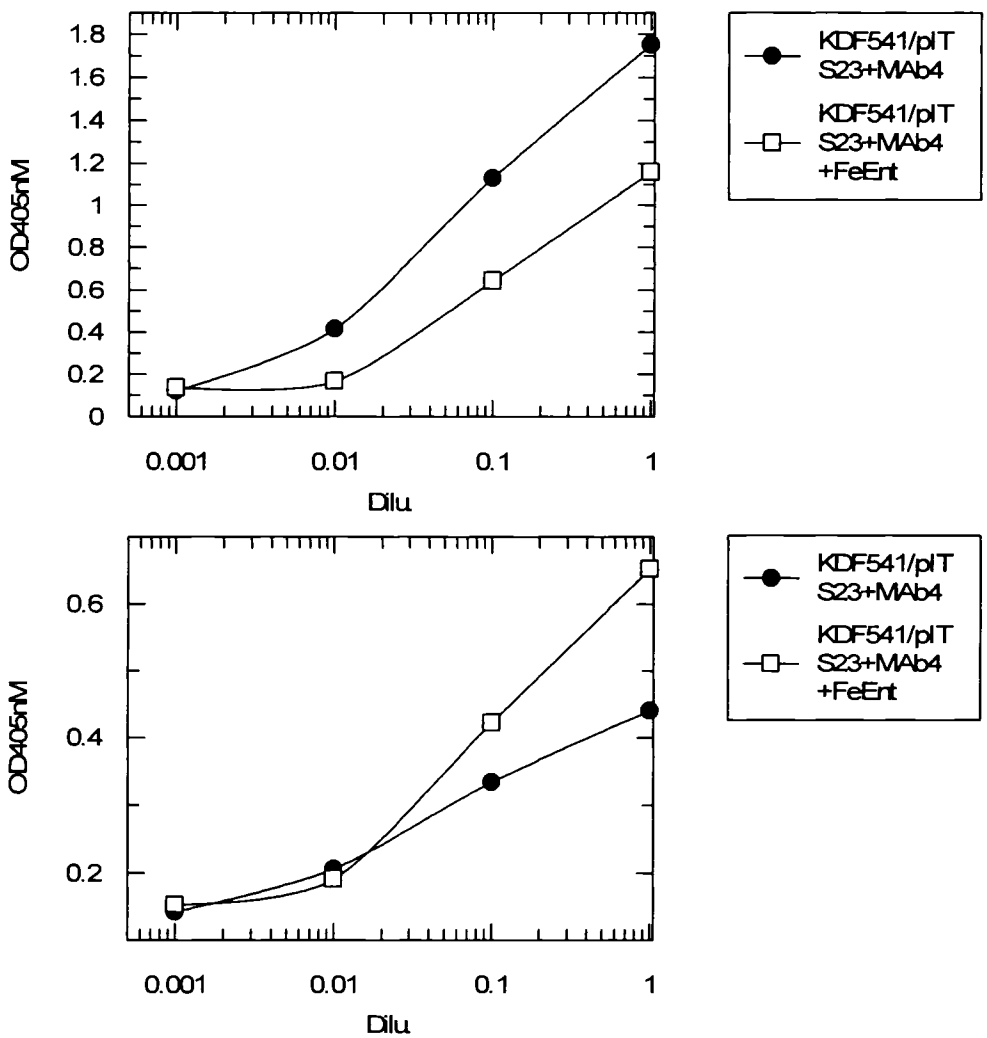

Fig. 4.3.8 ELISA of KDF541/pITS23 cells that were shocked with MAb4 ascites fluids and then incubated at 37°C either with or without the presence of FeEnt. Samples were dried in a 96-well microtiter plate. The plate was coated with the Goat-anti-Mouse IgG coupled with alkaline phosphatase (AP). The plate was then developed with the phosphatase substrate sigma 104 (p-Nitrophenyl Phosphate).

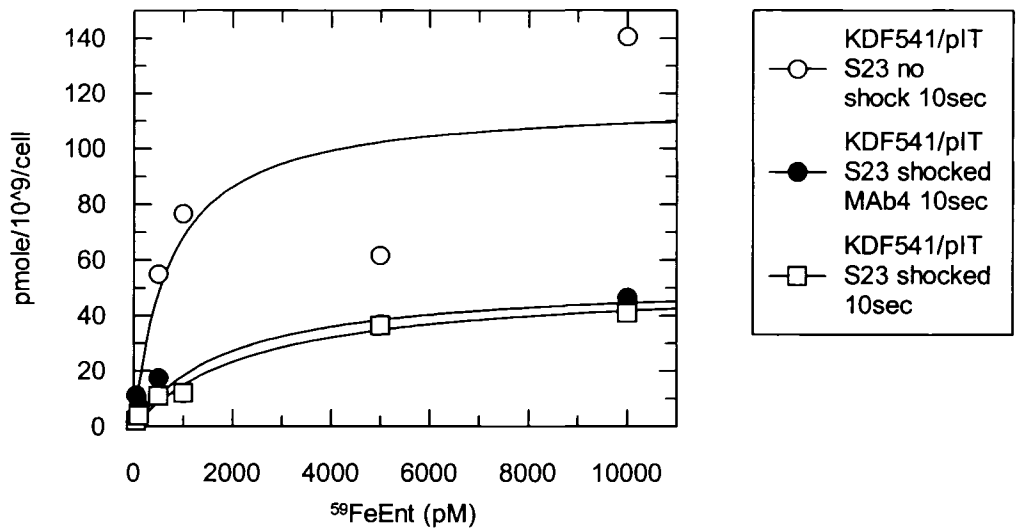

none

Parameter	Value	Std. Error
Vmax	116.7399	26.0285
Km	706.5983	585.1883

shocked

Parameter	Value	Std. Error
Vmax	52.2398	4.4987
Km	2498.6580	626.8017

shocked MAb4

Parameter	Value	Std. Error
Vmax	53.0905	10.9096
Km	1896.7642	1203.1210

Fig. 4.3.9 ^{59}FeEnt 10-second uptake of KDF541/pITS23 cells and cells that were shocked with or without MAb4 ascites fluids.

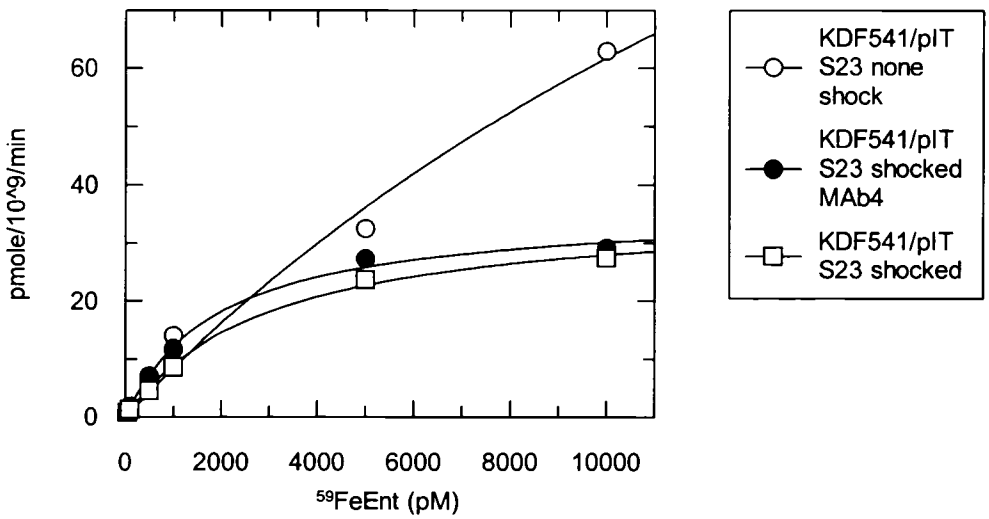

none

Parameter	Value	Std. Error
Vmax	209.3663	115.5473
Km	23918.7607	17734.3930

shocked

Parameter	Value	Std. Error
Vmax	36.6152	1.5624
Km	3064.1831	359.9766

shocked MAb4

Parameter	Value	Std. Error
Vmax	36.1350	1.5421
Km	1982.1768	264.1880

Fig. 4.3.10 ^{59}FeEnt two-hour uptake of KDF541/pITS23 cells and cells that were shocked with or without MAb4 ascites fluids.

Uptake of FeEnt requires energy from proton motive force. It concurs with the pH drop in the periplasm. Upon binding of FeEnt, the N domain may exit the β-barrel and enter the periplasm which is more acidic. So if I mimic the acidic environment of the periplasm, the N-domain could exit to the periplasm. To do this, I will make outer membrane vesicles. Some will have the periplasmic side of the OM facing outside of the vesicles. I will then adjust the pH of the vesicles suspension to lower pH. If the N domain comes out of the vesicles because of the pH drop, I will be able to use anti N-domain antibodies to detect it in ELISA.

To make the vesicles, I subcultured the overnight culture of KDF541 or KDF541/pITS23 in 100mL MOPS minimum media, and allow the culture to grow to OD600~0.5. I resuspended cells in 10mL of TBS with DNase and RNase, applied cells to French-Press, and separated inner membrane and outer membrane by centrifugation for 45 minutes at 20000*g. I then resuspended the outer membrane in 4mL coating buffer (ammonium acetate and ammonium carbonate, pH8.3). To denature the samples, I add 1% SDS and boiled the samples for five minutes. Finally, I applied regular samples or denatured samples to microtiter plate and incubated the plate in cold room overnight. Next day, I wash the plate with TBS-0.5% Tween 20, block the plate with 2% BSA in TBS for 30 minutes, and wash again. I then incubate different wells with 50 mM $NaHPO_4$ with different pH, 2.5, 3.5, 5.5, 6.5 and 7.5. Buffer is removed in 5 minutes. Dilutions of anti N-domain antibodies are added to the plate. After 1 hour, I wash the plate, coat it with goat-anti-mouse IgG plus 1:1000 alkaline phosphatase in 1% blocking buffer. I wash the plate again in 1 hour, and add the substrate sigma 104 in diethanolamine buffer at 1mg/ml. 50 μl of 2 N NaOH is added when the color of the

reaction is bright yellow. Although the name of alkaline phosphatase implies that a basic pH is preferred optimum, it has activity at acidic pH *in vitro* too.

I tried MAb1 for KDF541 and KDF541/pITS23 at pH 2.5 and 6.5. Results showed that (Fig. 4.3.11) KDF541 was not reactive to MAb1 under both pHs. KDF541/pITS23 was not reactive to MAb1 under both pHs when it is not denatured, and strongly reactive when it was denatured. However, ELISA titer seemed to be the same. I then tried MAb 2, 4, 12, 26, 27, 29, 33, 41, and got the same results (data not shown here) as MAb1. MAb45 was a control, because it is reactive to surface epitope. MAb45 should be reactive to FepA no matter whether it is denatured or not. Results (Fig. 4.3.12) reaffirmed it.

Then I compared ELISA (Fig. 4.3.13) with more pH conditions, 2.5, 3.5, 5.5, and 7.5. Results with MAb1 showed that KDF541 and KDF541/pITS23 undenatured were not reactive to MAb1 under all pHs. For KDF541/pITS23 denatured, there was almost no reactivity under pHs 2.5 and 3.5, but strongly reactive under pHs 5.5 and 7.5. I also used MAb2, 4, 27, 29. Results (data not shown here) were consistent, except there was some reactivity with MAb 27 and 29 under pH 3.5 too.

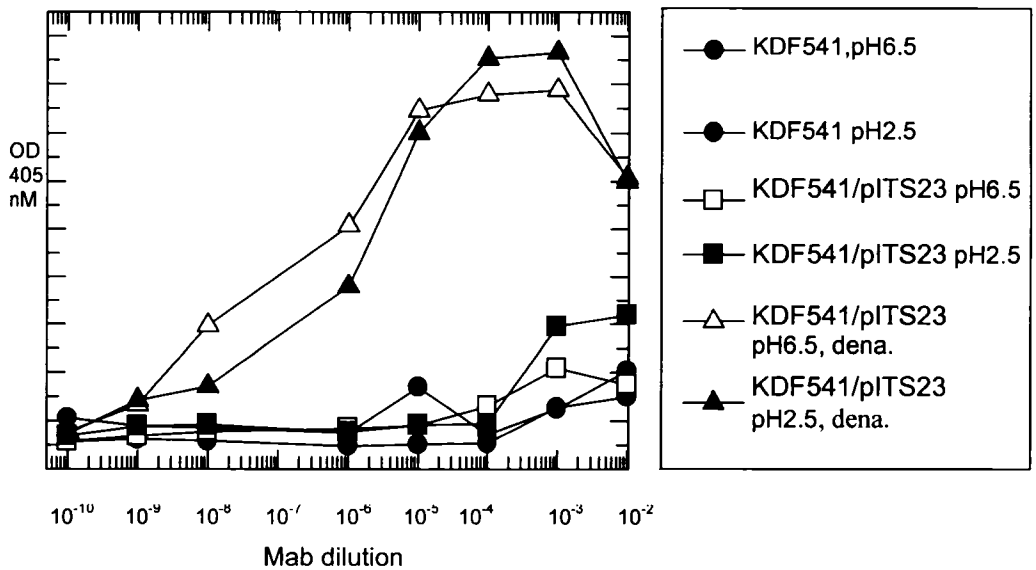

Fig. 4.3.11 KDF541 and KDF541/pITS23 samples or denatured samples incubated with serial dilutions of MAb1 ascites fluids at pH2.5 or 6.5. Bacterial samples were dried in a 96-well microtiter plate. The plate was coated with serial dilutions of MAb1 ascites fluid, followed by the Goat-anti-Mouse IgG coupled with alkaline phosphatase (AP). The plate was then developed with the phosphatase substrate sigma 104 (p-Nitrophenyl Phosphate).

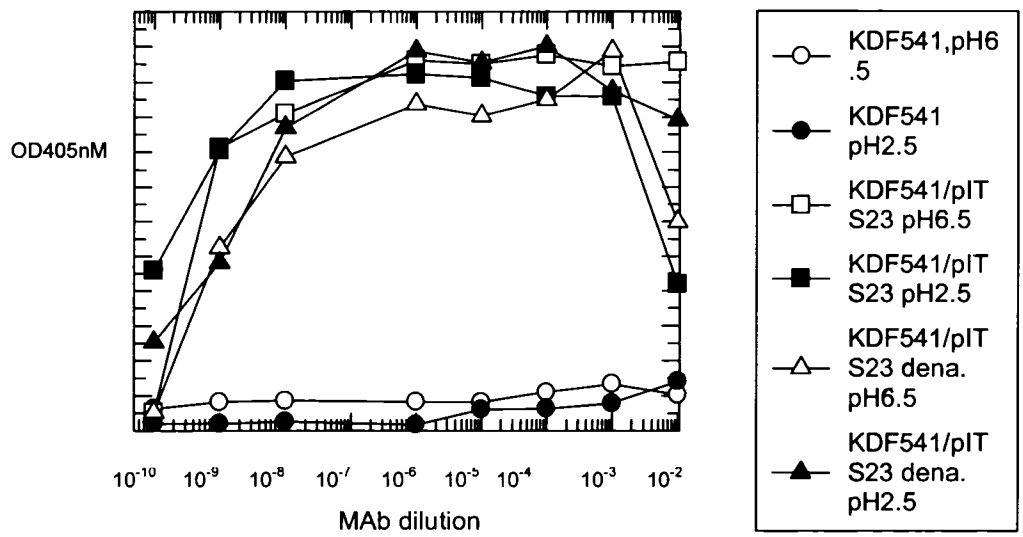

Fig. 4.3.12 KDF541 and KDF541/pITS23 samples or denatured samples incubated with serial dilutions of MAb45 ascites fluids at pH2.5 or 6.5. Bacterial samples were dried in a 96-well microtiter plate. The plate was coated with serial dilutions of MAb45 ascites fluid, followed by the Goat-anti-Mouse IgG coupled with alkaline phosphatase (AP). The plate was then developed with the phosphatase substrate sigma 104 (p-Nitrophenyl Phosphate).

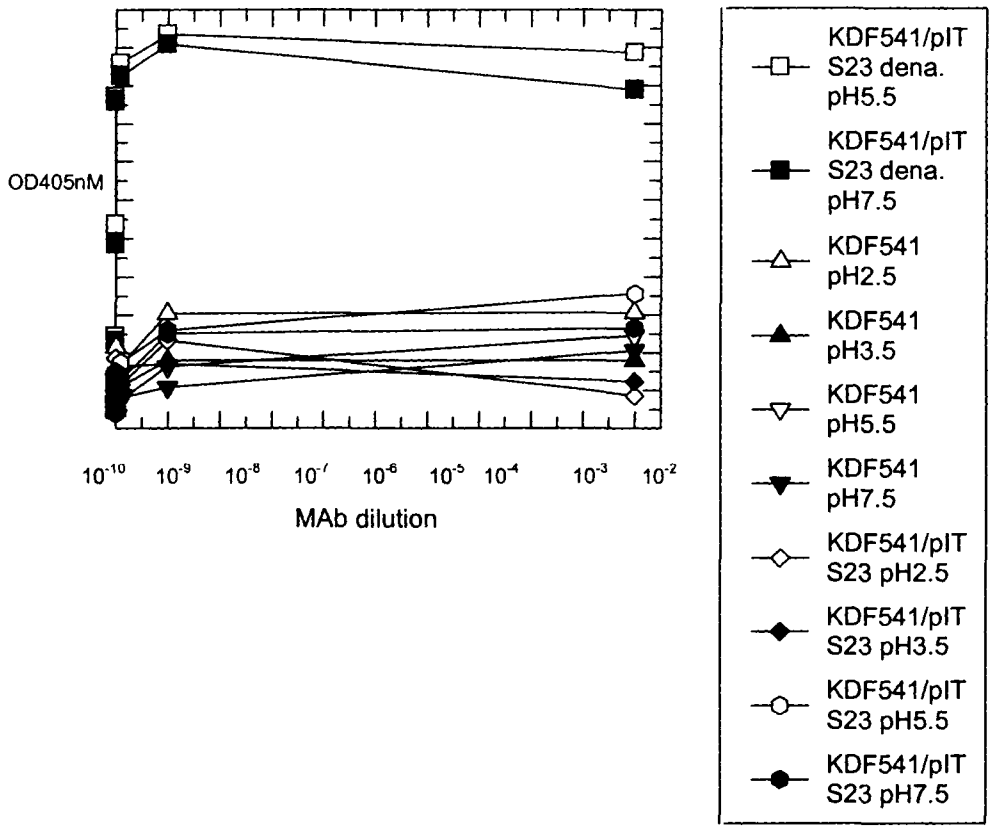

Fig. 4.3.13 KDF541 and KDF541/pITS23 samples or denatured samples incubated with serial dilutions of MAb1 ascites fluids at pH2.5, 3.5, 5.5 or 7.5. Bacterial samples were dried in a 96-well microtiter plate. The plate was coated with serial dilutions of MAb1 ascites fluid, followed by the Goat-anti-Mouse IgG coupled with alkaline phosphatase (AP). The plate was then developed with the phosphatase substrate sigma 104 (p-Nitrophenyl Phosphate).

In summary, using the osmotic shock procedure to introduce antibodies into the periplasm and ELISA to detect the presence of antibodies in the periplasm, a small amount of antibody seemed to exist in the periplasm after the procedure. Majority of the antibodies used in the procedure stayed outside of the cells. I used a few antibodies that recognized different epitopes on the N domain, and there were no different results obtained. The size of the antibodies (150 kDa) seemed to be too large for them to enter the pores produced in the outer membrane during the osmotic shock. Even though only a very small amount of the antibodies entered the cells, I tried to identify the interaction between the antibodies and the N domain and study if it affected the transport of FeEnt. However, the functionality of the cells does not seem to change much after the antibodies enter the periplasm, probably due to the small amount. The only functional difference observed (Fig. 4.3.9 and 4.3.10) in transport assays was related to the osmotic shock procedure. Among all the proteins involved in the transport of FeEnt, only FepB, the iron binding protein, is in the periplasm. FepB has a size less than 37 kDa (Sprencel *et al.*, 2000). During osmotic shock, certain amount of FepB protein will be equilibrated to outside of cells. This will certainly decrease the maximum amount of FeEnt that is transported to the inner membrane, which was seen in Fig. 4.3.9 and 4.3.10. Another possibility was that when the N domain enters the periplasm upon the binding of FeEnt, it could maintain the original conformation as in the barrel. So the epitopes that were recognized by anti N-domain antibodies when FepA protein was denatured may not be exposed. This experiment is not informative unless a larger amount of antibodies could be introduced into the periplasm in the future. Also more anti N-domain antibodies that recognize different epitopes need to be applied.

4.4 Introduction of MAb ascites fluid into periplasm and detection by SDS-PAGE and Western blot (2)

To study the movement of the N-terminal domain, here I used anti FepA N-terminal domain antibodies. If an anti FepA N-terminal domain antibody is introduced into the periplasmic space, then the antibodies will interact with the N domain when and if it exits the β-barrel. If the interaction happens, then the N domain will be stuck in the periplasm by the antigen-antibody interaction which is strongly stabilized and specified by hydrogen bonds, van der Waals forces, hydrophobic interactions, and/or electrostatic forces. In addition, antibodies are too large to enter the barrel. Later on, when I add FeEnt to the extracellular environment, the surface loops will bind the FeEnt. However, it may show completely different transport kinetics because the N domain is not in the native position and conformation after it is bound by antibodies in the PP. Upon the binding of the FeEnt, the N domain undergoes conformational changes. It is likely that epitopes recognized by the antibodies will still not be exposed to the periplasm. But, if the N domain exits the β-barrel partially or completely, then antibodies will have an excellent chance to interact with its exposed surfaces. I used SDS-PAGE and Western blots to detect the amount of MAb that entered the periplasm of *E. coli* after osmotic shock procedure. I did not adopt radioactive Immunoblot using goat-anti-mouse IgG and I^{125}-protein A because it was not very reactive to anti FepA N-domain antibodies (Fig. 4.4.1), although it was reactive to MAb45, which recognizes the epitopes on the surface loops.

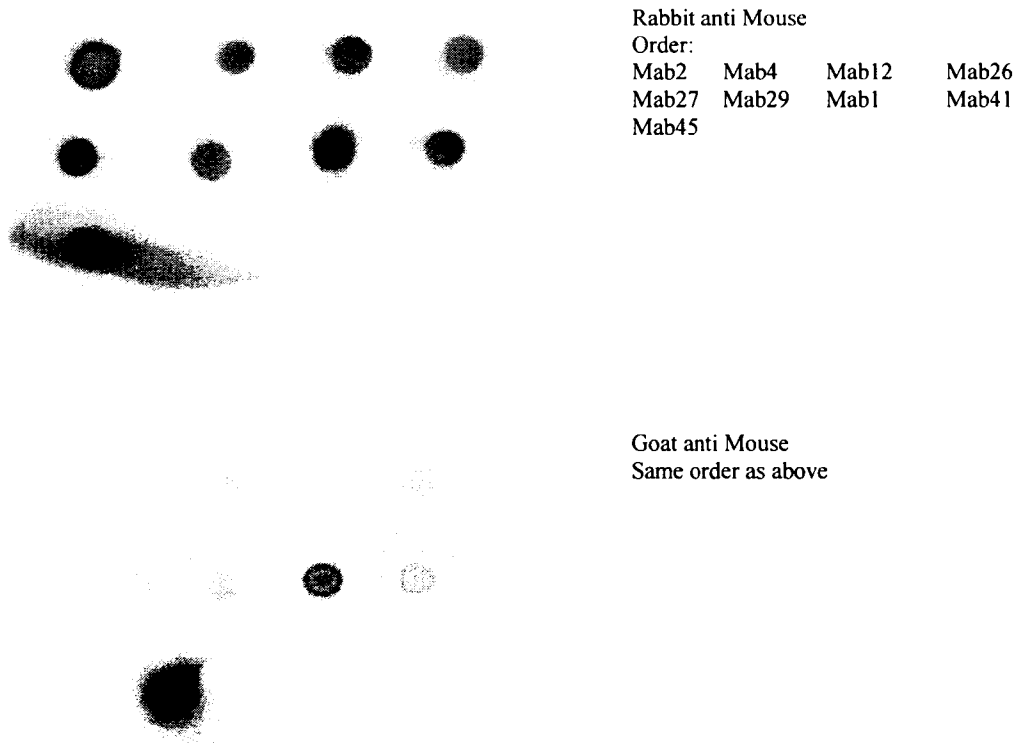

Fig. 4.4.1 Spot Immnoblot to test the reactivity of anti FepA N-domain antibodies to goat-anti-mouse or rabbit-anti-mouse with I^{125}-proteinA. Anti FepA N-domain antibodies were first spotted and dried on a piece of nitrocellulose membrane. Then the membrane was incubated with either anti-mouse antibody, followed by I^{125}-proteinA. Finally the image was transferred to phosphoimage screen, and the screen was scanned by a STORM scanner.

There were a few anti FepA N-domain antibodies available, including MAb1, 2, 4, 12, 20, 26, 27, 29, 33, 38, 39, and 41. According to the availability and their titers (Table 4.4.1) in ELISA, MAb4 was chosen as the first antibody for the experiment.

Using osmotic shocking procedure (Brass, 1986), I tried to shock MAb4 ascites fluid into KDF541/pITS23 with Tris/0.1M $CaCl_2$ buffer in a period of 30 minutes. However, I did not see any antibody in the cell fluid (Fig. 4.4.2). I only saw a small amount bound on the cell membrane and it is not specific to FepA (Fig. 4.4.2). I applied the same samples to western blot (Fig. 4.4.2), and the same results appeared. I also applied the same samples to ELISA (Fig. 4.4.3). I was also able to see reactivity to FepA in cell membrane. But there was no difference whether the incubation at 37°C after the shock procedure contained FeEnt or not.

Next, I tried a two-hour shocking procedure, but results (Fig. 4.4.4) remained the same. I used these cells to do ^{59}FeEnt uptake experiment. The 10-second uptake experiment (Fig. 4.4.5) showed that bacteria shocked without MAb4 seemed to act like wild type in uptake. However, bacteria shocked with MAb4 had almost 10-fold decreased V_{max}. I also did uptake for 30 minutes and 2 hours (Fig. 4.4.5). Bacteria that were not shocked showed a non-saturated curve. Bacteria shocked with or without MAb4 showed a saturated curve.

Table 4.4.1 ELISA of anti FepA N-domain antibodies.

MAb	Epitopes*	ELISA titer
1	27-37	$4*10^5$
4	100-178	$4*10^5$
26	27-37	$4*10^5$
27	100-178	$4*10^4$
39	100-178	$4*10^5 - 4*10^6$
41	100-178	$4*10^4 - 10*10^5$

Denatured FepA protein was dried in a 96-well microtiter plate at 37°C. The plate was coated with serial dilutions of different anti N-domain antibodies, followed by the Goat-anti-Mouse IgG coupled with alkaline phosphatase (AP). The plate was then developed with the phosphatase substrate sigma 104 (p-Nitrophenyl Phosphate).

* Amino acids numbering in the peptides (Murphy *et al.*, 1990).

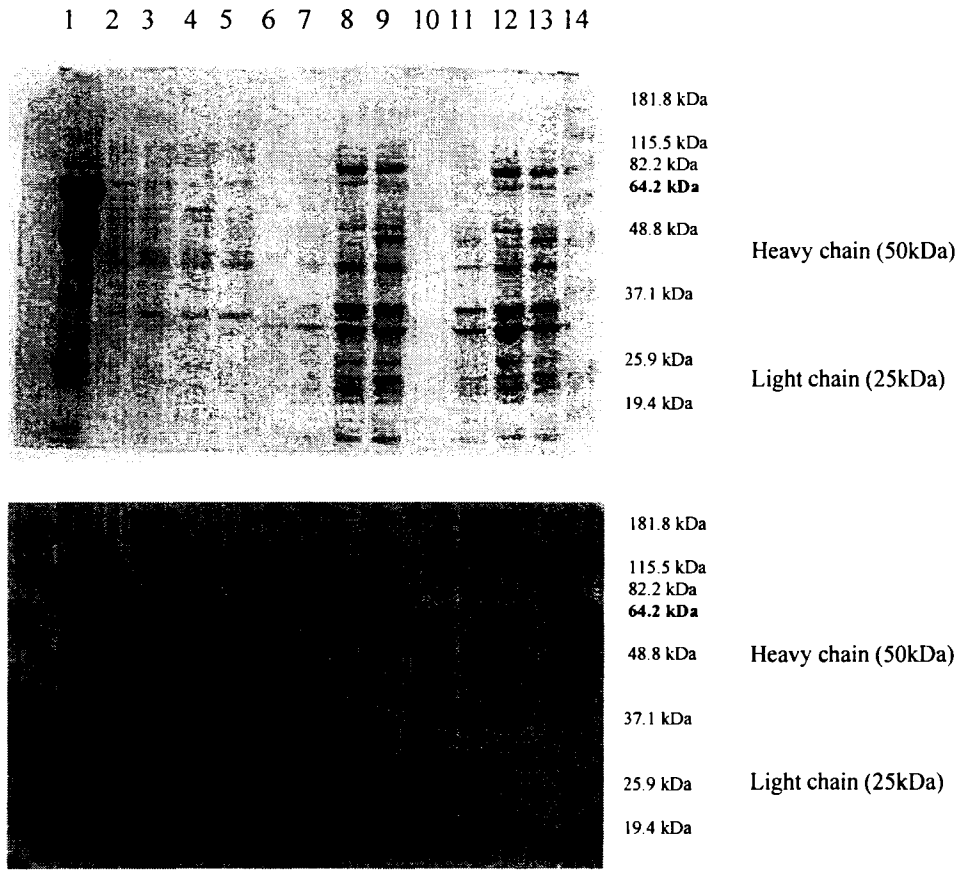

Fig. 4.4.2 10% SDS-PAGE of KDF541 and KDF541/pITS23 cell fluid after osmotic shock. Lane 1 was 1μL of MAb4 stock. Lane 14 was protein ladder. Lane 2 to 5 was the supernatant (cell fluid) after French-Press of the bacteria cells osmotically shocked with or without MAb4 ascites fluids. Lane 2 was p23 shocked without MAb4. Lane 3 was p23 shocked with MAb4. Lane 4 was p23 shocked without MAb4 followed by FeEnt incubation at 37°C. Lane 5 was p23 shocked with MAb4 followed by FeEnt incubation at 37°C. Lanes 6 to 14 were pellet (membranes) after French-Press of the bacteria cells osmotically shocked with or without MAb4 ascites fluids. Lane 6 was KDF541 shocked without MAb4. Lane 7 was KDF541 shocked with MAb4. Lane 8 was p23 shocked without MAb4. Lane 9 was pITS23 shocked with MAb4. Lane 10 was KDF541 shocked without MAb4 followed by FeEnt incubation at 37°C. Lane 11 was KDF541 shocked with MAb4 followed by FeEnt incubation at 37°C. Lane 12 was p23 shocked without MAb4 followed by FeEnt incubation at 37°C. Lane 13 was shocked with MAb4 followed by FeEnt incubation at 37°C.

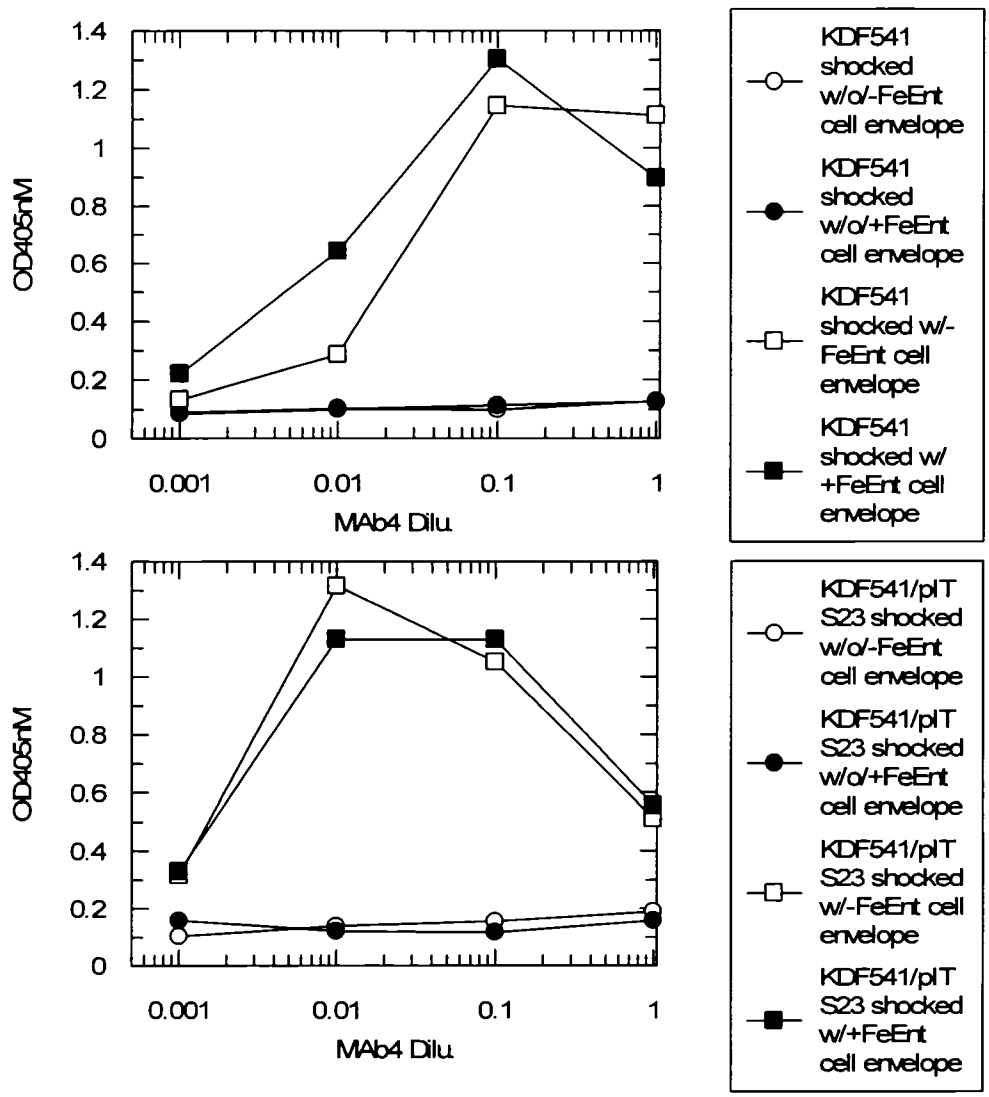

Fig. 4.4.3 ELISA. Samples were the same as in Fig. 4.4.2. Bacterial samples were dried in a 96-well microtiter plate. The plate was coated with the Goat-anti-Mouse IgG coupled with alkaline phosphatase (AP). The plate was then developed with the phosphatase substrate sigma 104 (p-Nitrophenyl Phosphate).

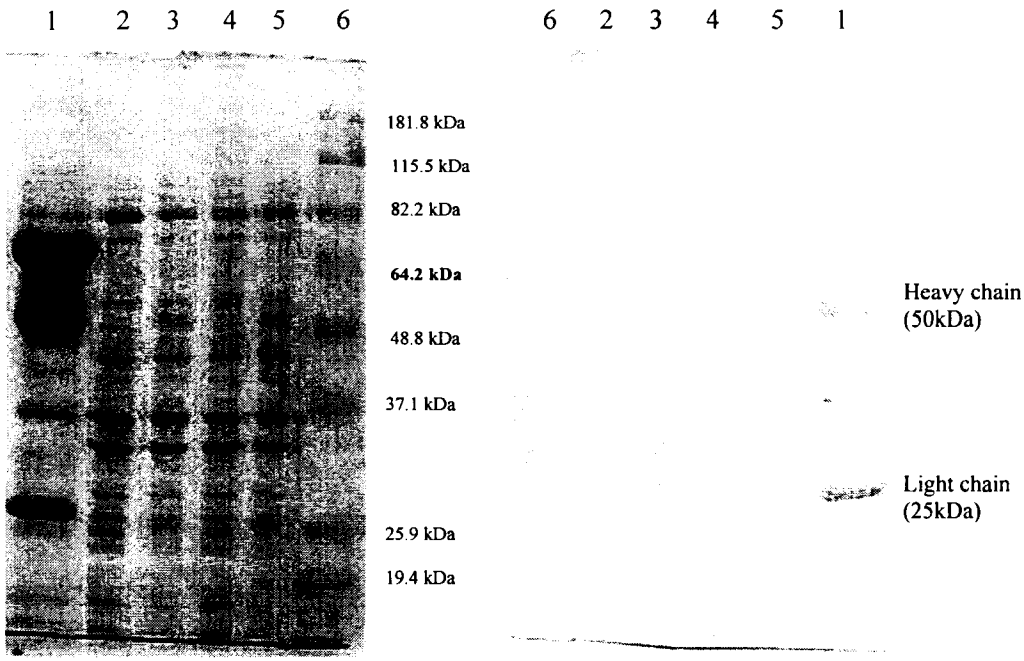

Fig. 4.4.4 Same experiment as in Fig. 3, but shocking was 2 hours. Left panel, lane 1 was MAb4 stock, lane 6 was protein ladder. Lane 2 to 5 was cell envelope. Lane 2 was KDF541/pITS23 shocked without MAb4, lane 3 was with MAb4, lane 4 was KDF541/pITS23 shocked without MAb4, followed by FeEnt incubation, and lane 5 was with MAb4 and FeEnt. Right panel: same samples are labeled with same numbers from 1 to 6.

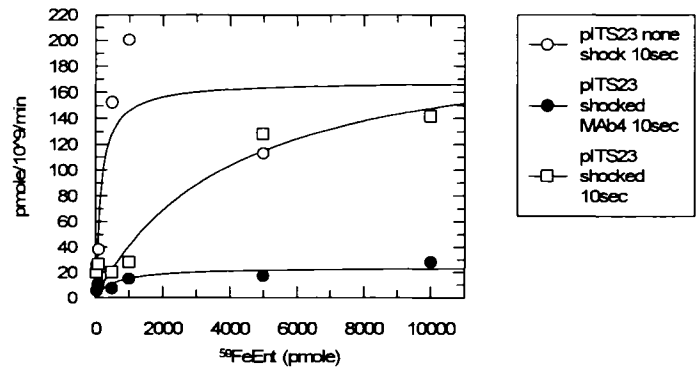

	Parameter	Value	Std. Error
none	Vmax	168.0200	44.3905
	Km	148.8616	185.5601

	Parameter	Value	Std. Error
shocked	Vmax	207.5408	51.9622
	Km	4016.2915	2497.2897

	Parameter	Value	Std. Error
shocked MAb4	Vmax	23.8851	5.0251
	Km	563.9450	440.8099

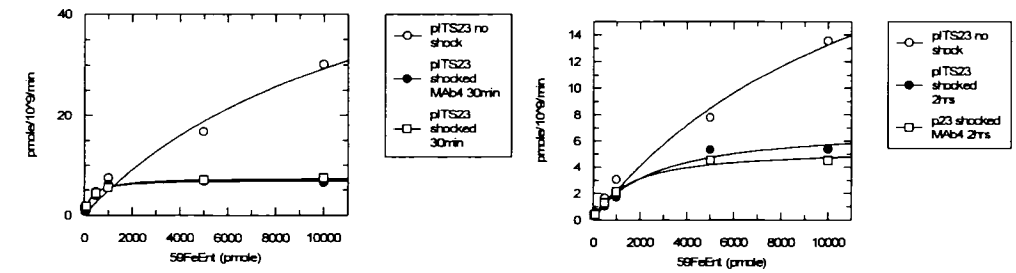

	Parameter	Value	Std. Error
none	Vmax	65.8158	22.6040
	Km	12480.4269	6938.5515

	Parameter	Value	Std. Error
shocked	Vmax	7.5156	0.1878
	Km	342.8657	37.8265

	Parameter	Value	Std. Error
shocked M4	Vmax	7.0366	0.3044
	Km	274.7939	55.3715

	Parameter	Value	Std. Error
none	Vmax	30.0989	8.3360
	Km	12691.5977	5659.3652

	Parameter	Value	Std. Error
shocked	Vmax	5.4309	0.3057
	Km	1479.1702	279.6976

	Parameter	Value	Std. Error
shocked M4	Vmax	7.2086	0.8147
	Km	2596.4318	858.4979

Fig. 4.4.5 ^{59}FeEnt uptake of KDF541/pITS23 shocked with MAb4 for 10 seconds, 30 minutes, or two hours.

I tried different concentrations of Tris in the reconstitution buffer. Both 0.2 M and 0.3 M Tris (Fig. 4.4.6) in two-hour shocking period did not increase the amount that was shocked into the cells. SDS-PAGE showed that the cell fluid only contained a small amount of MAb4, the cell envelope did not have any MAb4 attached, and most of the MAb4 used in the procedure appeared in the supernatant after NaCl wash. However, western blot showed equal amounts of MAb4 in the supernatant, cell fluid, and cell envelope I loaded. A decent amount of mouse serum albumin (MSA) was shocked into cells probably because BSA is less than half of the size of antibodies.

I did ^{59}FeEnt uptake (Fig. 4.4.7) for these cell samples without French-Press. Cells shocked with or without MAb4 had decreased V_{max}. Cells shocked with MAb4 had smaller V_{max} than cells shocked without MAb4.

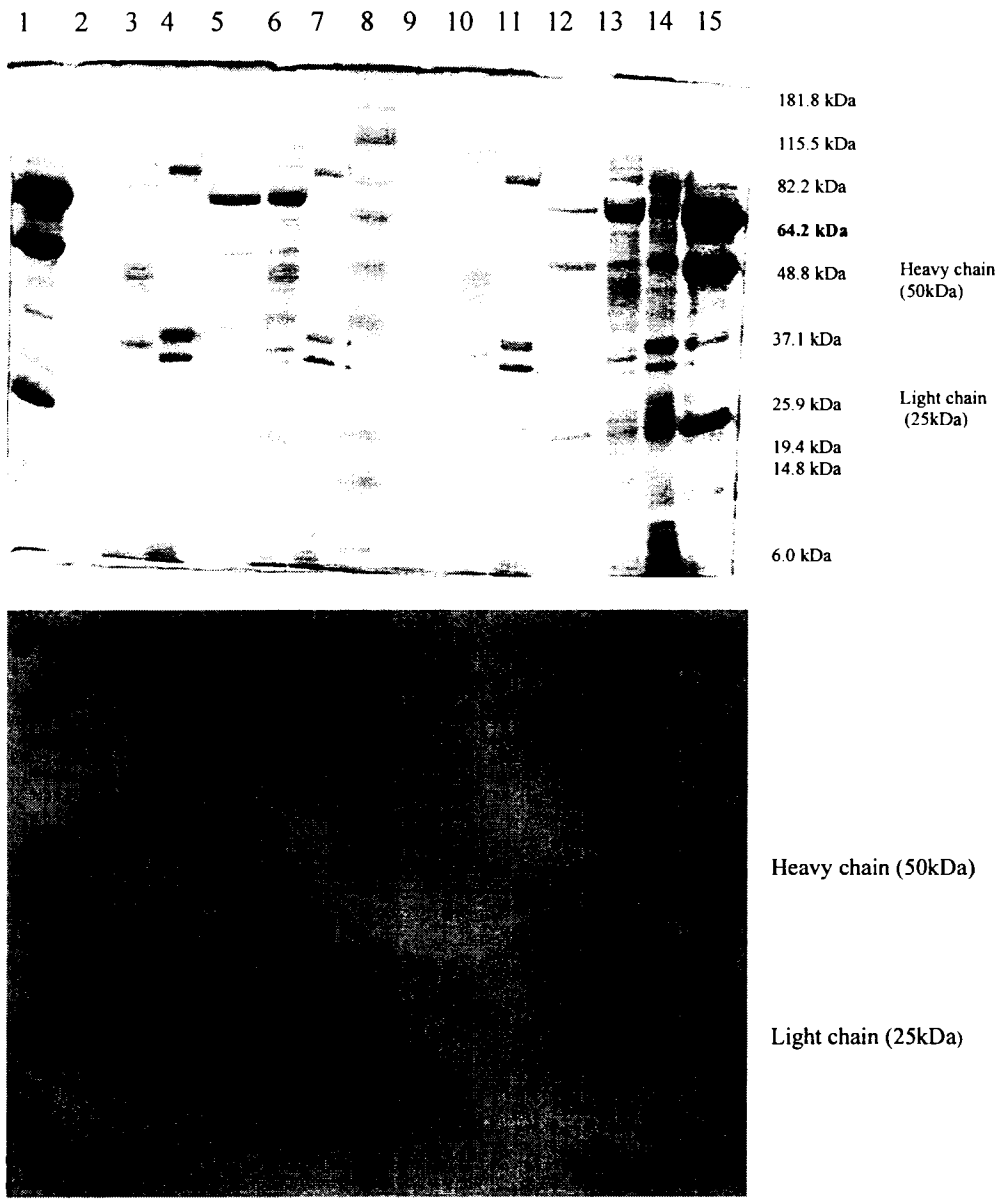

Fig. 4.4.6 SDS-PAGE and Western blot of same samples of KDF541/pITS23 cell lysates. Lanes 1 and 15 were MAb4 ascites fluid dilution. Lane 8 was protein ladder. Lanes 2 to 7 were cells shocked in 0.3 M Tris/$CaCl_2$ buffer. Lanes 2 to 4 were cell samples shocked without MAb4. Lane 2 was supernatant after NaCl wash. Lane 3 was cell fluid. Lane 4 was membrane envelope.

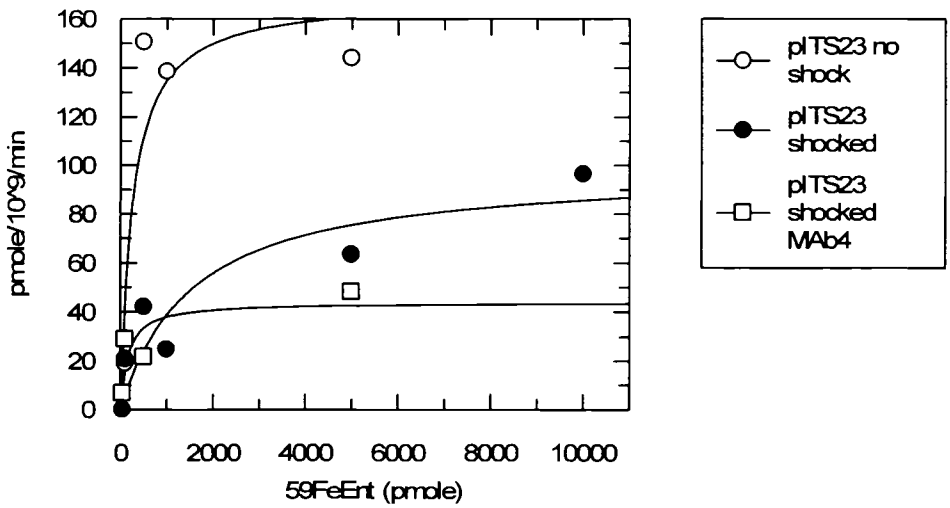

none

Parameter	Value	Std. Error
Vmax	168.8617	36.9073
Km	252.2219	233.6371

shocked

Parameter	Value	Std. Error
Vmax	98.5475	20.7809
Km	1523.5290	1022.9704

shocked M4

Parameter	Value	Std. Error
Vmax	43.9123	13.0691
Km	154.1525	179.0983

Fig. 4.4.7 ^{59}FeEnt uptake of KDF541/pITS23 shocked with MAb4.

I then compared shocking procedure for 5 minutes, 15 minutes, 30 minutes, and 2 hours. 15-minute shocking (Fig. 4.4.8) seemed to get best results if there was any difference at all. In addition, cells should be more viable in 15 minutes compared to 30 minutes and 2 hours, although the viabilities in all the experiments were above 60% (data not shown).

I used TEV protease as a control in the osmotic shock procedure. As Fig. 4.4.9 showed, a decent amount of TEV protease was present in the cells although only 1 μL of the enzyme was used in the procedure. However, only a small amount of antibody was present. An apparent explanation is that TEV protease has a size of 27 kDa which is small enough to equilibrate in and out the OM during the osmotic shock procedure. On the other hand, IgG is 150 kDa. Another difference was that the TEV protease I used was pure recombinant proteins, and the ascites fluids I used contained a large amount of other proteins, such as MSA. The large percentage of impurities that are smaller than IgG could also make it difficult for IgG to enter the PP.

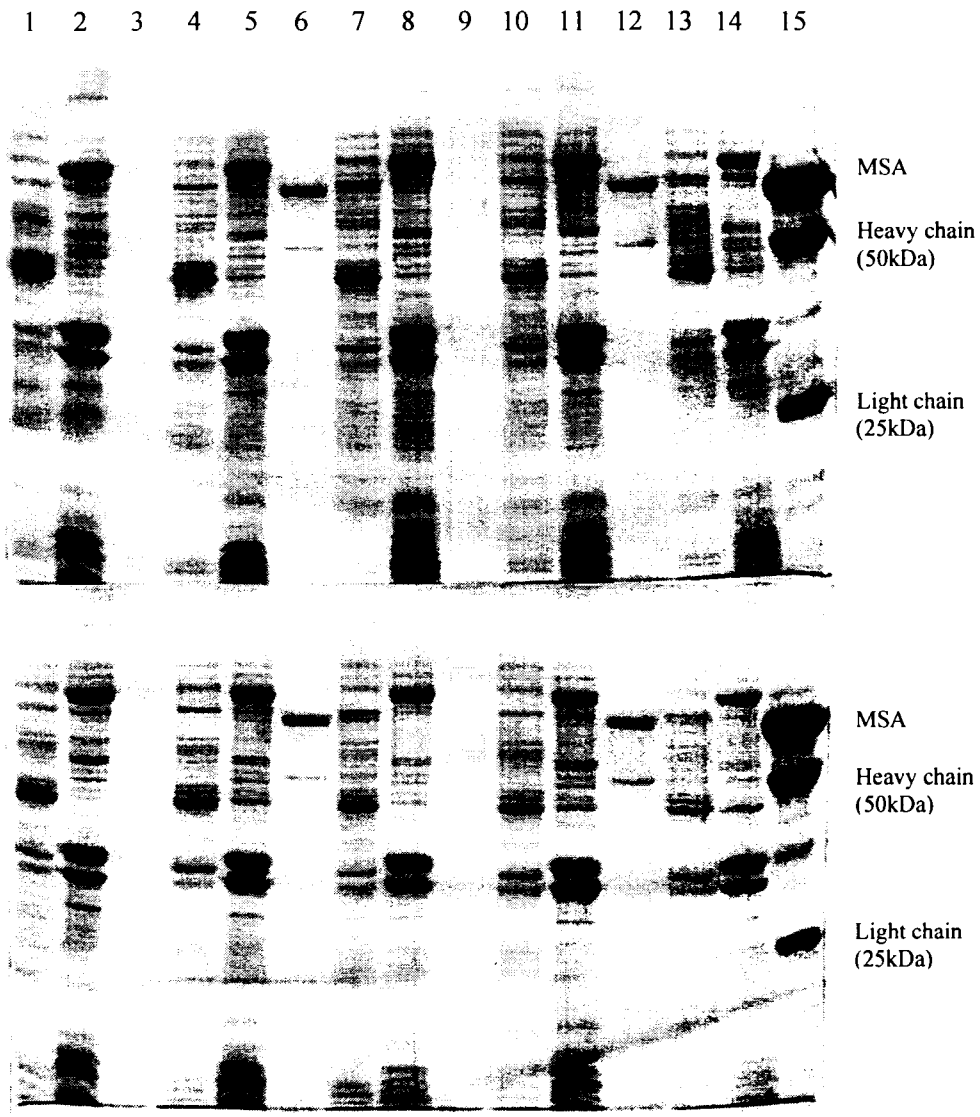

Fig. 4.4.8 SDS-PAGE of KDF541/pITS23 shocked with MAb4 for 5 minutes, 15 minutes, 30 minutes and two hours.

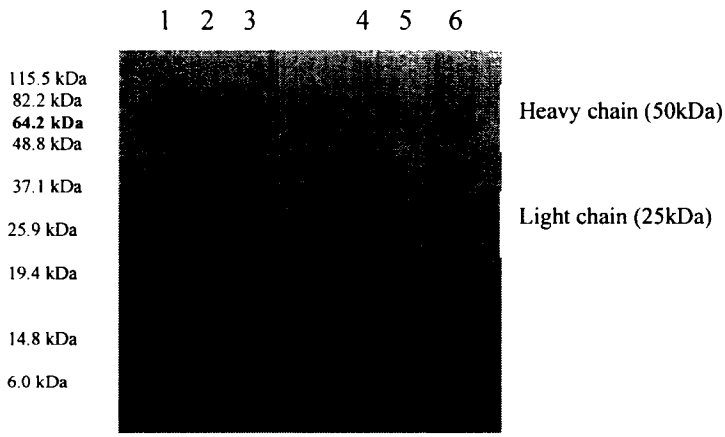

Fig. 4.4.9 Western blot. Cell samples were run on 10% SDS-PAGE. Gel was then transferred onto nitrocellulose membrane. The membrane was incubated with anti-TEV protease antibody or anti FepA N-domain antibody (MAb4), followed by goat-anti-mouse IgG conjugated with alkaline phosphatase, and developed with the substrate (sigma 104). Lanes 1 to 2 were KDF541/pITS23 shocked without and with TEV protease respectively. Lane 3 was protein ladder. Lane 6 was MAb4 stock. Lanes 4 and 5 were cell fluid of KDF541/pITS23 shocked in 0.2M Tris/0.3M $CaCl_2$ with 10 μl and 20 μl of MAb4 respectively.

Next, I used MAb1 to study. Results (Fig. 4.4.10) showed that a large amount of MSA, but little MAb1, was shocked into cells. MSA appeared in the supernatant, cell fluid, and membrane probably because MSA nonspecifically associated with the membrane as well as being equilibrated into the periplasm and the cytoplasm.

I did nutrition tests (Table 4.4.2) after I use osmotic shock to introduce MAb1 into bacteria. Results showed that bacteria after shocking procedure without antibodies always gave larger halos than bacteria without shocking. Bacteria after shocking with antibodies always gave smaller halos than bacteria shocked without antibodies.

I increased amount of MAb1 in the procedure. Results (Fig. 4.4.11) showed increasing of MAb1 will increase the amount of BSA in cell fluid, but not the amount of MAb1. NaCl wash got rid of non specific bindings.

I also incubated bacteria at 37°C with or without FeEnt after osmotic shock. Cells were applied to SDS-PAGE and ELISA assays. Results (Fig. 4.4.12) did not show any difference whether FeEnt was present or absent because of the small amount of antibodies in the periplasm initially.

Since KDF541 was found to contain a small portion of N domain to complement the function in N-domain deletion mutants (Postle et al., 2002), I also used OKN3, a site-directed chromosomal *fepA* deletion derivative of BN1071 (Fig. 4.4.13). Still no desired results were observed.

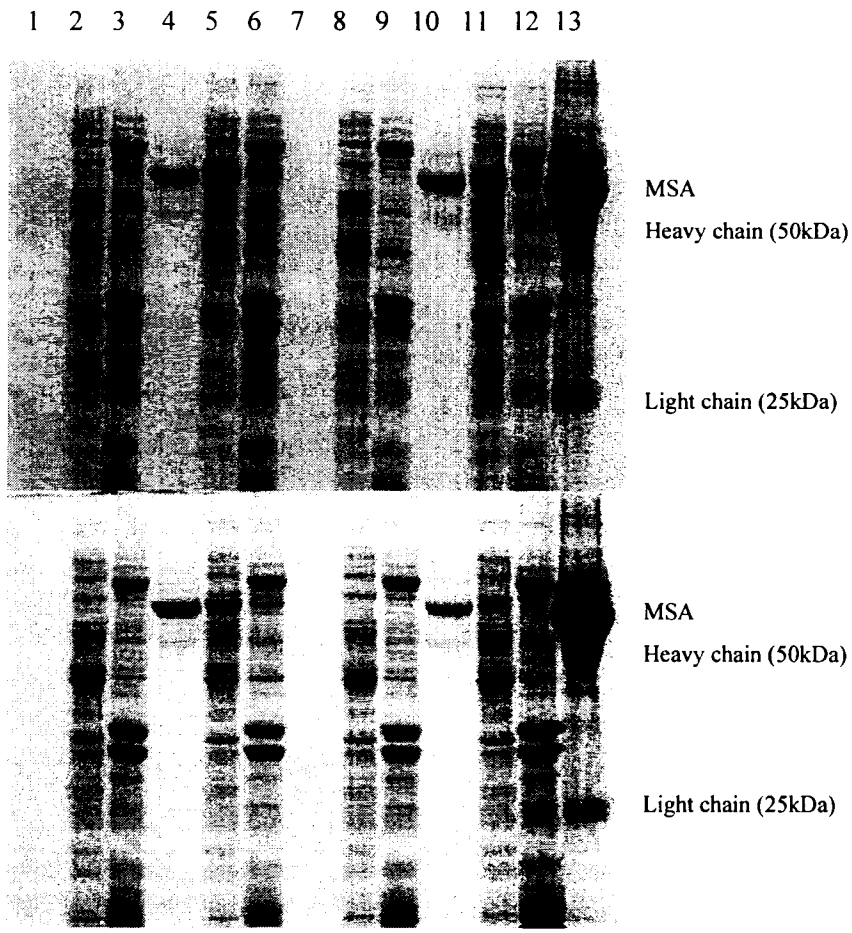

Fig. 4.4.10 Osmotic shock of KDF541/pITS23 with MAb1. Top, lane 13 was MAb1 stock dilution. Lanes 1 to 6 were cells shocked with 0.2M Tris/0.3M $CaCl_2$. Lane 1 was supernatant after NaCl wash of cells shocked without MAb1. Lane 1 was cell fluid of cells shocked without MAb1. Lane 3 was membrane of cells shocked without MAb1. Lanes 4 to 6 were same order as 1 to 3, but with MAb1. Lanes 7 to 12 were same order as 1 to 6, but shocked in 0.2M Tris/0.15M $CaCl_2$. Bottom, just like top, but lanes 1 to 6 were cells shocked with 0.2M Tris/0.1M $CaCl_2$; lanes 7 to 12 were cells shocked with 0.2M Tris/0.025M $CaCl_2$.

Table 4.4.2 Nutrition tests of bacteria after osmotic shock with MAb1.

	Strains	halo(mm)	appearance
NB Top agar	pITS23	17.5	sharp
	0.1M$CaCl_2$	22	faint
	0.1M $CaCl_2$/MAb1	18	sharp
	0.15M $CaCl_2$	22.5	faint
	0.15M $CaCl_2$/MAb1	18	faint
	0.3M $CaCl_2$	24	faint
	0.3M $CaCl_2$/MAb1	19.5	faint
LB Top agar	pITS23	16.5	sharp
	0.1M $CaCl_2$	17.5	faint
	0.1M $CaCl_2$/MAb1	15	sharp
	0.15M $CaCl_2$	19	faint
	0.15M $CaCl_2$/MAb1	16	sharp
	0.3M $CaCl_2$	21	faint
	0.3M $CaCl_2$/MAb1	17	faint
Trp Top agar	pITS23	16.5	sharp
	0.1M $CaCl_2$	18	faint
	0.1M $CaCl_2$/MAb1	16	sharp
	0.15M $CaCl_2$	19	faint
	0.15M $CaCl_2$/MAb1	16	sharp
	0.3M $CaCl_2$	21	faint
	0.3M $CaCl_2$/MAb1	17	faint

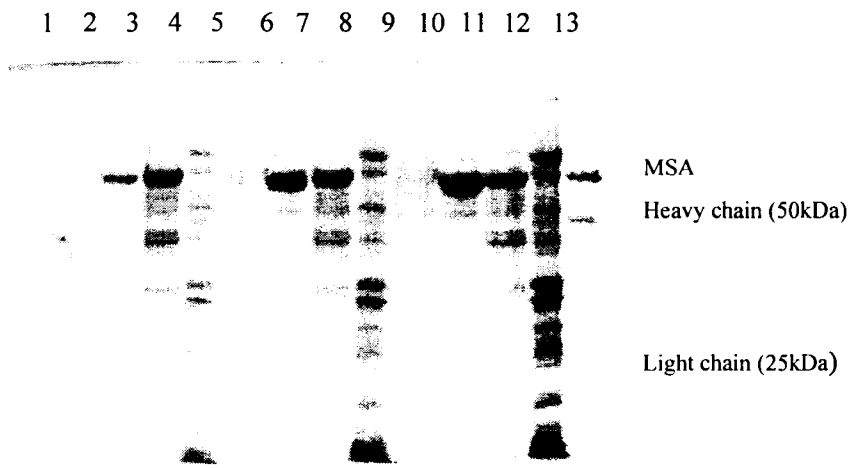

Fig. 4.4.11 Osmotic shock of KDF541/pITS23 with MAb1. Lanes 1-4 were cells shocked with 15 μL MAb1. Lanes 1 to 4 were supernatant after shock, supernatant after NaCl wash, cell fluid and membrane respectively. Lanes 5 to 8 and 9 to 12 were same order, but shocked with 25 μL and 35 μL MAb1 respectively. Lane 13 was MAb1 control (0.12 μL).

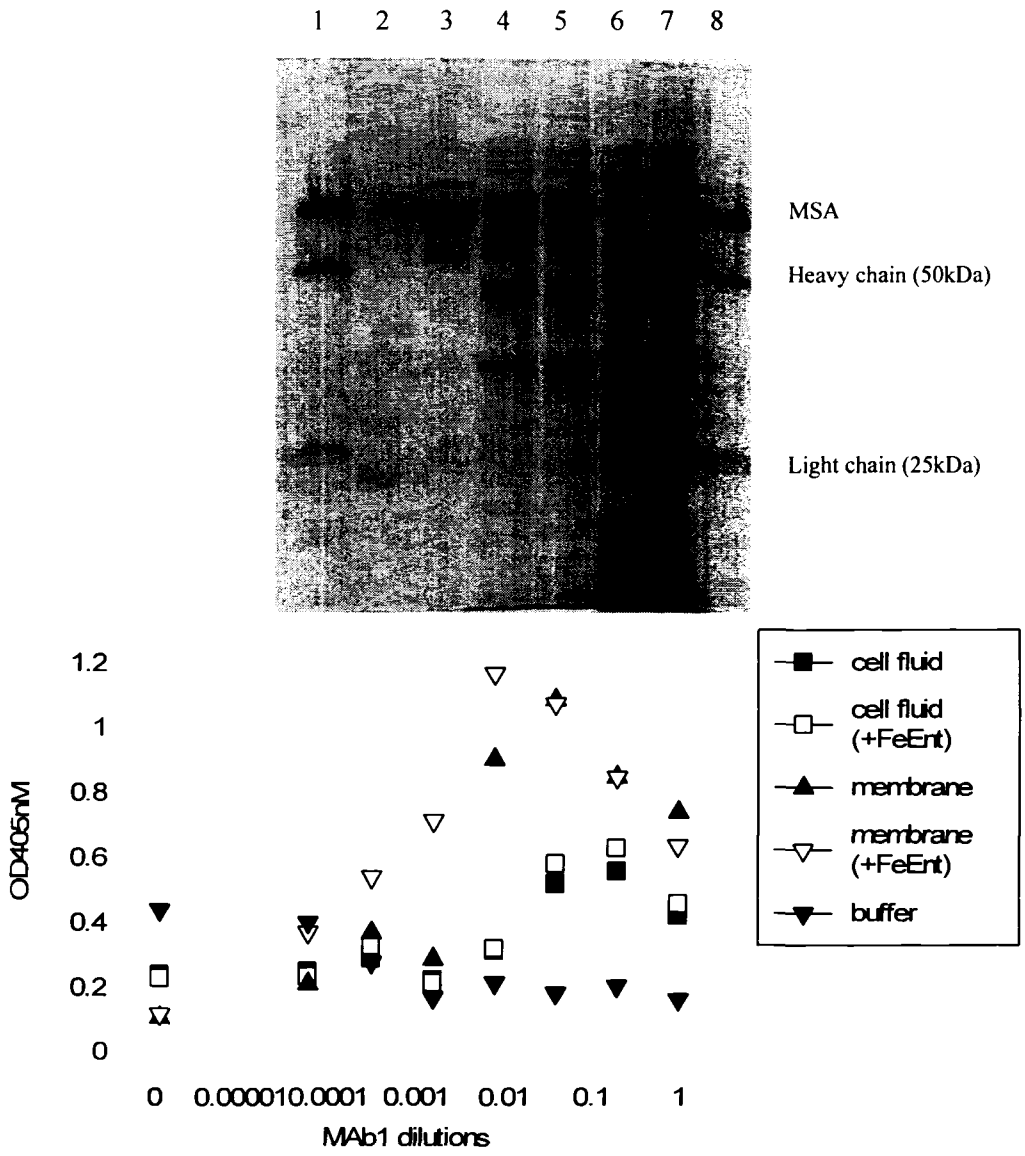

Fig. 4.4.12 Top, SDS-PAGE of osmotic shocked cells, followed by incubation at 37°C with or without FeEnt (10 μM). Lane 1 was MAb1 stock 0.17 μL. Lane 2 was the supernatant after shock. Lane 3 was the supernatant after NaCl wash. Lane 4 was cell fluid of cells shocked with MAb1, but incubated without FeEnt. Lane 5 was as 4 but with FeEnt. Lane 6 was as 4, but it was cell envelope. Lane 7 was as 5, but it was cell envelope. Lane 8 was MAb1 stock 0.12 μL. Bottom, ELISA of same treated cells. Bacterial samples were dried in a 96-well microtiter plate. The plate was coated with the Goat-anti-Mouse IgG coupled with alkaline phosphatase (AP). The plate was then developed with the phosphatase substrate sigma 104 (p-Nitrophenyl Phosphate).

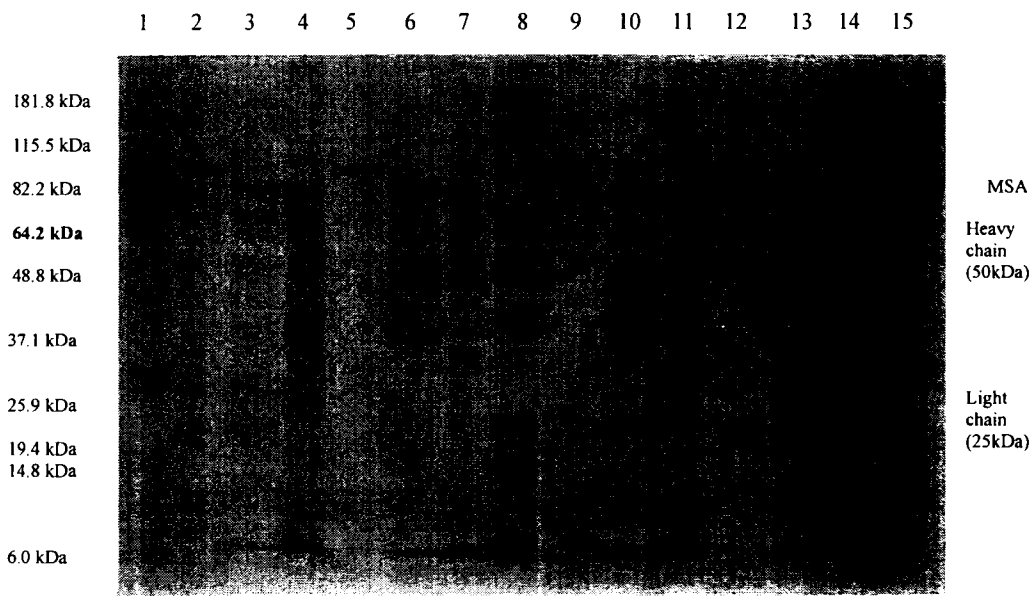

Fig. 4.4.13 Lanes 1 and 15 were MAb4 stock 0.12 µl and 0.23 µl respectively. Lane 8 was protein ladder. Lanes 2 to 4 were KDF541/pITS23 cells shocked with MAb4 NaCl wash, cell fluid, and cell envelope respectively. Lanes 5 to 7 were same as lanes 2 to 4 except cells were incubated with FeEnt after shocking. Lanes 9 to 14 were same as lanes 2 to 7, but strain was OKN3/pITS23.

Discussion:

Proteins that are smaller than 30 kDa were introduced into the periplasm by osmotic shock procedure (Zgurskaya *et al.*, 1999). Periplasmic maltose-binding protein (less than 40 kDa) were introduced into the periplasm by another method (Brass, 1986). Molecular weight of TEV protease and BSA is 27 kDa and 67 kDa, respectively. The osmotic shocking experiment proved that a decent amount of both of them can be easily introduced into cells by the second method due to their relatively smaller size, even though MSA is larger than 40 kDa. However, molecular weight of MAb is 150 kDa. I was not able to see a large amount of MAb1 introduced into cells. 0.2 M Tris/0.15-0.3 M $CaCl_2$ can introduce a very small amount of antibody into cells. I could not see incubation of cells with FeEnt at 37°C after osmotic shock decreased the amount of antibody in the periplasm, using SDS-PAGE, western blot, and ELISA. Only ^{59}FeEnt uptake experiments showed different results. Using the two osmotic shocking procedures, cells shocked with MAb4 had much decreased V_{max} (10- and 2- fold) compared to cells shocked without MAb4 and cells that were not shocked, in the 10-second uptake measurement. However, in 30-minute and 2-hour uptake measurements, no such differences were observed. Nutrition tests were done for cells shocked with MAb1. Cells after being shocked without antibodies seemed to have larger halos than normal cells. But when MAb1 was included in the shocking procedure, cells had smaller halos, sometimes even smaller than that of normal cells. Lots of possibilities exist. One is probably due to the small amount of antibody available in the cells for analysis. Second, no large amount of FepA proteins present in cells could interact with enough antibodies to make the difference visible in

SDS-PAGE and western blot. Third, the N domain may not exit the barrel to periplasm, which may not be consistent to other data (fluorescence labeling by colleagues in our lab).

Another problem was the recovery of cell membranes. When I tried to introduce TEV protease into the PP, bacteria looked normal with one time washing of 0.9% NaCl after osmotic shock. However, when I tried to introduce ascites fluids, I had to wash the bacteria several times with 0.9% NaCl before bacteria looked close to normal instead of aggregating together. Sometime bacteria were lysed no matter how many times I washed them. It seemed that some components in the ascites fluids alone or with $CaCl_2$ were responsible for bacteria lysis.

Because of the successful introduction of BSA into the periplasm, Fab fragment, 50 kDa, becomes a good candidate for the osmotic procedure, which I will discuss next.

Overall, this osmotic shocking experiment with anti N-domain antibodies was not successful.

4.5 Osmotic Shock of Fab Fragment

Immunoglobulins are large proteins (~150 kDa) that are composed of two heavy chains (~50 kDa each) and two light chains (~25 kDa each). The basic architecture of an antibody molecule is shown in Fig. 4.5.1. Two "arms" of the antibody, called F_{ab}, bind the antigens. The rest of the antibody is a conserved region called F_c. Between the Fab arms and the Fc is a flexible region called the hinge, that sensitive to proteolysis. Two disulfide bonds are present in the hinge (Fig. 4.5.1). Papain digestion usually occurs slightly above the disulfide bonds, releasing two 45 kDa fragments (F_{ab}). The production of F_{ab} has a couple of advantages over unprocessed ascites fluids in my experiments. One is its smaller size that makes it easier for me to introduce it into the periplasm of *E. coli* by osmotic shock procedure. The other is that the F_{ab} fragment contains the antigen binding domain but not the F_c fragment and it reacts more specifically to the antigen, although with lower affinity. So it will not produce as much nonspecific interaction as ascites fluids do.

The procedure of purification of mouse IgG and Fab fragments (Smith, 1993) will be discussed below. I chose anti-FepA MAb2 antibody because it recognizes the epitope around FepA amino acids 100 to 142 (Rutz *et al.*, 1991) and larger amount of ascites fluids of MAb2 was available in the lab. This epitope is only recognized by MAb2 when FepA is denatured, but not recognized when FepA is in native conformation. On the first day, I precipitated 25 mL of MAb2 ascites fluids using 60% ammonium sulfate, then solubilized and dialyzed the precipitate against 50 mM Tris buffer, pH8.0. Although this step is not absolutely necessary, removing irrelevant proteins will help with running a clean column later. The next day, I loaded the dialyzed ascites fluid on DE-52 column at

room temperature. I then washed the column and eluted with a 0-0.3 M NaCl gradient. I collected all the eluted fractions and used UV absorbance at 280nm to determine the protein concentration (Fig. 4.5.2). In the reference, a Mono-Q column was used to show that peak two was IgG molecules. Because I was using DE-52 column, and also each antibody is expected to run differently on the column, I used SDS-PAGE (Fig. 4.5.3), Western blot (Fig. 4.5.4), and ELISA (Fig. 4.5.5) to confirm the fractions that contain IgG molecules.

As shown in Fig. 4.5.3, fractions 82, 144, and 156 had one thick band above 64 kDa which represented the MSA. Fraction 46 and 54 had much less MSA. Fraction 144 also had a thick band at both 50 kDa and 25 kDa, which could represent the heavy chain and the light chain. Fraction 46 and 54 had a weak band around 50 kDa, which was probably the heavy chain. The light chain, however, was not visible. To confirm the identification of the bands, I did western blot with the same samples, as shown in Fig. 4.5.4. It turned out that the thick bands (50 kDa and 25 kDa) in fractions 144 were not reactive to goat-anti-mouse IgG, which suggested that those proteins were not heavy and light chains. Fraction 46 and 54 showed both heavy chain and light chain in the blot. Also, fraction 54 was much more strongly reactive. ELISA also confirmed the reactivity of fraction 46 to 62 to FepA proteins. ELISA titer was determined by the highest dilution that can give an absorbance of double the number of the negative control. Therefore, I pooled fraction 46 to fraction 62 for further purification.

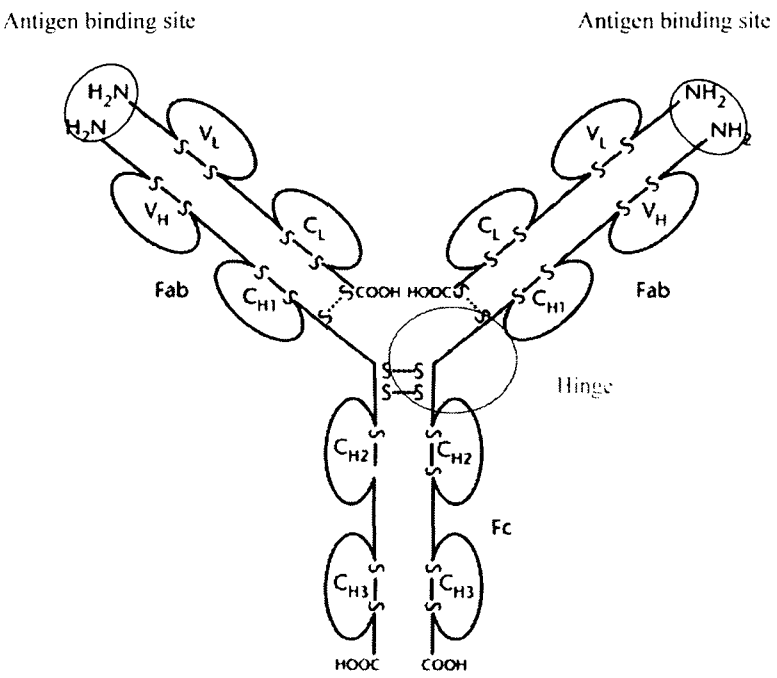

Fig. 4.5.1 Schematic drawing of an IgG molecule.

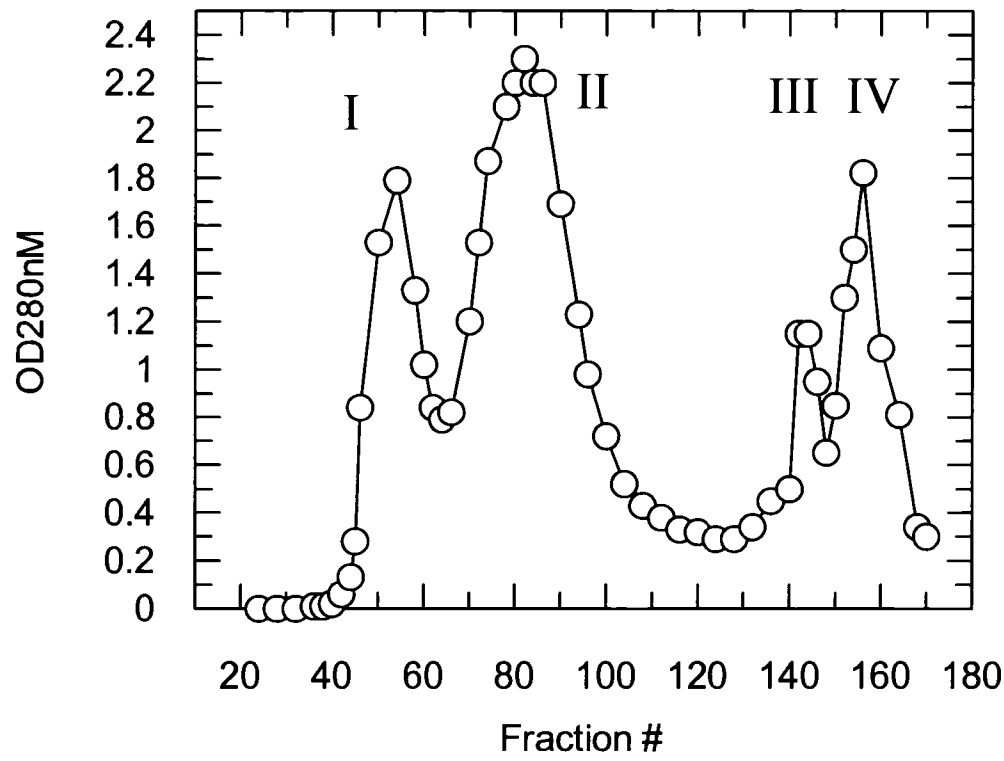

Fig. 4.5.2 Protein concentration was determined by UV absorbance at 280 nm for the DE-52 fractions of ascites fluids of MAb2.

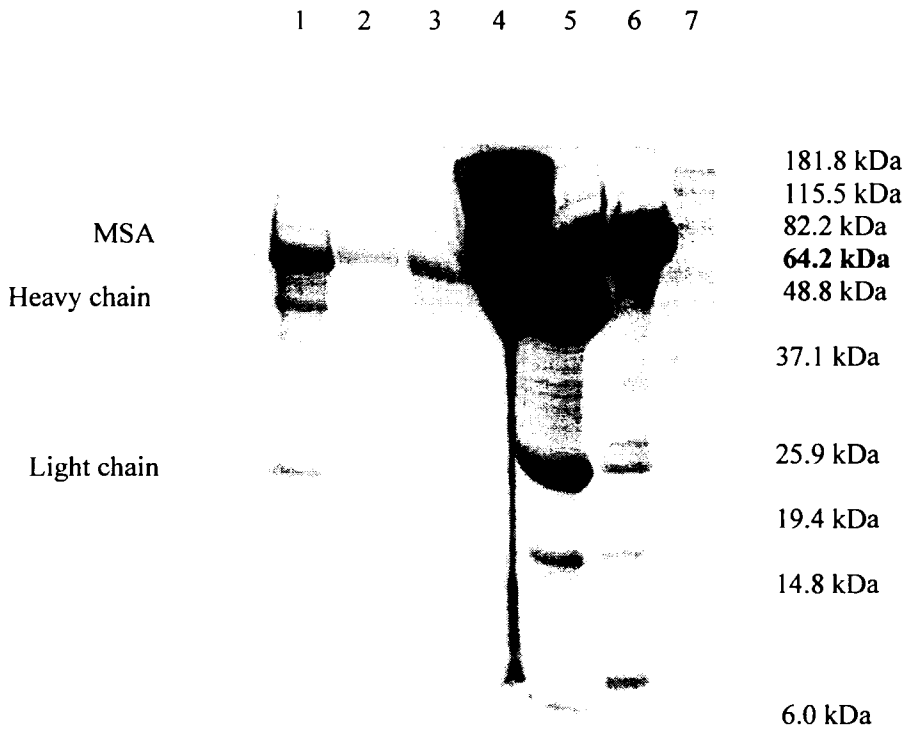

Fig. 4.5.3 SDS-PAGE of DE-52 fractions of ascites fluids of MAb2. Lane 1 was ascites fluid (1:300 dilutions); lanes 2 to lane 6 were fractions 46, 54, 82, 144 and 156, respectively; lane 7 was the protein ladder.

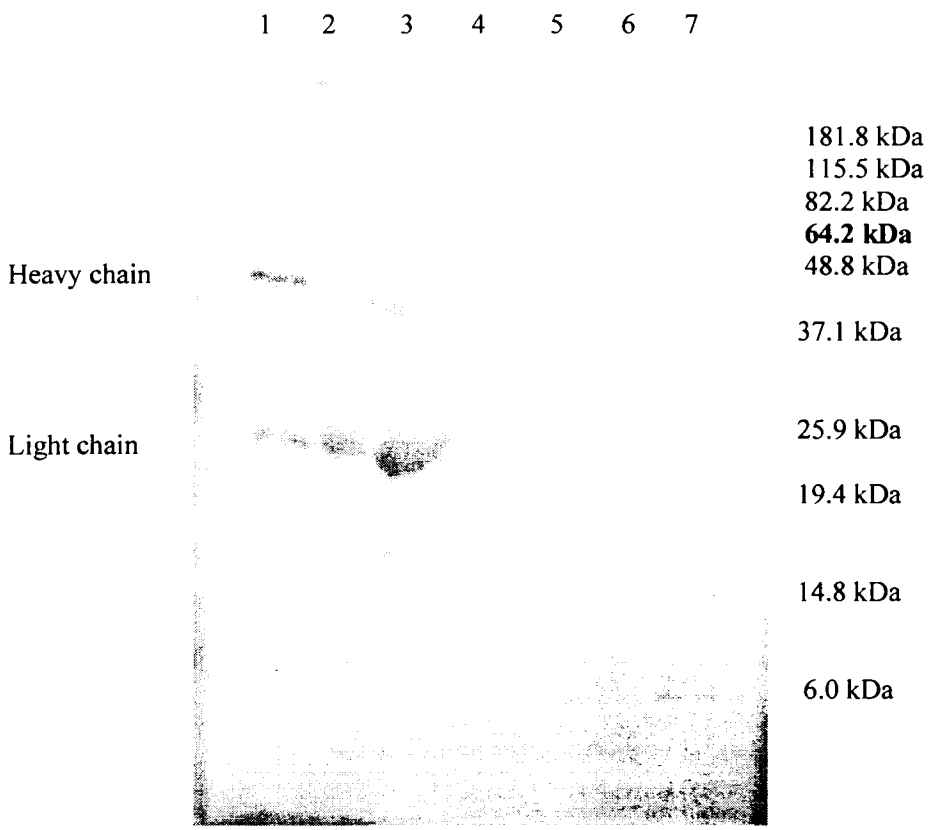

Fig. 4.5.4 Western blot of DE-52 fractions. Samples and their order were exactly same as those in Fig. 4.5.3. Samples run on 10% SDS-PAGE were transferred onto a nitrocellulose membrane. The membrane was then coated with goat-anti-mouse IgG coupled with alkaline phosphatase, and developed with the substrate sigma 104.

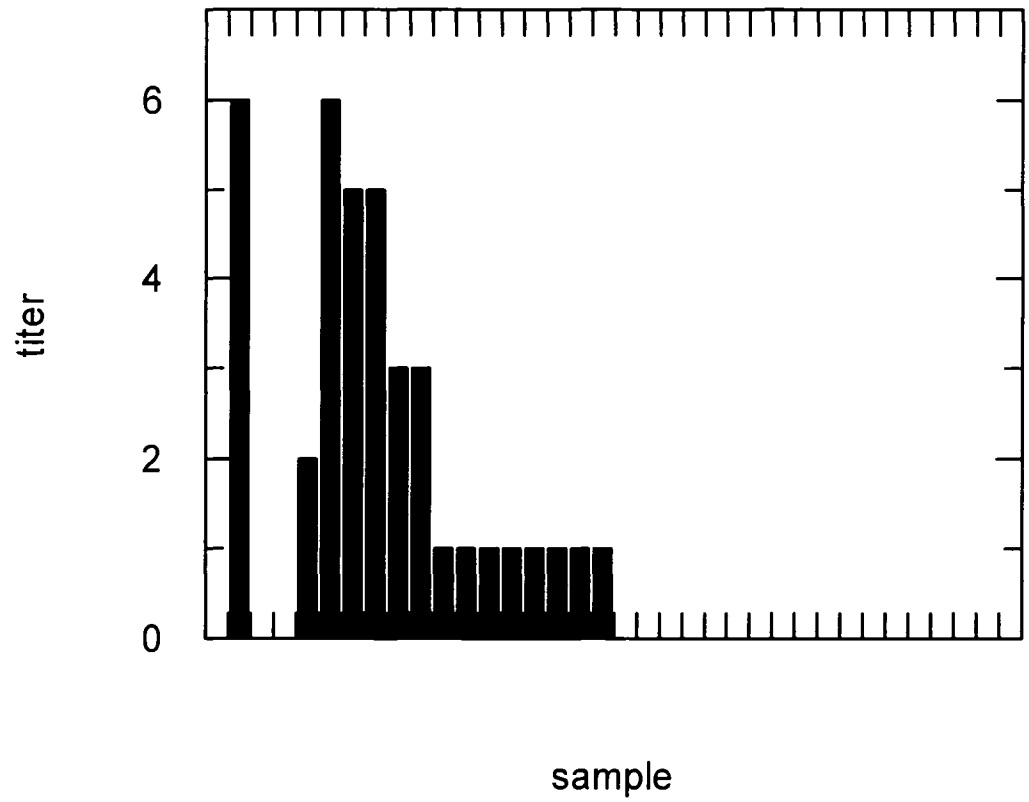

Fig. 4.5.5 ELISA of DE-52 column fractions. Procedure was the same as in chapter 4.3. Plates were first coated with 2 μg/ml of FepA proteins before different fractions were loaded. The left-most sample was ascites fluid. Starting from the second green bar were fractions 46, 50, 54, 58, 60, and 62. The rest was from 64 to the last fraction.

Once purified antibody was obtained, the next step was to cleave the antibodies with papain to achieve the F_{ab} fragment (Porter, 1959). Papain digestion condition was optimized with a serious of pilot experiments. Western blot (Fig. 4.5.6) showed that when BME was not added, IgG is 150 kDa (lane 1). When BME was added, I can see two major bands, corresponding to 50 kDa and 25 kDa (lane 15), as expected to be the heavy chain and light chain. After the papain digestion, the main band became 50 kDa without BME (lanes 2, 4, 6), which was the F_{ab} or the F_c fragment. When BME was present, I can see two bands (lanes 9, 11, 13). One was 50 kDa, which represented the F_{ab} fragment. The other was 25 kDa, which represented either the light chain part or the heavy chain part of the F_{ab} fragment, or half of the Fc fragment. I was not able to observe any difference when EDTA was added to the digestion reaction (lanes 3, 5, 7, 10, 12, 14). Also 10 hours did not improve the percentage of digestion when I compared lane 6 with lane 2.

To test if longer incubation time will improve the digestion, I digested the IgG with papain for up to 23 hours. Results (Fig. 4.5.7) showed that 23 hours digestion was almost complete digestion to 50 kDa without BME and 25 kDa with BME.

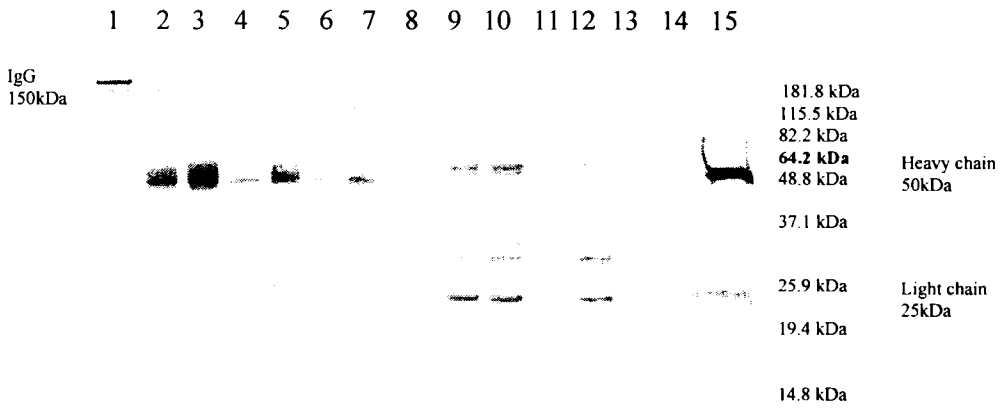

Fig. 4.5.6 Western blot of papain digestion of IgG. Lanes 1 to 7 were samples run without BME added in the sample buffer. Lane 1 was the Mab2 IgG; lanes 2 and 3 were digestion without and with EDTA for one hour, respectively; lanes 4 and 5 were digestion without and with EDTA for five hours, respectively; lanes 6 and 7 were digestion without and with EDTA for ten hours, respectively. Lane 8 was protein ladder. Lanes 9 to 15 were samples run with BME added in the sample buffer. Lanes 9 to 14 were the same sample order as lanes 2 to 7. Lane 15 was the Mab2 IgG with BME.

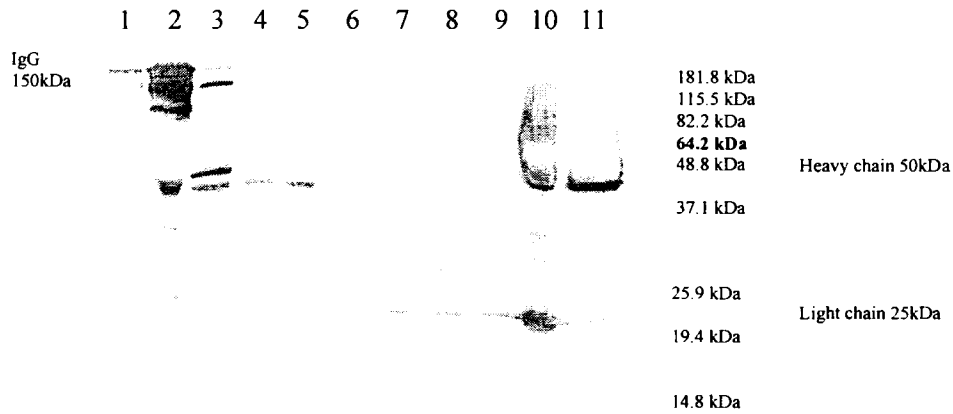

Fig. 4.5.7 Western blot of papain digestion reaction. Lanes 1 to 5 were samples without BME. Lane 1 was ascites fluid; lane 2 was concentrated IgG; lanes 3 to 5 were IgG digested with papain for 5, 10 and 23 hours, respectively. Lane 6 was protein ladder. Lanes 7 to 9 were same sample order as lanes 2 to 4. Lane 10 was concentrated IgG; lane 11 was ascites fluid.

After the papain digestion, I loaded the reaction onto a DE-52 column. I first washed the column with 0.02 M Tris buffer, pH7.8, and collected the wash, which was supposed to be my F_{ab} fragment (Fig. 4.5.8). Then I eluted the column with a 0-0.1M sodium chloride gradient, and collected the elutes (Fig. 4.5.8). As shown in Fig. 8, the washes (lanes 3 and 4) contained very pure Fab fragments, which were supposed to be 50 kDa. When BME was added to the samples (lanes 10 and 11), Fab fragment was reduced to 25 kDa because the disulfide bonds were disrupted.

To test the relative reactivity of the Fab fragment to FepA protein *in vivo,* and with goat-anti-mouse IgG, I ran whole cell lysates of KDF541 (*fepA*-) and KDF541/pITS23 (*fepA+)* on SDS-PAGE, transferred the gel to nitrocellulose membrane, and then coated the membrane with 1:500 MAb2 ascites fluid, 1 :100 MAb2 IgG, and 1 :100 MAb2 F_{ab} fragment for overnight. The next day, I coated the membrane with goat-anti-mouse IgG, and developed the membrane. Results (Fig. 4.5.9) showed that at certain dilution factor, they had similar reactivity to FepA proteins and goat-anti-mouse IgG together. However, F_{ab} fragment had much less non-specific reactivity.

The purification and the functionality of MAb2 F_{ab} fragment was completed and confirmed in the pilot experiments. Large scale purification was then carried out and results were shown in Fig. 4.5.10. The final purified F_{ab} fragment was shown in lane 10 in Fig. 4.5.10 (A) as compared to the previously purified F_{ab} fragment in small scale experiment (lane 1). However, elute 1 and 2 also contained quite a lot of F_{ab} fragment. So I performed another western blot (Fig. 4.5.10 (B)) to look at all the other elutes from DE-52 column. I found that elute 1 to 4 did contain lots of Fab fragment. Elute 5 to the last contained F_c fragment which is a little larger than F_{ab} fragment. To study how the F_{ab}

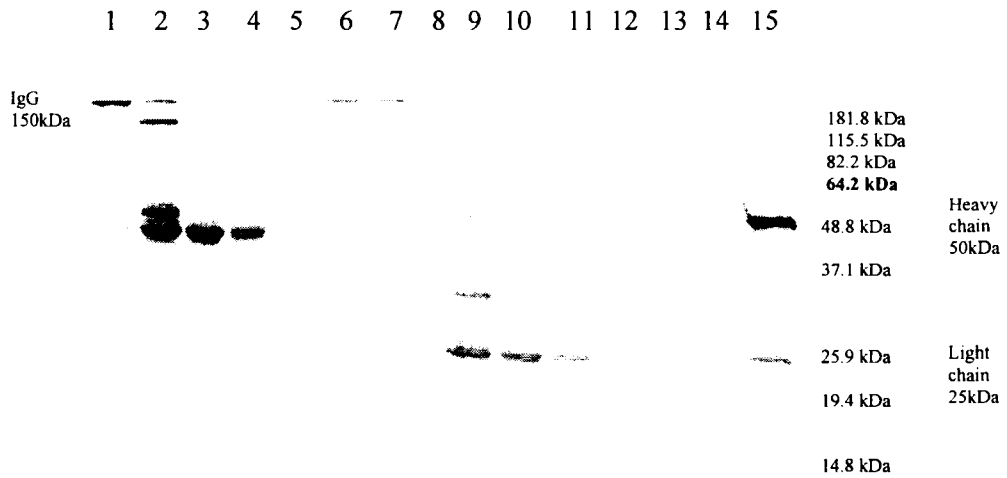

Fig. 4.5.8 Western blot of large scale papain digestion of MAb2. Lanes 1 to 7 were samples without BME. Lane 1 was ascites fluid; lane 2 was digestion reaction; lanes 3 and 4 were different washes after the papin digestion was loaded onto the DE-52 column; lanes 5 to 7 were different elutes. Lane 8 was protein ladder. Lanes 9 to 15 were samples with BME. Lane 9 was concentrated IgG; lanes 10 to 14 were the same order as lanes 3 to 7; lane 15 was ascites fluid.

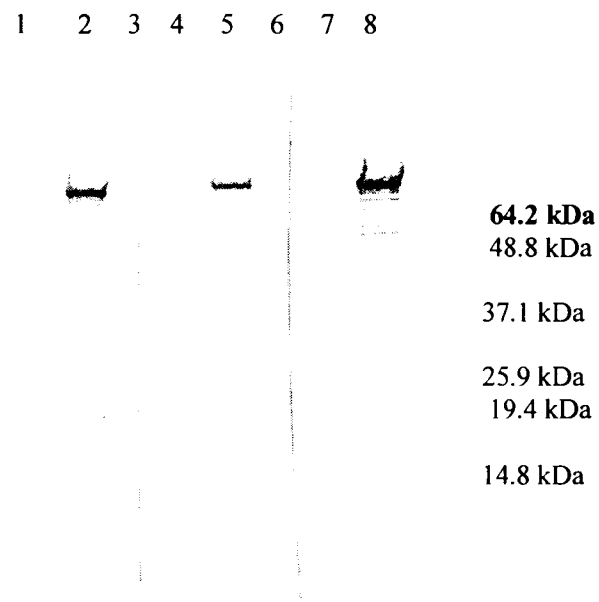

Fig. 4.5.9 Western blot. Lanes 1, 4, and 7 were whole cell lysates of KDF541. Lanes 2, 5 and 8 were whole cell lysates of KDF541/pITS23. Lanes 1 and 2 were coated with MAb2 IgG. Lanes 4 and 5 were coated with Mab2 Fab fragment. Lanes 7 and 8 were coated with MAb2 ascites fluid. Lanes 3 and 6 were protein ladders.

fragments can be stored, I froze 0.5 mL of purified F_{ab} fragment and also 0.5 mL of F_{ab} fragment with 20% glycerol added at -20°C. The rest stayed at 4°c in the cold room. A few days later, I thawed out the frozen F_{ab} fragment, and did western blot (Fig. 4.5.10 C) and ELISA (Fig. 4.5.11) with them. It turned out that F_{ab} fragments were intact and still had the same ELISA titer after being frozen for a few days, indicating that they could be stored at -20°c with or without glycerol.

ELISA was then used to check the purified F_{ab} fragment. As shown in Fig. 4.5.11, the F_{ab} fragment (elute fractions 1 and 2) was very reactive to the purified FepA protein although the ELISA titer was not as high as the titer of the MAb2 ascites fluid. Elute fractions 6-11 from the DE-52 column showed very high ELISA titer because of the presence of the impurity of MAb2 IgG.

To summarize, the purified F_{ab} fragment has very good specificity and very high reactivity to the FepA protein compared to the MAb2 ascites fluid. The weak point of this purification was that it takes a lot of ascites fluids to make a decent amount of F_{ab} fragment because lots of proteins were lost in various steps, including ammonia sulfate precipitation, papain digestion, and ion exchange chromatography.

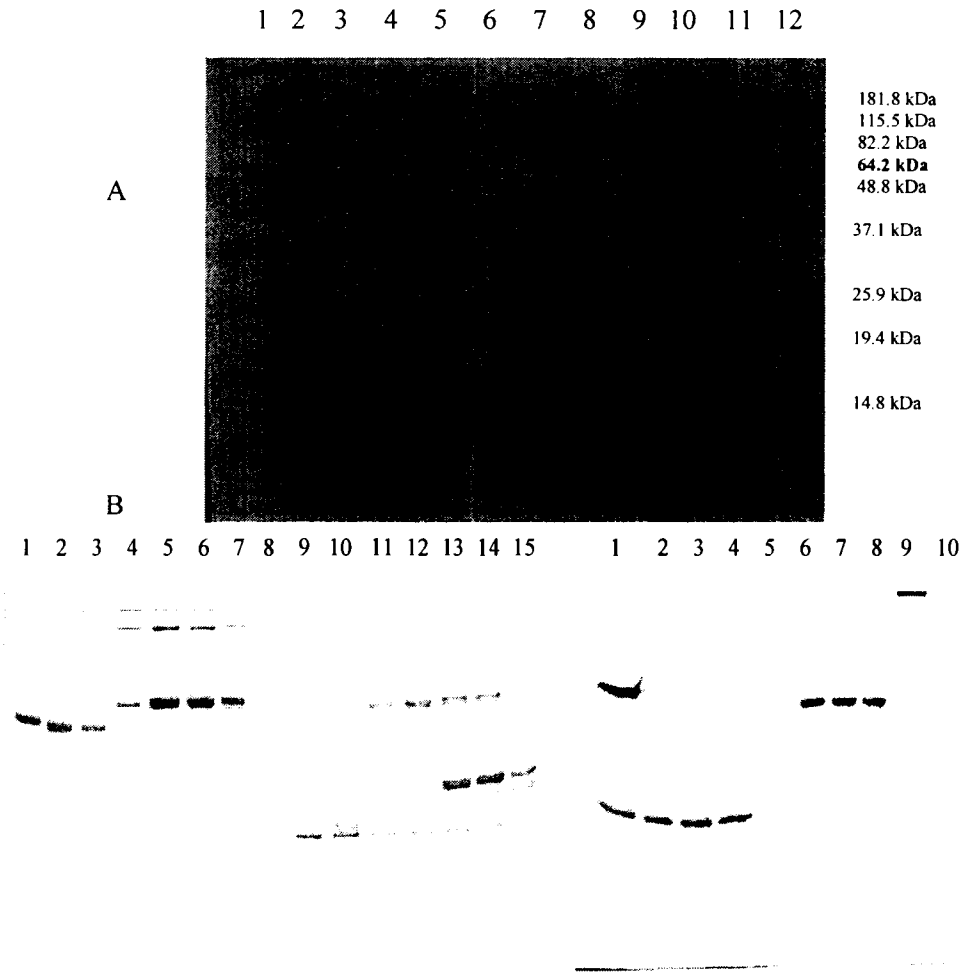

Fig. 4.5.10 Western blot of samples from purification of F_{ab} fragment. A. Lanes 1 to 5 were samples without BME. Lane 1 was Fab fragment from the pilot experiment; lane 2 was Fab washed off the DE-52 column after papain digestion; lanes 3 to 5 were elute 1.2 and 6. Lanes 6 and 12 were protein ladders. Lanes 7 to 11 were the same as lanes 1 to 5, except BME is added. B. Lanes 1 to 7 was samples without BME. They were elute fractions 1, 3, 4, 5, 7 and 8, respectively; Lane 8 was protein ladder. Lanes 9 to 15 were the same sample order as lanes 1 to 7, except BME was added. C. Lanes 1 to 4 was samples with BME. Lanel was diluted MAb2 ascites fluid; lane 2 was F_{ab} fragment stored in the cold room; lane3 was Fab fragment frozen at -20°C; lane 4 was F_{ab} fragment frozen at -20°c with 20% glycerol. Lanes 5 and 10 were protein ladders. Lanes 6 to 9 were the same sample order as lanes 2 to 5, except BME was not present.

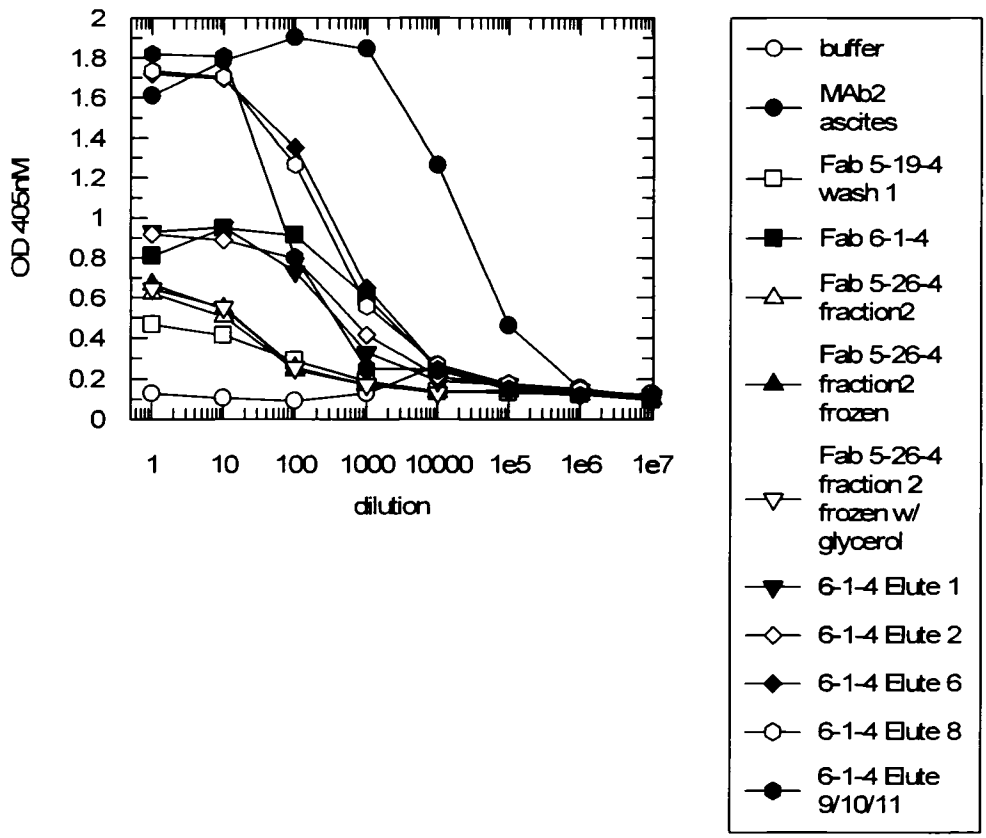

Fig. 4.5.11 ELISA with coated purified FepA protein on the microtiter plate. Samples were as labeled on the right side of the graph. From top to bottom on the right panel, first sample is ELISA washing buffer as a negative control; 2nd to 7th samples are Fab fragments from different dates; rest of them are fractions of elutes containing presumably Fc fragments and undigested IgG molecules. Procedure was the same as in chapter 4.3.

Osmotic shock procedure was performed with purified MAb2 F_{ab} fragments. However, I cannot shown a very clear presence of Fab fragment inside of the periplasmic space where I desired. This suggested that not enough amount of F_{ab} fragment entered the periplasm during osmotic shock, although I was able to find a small amount of F_{ab} fragment present in the cells in about 50% of the osmotic shock experiments (Fig. 4.5.12). 10 μl of F_{ab} fragment seemed to give a clear band about 50 kDa and a faint band of around 25 kDa (only seen on the actual nitrocellulose membrane) in lane 11. I could only see very faint band around 50 kDa and 25 kDa when less or more amount of F_{ab} fragment was added to the cells. However, I could not see F_{ab} fragment in the buffer that I used to wash the cells after it was mixed with F_{ab} fragment (lane 3 to 8). So it seemed that most of the F_{ab} fragments that were added to the cells were missing. Then I tested the supernatant after centrifugation of the osmotic shocked bacteria (Fig. 4.5.13). Still, not very much F_{ab} fragment was present as shown in lane 2 to 7.

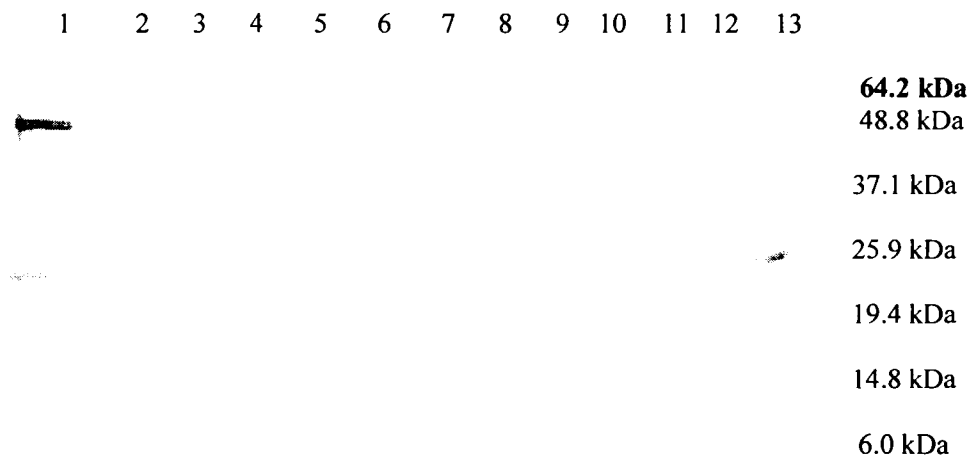

Fig. 4.5.12 Western blot of the osmotic shock samples. Lane 1 was diluted MAb2 ascites fluid. Lane 13 was diluted MAb2 F_{ab} fragment. Lane 8 was protein ladder. Lanes 2 to 6 were supernatant after spinning down the osmotic shocked cells. Lane 2 was cells shocked without F_{ab} fragment. Lanes 3 to 6 were cells shocked with increasing amount of F_{ab} fragment, 2 μl, 10 μl, 20 μl, and 50 μl respectively. Lanes 8 to 12 were whole cell lysates with the same order as lanes 2 to 6.

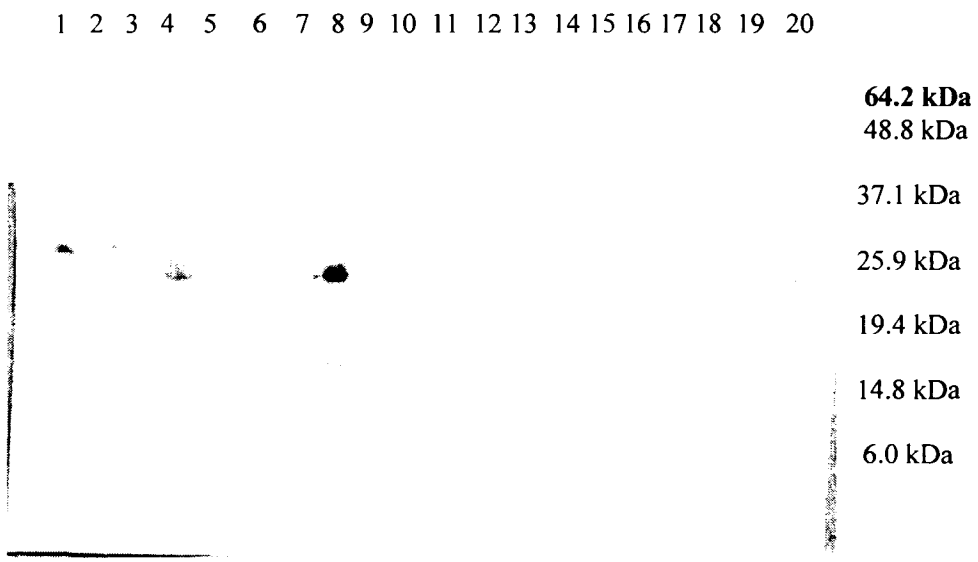

Fig. 4.5.13 Western blot of bacteria after osmotic shock. Lanes 1 and 8 were diluted MAb2 F_{ab}. Lane 14 was protein ladder. Lanes 2 to 4, 9 to 13, and 15 to 20 were bacteria shocked for 30 minutes. Lanes 2 to 4 were the supernatant right after the shocking procedure and centrifugation of the bacteria shocked without F_{ab}, with 10 μl of F_{ab} and with 100 μl of F_{ab}, respectively. Lanes 9 to 11 were the buffer that is used to wash the bacteria after osmotic shock, same order as lanes 2 to 4. Lanes 15 to 17 were the final whole cell lysate. Rest lanes, 5 to 7, 12 to 13 (sample for shocking without F_{ab} is missing), and 18 to 20, were bacteria shocked for two hours. They were the same order as the three samples right by their left side.

One possibility of missing total F_{ab} fragment is that F_{ab} actually entered the periplasm, but somehow it got degraded by proteases. To test this idea, I used an *E. coli* strain called SF120 (Baneyx *et al.*, 1991). Several proteases associated with the cell envelope of *E. coli* have been isolated. Four of them, OmpT (Sugimura *et al.*, 1988 a and b), DegP (Strauch *et al.*, 1988 and 1989), protease III (Dykstra *et al.*, 1984; Finch *et al.*, 1986), and protease IV (Ichihara *et al.*, 1984 and 1986), have been cloned and characterized. SF120 is an *E. coli degP ptr ompT* mutant. In this strain, *OmpT* is inactivated by the insertion of a chloramphenicol cartridge into the *ompT* gene, protease III is inactivated by insertion into *degP* gene, and so is *ptr*. I then transformed pITS449 (*fepA*+) into SF120 and tried to shock the Fab fragment into the bacteria. However, I achieved exactly the same results (data not shown, but looked just like Fig. 4.5.12) as I saw with KDF541/pITS23. I still could not find where most of the F_{ab} fragment was, although I was able to see a small amount of F_{ab} present as size of 50 kDa and 25 kDa in the bacteria.

I also tested the functionality of FepA protein in the shocked bacteria by performing ^{59}FeEnt quantitative transport assay. Bacteria used were BN1071 (chromosomal FepA) and KDF541/pITS23 (*fepA*+ in pHSG575). Results (Fig. 4.5.14 A) showed that osmotic shock procedure did not compromise the bacteria a lot. It also told me that bacteria still transported when F_{ab} was present, which suggested that the presence of a small amount of F_{ab} fragment inside of the cells did not interact with the periplasmic side of FepA and then block the channel. In another transport experiment (Fig. 4.5.14 B), I found that bacteria almost stopped transporting iron after two hours, probably because all the FeEnt was used up. When I looked at the viability of bacteria after osmotic shock,

I found more than 75% of the bacteria were able to survive after the osmotic shock procedure.

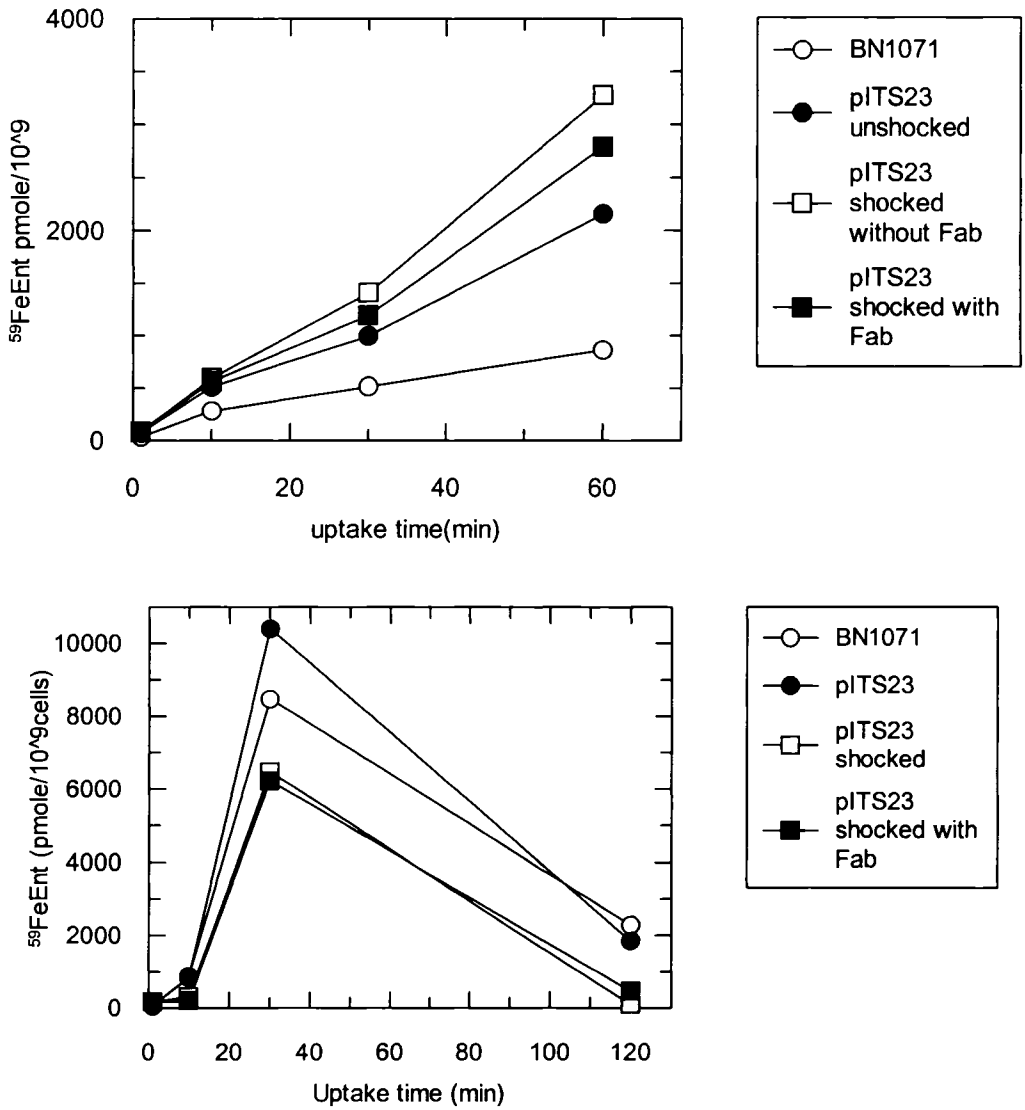

Fig. 4.5.14 ^{59}FeEnt transport assay of KDF541/pITS23 cells after osmotic shock with F_{ab} fragment. Samples are explained on the right panels of the graphs.

In summary, I was able to get very pure F_{ab} fragment purified from anti FepA N-terminal MAb2 ascites fluids. The purified F_{ab} fragment was highly reactive to purified FepA protein and FepA protein expressed *in vivo*. However, I could not observe a large amount of the F_{ab} fragment in the periplasmic space of bacteria, although the size of F_{ab} fragment is small enough. After osmotic shock and French-Press, majority of the F_{ab} fragment I used in the experiments were not detected in either the supernatant after shock, supernatant from washing steps, cell fluids, or cell envelopes. Also the experiments with proteases defective strains did not prove the possibility that the proteases degraded the Fab fragment in the cells. I was not able to find where most of the F_{ab} fragment used in the procedure went. Only a small amount of F_{ab} fragment was in the cells. The only other possibility in my mind, which is very unlikely though, was that the structure of the F_{ab} fragment changed in the reconstitution buffer which contains high concentration of calcium chloride so that the goat-anti-mouse IgG could not recognize it any more. This possibility requires either complete disruption of the structure of the F_{ab} fragment or the epitopes recognized by goat-anti-mouse IgG being hided due to the structural changes because the goat-anti-mouse IgG can recognize it even when the F_{ab} fragment is denatured by SDS. This possibility can be tested in the future by simply incubating the Fab fragment in the reconstitution buffer for certain amount of time and then applying it to Western blot to see if it can be recognized and show a band at the right size. However, this is unlikely because MSA and TEV protease can be detected after the osmotic shock experiment with ascites fluids. Quantitative ^{59}FeEnt uptake experiment did not show any difference between the bacteria shocked with and without a small amount of F_{ab} fragment.

Discussion:

Before I tried all the above methods, I tried Tobacco Etch Virus (TEV) NIa protease first. TEV protease is a very useful tool in molecular biology. It recognizes a seven amino acid consensus sequence, Glu-X-X-Tyr-X-Gln-Ser/Gly, where X can be various amino acids, and last residue can be either Ser or Gly. Cleavage occurs between the Gln and Ser or Gly residues. TEV protease is a small protein about 27 kDa that can get into the periplasm of *E. coli*. I engineered TEV cleavage site into different location of the N domain of FepA. If the N domain or a part of the N domain that contains the TEV cleavage site exits β-barrel, the TEV cleavage site may be exposed in the periplasm. Once TEV protease enters the periplasm, it will find and cleave the target. As a result, size of the FepA protein will get smaller that can be detected in SDS-PAGE and Western Blot. A FepA mutant with residues 94 to 100 replaced by TEV cleavage site was shown to grow upon FeEnt. Also, I was able to introduce a decent amount of TEV protease into the PP of E. coli (Fig. 4.4.9). However, I did not observe a smaller FepA protein in a few initial experiments although the experiment needs to be optimized as far as the cleavage condition in the periplasm is concerned, which one of my colleagues was working on. I did find that at 37°C, some proteins are subject to cleavage. I also constructed three more FepA mutations (see methods) that contained the TEV protease recognition sequence in different location of the N domain. However, they were not able to grow upon FeEnt in nutrition assays, which suggested that the structure of FepA were not intact in the OM and it was not functional in the OM. In the future, more such mutants could be constructed, and they can be used to test the activity of TEV protease in the PP as long as the mutants are functional at FeEnt transport.

This chapter contained most of my unpublished data. In chapter 4.3, 4.4, and 4.5, data did not seem to explain what I wanted to show. Although TEV protease and BSA could easily enter the PP, the same method could not be applied to either ascites fluids or F_{ab} fragments. The large size of IgG may explain why it could not enter the PP, but F_{ab} fragment, which is smaller than MSA, showed an unexpected result: it disappeared.

4.6. Transport in the Periplasm only

Escherichia coli FeEnt transport apparatus contains outer membrane transporter (FepA), periplasmic FeEnt binding protein (FepB), inner membrane iron transport system (FepDCG), and TonB/ExbB/ExbD (presumably energy supply system). Although the mechanism of inner membrane iron transport is not yet clear, FepC protein is presumably an ATP-binding component of the inner membrane iron transport system. I looked at outer membrane transport process of *E. coli* by comparing the FeEnt uptake between strains containing *fepC* and strains with *fepC* deleted. Without FepC, I expect bacteria will not be able to iron transport across the inner membrane will not occur.

TJB1 and TJB1/fepC- strains were from Dr. McIntosh's lab. ^{59}FeEnt uptake of these two strains (Fig. 4.6.1) showed that uptake by TJB1 strain was almost linear to the concentration of ^{59}FeEnt, indicating that this strain was transporting iron throughout the whole hour. However, the iron uptake of TJB1 *fepC*- strain was saturated at very low concentration of iron (below 1 nM).

UT5600 and UT2300 strains (Elish *et al.*, 1988; McIntosh *et al.*, 1979) were the other pair of strains tested. Both strains were spontaneous *fepA* mutants of *E. coli* (Elish *et al.*, 1988; McIntosh *et al.*, 1979). They are *fepA* derivatives of RW193 (*fepA+*, *fhuA+*,

Leong & Neilands, 1976), which is a derivative of AB1515 (*fepA*+, *E. coli* Genetic Stock Center). UT2300 has complete deletion of *fepC* gene (Elish *et al.*, 1988). I then transformed pITS23 plasmid (pHSG575 plasmid cloned with complete *fepA* gene) into both UT5600 and UT2300. Results (Fig. 4.6.2) were very similar to what I have already seen with TJB1 and TJB1 *fepC*, but still not exactly same. When the near complete uptake apparatus is present (UT5600/pITS23, a very small portion of *fepC* is missing), utilization of iron within one hour time period seemed to be a saturable process, with K_m~1.9 nM and V_{max} 28 pmole/10^9/min. When *fepC* is fully deleted (UT2300/pITS23), the uptake reached maximum rate of only 1 pmole/10^9/min at 2 nM concentration. And the difference of transport affinity between these two strains is negligible.

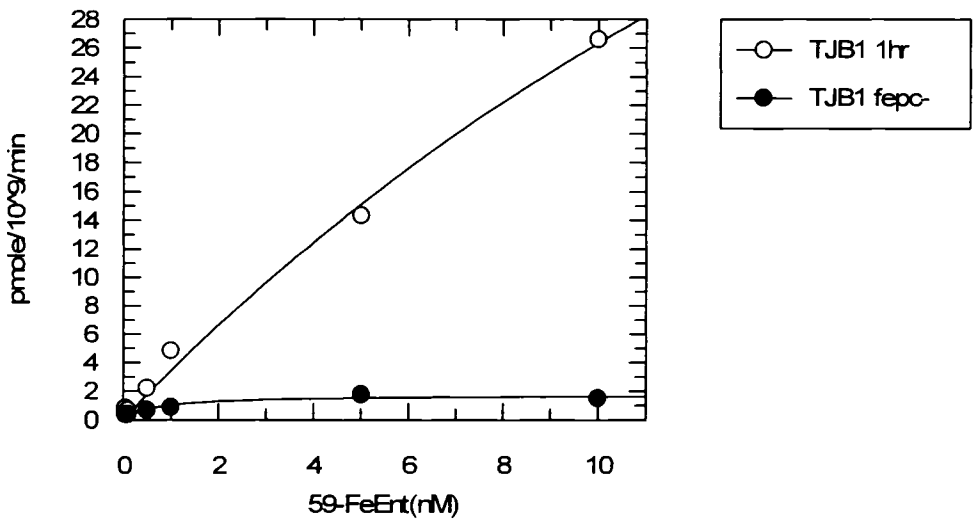

Parameter	Value	Std. Error
Vmax	101.7656	38.6683
Km	28.6160	14.0379

Parameter	Value	Std. Error
Vmax	1.7197	0.2047
Km	0.6741	0.3030

Fig. 4.6.1 One hour ^{59}FeEnt uptake of TJB1 and TJB1 *fepC*- strains.

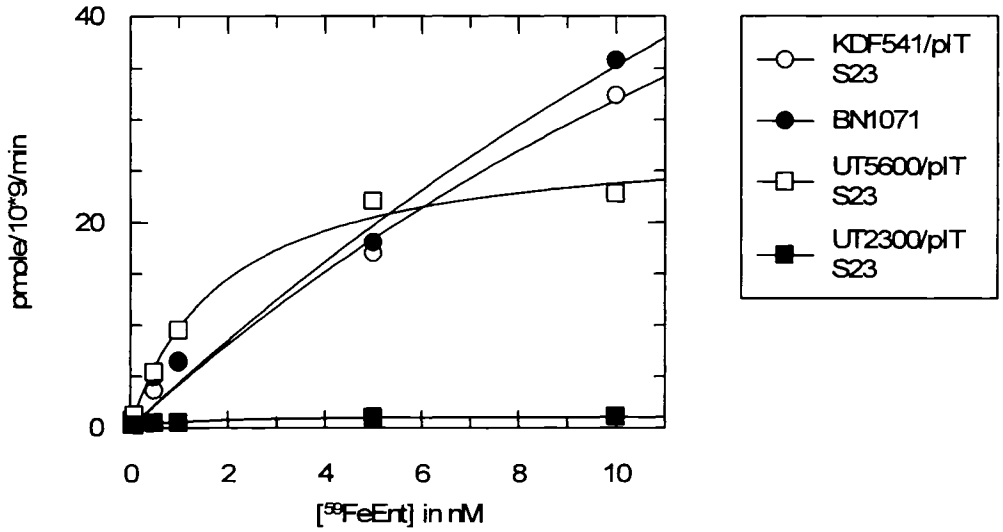

Parameter	Value	Std. Error
Vmax	119.8532	59.9301
Km	27.5424	17.9266

Parameter	Value	Std. Error
Vmax	163.7123	108.6700
Km	36.4440	29.7649

Parameter	Value	Std. Error
Vmax	28.3328	1.4823
Km	1.9054	0.3104

Parameter	Value	Std. Error
Vmax	1.1538	0.1462
Km	0.9268	0.4207

Fig. 4.6.2 One hour ^{59}FeEnt uptake of UT5600 and UT2300 (presumably *fepC*-) strains.

4.7 Examine Residue 2-12 of FepA

TonB box (residue 13 to 19 of FepA; Larsen *et al.*, 1997), which is located near the amino terminus as a highly conserved seven-residue motif, was shown to be essential for the interaction between TonB protein and FepA protein. Certain mutations in the TonB box abolish the transport of TonB-dependent ligands without altering the ability of the receptor to bind ligand. However, two studies (Braun *et al.*, 1999; Scott *et al.*, 2001) showed that, without the N domain, the β-barrel still bound and transported FeEnt although with impaired affinity. This suggested that FepA functions without the N domain and this finding contradicted with the previous finding that the interaction of the N domain with TonB is essential for the transport of FeEnt.

What is the role of the residues upstream of the TonB box? Are they also involved in the interaction with TonB? To study these questions, I constructed a residue 2 to 12 (EPTDTPVSHDD) deletion mutant on FepA. These 11 residues include four negatively charged residues that may interact with the C terminus of TonB where positively charged residues seem to dominate over negatively charged residues on the surface of the C-terminus of TonB and a KP repeat (Larsen *et al.*, 1993) of TonB was proposed to interact with FhuA. Nutrition test of the mutant (Table 4.7.1) showed no difference from the wild type. This result confirmed the results of Braun's and Scott's studies that the N domain is dispensable for the uptake of FeEnt. Transport assay needs to be performed to find out the effect of the deletion on the transport kinetics. However, in colicin killing assay (Table 4.7.1), the mutant showed 3- to 4-fold decrease of colicin sensitivity. One possible explanation is that colicins may interact with residue 2 to 12 during the binding process due to the large sizes of the colicins.

Table 4.7.1 Phenotypes of residue 2-12 deletion mutant of FepA.

Strains	Nutr. (mm)	ColB	ColD
KDF541	-	-	-
KDF541/pITS23	17.5	$8*10^6$	$3*10^4$
KDF541/pITS23/Δ2-12	17.5	$2*10^6$	10^4

Discussion:

FepC (Shea, 1991) is the inner membrane ABC binding component of FeEnt transport system in *E. coli.* No study has been done with this protein so far. This study showed a linear increase of iron uptake in one hour period. However, iron uptake was saturated quickly (very low K_m) without FepC present in the cytoplasm. What happens is probably when FeEnt is transported into the periplasm by FepA, presumably the iron-binding protein, FepB, will bind FeEnt and transfer it to the cytoplasm, where the FepDGC system will transport FeEnt into the cytoplasm before FeEnt is degraded by Fes protein and Fe^{3+} then is reduced to Fe^{2+} that is used in metabolisms. This whole process will keep a constantly low concentration of Fe^{3+} in the periplasm and cytoplasm. As a result, FepA will transport more iron until extra ferrous iron together with the Fur protein forms a complex that binds the promoter region of FepA and represses the transcription of FepA protein, which did not happen in a one hour uptake period. Without FepC, however, Fe^{3+} will stay in the periplasm instead of going into the cytoplasm and being reduced there. Concentration of Fe^{3+} in the periplasm will quickly become very high. This will probably signal the FepA to terminate the transport of iron from extracelluar environment in an unknown pathway. Similarly, deletion of either the periplasmic iron-binding protein FepB or the cytoplasmic permeases FepD and FepG will also lead to fast saturation of iron transport, which can be done in the future.

Once FeEnt is internalized into the PP, the iron binding protein, FepB will bind FeEnt. 4000 copies of FepB (Sprencel *et al.,* 2000) are expressed from the chromosome in one cell. So there are $4*10^{12}$ copies of FepB in 10^9 cells. If one FepB protein binds to one molecule of FeEnt, then $4*10^{12}$ molecules of FeEnt can be bound maximally, which

correspond to about 6 pmole of FeEnt. Considering of the V_{max} (1.2 pmole/10^9/min) of FeEnt transport by UT2300/pITS23, the FepC deficient strain, approximately every 4-5 copies of FepB bind to one molecule of FeEnt. In TJB1/*fepC*- strain, approximately every 3-4 copies of FepB bind to one molecule of FeEnt. This indicates that before more FepB proteins bind to FeEnt, bacteria produce some kind of signal to stop the OM transport process. On the other hand, ratio of FeEnt to FepB proteins is larger than 16:1 in TJB1 strain and 27:1 in BN1071. This suggests that, in wild-type strain, once FeEnt is bound by FepB in the PP, FepB will quickly transfer FeEnt to the IM ABC transport system and the IM transporters will then quickly transport FeEnt into the cytoplasm (CM). This whole process from the PP to the CM must be quick enough to keep extra FepB proteins available in the PP and drive the OM transport process towards the direction of PP by keeping the iron concentration in the PP low. However, I was surprised to find out that even in FepC deficient strain, majority of the FepB proteins (80% in UT2300/pITS23 and 70% in TJB1/*fepC*-) were still free to bind more FeEnt. This suggests two things. One is that the expression of FepB is related to the expression of FepDGC. The other is that extra copies of iron-binding protein may be one way how bacteria respond to the intracellular iron concentration in iron-replete or iron-deplete environments.

Chapter 5. Iron Uptake of Gram-positive bacteria

5.1 *Listeria monocytogenes*

Interested operons. The genome sequence of *L. monocytogenes* (2,944,528 base pairs) (Glaser *et al.*, 2001) was completed in 2001. Four potential Fur-regulated iron transport systems (Fig. 5.1.1), at 2.031mb (the *fur* region), 2.184 Mb (the *feo* region), 2.27 Mb (the *srtB* region), and 2.499 Mb (designated the *hupDGC* region), were chosen to study based on their homology, which will be discussed later, to other known iron uptake systems. They all contain a well-conserved Fur box. Among these, the *srtB* region has been studied (Newton *et al.*, 2005). This region is shown to be regulated by Fur. SrtB is surface located, and SvpA is a secreted protein that is identified by LPxTG motif. However, neither SvpA nor SrtB is identified to be involved in the transport of heme, hemoglobin or ferrichrome.

Site-directed in-frame chromosomal deletions. I generated chromosomal deletion mutants in a wild-type *Listeria monocytogenes* strain: EGD-e (Glaser *et al.*, 2001). The putative membrane permease encoded by *lmo2183* was deleted, and combined with another deletion mutant *Δlmo1960* (a putative ATP-binding protein) to make a double mutants. Also other mutants were made in our lab, including *Δlmo2429* (*ΔhupC*), *Δlmo1959* (*ΔfhuD*), *Δlmo1960* (*ΔfhuC*), *Δlmo1961* (*Δor*), *Δlmo943* (*Δfri*), *Δlmo1956* (*Δfur*), *Δlmo2105* (*ΔfeoB*), *Δlmo929* (*ΔsrtA*), *Δlmo2181* (*ΔsrtB*), *ΔsrtAB*, *ΔInLAB*, and *ΔPrfA*. In total, 14 mutants were assessed together with the wild-type strain. The deletion mutations of the rest genes in these four operons need to be completed in the future.

The site-directed chromosomal deletion procedure includes a few major steps (Fig. 5.1.2 and Fig. 5.1.3). First, I amplified two fragments with proper restriction digestion sites incorporated upstream and downstream of the target gene. Then I amplified the ligation product of the two fragments and cloned it into the thermo-sensitive vector pKSV7 (Smith *et al.*, 1992). The clone was transformed into an *E. coli* strain DH5α. Plasmids were purified and verified by PCR. Then the correct plasmid was transformed into *Listeria monocytogenes* competent cells. Bacteria were incubated at 30°C and transformants were verified by PCR with a small portion of bacteria. Transformants were then grown at 30°C, subcultured in LB with 5 μg/mL of chloramphenicol, and shaken at 37°C or 42°C. I plated out the final culture on LB plus chloramphenicol (5 μg/mL) plates, and incubated the plates at 37°C. Because pKSV7 only replicates at 30°C, any colony developed on the plates at 37°C should be integrants. Then I inoculated the integrants and passed through at least 6 times at 42°C in LB without chloramphenicol. Finally, I plated out the culture on the LB plates and screened for chloramphenicol sensitive clones. Final verification by colony PCR was done to show the deletion on chromosome. Sequence analysis was also completed later to confirm the deletion.

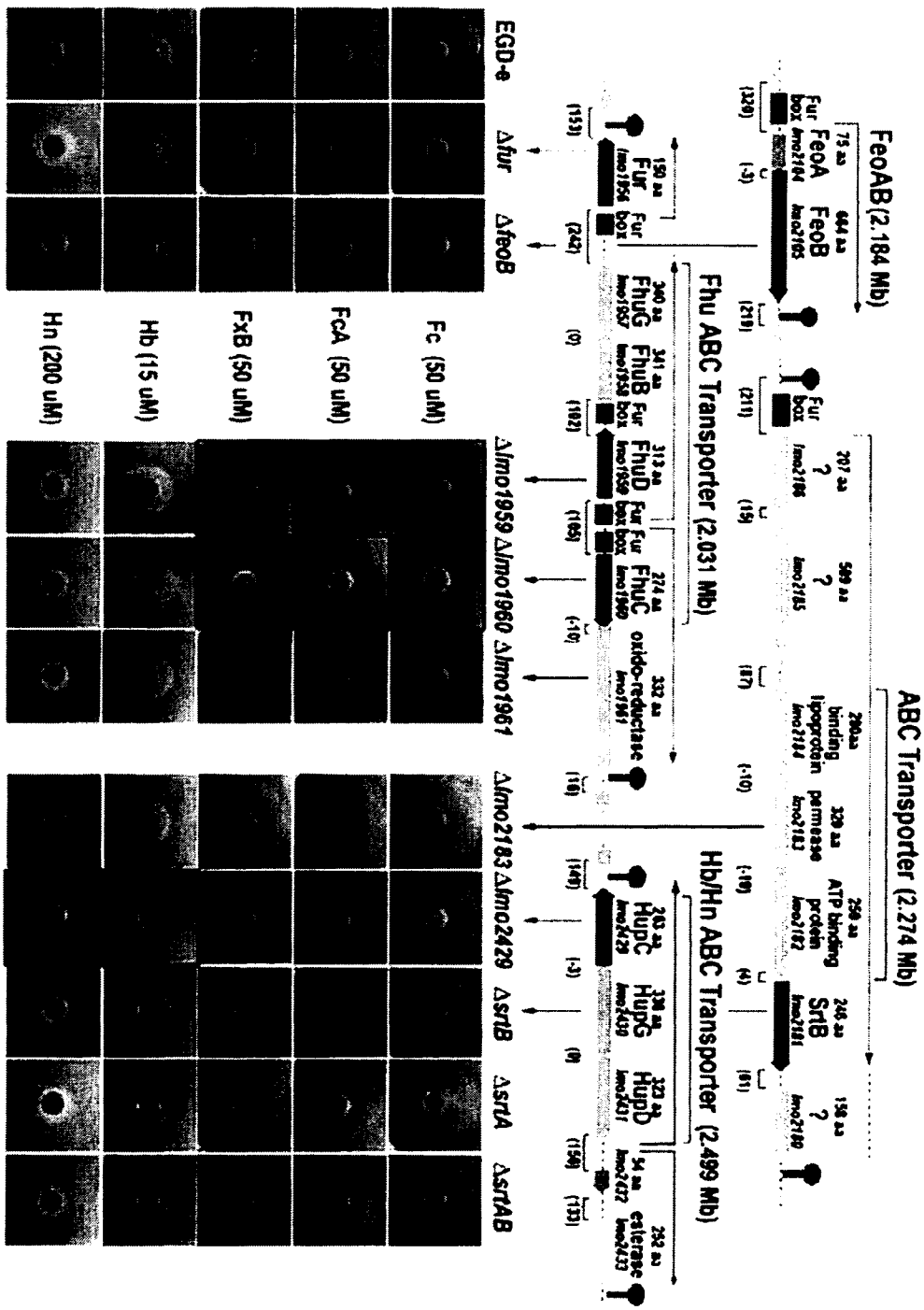

Fig. 5.1.1 Target operons that may be involved in the iron utilization and nutrition tests of EGD-e strain and its derivatives.

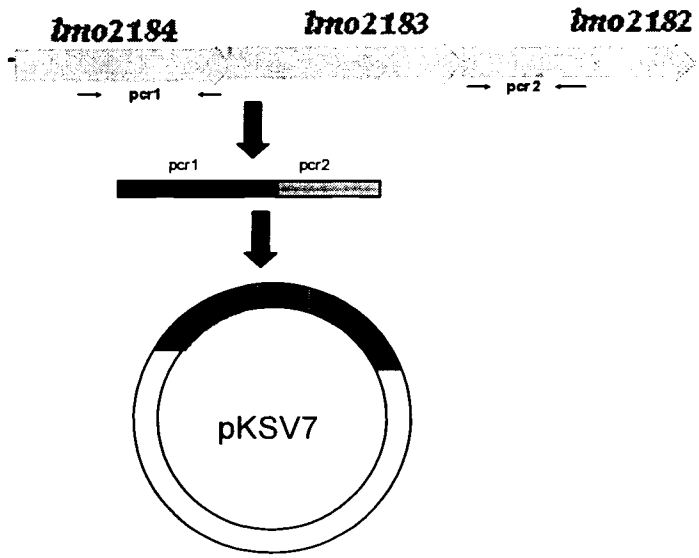

Fig. 5.1.2 Cloning of deletion mutation in pKSV7. To delete gene *lmo2183*, I cloned two PCR products, upstream "pcr1" and downstream "pcr2", onto a thermosensitive vector pKSV7, then transformed the clone into *E. coli* for its expression.

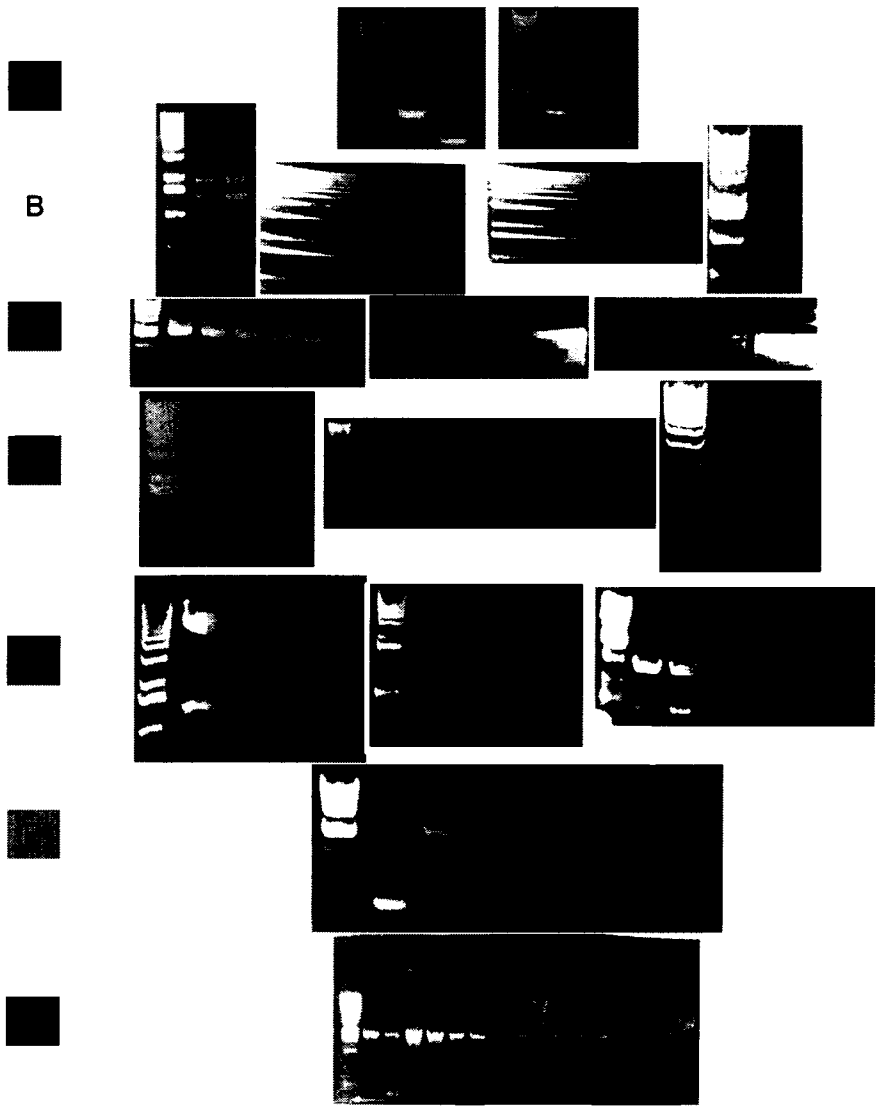

Fig. 5.1.3 1% agarose gel pictures showing the complete cloning process. A. PCR of two fragments upstream and downstream of my target gene. B. Ligation of the two PCR products and purified from agarose gel. C. PCR of the ligation product. D. Clone the ligation product onto pKSV7, transform into DH5α, and confirm the transformants by colony PCR with M13 primers. E. Confirm transformants by restriction digestion and confirm they are *Listeria*. F. Confirm integrants by primers designed separately to check integrants. G. Confirm final chromosomal deletion mutant with either new designed "check" primers or the two "extremity" primers: one is the upstream primer of of PCR1; the other is the downstream primer of PCR2.

Table 5.1.1 Siderophore nutrition tests and mouse infection experiments with EGD-e and its mutant derivatives.

Strain	Region	Transport										LD_{50}
		Fc/A		FxB		Hb	Hn	HTf	Ftn	FeCit	$FeSO_4$	
		50	1	50	1	15	200	13	9	20	20	
EGD-e	NA	25	16	23	14	15	10	20	14	15	14	$10^{4.5}$
Δfri (lmo943)	*fri*	28	17	28	18	15	10	20	12	14	14	ND
Δfur (lmo1956)	*fur*	31	22	28	18	16	10	14	11	12	12	$10^{7.5}$
ΔfhuD (lmo1959)	"	**0**	**0**	**0**	**0**	15	10	19	14	15	15	$10^{4.5}$
ΔfhuC (lmo1960)	"	**0**	**0**	**0**	**0**	16	10	18	14	14	14	ND
Δor (lmo1961)	"	23	15	22	10	15	9	18	14	14	14	$10^{4.5}$
ΔfeoB (lmo2105)	*feoAB*	25	15	25	13	14	9	19	15	15	15	$10^{4.5}$
ΔfhuC (lmo2183)	*srtB*	24	15	24	14	14	10	20	12	14	14	ND
ΔsrtB (lmo2181)	"	25	15	25	13	14	9	20	15	14	13	$10^{4.5}$
ΔhupC (lmo2429)	*hupDGC*	25	14	22	12	**0**	**0**	18	15	15	15	$10^{6.2}$
ΔsrtA (lmo929)	*srtA*	23	14	22	12	14	9	18	11	15	15	$10^{6.4}$
ΔsrtAB	NA	25	15	25	13	14	9	17	11	14	14	ND
ΔPrfA	NA	25	16	23	13	14	ND	ND	ND	ND	ND	ND
ΔInlAB	NA	30	17	21	12	18	ND	ND	ND	ND	ND	ND

For nutrition tests, the tabulated values represent the diameter (in mm) of the halo of growth surrounding a paper disc embedded with 10 μL aliquots of the test compound. Fc, FcA, FxB Hb and Hn were tested on BHI agar containing 0.1 mM BP; HTf, Ftn, FeCit and $FeSO_4$ were tested on KRMT agar plates. Fc and FcA were evaluated at 50 and 0.5 μM; the two hydroxamate siderophores always gave similar growth halos with all the strains, and the results of 3 or 4 experiments with each compound were averaged and tabulated in column (Fc/A). The concentrations of all other iron compounds are also micromolar; each tabulated value represents the mean of 3 or 4 tests, which had minimal variation. NA, not applicable; ND, no data.

Qualitative iron uptake: siderophore nutrition tests. To determine the ability of *L. monocytogenes* EGD-e wild-type strain and its derivatives to utilize different iron sources to support their growth, I applied nutrition tests. I used apoferrichrome A as the chelator to remove the residual iron existing in the medium when I examed Gram-negative bacteria (Annamalai *et al.*, 2004). However, Gram-positive bacteria were shown to utilize apoferrichrome A as their iron source (Fig. 5.1.1). As a result, I used α, α'-bipyridyl (BP) as the iron chelator in the medium. BP restricted growth of *L. monocytogenes* in BHI media and nutrition tests on BHI agar plates when 0.1 mM of BP was applied. Siderophores that I tested on BHI agar plates include ferrichrome (Fc), ferrichrome A (FcA), ferrioxamine B (FxB), hemin (Hn), and hemoglobin (Hb). Data here (Table 5.1.1) also includes human transferrin (HTf), ferritin (Ftn), ferric citrate (FeCit), and ferrous sulfate ($FeSO_4$), which were tested by Dr. Klebba on KRMT agar plates. I first grew bacteria in BHI overnight. Next day, I subcultured them in BHI to OD_{600nm}=0.1, added BP to 0.1 mM, and allowed them grow a few hours to mid-log at 150 rpm and 37°C.

Results (Fig. 5.1.1; Table 5.1.1) of nutrition tests showed that all the compounds could stimulate the growth of wild-type EGD-e on the plates. All derivatives could utilize all the compounds more or less, except that ferrichrome, ferrichrome A, and ferrioxamine B could not stimulate the growth of *ΔfhuD (Δlmo1959)* and *ΔfhuD (Δlmo1960)*, and hemin and hemoglobin could not stimulate the growth of *ΔhupC (Δlmo2429)*. Because of the poor solubility of Hn and Hb, the halos displayed by wild type and its derivatives were very small. These results suggested that the *hupDGC* might encode a hemin and hemoglobin uptake system, and *fhuDGC* might encode an Fc, FcA, and FxB uptake system. This required further quantitative and kinetic binding and transport assays to

characterize and confirm. Furthermore, *Δfri* and *Δfur* had different phenotypes. Although they utilized Fc, FcA, and FxB, the growth halos were much larger compared to the halos of the wild type. And *Δfur* had a much smaller halo when HTf was applied. This also required future investigation. Although I was not able to show stimulation of growth of *L. monocytogenes* by FeEnt and FeTrn, subsequent radioactive binding and transport assays showed that *L. monocytogenes* transported these two siderophores at very low rates, which might explain why I did not see halos in nutrition tests. I also tested *ΔPrfA and ΔInlAB* with Fc, FcA, FxB, Hb and Hn. Their growth halos (Table 5.1.1) were similar to that of wild type except that the growth halos of *ΔInlAB* were generally larger.

Quantitative binding and transport assays. Because *L. monocytogenes* grew poorly in existing minimal media (Premaratne *et al.,* 1991; Phan-Thanh *et al.,* 1997; Pine *et al.,* 1989), Dr. Klebba developed KRM medium based on RPMI 1640 (sigma), which renders *L. monocytogenes* iron-deficient. To do the experiments, I grew bacteria in BHI overnight. Next morning, I subcultured bacteria in KRM, and allowed them grow to stationary phase. That same night, I subcultured bacteria again in KRM, letting them grow to mid-log phase. Then the same procedures for ^{59}FeEnt binding and transport assays (Annamalai *et al.,* 2004) were conducted, except that I did a one-hour transport because the normal one-minute transport I did initially did not show any transport, indicating that the transport process was very slow. Due to the availability, I used ^{59}FeEnt, ^{59}FeTrn, and ^{59}Fc as the ligands. Specific activity of radioactive siderophores was usually between 150 to 1000 cpm/pmole.

EGD-e strain

I first studied the binding and transport of ^{59}FeCrn. Despite the negative results on nutrition tests, results of radioactive binding assay (Fig. 5.1.4) showed that below 10 nM concentration, EGD-e had a saturable binding process, indicating the binding by receptors although nonspecific adsorption existed as well. However, when concentration reached up to 500 nM, I observed an almost linear relationship (data not shown), suggesting that non-specific interaction between FeCrn and *L. monocytogenes* cell surface dominated over the actual binding of the ligands by the receptors at a concentration of 10 nM or above. The capacity was 6 pmole/10^9 cells, and K_d was 0.04 nM. These results suggested that *L. monocytogenes* bound FeCrn. When I added about 2 μM cold FeEnt to the growth of *L. monocytogenes*, the binding properties of ^{59}FeCrn did not change much. Capacity was lowered from 6 to 5 pmole/10^9 cells. K_d increased from 0.04 nM to 0.16 nM. Transport, on the other hand, gave a saturation curve (Fig. 5.1.4) when the concentration of ^{59}FeCrn was used up to 100 nM. The transport K_m was 43 nM, and the V_{max} was 1.7 nM. However, no other corynebactin transport system has been identified, and FepA does not transport FeCrn (Annamalai *et al.*, 2004), so my results are not comparable to any other data. When FeCrn was added to the growth of EGD-e, the transport properties did not change much either. K_m changed from 43 nM to 48 nM, and Vmax changed from 1.7 to 2.5 pmole/10^9/min. This suggested that uptake of FeCrn might be positively regulated, if at all, by FeCrn in *L. monocytogenes*.

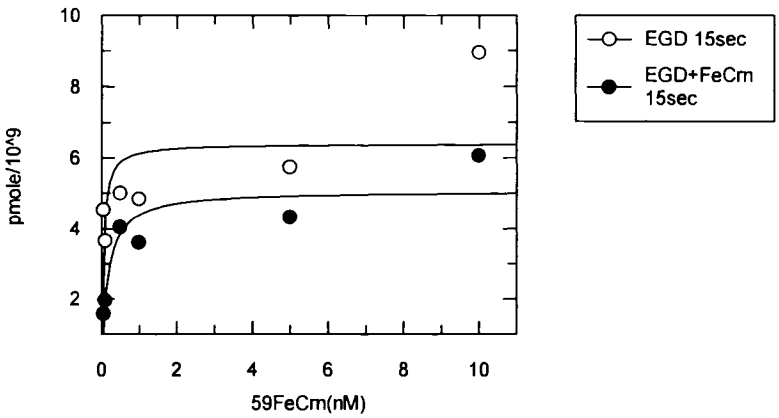

Parameter	Value	Std. Error
Cap	6.3891	0.9611
Kd	0.0443	0.043
Parameter	Value	Std. Error
Cap	5.0678	0.5064
Kd	0.1567	0.0779

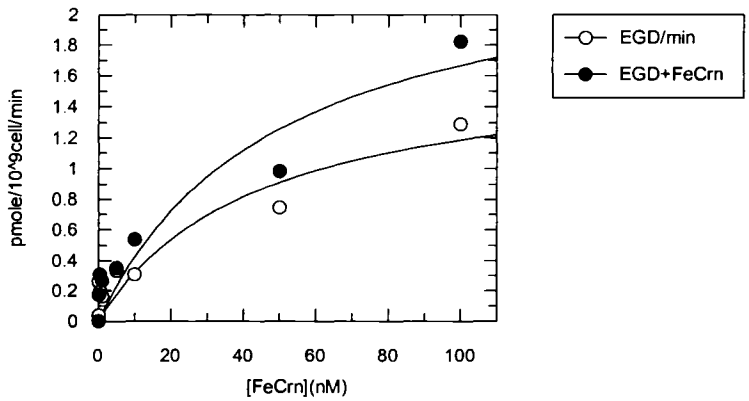

Parameter	Value	Std. Error
Vmax	1.6974	0.4956
Km	43.0850	29.5980
Parameter	Value	Std. Error
Vmax	2.4736	0.7355
Km	48.3268	32.6999

Fig. 5.1.4 Binding (top) and transport (bottom) of ^{59}FeCrn by EGD-e grown in KRM media without or with FeCrn (2μM).

The second iron-siderophore complex I tested was ^{59}FeEnt (Fig. 5.1.5). EGD-e again showed non-specific binding when the concentration of ^{59}FeEnt reached above 100 nM. Binding affinity (K_d~349 nM) was much higher than that of *E. coli* FepA (K_d~0.3 nM; Annamalai et al., 2004), indicating much lower efficiency. The capacity, though, was comparable to that of FepA (Cap~67 pmole/10^9). This binding characterization might not be very accurate because of the lacking of a binding deficient strain from which I could subtract the binding. But it did tell me that EGD-e bound FeEnt. When FeEnt, 2 μM, was added to the culture during the growth of *L. monocytogenes*, the binding properties again remained the same. Transport displayed a 47 nM K_m, that was much higher than that of FepA (0.4 nM; Annamalai *et al.*, 2004), and a V_{max} 23 pmole/10^9/min, which was about 5-fold less than that of FepA. When 2 μM of FeEnt was present in the growth of bacteria, V_{max} seemed to increase by 50%, and K_m remained the same. This suggested that the uptake of FeEnt by *L. monocytogenes* might be under positive regulation, if at all, by FeEnt.

The last iron-siderophore complex that I tested was ^{59}Fc (Fig. 5.1.6). Interestingly, EGD-e transported Fc at a comparable level as *E. coli* FhuA (Annamalai *et al.*, 2004). Even more interestingly, the presence of Fc in the growth of bacteria decreased the V_{max} by 8-fold, leaving some residual transport, and indicating a negative regulation by Fc.

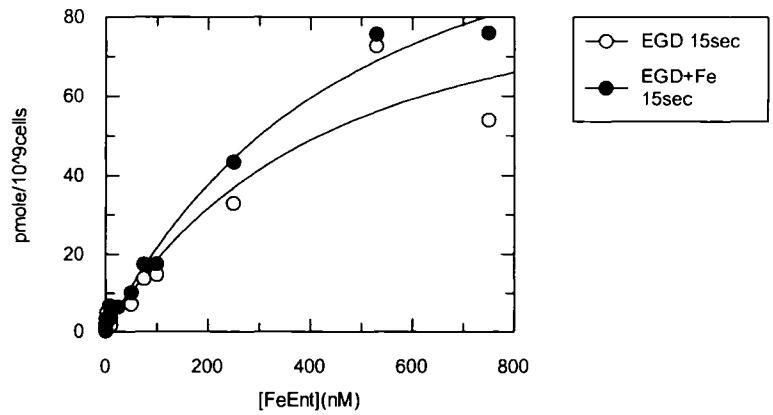

Parameter	Value	Std. Error
Capacity	97.4497	22.0421
Kd	349.1087	177.7994

Parameter	Value	Std. Error
Capacity	125.4528	13.0515
Kd	377.2372	83.8465

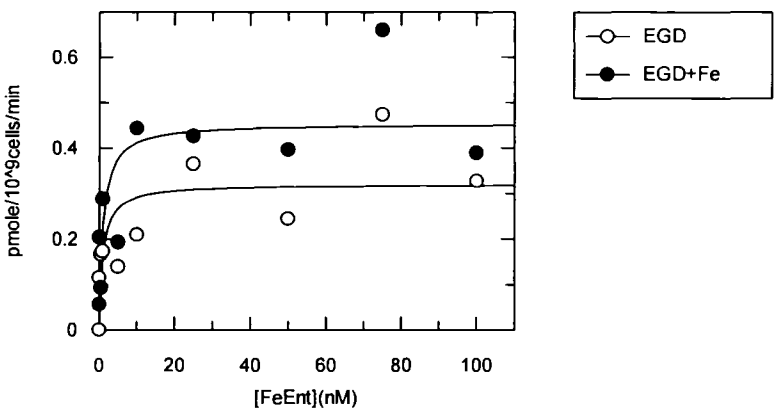

Parameter	Value	Std. Error
Vmax	0.3214	0.0451
Km	0.9955	0.9101

Parameter	Value	Std. Error
Vmax	0.4539	0.0592
Km	1.0280	0.7472

Fig. 5.1.5 Binding (top) and transport (bottom) of ^{59}FeEnt by EGD-e grown in KRM media without or with FeEnt (2μM).

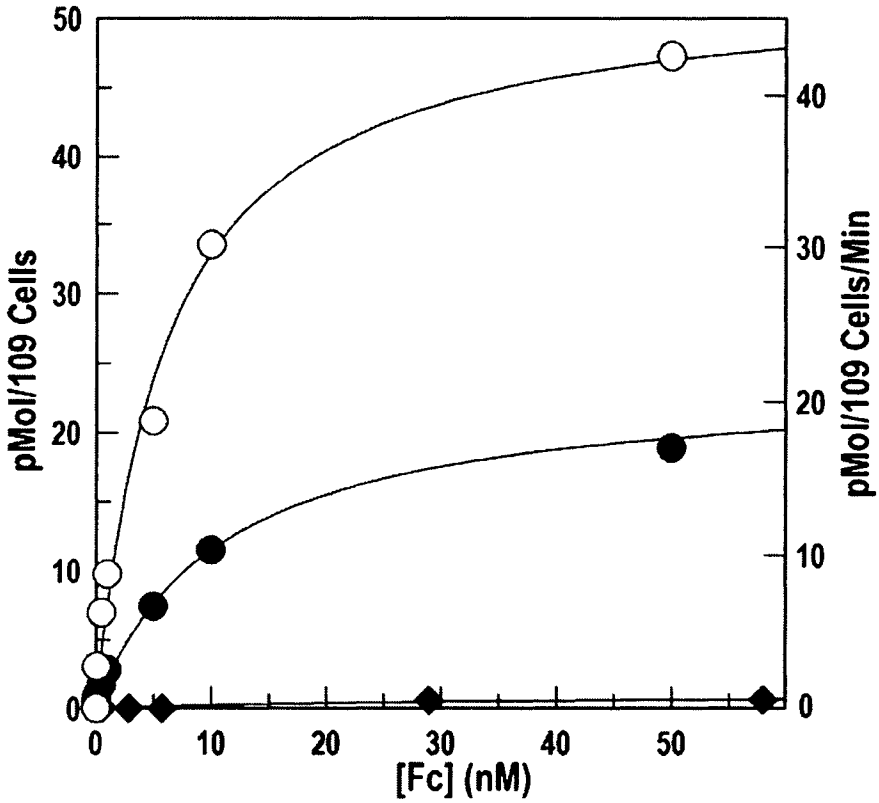

Fig. 5.1.6 Binding and transport of ^{59}Fc by EGD-e. Binding (open symbols) and transport (closed symbols) of Fc was measured as described for FeCrn and FeEnt. Bacteria were grown in KRM (circles) or KRM containing 2 μM Fc (diamonds), which repressed its own uptake reaction.

Derivatives

First, I identified that the *fhuDGC* (*lmo1957* to *lmo1961*) operon encoded for a ferrichrome uptake system. Deletion of *lmo1959* (*fhuD*, an iron-binding protein) almost completely diminished the uptake of ^{59}Fc (Fig. 5.1.7). However, this deletion did not affect the uptake of ^{59}FeCrn (Fig. 5.1.7). This indicated that FhuD was specifically involved in the uptake of Fc for *L. monocytogenes*. Deletion of *lmo1960* (*fhuC*, an ATP-binding protein), also severely impaired the uptake of ^{59}Fc. I did not measure the uptake of ^{59}FeCrn by Δ*fhuC*. Deletion of *lmo1961* (an oxido-reductase) did not impaired the uptake of either ^{59}Fc (Fig. 5.1.8) or ^{59}FeCrn (Fig. 5.1.10), although V_{max} of ^{59}FeCrn was slightly higher than that of EGD-e. We still needed to make deletion mutants of *lmo1957* *(fhuG)* and *lmo1958 (fhuB)*. In any case, above results indicated this *fhuDGC* operon encoded an Fc utilization uptake in *L. monocytogenes*.

Second, I compared the binding and transport of ^{59}FeCrn by Δ*fri* (Fig. 5.1.9) with the wild-type EGD-e strain. They had similar binding affinity and capacity. But surprisingly, uptake results showed that Δ*fri* had higher affinity (K_m decreased by 8-fold), and larger V_{max} (increased by 2-3-fold). Δ*fri* eliminated bacterioferritin, and retarded bacterial growth in defined medium (Olsen *et al.,* 2005). The growth curve of Δ*fri* completed by Dr. Klebba also confirmed it. So this internal iron depletion might be responsible for the increased transport affinity. And overexpression of the iron transporters, due to the low iron availability, might explain why V_{max} became larger. However, Δ*fri* diminished the transport of ^{59}Fc (Table 5.1.1; Fig. 5.1.8), although the Fc transport system (*fhuCDBG*) is negatively regulated by iron. This required further investigation.

Third, *lmo2429* (*hupC*) is a putative membrane ATP-binding protein. Siderophore nutrition tests showed that Δ*lmo2429* was not able to grow on BHI agar plates with either heme or hemoglobin at 200 and 15 μM respectively. However, this mutant was able to utilize ^{59}Fc (Fig. 5.1.8) normally in binding and transport assays. Also in nutrition assay, *ΔhupC* could utilize all the other iron complexes tested. This indicated that *hupC* is specifically involved in the utilization of Hn and Hb.

Fourth, *ΔfeoB* acted like wild type in both nutrition tests (Table 5.1.1; Fig. 5.1.1) and binding and transport assays (Table 5.1.2; Fig. 5.1.10).

Fifth, I also took a look at *Δfur*. Although it showed impaired utilization of iron hydroxamates (Table 5.1.1), it seemed to have a normal transport of ^{59}FeCrn (Fig. 5.1.11).

Last, *Δlmo2183*, deletion of a putative Fc permease of an ABC-type transport system, did not show any effect in either nutrition tests (Table 5.1.1; Fig. 5.1.1) or ^{59}Fc transport assays (Table 5.1.2; Fig. 5.1.8)

Protein expression profile

I looked at the protein expression profile very briefly (Fig. 5.1.12). I subcultured the overnight EGD-e BHI culture in MOPS minimum medium either with or without iron added. Then I ran whole cell lysates on 10% SDS-PAGE, followed by staining with Coomassie Blue, and destaining with 10% acetic acid. Although I need much more careful characterization, (for example, I would try KRM medium, SDS-PAGE with better resolution, and better normalization of bacteria cell number), I was able to see a 23 kDa protein that was expressed more when iron was not present in the medium. Several

proteins were expressed more (Fig. 5.1.12) when iron was present in the medium. Further investigation is needed. We can determine the protein sequence by either traditional nitrocellulose western blot elution and N-terminal sequence analysis or proteomics.

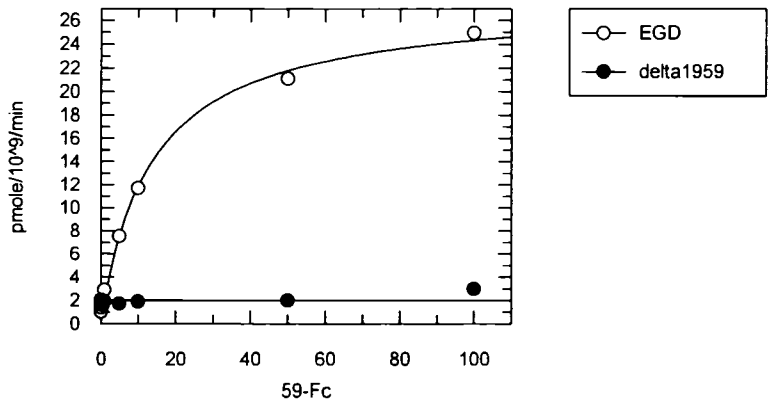

Parameter	Value	Std. Error
Vmax	27.5258	1.1230
Km	13.2002	1.8330

Parameter	Value	Std. Error
Vmax	2.0062	0.1902
Km	0.0016	0.0123

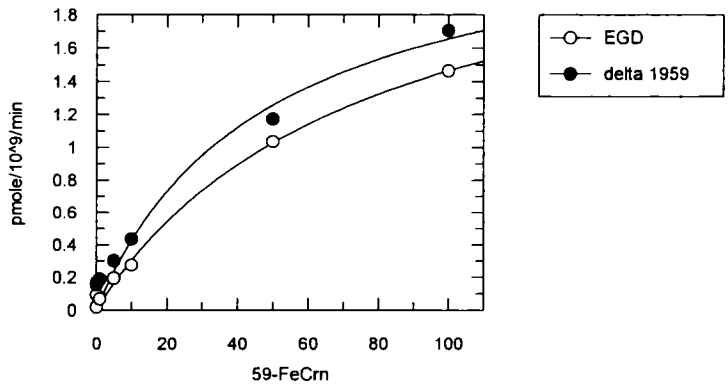

Parameter	Value	Std. Error
Vmax	2.5431	0.2956
Km	73.5174	16.8293

Parameter	Value	Std. Error
Vmax	2.4205	0.4562
Km	46.1492	20.4800

Fig. 5.1.7 ^{59}Fc (top) and ^{59}FeCrn (bottom) uptake of Δ*lmo1959* compared to the wild type strain EGD-e.

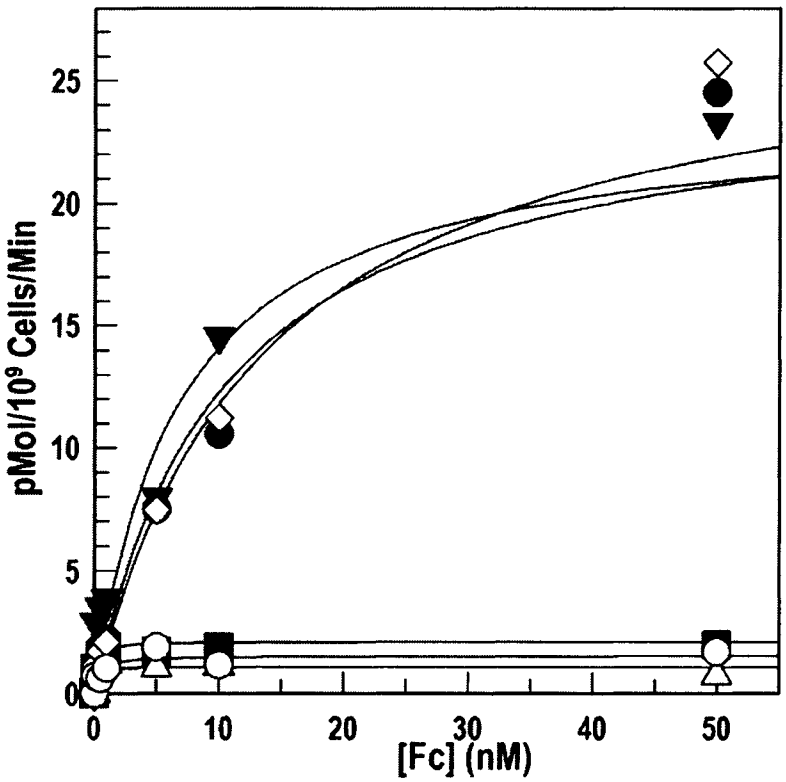

Fig. 5.1.8 ^{59}Fc uptake of *Δlmo2429* (*hupC* •), *lmo1959* (*fhuD* ■), *lmo1960* (*fhuC* Δ), *lmo1961* (▼), *lmo2183* (◊) and *fri* (○).

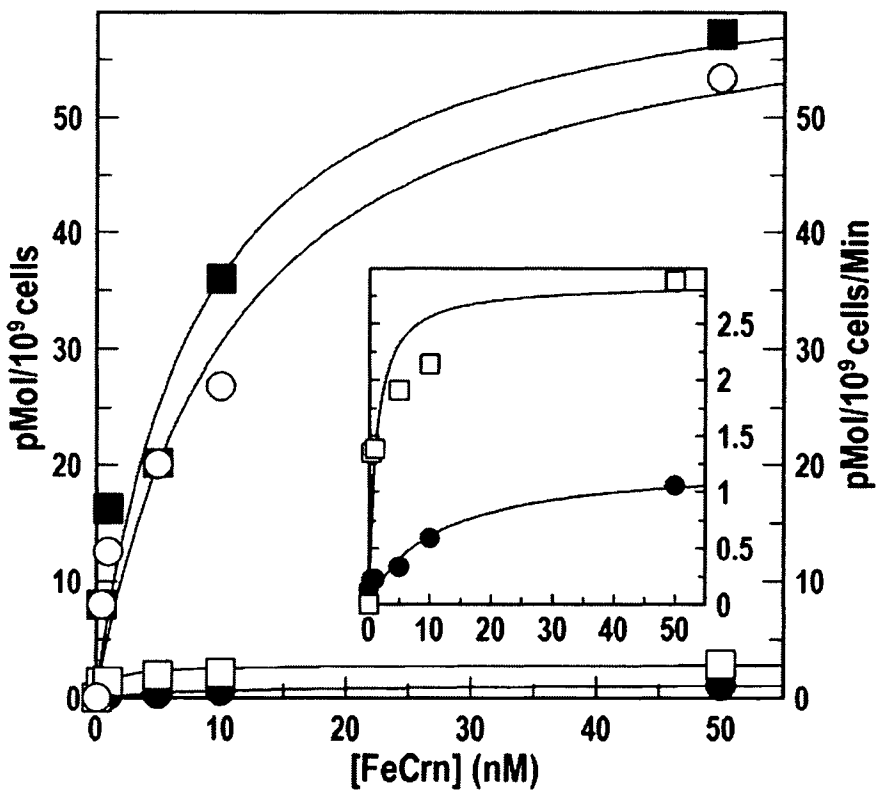

Fig. 5.1.9 Binding and transport of ^{59}FeCrn by *)fri* compared to EGD-e. Binding by *)fri* (■) and EGD-e (○), transport by *)fri* (□) and EGD-e (●).

Table 5.1.2 Transport properties of EGD-e and its derivatives.

Strain	^{59}Fe Transport			
	FeCrn		Fc	
	K_m	V_{max}	K_m	V_{max}
EGD (++)	10	1.2	10	24
)*fri (lmo943)*	1.2	2.9	.4	1.5
)*fhuD (lmo1959)*	26	1.8	.2	2.1
)*fhuC (lmo1960)*	ND	ND	.1	1.1
)*or (lmo1961)*	8	1	7	24
)*feoB (lmo2105)*	8	1.2	ND	ND
)*lmo2183*	ND	ND	10.4	25
)*hupC(lmo2429)*	ND	ND	13.5	25

Bacteria were cultured in BHI broth overnight, subcultured in KRM media to stationary phase, and subcultured a second time in KRM to mid-log. Uptake of ^{59}Fe complexes of corynebactin and apoFc was determined and plotted by Grafit 5.09 (Erithacus Ltd., London). K_m (nanomolar) and V_{max} (pMol/10^9cells/min) were calculated using the "Enzyme Kinetics" algorithm. The mean standard deviations of K_m and V_{max} determinations for FeCrn and Fc were 42% and 14%, and 41% and 8.5%, respectively.

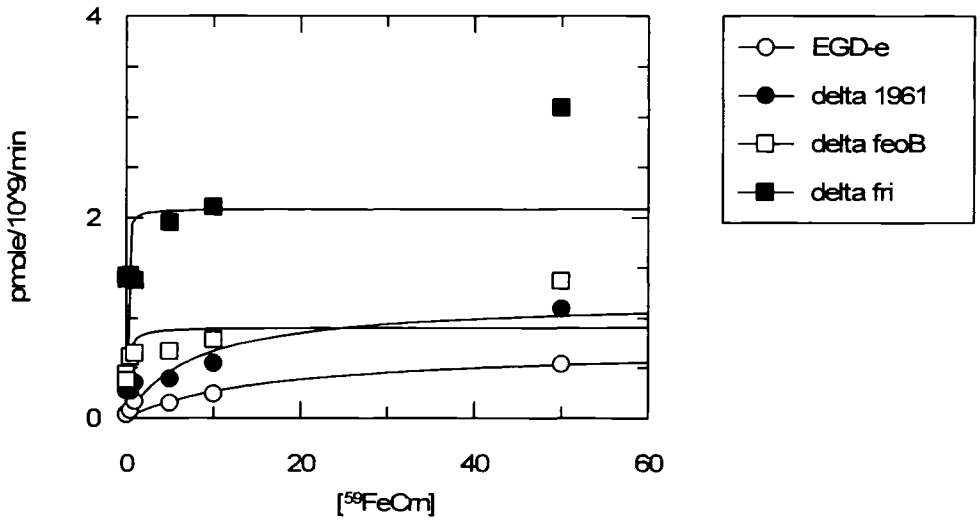

Parameter	Value	Std. Error
Vmax	0.7036	0.1642
Km	16.5849	9.3070

Parameter	Value	Std. Error
Vmax	1.1822	0.3541
Km	7.7062	6.4274

Parameter	Value	Std. Error
Vmax	0.9037	0.1490
Km	0.1498	0.1494

Parameter	Value	Std. Error
Vmax	2.0884	0.2941
Km	0.0454	0.0462

Fig. 5.1.10 ^{59}FeCrn uptake of EGD-e, *Δlmo1961, ΔfeoB, and Δfri.*

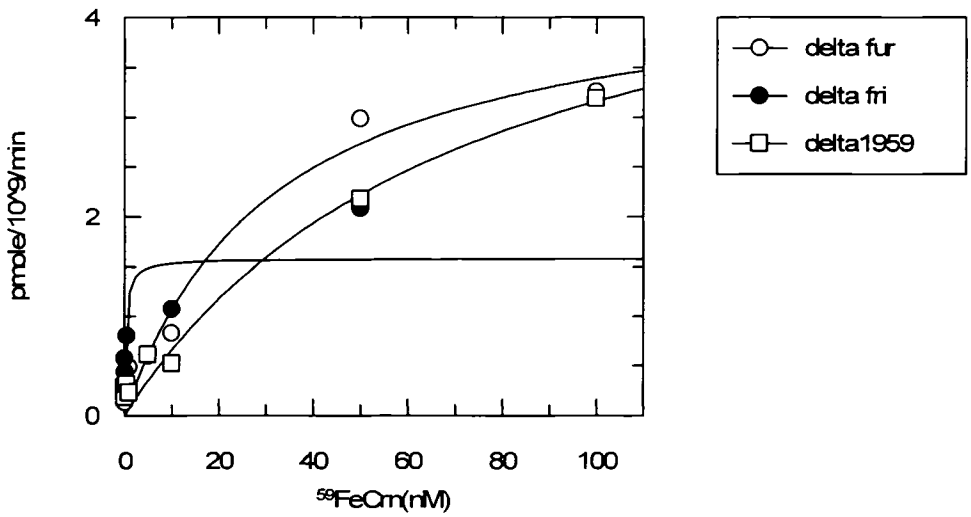

Parameter	Value	Std. Error
Vmax	4.4651	0.5788
Km	31.6002	11.1564

Parameter	Value	Std. Error
Vmax	1.5789	0.3356
Km	0.2965	0.2732

Parameter	Value	Std. Error
Vmax	5.4671	1.3786
Km	72.8550	36.3059

Fig. 5.1.11 ^{59}FeCrn uptake of *Δfur*, *Δfri*, and *Δlmo1959*.

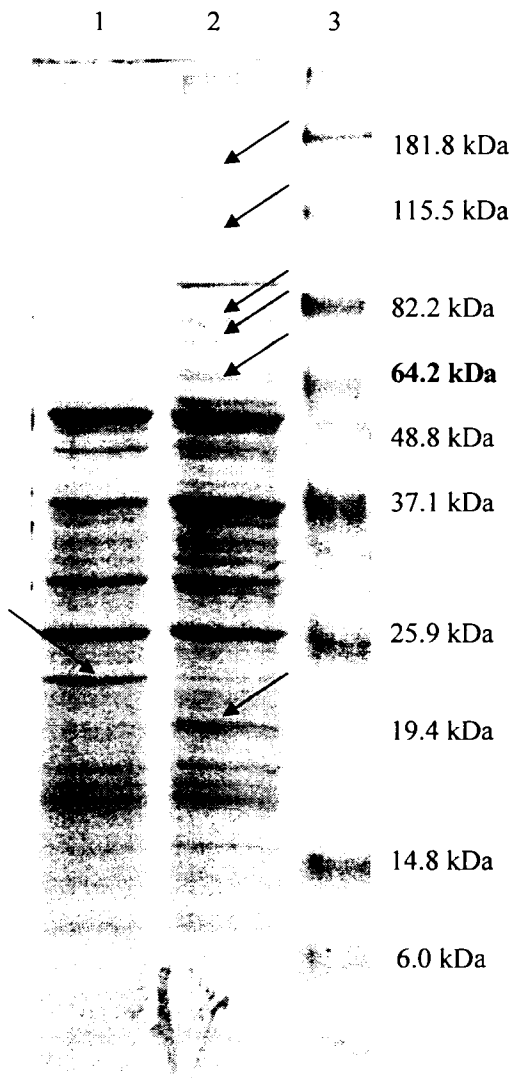

Fig. 5.1.12 SDS-PAGE of *L. monocytogenes* EGD-e strain cell envelope in the absence or presence of iron in MOPS minimum medium. Lane 1 was envelope of cells that was grown in MOPS. Lane 2 was envelope of cells that was grown in MOPS with iron. Lane 3 was protein ladder.

Discussion

Iron has been shown to be important for the growth of *listeria* during experimental infection (Sword, 1966). Most bacteria acquire iron through the secretion of high-affinity chelating agents, known as siderophores. Siderophores have not been detected, however, in organisms such as *Yersinia spp.* (Une *et al.*, 1984) and *Legionella spp.* (Reeves *et al.*, 1983).

The tight relationship between iron acquisition and pathogenicity suggests that host iron metabolism may play a part in the onset and progress of listerial infections (Sword, 1966). Although *Listeria monocytogenes* is known not to secrete siderophores (Cowart *et al.*, 1985), like *Streptococcus pneumoniae* (Tai *et al.*, 1993), *Listeria monocytogenes* acquires iron from variety of siderophores produced by various microorganisms or natural catecholate compounds widespread in the environment and other iron-chelating compounds, but not ferrichrome (Simon *et al.*, 1995). Most of the siderophores I tested, except ferrichrome and ferrioxamine B, do not overlap with the siderophores tested by Simon. In addition, we had exactly opposite results concerning ferrichrome, probably because we used different strains of *listeria*. In the presence of iron-chelating agent, growth of *listeria* is completely inhibited (Coulanges *et al.*, 1997). The growth inhibition can be relieved by addition of iron complexes (Coulanges *et al.*, 1997; 1996), indicating the importance of iron acquisition from these compounds to bacterial growth.

Gram-negative bacteria, like *E. coli* and its relatives, have an inner membrane (IM), an outer membrane (OM), and an aqueous space between them, the periplasm. This cell envelope contains the proteinaceous components that catalyze the uptake of

metabolic solutes, including sugars, amino acids, nucleotides, vitamins, and metals. When ferric siderophores traverse the Gram-negative cell envelope, they first encounter OM receptor proteins (Buchanan *et al.*, 1999; Locher *et al.*, 1998; Ferguson *et al.*, 1998). The high affinity of these proteins for their ligands (Newton *et al.*, 1999; Cao *et al.*, 2000; Scott *et al.*, 2001) is the foundation of efficient uptake: it permits the adsorption of ferric siderophores, even at the low concentrations that are common in the environment, probably never exceeding micromolar levels. After passage through the OM, iron chelates bind to proteins in the periplasm (with slightly lesser affinity; Kuan *et al.*, 1995; Braun *et al.*, 1998; Dassa *et al.*, 2001), which deliver them to IM ABC-type permeases (Kuan *et al.*, 1995; Braun *et al.*, 1998; Dassa *et al.*, 2001; Saier *et al.*, 2002). The cell envelope of Gram-positive bacteria, on the other hand, contains a cytoplasmic membrane (CM) surrounded by multilamellar peptidoglycan (Dmitriev *et al.*, 1999; Navarre *et al.*, 1999), to which sortase-anchored proteins (Mazmanian *et al.*, 2002 and 2003; Skaar *et al.*, 2004) and other molecules, like techoic acids, covalently or non-covalently associate. It is not yet known how metals like iron pass through the Gram-positive cell envelope, but its architectural differences pose a question: without an OM, and hence, without high affinity receptor proteins, how do Gram-positive organisms like *Listeria*, *Bacillus*, *Corynebacterium*, *Staphylococcus*, and *Streptococcus* acquire sufficient iron to meet their metabolic needs? Either their ABC transporters in the CM function in a novel way, as the initial binding site for iron-containing molecules, or perhaps high affinity iron binding proteins exist within the PG surface layer, as suggested by experiments with *S. aureus* (Mazmanian *et al.*, 2003; Skaar *et al.*, 2004). It is unclear, nevertheless, how binding proteins anchored within PG may facilitate iron uptake. Once bound to such proteins, no

obvious driving force exists to transfer iron, or ferric siderophores, or hemin, or hemoglobin, or Fe-transferrin to CM permeases. One result of our study was that the individual deletion of known sortase genes (Δ*srtA*, Δ*srtB*, and the double mutant Δ*srtAB*), did not impair iron acquisition from any of the ferric siderophores or iron binding proteins that we tested. These data are inconsistent with the idea that in *Listeria*, sortase anchored proteins play a predominant role in iron acquisition.

This study reiterated (Coulanges *et al.*, 1996 and 1997; Simon *et al.*, 1995) and further demonstrated the ability of *Listeria* to acquire iron from a variety of molecules. In contrast to the *Enterobacteriaceae*, which only transport the ferric siderophores for which they contain receptor proteins, *L. monocytogenes* used every iron source we tested, including several (FeCrn, FxB, Hb, Hn HTf, Ftn) that are not utilized by *E. coli*. The molecular basis of this broad transport ability is unknown. Although these data ostensibly support the postulate (Adams *et al.*, 1990; Deneer *et al.*, 1995; Cowart, 2002; Barchini *et al.*, 1996) of a membrane reductase with broad specificity, the identification of two ABC-transporters with diverse selectivity for ferric hydroxamates and Hn/Hb demonstrates another efficient way for bacteria to achieve iron. Apparently Fc, FcA and FxB enter the cytoplasm by a pathway that is comparable to those observed in Gram-negative bacteria, via a specific ABC-transporter. This system may equate with a hydroxamate transporter previously described in *Bacillus* (Schneider *et al.*, 1993). Furthermore, the elimination of the putative oxidoreductase in the same locus did not impair uptake of the same ferric siderophores. The uptake of Hn/Hb similarly depends on a different ABC-transporter.

The *feoAB* locus encodes a membrane transport system for uptake of ferrous iron, but we did not find defects in the ability of EGD-e/Δ*feoB* to obtain iron from either ferric

siderophores or eukaryotic iron-binding proteins. Neither was the Δ*feoB* strain attenuated in the mouse model system (LD_{50} in Table 5.1.1). However, further experiments are needed to fully evaluate this mutant (Kammler *et al.*, 1993). In *Helicobacter pylori* (Velayudhan *et al.*, 2000) and *Legionella pneumoniae* (Robey *et al.*, 2002) FeoAB homologues contribute to bacterial virulence; in *S. typhimurium* conflicting results exist on the connection between the FeoAB system and pathogenesis (Tsolis *et al.*, 1996; Boyer *et al.*, 2002).

Δ*fri* showed a phenotype that was hard to understand. *fri* encodes for bacterioferritin, the iron storage protein. Deletion of this protein may lead to low intracellular iron availability and probably increased extracellular iron utilization. Since transport of FeCrn and FeEnt was shown to be positively regulated by iron and transport of Fc was shown to be negatively regulated by iron, one may expect to see that Δ*fri* would decrease the transport of FeCrn and FeEnt, and increase the transport of Fc. However, the results I obtained were exactly opposite. The uptake of ^{59}FeCrn had a 2- to 3-fold increase of V_{max} (from 1.2 to 2.9 pmole/10^9/min) and an 8-fold higher affinity (K_m from 10 nM to 1.2 nM). The uptake of ^{59}Fc had a 16-fold decreased V_{max} (from 24 to 1.5 pmole/10^9/min), although the affinity still increased from 10 nM to 0.4 nM. This suggested a new and not yet understood correlation between the intracellular iron storage and extracellular iron acquisition. One possible explanation is that bacteria respond to the iron concentration in solutions instead of the overall intracellular iron availability and Fri is the protein that regulates the iron concentration in solutions. When iron availability is high in solutions, Fri will store extra iron and lower the iron concentration. This lower iron concentration will then result in less transport of FeCrn and FeEnt and more

transport of Fc. On the other hand, when iron availability is low in solutions, Fri will release iron and increase the iron concentration. This higher concentration will then result in more transport of FeCrn and FeEnt and less transport of Fc, which was seen in the experiments (Fig. 5.1.4; Fig. 5.1.5; Fig. 5.1.6).

The experiments reported within provide the first biochemical characterizations of Gram-positive bacterial iron transport processes, the first such analysis of iron acquisition by an intracellular bacterial pathogen, and the first identification of listerial membrane transport systems for particular iron-containing compounds. The determinations of listerial binding affinity for ^{59}Fe-siderophores were hampered by the lack of mutants that are unable to bind specific iron complexes, and by a high nonspecific adsorption of siderophores to EGD-e and its derivatives. As a result, the amounts of ferric siderophores bound to listerial cells well exceeded the amount transported per minute. This is not the case in Gram-negative cells, in which high non-specific binding does not occur (Newton *et al.,* 1999): in *E. coli*, ferric siderophores adsorb to their receptor proteins, and are immediately transported. In spite of these difficulties, the uptake experiments with EGD-e gave unambiguous results about the capabilities and affinities of listerial cell envelope iron uptake systems. *Listeria* does not manifest as high an affinity for ferric siderophores as do *E. coli* and its relatives, and its rates of ferric siderophore uptake were lower than those of Gram-negative bacteria, especially with regard to ferric catecholates. Nevertheless, *L. monocytogenes* efficiently proliferated on sub-micromolar concentrations of Fc and FcA, at even lower concentrations than those required for growth of *E. coli*. Does this superior ability exclusively derive from ABC-transporter

systems in the CM, or do other, currently unknown cell envelope proteins make contributions that enhance it?

The acquisition of iron from mammalian proteins is a common attribute of pathogenic bacteria (Cornelissen and Sparling, 1994 a and b), as evidenced by the TonB-dependent lactoferrin/transferrin receptors of *Neisseria* (Schryvers *et al.*, 1998 and 1999; Gray-Owen *et al.*, 1996; Bonnah *et al.*, 1995; Cornelissen and Sparling, 1994 a and b), the hemin/hemoglobin-haptoglobin/hemopectin uptake systems of *Haemophilus* (Jarosik *et al.*, 1995; Jin *et al.*, 1999; Stevens *et al.*, 1996; Sanders *et al.*, 1994; Morton *et al.*, 1999; Ren *et al.*, 1998; Elkins *et al.*, 1998; Thomas *et al.*, 2001; Elkins *et al.*, 1995) and *Neisseriae* (Richardson *et al.*, 1999; Stojiljkovic *et al.*, 1997; Zhu *et al.*, 2000), and the tendency of siderophores to remove iron from transferrin and ferritin (Konopka *et al.*, 1984; Tidmarsh *et al.*, 1983). Our experiments demonstrate that *L. monocytogenes*, an intracellular pathogen that crosses several physical barriers in the human body, also efficiently utilizes eukaryotic proteins as iron sources, and that the elimination of its ability to obtain iron from Hn/Hb significantly decreases its pathogenesis in mice.

By analysis of signal peptides using SignalP 3.0 program (http://www.cbs.dtu.dk/services/SignalP), *Lmo1960* was predicted to code for a non-secretary protein. By sequence comparison and alignment, I found that Lmo1960 was similar to ATP-binding component of ABC-type membrane permeases. Lmo1960 has 69% homology to the *Escherichia coli* ferric enterobactin transport ATP-binding protein FepC, 63% homology to the *Escherichia coli* hydroxamate transport ATP-binding component FhuC, and 68% homology to *Escherichia coli* citrate-dependent iron (III) transport ATP-binding component FecE. Also they had all the features (Fig. 5.1.13) that

other ATP-binding proteins shared with each other, for example, Walker A sequence (GxxGxGKS/T, "x" represents any amino acid; Walker *et al.*, 1982), Walker B sequence (hhhhD, "h" represents any aliphatic residue), ABC Signature motif (LSGGQQ/R/KQR, Jha *et al.*, 2003; Hopfner *et al.*, 2000; Verdon *et al.*, 2003), Q-loop (Hopfner *et al.*, 2000; Verdon *et al.*, 2003; Jones *et al.*, 2002), H-loop (Hopfner *et al.*, 2000; Verdon *et al.*, 2003), and D-loop (Hopfner *et al.*, 2000; Verdon *et al.*, 2003). Using SignalP 3.0 Lmo1959 was predicted to be a secretary protein. Also Lmo1959 was close to periplasmic binding proteins, such as FecB, FepB of *Escherichia coli*. Lmo1961 was predicted to be a non-secretary protein, and close to thioredoxin reductases. Lmo2429 was predicted to be non-secretary proteins. It was similar to ATP-binding protein of ABC transport system and it had 65%, 60%, and 63% homology to *E. coli* FepC, FhuC and FecE, respectively. *Lmo2430* was similar to ABC transport permease and had 58% homology to citrate transport system inner membrane permease FecD of *Escherichia coli*, and 54% homology to ferric enterobactin transport system inner membrane permease FepG. Lmo2431 was similar to periplasmic binding protein, and it had 48% homology to *Escherichia coli* Vitamin B12 binding protein BtuF. Lmo2182 had 65% homology to *Escherichia coli* ATP-binding protein FepC and 60% homology to FhuC. Lmo2183 had 54% homology to *Escherichia coli* inner membrane permease FecD, 53% to FecC, 53% to FepD, 54% to FepG and 54% to FhuB. Lmo2184 had 47% homology to *E. coli* periplasmic binding protein BtuF. In summary, each operon contains at least three proteins. Among the three proteins, one is similar to periplasmic binding protein, one is similar to ATP-binding protein, and another is similar to inner membrane permease. This displays a typical iron utilization system in gram-positive bacteria.

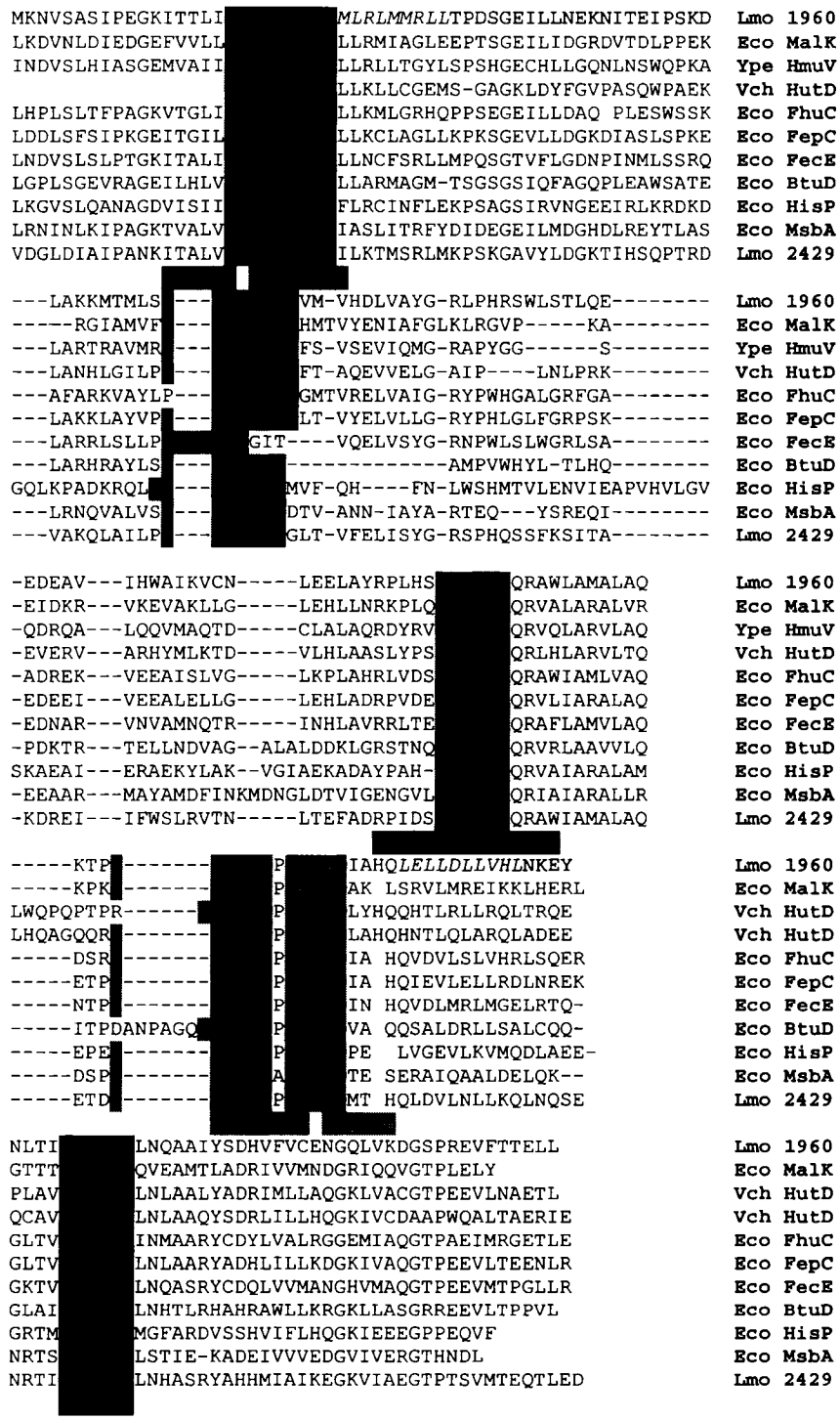

Fig. 5.1.13 Protein sequence alignment of *lmo1960, lmo2429* with other closely related proteins.

5.2 *Bacillus subtilis*

Research target. I specifically studied the possible operons that may be involved in ferrichrome uptake. I found a huge regulon (Fig. 5.2.1) consisting of a few operons. The only study done was about *fhuD* (Schneider and Hantke, 1993). Among these operons, the *yfm* operon contains three genes: *yfmC*, *yfmD*, and *yfmE*. YfmE has 67% homology to *E. coli* citrate transport system inner membrane permease protein FecD, 57% to membrane permease protein FecC, 57% to ferric enterobactin transport system ATP-binding protein FepC, 58% to the membrane permease FepG. YfmC has 59% homology to periplasmic binding protein FecB, 42% to ferric enterobactin transport system periplasmic binding protein FepB, 45% to ferrichrome transport system membrane permease FhuD. YfmD has 61% homology to FecC, 61% to FecD, 58% to membrane permease FepD. Although another gene, *yusV* has higher homology to citrate transport permease; it is a single gene that does not relate to other genes. So I chose *yfm* operon to start my study.

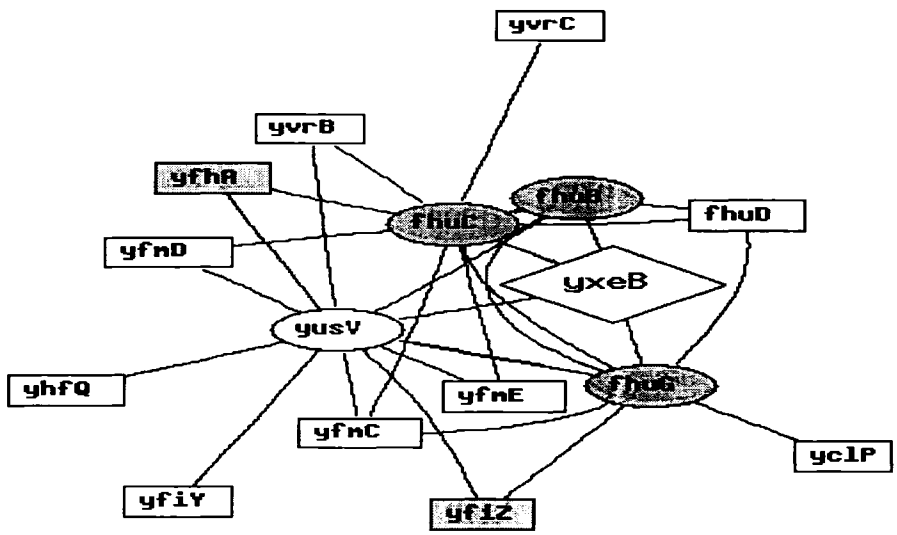

Fig. 5.2.1 Predicted regulon that may be involved in the utilization of Fc in *B. subtilis* (http://vimss.lbl.gov).

Nutrition assays. I first did nutrition assay to see what kind of iron complexes *B. subtilis* utilizes. Results (Fig. 5.2.2) showed that FeCrn, FeEnt, Fc, and Hb could stimulate the growth of *B. subtilis* very well, all though the growth halo for Hb was fuzzy. There was a small halo just around the disk that were applied with Hn, which needed further investigation. *B. subtilis* did not seem to release and utilize iron from Ftn.

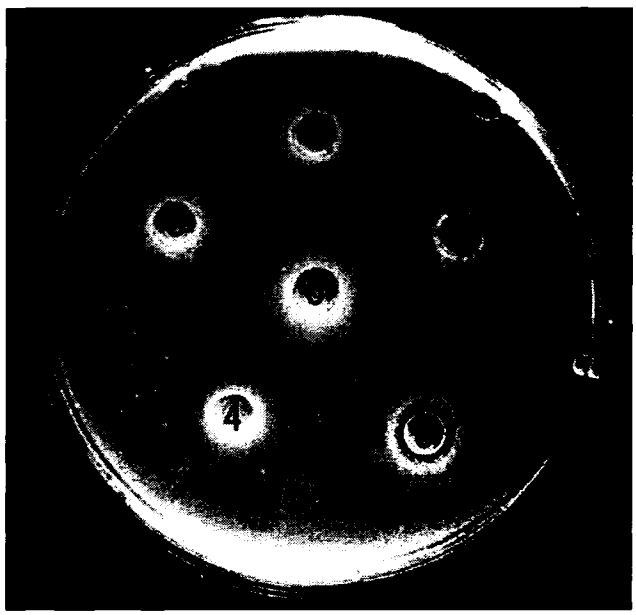

Fig. 5.2.2 Nutrition test of *B. subtilis168* strain with different iron sources. Iron sources from 1 to 6 were FrCrn, Hb, Hn, Ftn, FeEnt, and Fc, respectively.

^{59}Fe binding and uptake assays. I used ^{59}FeCrn, ^{59}FeEnt, and ^{59}Fc to test the ability that *B. subtilis 168* strain utilizes these three iron siderophore complexes.

Similar to *L. monocytogenes*, within the range of 10 nM, binding of ^{59}FeCrn (Fig. 5.2.3) showed saturation. But above 10 nM, up to 500 nM that I tested, binding showed linear relationship to the concentration of ^{59}FeCrn. The K_d was 0.085 nM, and capacity was 21.1 pmole/10^9. This high binding affinity was not surprising at all, because FeCrn is the native siderophore of *B. subtilis*. However, K_m was only 15 nM, and V_{max} was 1.3 pmole/10^9/min, which did not indicate an eager uptake.

^{59}FeEnt did not show a saturable binding process either (Fig. 5.2.4). So its binding K_d and capacity should not be trusted. Its transport properties, K_m~6.5 nM, V_{max}~3.3 pmole/10^9/min, were not comparable to the transport of ^{59}FeEnt by *E. coli* FepA, either. But *B. subtilis* was able to utilize both FeCrn and FeEnt, and *E. coli* can only utilize FeEnt.

Fc, on other hand, seemed always to be the favorite siderophore (also for *L. monocytogenes*; Table 5.2.1). ^{59}Fc binding showed a K_d of 9.7 nM and a large capacity in a saturable process (Fig. 5.2.5), although this did not mean there was no non-specific absorption. The transport also showed us that *B. subtilis* prefers Fc with 13 nM K_m and 38.1 pmole/10^9/min maximum rates.

Another experiment I did was to look at the iron regulation (Fig. 5.2.4) by FeEnt. When I added around 2 μM of FeEnt during the growth of bacteria, *B. subtilis* showed a 3- to 4- fold increase of V_{max} and a 2- to 3- fold increase of K_m. This suggested that FeEnt uptake by *B. subtilis* might be under positive regulation by iron, which was also seen in *L. monocytogenes*.

To summarize, *B. subtilis* utilized FeCrn, FeEnt, and Fc (Table 5.2.1) with different affinity and rates. It might also prefer Fc.

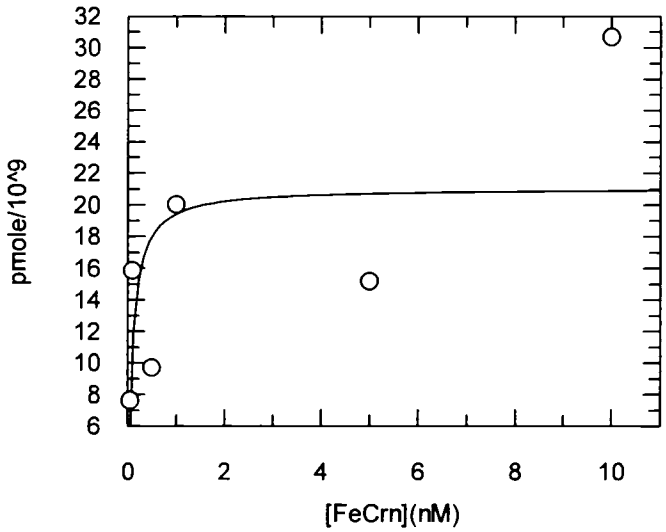

Parameter	Value	Std. Error
Cap	21.1	4.5
Kd	0.085	0.1

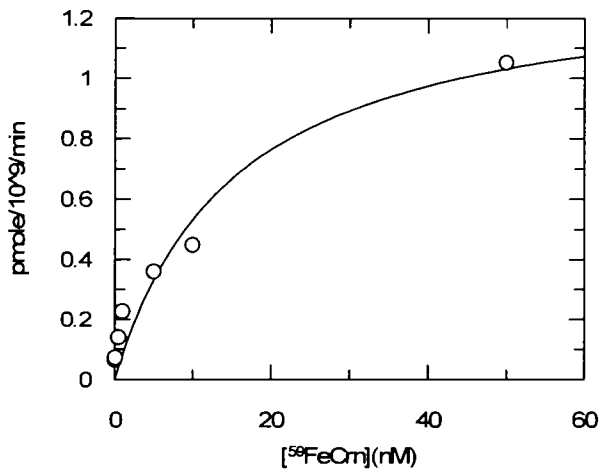

Parameter	Value	Std. Error
Vmax	1.3457	0.2145
Km	15.2471	6.0111

Fig. 5.2.3 ^{59}FeCrn uptake of *B. subtilis*.

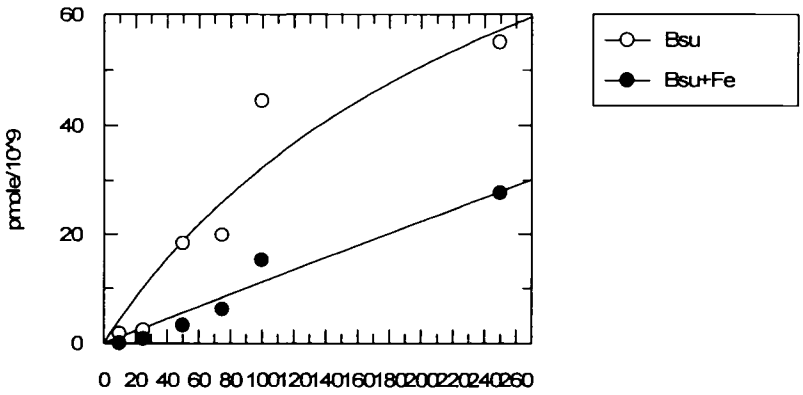

Parameter	Value	Std. Error
Cap	117.24	60.97
Kd	262.78	216.8
Parameter	Value	
Cap	5415	25560
Kd	48282	228742

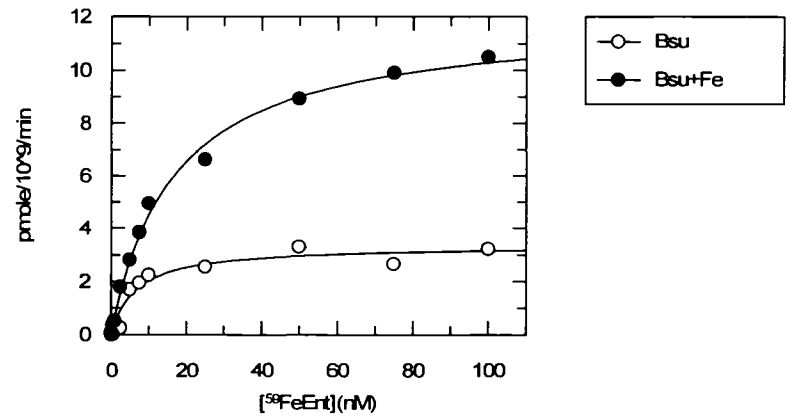

Parameter	Value	Std. Error
Vmax	3.3504	0.2251
Km	6.5568	1.6361
Parameter	Value	Std. Error
Vmax	11.9817	0.3212
Km	16.5228	1.3616

Fig. 5.2.4 ^{59}FeEnt uptake of *B. subtilis* grown in MOPS without or with FeEnt (2μM).

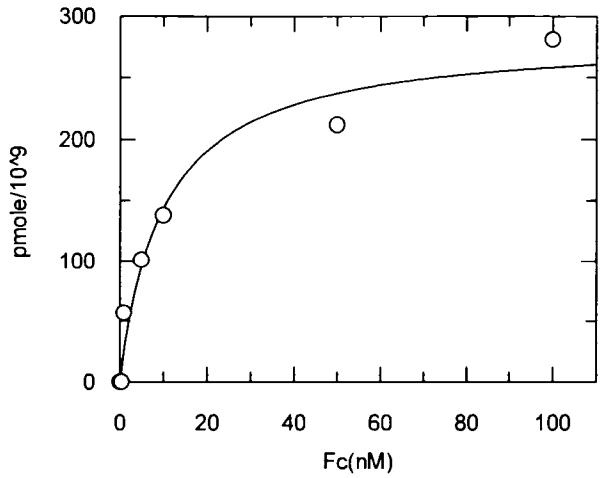

Parameter	Value	Std. Error
Cap	283.2059	21.3471
Kd	9.721	2.5674

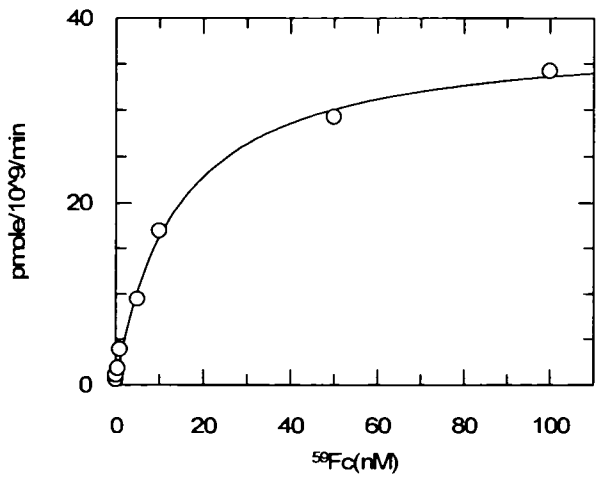

Parameter	Value	Std. Error
Vmax	38.0935	1.1473
Km	13.4150	1.3712

Fig. 5.2.5 ^{59}Fc binding and uptake of *B. subtilis*.

Table 5.2.1 Summary of siderophore binding and uptake by *B. subtilis*.

Siderophores	Binding		Transport	
	K_d(nM)	Cap(pmole/10^9)	K_m(nM)	V_{max}(pmole/10^9/min)
FeCrn	0.085	21.1	15.2	1.34
FeEnt	263	117	6.5	3.3
Fc	9.7	283	13.4	38.1

Growth curve. I took a brief look at the growth curve (Fig. 5.2.6) of *B. subtilis* in MOPS minimum media. When 1.7 μM of iron was added, *B. subtilis* seemed to growth a little faster starting at 200-minute point, and also reached slightly higher final OD at 600 nM.

Mutation derivatives. I used the same in-frame chromosomal deletion procedure that I did for *L. monocytogenes* to make deletions in *yfm* operon. I constructed *ΔyfmE*, deletion of a putative membrane permease. *Bsu/ΔyfmE* showed wild-type growth in the nutrition test. It was not yet fully characterized. I am currently making deletion of *yfmC and yfmD*.

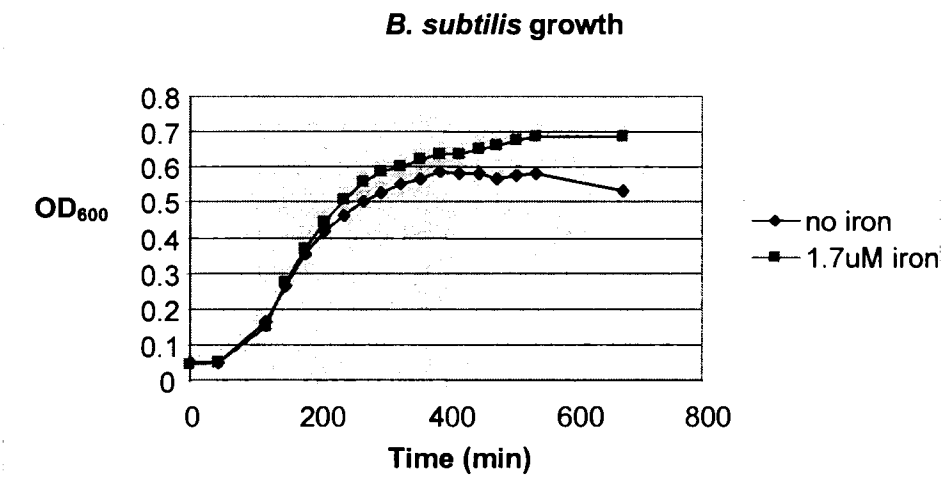

Fig. 5.2.6 Growth curve of *B. subtilis* in MOPS minimum media.

Discussion: *Bacillus subtilis* has been well studied. However, iron uptake is very poorly known, except Dr. Hantke identified an iron binding protein, FhuD, whose deletion eliminated the ferrichrome transport. This study showed that *Bacillus subtilis 168 (Bsu)* strain can utilize several kinds of iron complexes, including FeEnt, Fc, FeCrn, Hb, and Hn. Although Crn is the native siderophore of *B. subtilis*, bacteria did not show any preference over Crn. This was displayed (Table 5.2.1) by the K_m (15.2 nM), which was similar to the K_m of ^{59}FeEnt and ^{59}Fc uptake, and V_{max} (1.34 pmole/10^9min), which was the smallest. Surprisingly, ^{59}Fe transport experiments (Table 5.2.1) showed that, just like *L. monocytogenes, Bsu* favors Fc by possessing a V_{max} of 38.1 pmole/10^9min, which was 28-fold and 11-fold larger than the V_{max} of ^{59}FeEnt and ^{59}Fc uptake, respectively. Deletion of *yfmE*, the putative membrane permease, did not impair the transport of FeEnt in nutrition test probably because of the presence of the redundant two copies of permeases, YfmE and YfmD. I need to make the double mutant *ΔyfmDE*. I am currently making the deletion of *yfmC*, the putative binding protein.

There was a big problem with the construction of chromosomal deletion in *Bsu*. Although pKSV7 is constructed from *Bsu*, it is not stable. It could be lost in just a few generations after it was transformed into *Bsu*. So in the future, other cloning vectors, which stay stably in *Bsu,* should be considered.

Chapter 6. Discussion

The acquisition of iron is possibly the major determinant as to whether a bacterium that finds itself within a host is able to survive. The concentration of free iron in solution at pH7 is usually 10^{-18} M. This forces bacteria to look for other iron sources. On the other hand, in order to defense themselves, animals withhold the iron from infecting bacteria and keep the iron availability very low. It has been shown that treatment with iron for patients with bacteria, viral or parasitic infection could be deadly (Weinberg, 1993).

In humans and other vertebrates, iron is attached to glycoprotein transferrin (Tf). There are three major classes of Tf: serum Tf (or serotransferrin); lactoferrin (Lf) or lactotransferrin, which is found in many extracellular fluids; and ovotransferrin, which is found in the albumen of eggs. They are single-chain glycoproteins of molecular weight 80 kDa and they have two similar but not identical binding sites for iron. Both sites have binding constants for iron of 10^{20}. It is important that Tf is never fully saturated with iron. This capacity is crucial to adsorb any iron that may arise in the fluids during infection and to ensure that no free iron is available. Besides Tf, bacteria may also acquire iron from hemoglobin. Bacteria could destruct the erythrocytes and hydrolyze hemoglobin, take iron containing heme out of hemoglobin, or directly reduce the Fe^{3+} of hemoglobin to Fe^{2+} that is more soluble. Another source of iron is ferritin, which in fact may be the major target of invaders. Ferritins are the primary iron storage compounds of most organisms. The molecular weight of ferritin is 500 kDa. It is composed of 24 protein subunits that form a hollow sphere that can accommodate more than 4000 atoms of Fe^{3+}.

The bacterioferritin that is different from the ferritins in animals and plants has a heme group attached. Ferritin stores iron in iron-replete cells.

Bacteria have developed two main systems to achieve acquisition of iron from their host. They could directly contact the iron sources (Tf, heme, or heme proteins) and remove the iron by its reduction and uptake. Alternatively, they could synthesize compounds that possess much higher affinity to iron than their host iron binding proteins and capture the iron from the host proteins. This kind of compounds is called siderophores. Then bacteria will adopt sophisticated systems to transport iron-siderophore complexes back and reduce the Fe^{3+} to Fe^{2+}. However, such systems may also transport iron binding proteins (Tf, heme, or heme proteins). Siderophores are produced by many microorganisms, including Gram (+) bacteria, Gram (-) bacteria, yeast, and fungi. There are more than 500 different siderophores. They are basically divided into three categories based on their structures: hydroxamate, catecholate, and mixed. Among the catecholates I studied, FeEnt that is produced by both Gram (-) and Gram (+) bacteria; FeCrn that is produced by Gram (+) bacteria; Ferric MECAM and Ferric TRENCAM (FeTrn) are two synthetic catecholates. Among the hydroxamates I studied, Fc is produced by fungi and FxB is produced by Gram (+) bacteria.

However, what I am interested in is not how siderophores remove iron from host iron containing proteins, but how bacteria, including *E. coli*, *L. monocytogenes*, and *Bacillus subtilis*, can utilize the iron-siderophore complexes and iron containing proteins. It turns out that *L. monocytogenes* and *Bacillus subtilis* can utilize all the siderophores I tested, which suggests that both bacteria have very broad substrate specificity as observed with *L. monocytogenes* ten years ago by Simon (1995) although we used different wild-

type strains of *L. monocytogenes*. In addition, *L. monocytogenes* may have developed different uptake systems for different siderophores. For example, the *fhu* operon of *L. monocytogenes* encodes a binding protein-dependent uptake system that transports Fc specifically, but not other siderophores and iron proteins. Another example will be the *Hup* operon of *L. monocytogenes,* which encodes an uptake system for heme and hemoglobin but not other siderophores I tested even though more experiments need to be completed to confirm. This indicates that specific iron uptake system in *L. monocytogenes* has very narrow substrate specificity, which is also observed in *E. coli*. *E. coli* can utilize FeEnt, Fc, and other siderophores. Data also showed that ^{59}FeEnt uptake by FepA was not competed by the presence of either hydroxamate (Fc) or catecholate (ferric agrobactin), but only competed by the presence of FeEnt and only a little bit by the structural homolog FeTrn. Also, FepA does not recognize and bind the hydroxamate Fc and catecholate FeCrn, a native siderophore of Corynebacterium. All these data indicate that both Gram (-) and Gram (+) bacteria may be able to acquire iron from all kinds of iron sources, and at the same time they also develop very specific uptake systems to specific iron sources. An obvious difference between the three bacteria is that *E. coli* makes enterobactin; *Bacillus subtilis* makes corynebactin; but *L. monocytogenes* does not produce any type of siderophores. This may suggest an unknown relationship between the production of siderophores and the pathogenicity of the bacteria since *L. monocytogenes* is the only pathogen among them.

Most iron uptake systems in Gram (-) bacteria are negatively regulated by iron via Fur protein (repressor). Usually when the amount of the ferrous iron meets the needs of metabolism, extra Fe^{2+} will form a complex with Fur protein. The complex will then bind

the promoter region (Fur box) of a particular iron uptake system probably depending on the type of iron source available. Therefore, RNA polymerase can not bind the promoter and transcription will stop. This negative regulation also applies to FepA protein. However, regulation is different in *L. monocytogenes* and *Bacillus subtilis.* In *Bacillus subtilis,* FeEnt actually shows positive regulation, which means bacteria FeEnt uptake is enhanced when FeEnt is present during growth and later on removed by centrifugation and washing for three times. Other siderophores will be tested in the same way in the future. For *L. monocytogenes,* FeEnt, FeCrn, and Fc were tested and different results were achieved. Fc definitely shows a strong negative regulation as in Gram (-) bacteria, which is consistent with the fact that there is a Fur box upstream of the Fc transport *fhu* operon. However, FeEnt and FeCrn show a weak positive regulation (about 2 folds enhancement of uptake) if there is any at all. Combined with the facts that both *L. monocytogenes* and *Bacillus subtilis* have much higher transport V_{max} for Fc (comparable to that of *E. coli*) than for FeEnt and FeCrn, I think that in extracellular environments these two Gram (+) bacteria favor and utilize primarily Fc, a hydroxamate type of siderophore although bacteria themselves do not synthesize Fc. Fc is secreted by fungus and fungus originates later than bacteria. So it is possible that Fc is the first siderophore that bacteria use to acquire iron before they synthesize their own. Also because Gram (-) bacteria utilize both catecholates and hydroxamates equal efficiently, this may suggest that Gram (+) bacteria originate earlier than Gram (-) bacteria. This could suggest that Fc is one of the earliest siderophores that utilized by Gram (+) bacteria. Only the presence of FeEnt and FeCrn, two catecholate siderophores, will induce the transport of themselves. Their transport is also regulated by proteins (probably inducers) other than Fur. This is

consistent with the data of Fur deletion mutant. When Fur protein is not present in *L. monocytogenes,* the transport of FeCrn is not affected. This suggests that the regulation by FeCrn is not via Fur protein which usually involves in negative regulation. FeEnt and Fc need to be tested, and I predict that transport of Δ*fur* will affect the Fc transport but not the FeEnt transport and Fc regulates iron transport via Fur protein. This also may explain the phenomenon of ferritin deletion mutant. Δ*fri* showed severely impaired Fc transport and slightly enhanced FeCrn transport. When ferritin is absent in bacteria, extra iron may be available in fluids. In result, extra Fc inhibits the transport of Fc and extra FeCrn enhances the transport of FeCrn.

Bacterial pathogenesis always seems to be crucial to its iron acquisition through either siderophores or host iron binding proteins. Lots of the iron binding proteins contain heme. The results that *ΔhupC* decreased LD_{50} by 50%, and *ΔfhuC* did not affect LD_{50} suggested a relationship between heme acquisition and bacteria pathogenicity. Heme, the iron protoporphyrin IX molecule, is a prosthestic group consisting of many enzymes. However heme is toxic because it is a hydrophobic molecule that can partition into membranes and promote nonenzymatic redox reactions. This explains why heme is scarcely found free although it is the most abundant form of iron-containing compounds. In laboratory conditions, many bacteria, such as *Streptococcus* (Liu and Lei, 2005; Lei *et al.,* 2003; Bates *et al.,* 2003), *Serratia marcescens* (Letoffe *et al.,* 2005), *Staphylococcus aureus* (Skaar *et al.,* 2004), *Vibrio anguillarum* (Mourino et al., 2004), *Vibrio cholerae* (Wyckoff *et al.,* 2004), and *Actinobacillus pleuropneumoniae* (Archambault *et al.,* 2003), can use heme as their sole iron source for growth and some components of the acquisition systems have been identified. Heme in the nanomolar range is usually sufficient. Like

those bacteria, *L. monocytogenes* can use heme as its sole iron source for growth (Fig. 5.1.1). In addition, *L. monocytogenes* also grows much faster (data not shown) when Hn (2 μM) is present in KRMI media. This could suggest that the utilization of Hn is under positive regulation. Most bacteria have several uptake systems for iron sources. It would be a substantial waste of energy to induce all the acquisition systems in response to iron limitation since most environments are iron limited. Especially this could true for those pathogenic bacteria. Although the ^{59}Hn uptake experiment is not yet completed, a couple of initial experiments (data not shown) show that the transport rate is probably faster than the transport of iron-siderophore complexes, such as FeEnt and FeCrn, by *L. monocytognes*. When the concentrations of ^{59}Hn are equal to or below 100 nM in a two-hour transport experiment, the transport rate is almost linear to the increasing concentration of ^{59}Hn. This is very similar to the one-hour FeEnt transport by E. coli FepA (Fig. 4.6.2), which also shows a linear relationship between the transport rate and the concentration of ^{59}FeEnt that is in nanomolar range. This could be very true because extracellular environments of pathogenic bacteria usually contain very low concentration of iron. However when the concentrations are higher than 100 nM, the transport rate decreases rapidly, even to negative numbers. This indicates that when iron concentration is high, which does not usually happen in hosts' body fluids, different mechanism of iron acquisition may occur. This is also suggested by the transport studies of *Δlmo2429*. *Δlmo2429* cannot grow with Hn as the sole iron source in the nutrition assays (Fig. 5.1.1), but the deletion of *hupC* does not completely (probably around 50%) diminish the transport of ^{59}Hn, even though those experiments need to be repeated. Another possibility is that higher concentration of Hn may inhibit the utilization of Hn by an unknown

mechanism. Also Hn utilization may be regulated by iron via Fur protein depending on the extracellular concentration of Hn. Two things should be tested immediately. One is that although the rate of the siderophore transport by *L. monocytogenes* is low, I should test the ability of *L. monocytogenes* to utilize Hn in a shorter time period than two hours. Two is that I should look at the effect of nonradioactive Hn that is added to KRMI media during the growth of *L. monocytogenes* to the transport of ^{59}Hn. The possibility that the utilization rate of Hn is faster than that of the siderophore is consistent to the fact that pathogenic bacteria prefer Hn (Rouault, 2004), and that *L. monocytogenes* does not produce any type of siderophores.

I studied both nonpathogenic and pathogenic bacteria. I also studied both Gram (-) and Gram (+) bacteria. Among *E. coli*, *Bacillus subtilis*, and *Listeria monocytogenes*, mechanism of iron acquisition may be one of the biggest differences between them. *E. coli k12* is a nonpathogenic Gram (-) bacteria. It produces and secretes a catecholate siderophore: enterobactin. It then adopts a whole system, including OM transporter (FepA), PP iron binding protein (FepB), and IM ABC type transport system (FepDGC), to bind and transport FeEnt to the cytoplasm, and then ferric esterase in the cytoplasm will break the FeEnt and reduce Fe^{3+} to Fe^{2+} for its metabolism. *Bacillus subtilis* is a nonpathogenic Gram (+) bacteria. It also produces and secretes a catecholate siderophore: corynebactin. Although no FeCrn acquisition system has been studied, FeCrn can support its growth on a solid medium plate (Fig. 5.2.2). Both of *E. coli k12* and *Bacillus subtilis* are nonpathogenic. No heme transporter has been identified within these two species, but a number of different siderophore transport systems have been found in *E. coli*. *Listeria monocytogenes* is a pathogenic Gram (+) bacteria. It does not secrete siderophores

although it does utilize them. Just like lots of other pathogenic bacteria, *L. monocytogenes* has heme utilization systems. It may also utilize heme at a very fast rate (data not shown). To combat microbial infections, hosts always strictly limit the availability of free iron in their blood and tissues. They do this by ensuring that iron is carried by high-affinity iron-binding proteins, which usually also contain heme. Due to the low availability of free iron, secretion of siderophores will not contribute very much to iron acquisition and bacterial survival. On the other hand, iron can be acquired from heme in hosts if bacteria can get free heme or get heme out of heme-containing proteins. So it is possible that *L. monocytogenes* also prefers heme as its major iron source just like *S. aureus* (Rouault, 2004). All these seem to suggest that nonpathogenic and pathogenic respond differently to their extracellular environments. In lab condition, however, all bacteria show very broad substrate specificity despite of their possible preferences, indicating the power of evolution.

In summary, both Gram (-) and Gram (+) bacteria have developed very sophisticated iron uptake systems that are specific to siderophores, free heme, or iron-containing proteins so that they can survive different environments.

References:

Adams TJ, V. S., Cowart RE. (1990). "Iron acquisition systems of Listeria monocytogenes." Infect Immun. 58(8): 2715-8.

Ahmer BM, T. M., Larsen RA, Postle K. (1995). "Characterization of the exbBD operon of Escherichia coli and the role of ExbB and ExbD in TonB function and stability." J Bacteriol. 177(16): 4742-7.

Alan Cockayne, P. J. H., Nick B. L. Powell, keith Bishop, Cate Sims, and Paul Williams (1998). "Molecular Cloning of a 32-Kilodalton Lipoprotein Component of a Novel Iron-regulated Staphylococcus epidermidis ABC Transporter." Infect Immun. 66(8): 3767-74.

Andersen C, B. C., Tauber H, Benz R, Wang J, Michel V, Newton SM, Hofnung M, Charbit A. (1999). "In vivo and in vitro studies of major surface loop deletion mutants of the Escherichia coli K-12 maltoporin: contribution to maltose and maltooligosaccharide transport and binding." Mol Microbiol. 32(4): 851-67.

Anming Xiong, V. K. S., Guillermo Cabrera and Radheshyam K. Jayaswal (2000). "Molecular characterization of the ferric-uptake regulator, Fur, from Staphylococcus aureus." microbiology 146: 659-68.

Archambault M, L. J., Rioux CR, Dumas F, Thibault P, Elkins C, Jacques M. (2003). "Identification and preliminary characterization of a 75-kDa hemin- and hemoglobin-binding outer membrane protein of Actinobacillus pleuropneumoniae serotype 1." Can J Vet Res. 67(4): 271-7.

Armstrong, S. K., C. L. Francis, and M. A. McIntosh. (1990). "Molecular analysis of the Escherichia coli ferric enterobactin receptor FepA." J. Biol. Chem. 265: 14536-14543.

Barchini E, C. R. (1996). "Extracellular iron reductase activity produced by Listeria monocytogenes." Arch Microbiol. 166(1): 51-57.

Barnard TJ, W. M. J., McIntosh MA. (2001). "Mutations in the Escherichia coli receptor FepA reveal residues involved in ligand binding and transport." Mol Microbiol. 41(3): 527-36.

Bates CS, M. G., Woods CR, Vincent RM, Eichenbaum Z. (2003). "Identification and characterization of a Streptococcus pyogenes operon involved in binding of hemoproteins and acquisition of iron." Infect Immun. 71(3): 1042-55.

Bearden SW, P. R. (1999). "The Yfe system of Yersinia pestis transports iron and manganese and is required for full virulence of plague." Mol Microbiol. 32(2): 403-14.

Bearden SW, S. T., Perry RD. (1998). "An ABC transporter system of Yersinia pestis allows utilization of chelated iron by Escherichia coli SAB11." J. Bacteriol. 180(5): 1135-47.

Benfang Lei, L. M. S., Heather M. Menning, Jovanka M. Voyich, Subbarao V. kala, Frank R. Deleo, Sean D. Reid, and James M. Musser (2002). "Identification and Characterication of a Novel Heme-Associated Cell Surface Protein Made by Streptococcus pyogenes." Infect Immun. 70(8): 4494-4500.

Bengang Lei, M. L., Jovanka M. Voyich, Christopher I. Prater, Subbarao V. Kala, Frank R. DeLeo, and James M. Musser (2003). "Identification and Characterization of HtsA, a Second Heme-Binding Protein Made by Streptococcus pyogenes." Infect Immun. 71(10): 5962-9.

Benjamin WH Jr, T. C. J., Posey BS, Briles DE. (1986). "Salmonella typhimurium virulence genes necessary to exploit the Itys/s genotype of the mouse." Infect. Immun. 51(3): 872-8.

Benz R, F. G., Nakae T, Ferenci T. (1992). "Investigation of the selectivity of maltoporin channels using mutant LamB proteins: mutations changing the maltodextrin binding site."

Biochim Biophys Acta. 1104(2): 299-307.

Bergmann B, R. D., Kuhn M, Goetz M, Hom S, Goebel W. (2002). "InlA- but not InlB-mediated internalization of Listeria monocytogenes by non-phagocytic mammalian cells needs the support of other internalins." Mol. Microbiol. 43(3): 557-570.

Bierne H, D. S., Gratacap MP, Randriamampita C, Carpenter G, Payrastre B, Cossart P. (2000). "The invasion protein InlB from Listeria monocytogenes activates PLC-gamma1 downstream from PI 3-kinase." Cell Microbiol. 2(6): 465-476.

Bierne H, M. S., Trost M, Pucciarelli MG, Liu G, Dehoux P, Jansch L, Garcia-del Portillo F, Schneewind O, Cossart P; European Listeria Genome Consortium. (2002). "Inactivation of the srtA gene in Listeria monocytogenes inhibits anchoring of surface proteins and affects virulence." 43 4(869-881).

Bierne H., G., C., Pucciarelli, M.G., Sabet, C., Newton, S.M., del Portillo, F.G., (2004). "Sortase B, a new class of sortase in Listeria monocytogenes." J Bacteriol. 1972-82.

Bluhm ME, K. S., Dertz EA, Raymond KN. (2002). "Corynebactin and enterobacin: related siderophores of opposite chirality." J Am Chem Soc. 124(11): 2436-7.

Bonnah RA, Y. R., Schryvers AB. (1995). "Biochemical analysis of lactoferrin receptors in the Neisseriaceae: identification of a second bacterial lactoferrin receptor protein." Microb Pathog. 19(5): 285-97.

Boyer E, B. I., Malo D, Gros P, Cellier MF. (2002). "Acquisition of Mn(II) in addition to Fe(II) is required for full virulence of Salmonella enterica serovar Typhimurium." Infect Immun. 70(11): 6032-42.

Brackett, R. E. (1988). "Presence and persistence of Listeria monocytogenes in food and water." Food technol. 42(4): 162-4.

Brass, J. M. (1986). "Calcium-Induced Permeabilization of the Outer Membrane: A Method for Reconstitution of Periplasmic Binding Protein-Dependent Transport Systems in Escherichia coli and Salmonella typhimurium." Methods in Enzymology 125: 289-302.

Braun (1997). "Surface signaling: novel transcription initiation mechanism starting from the cell surface." Arch. Microbiol 167: 325-331.

Braun M, E. F., Killmann H, Braun V. (2003). "In vivo reconstitution of the FhuA transport protein of Escherichia coli K-12." J Bacteriol. 185(18): 5508-18.

Braun, M., H. Killmann, and V. Braun (1999). "The ß-barrel domain of FhuA5-160 is sufficient for TonB-dependent FhuA activities of Escherichia coli." Mol. Microbiol 33: 1037-1049.

Braun, V. (1989). "The structurally related exbB and tolQ genes are interchangeable in conferring tonB-dependent colicin, bacteriophage, and albomycin sensitivity." J. Bacteriol 171: 6387-6390.

Braun, V. (1995). "Energy-coupled transport and signal transduction through the gram-negative outer membrane via TonB-ExbB-ExbD-dependent receptor proteins." FEMS Microbiol Rev. 16(4): 295-307.

Braun, V. (2005). "Bacterial iron transport related to virulence." Contrib Microbilo. 12: 210-33.

Braun, V., Braun M, Killmann H. (2000). "Iron transport in Escherichia coli. Crystal structure of FhuA, an outer membrane iron and antibiotic transporter." Adv Exp Med Biol. 485: 33-43.

Braun, V., H. Killmann, and R. Benz. (1994). "Energy-coupled transport through the outer membrane of Escherichia coli small deletions in the gating loop convert the FhuA transport protein into a diffusion channel." FEBS Lett. 346: 59-64.

Braun, V., Hantke K, Koster W. (1998). "Bacterial iron transport: mechanisms, genetics, and regulation." Met Ions Biol Syst. 35(67): 67-145.

Braun, V., J. Frenz, K. Hantke, and K. Schaller (1980). "Penetration of colicin M into cells of Escherichia coli." J. Bacteriol. 142: 162-168.

Braun, V., K. Gunter, and K. Hantke (1991). "Transport of iron across the outer membrane." Biol. Met. 4: 14-22.

Braun, V., S. Gaisser, C. Herrmann, K. Kampfenkel, H. Killmann, and I. Traub (1996). "Energy-coupled transport across the outer membrane of Escherichia coli: ExbB binds ExbD and TonB in vitro, and leucine 132 in the periplasmic region and aspartate 25 in the transmembrane region are important for ExbD activity." J. Bacteriol. 178: 2836-2845.

Brown JS, G. S., Holden DW. (2001a). "A Streptococcus pneumoniae pathogenicity island encoding an ABC transporter involved in iron uptake and virulence." Mol Microbiol. 40(3): 572-85.

Brown JS, O. A., Woodrow MC, Holden DW, Paton JC. (2001b). "Immunization with components of two iron uptake ABC transporters protects mice against systemic Streptococcus pneumoniae infection." Infect Immun. 69(11): 6702-6.

Bsat N, H. J. (1999). "Interaction of Bacillus subtilis Fur (ferric uptake repressor) with the dhb operator in vitro and in vivo." J Bacteriol. 181(14): 4299-307.

Buchanan SK, S. B., Venkatramani L, Xia D, Esser L, Palnitkar M, Chakraborty R, van der Helm D, Deisenhofer J. (1999). "Crystal structure of the outer membrane active

transporter FepA from Escherichia coli." Nat Struct Biol. 6(1): 56-63.

Budzikiewicz, H. B., A.; Taraz, K.; Pandey, A.; Meyer, J. M. (1997). "Corynebactin, a cyclic catecholate siderophore from Corynebacterium glutamicum ATCC 14067 (Brevibacterium sp. DSM 20411)." Zeitschrift fuer Naturforschung, C: Biosciences 52(7-8): 551-4.

Bullen, J. J. (1974). "Proceedings: Iron and infection." Br J Haematol. 28(1): 139-40.

Bullen JJ, R. H., Griffiths E. (1978). "Role of iron in bacterial infection." Curr Top Microbiol Immunol. 80: 1-35.

C., B. (1993). "The proton motive force drives the outer membrane transport of cobalamin in Escherichia coli." J Bacteriol. 175(10): 3146-50.

Cadieux, N., C. Bradbeer, and R. J. Kadner. (2000). "Sequence changes in the Ton box region of BtuB affect its transport activities and interaction with TonB protein." J. Bacteriol. 182: 5954-5961.

Cafiso, D. S., and W. L. Hubbell. (1982). "Transmembrane electrical currents of spin-labeled hydrophobic ions." Biophys. J. 39: 263-272.

Cafiso, D. S., and W. L. Hubbell. (1983). "Electrogenic H+/OH– movement across phospholipid vesicles measured by spin-labeled hydrophobic ions." Biophys. J. 44: 49-57.

Cao, Z., P. Warfel, S. M. Newton, and P. E. Klebba (2003). "Spectroscopic observations of ferric enterobactin transport." J. Biol. Chem 278: 1022-1028.

Cao Z, Q. Z., Sprencel C, Newton SM, Klebba PE. (2000). "Aromatic components of two ferric enterobactin binding sites in Escherichia coli FepA." Mol Microbiol. 37(6): 1306-

17.

Chang C, M. A., Pluckthun A, Wlodawer A. (2001). "Crystal structure of the dimeric C-terminal domain of TonB reveals a novel fold." 276 29(27535-40).

Charbit (2003). "Maltodextrin transport through lamb." Front Biosci. 8: s265-74.

Charbit A, W. J., Michel V, Hofnung M. (1998). "A cluster of charged and aromatic residues in the C-terminal portion of maltoporin participates in sugar binding and uptake." Mol Gen Genet. 260(2-3): 185-92.

Chimento, D. P., A. K. Mohanty, R. J. Kadner, and M. C. Wiener. (2003). "Substrate-induced transmembrane signaling in the cobalamin transporter BtuB." Nat. Struct. Biol. 10(394-401).

Cornelissen CN, K. M., Hobbs MM, Anderson JE, Cannon JG, Cohen MS, Sparling PF. (1998). "The transferrin receptor expressed by gonococcal strain FA1090 is required for the experimental infection of human male volunteers." Mol Microbiol. 27(3): 611-6.

Cornelissen CN, S. P. (1994a). "Iron piracy: acquisition of transferrin-bound iron by bacterial pathogens." Mol Microbiol. 14(5): 843-50.

Cornelissen CN, S. P. (1994b). "Identification of receptor-mediated transferrin-iron uptake mechanism in Neisseria gonorrhoeae." Methods Enzymol. 235(356-63).

Cossart P, V. M., Mengaud J, Baquero F, Perez-Diaz JC, Berche P. (1989). "Listeriolysin O is essential for virulence of Listeria monocytogenes: direct evidence obtained by gene complementation." Infect Immun. 57(11): 3629-3636.

Coulanges V, A. P., Vidon DJ. (1996). "Esculetin antagonizes iron-chelating agents and increases the virulence of Listeria monocytogenes." Res Microbiol. 147(9): 677-85.

Coulanges V, A. P., Ziegler O, Buchheit L, Vidon DJ. (1997). "Utilization of iron-catecholamine complexes involving ferric reductase activity in Listeria monocytogenes." Infect Immun. 65(7): 2778-85.

Courcol RJ, T. D., Bissinger MC, Martin GR, Brown MR. (1997). "Siderophore production by Staphylococcus aureus and identification of iron-regulated proteins." Infect Immun. 65(5): 1944-8.

Cowan SW, S. T., Rummel G, Steiert M, Ghosh R, Pauptit RA, Jansonius JN, Rosenbusch JP. (1992). "Crystal structures explain functional properties of two E. coli porins." Nature 358(6389): 727-33.

Cowart, R. (2002). "Reduction of iron by extracellular iron reductases: implications for microbial iron acquisition." Arch Biochem Biophys. 400(2): 273-81.

Cowart RE, F. B. (1985). "Differential effects of iron on the growth of Listeria monocytogenes:minimum requirements and mechanism of acquisition." J Infect Dis. 151(4): 721-30.

Dale SE, D.-K. A., Lajoie G, Heinrichs DE. (2004b). "Role of siderophore biosynthesis in virulence of Staphylococcus aureus: identification and characterization of genes involved in production of a siderophore." Infect Immun. 72(1): 29-37.

Dale SE, S. M., Heinrichs DE. (2004a). "Involvement of SirABC in iron-siderophore import in Staphylococcus aureus." J Bacteriol. 186(24): 8456-62.

Dassa E, B. P. (2001). "The ABC of ABCS: a phylogenetic and functional classification of ABC systems in living organisms." Res Microbiol. 152(3-4): 211-229.

Davies JK, R. P. (1975). "Genetics of resistance to colicins in Escherichia coli K-12: cross-resistance among colicins of group A." J Bacteriol. 123(1): 102-17.

Deneer HG, H. V., Boychuk I. (1995). "Reduction of exogenous ferric iron by a surface-associated ferric reductase of Listeria spp." Microbiology. 141(8): 1985-92.

Dmitriev BA, E. S., Rietschel ET. (1999). "Layered murein revisited: a fundamentally new concept of bacterial cell wall structure, biogenesis and function." Med Microbiol Immunol (Berl). 187(3): 173-181.

Domann E, W. J., Rohde M, Pistor S, Hartl M, Goebel W, Leimeister-Wachter M, Wuenscher M, Chakraborty T. (1992). "A novel bacterial virulence gene in Listeria monocytogenes required for host cell microfilament interaction with homology to the proline-rich region of vinculin." EMBO J. 11(5): 1981-1990.

Drechsel H, F. S., Nicholson G, Haag H, Jung O, Zahner H, Jung G. (1993). "Purification and chemical characterization of staphyloferrin B, a hydrophilic siderophore from staphylococci." Biometals. 6(3): 185-92.

Dumas F, K. R., Winterhalter M, Van Gelder P. (2000). "Sugar transport through maltoporin of Escherichia coli. Role of polar tracks." J Biol Chem. 275(26): 19747-51.

Dutzler R, W. Y., Rizkallah P, Rosenbusch JP, Schirmer T. (1996). "Crystal structures of various maltooligosaccharides bound to maltoporin reveal a specific sugar translocation pathway." Structure 4(2): 127-34.

Dykstra, C. C., and S. R. Kushner (1985). "Physical and biochemical analysis of the cloned recB and recC genes of Escherichia coli K-12." J Bacteriol. 157: 21-7.

E. Gouaux (1997). "Channel-forming toxins: tales of transformation." Curr Opin Struct Biol. 7(4): 566-73.

Ecker, D. J., B. F. Matzanke, and K. N. Raymond. (1986). "Recognition and transport of ferric enterobactin in Escherichia coli." J. Bacteriol. 167: 666-673.

Ecker DJ, P. C., Emery T. (1982). "Role of two siderophores in Ustilago sphaerogena. Regulation of biosynthesis and uptake mechanisms." Biochim Biophys Acta. 720(3): 242-9.

ED, W. (1993). "the development of awareness of iron-withholding defense." Perspect. Biol. Med.(36): 215-21.

Elish ME, P. J., Earhart CF. (1988). "Biochemical analysis of spontaneous fepA mutants of Escherichia coli." J Gen Microbiol. 134(5): 1355-64.

Elkins C, C. C., Thomas CE. (1995). "Characterization of the hgbA locus encoding a hemoglobin receptor from Haemophilus ducreyi." Infect Immun. 63(6): 2194-200.

Elkins C, T. P., Olsen B, Thomas CE. (1998). "Role of the Haemophilus ducreyi Ton system in internalization of heme from hemoglobin." Infect Immun. 66(1): 151-60.

Emery, T. (1971). "Role of ferrichrome as a ferric ionophore in Ustilago sphaerogena." Biochemistry 10(8): 1483-1488.

Eric P. Skaar, A. H. G., and Olaf Schneewind (2004). "IsdG and IsdI, heme-degrading Enymes in the Cytoplasm of Staphylococcus aureus." J Biol Chem. 279(1): 436-443.

Evans LJ, C. A., Lakey JH. (1996). "Direct measurement of the association of a protein with a family of membrane receptors." J Mol Biol. 255(4): 559-63.

Ferguson, A. D., and J. Deisenhofer. (2002b). "TonB-dependent receptors-structural perspectives." Biochim. Biophys. Acta 1565: 318-332.

Ferguson AD, B. V., Fiedler HP, Coulton JW, Diederichs K, Welte W. (2000). "Crystal structure of the antibiotic albomycin in complex with the outer membrane transporter FhuA." Protein Sci. 9(5): 956-63.

Ferguson AD, H. E., Coulton JW, Diederichs K, Welte W. (1998). "Siderophore-mediated iron transport: crystal structure of FhuA with bound lipopolysaccharide." Science 282(5397): 2215-20.

Ferguson, A. D., J. Kodding, G. Walker, C. Bos, J. W. Coulton, K. Diederichs, V. Braun, and W. Welte. (2001). "Active transport of an antibiotic rifamycin derivative by the outer-membrane protein FhuA." Structure 9: 707-716.

Ferguson, A. D., R. Chakraborty, B. S. Smith, L. Esser, D. van der Helm, and J. Deisenhofer. (2002a). "Structural basis of gating by the outer membrane transporter FecA." Science 295: 1715-1719.

Fernandez-Beros ME, G. C., McIntosh MA, Cabello FC. (1989). "Immune response to the iron-deprivation-induced proteins of Salmonella typhi in typhoid fever." Infect Immun. 57(4): 1271-5.

Finch, P. W., R. E. Wilson, K. Brown, I. D. Hichson, and P. T. Emerson (1986). "Complete nucleotide sequence of the Escherichia coli ptr gene encoding protease III." Nucleic Acids Res. 14: 7695-7703.

Forst D, W. W., Wacker T, Diederichs K. (1998). "Structure of the sucrose-specific porin ScrY from Salmonella typhimurium and its complex with sucrose." Nat Struct Biol. 5(1): 37-46.

Foster, R. E. C. a. B. G. (1985). "Differential Effects of Iron on the Growth of Listeria monocytogenes: Minimum Requirements and Mechanism of Acquisition." The Journal of Infectious Diseases 151(4): 721-30.

Frisk A, S. J., Wang G, Bertucci DC, Marrero L, Hwang SH, Hassett DJ, Schurr MJ. (2004). "Transcriptome analysis of Pseudomonas aeruginosa after interaction with human airway epithelial cells." Infect. Immun. 72(9): 5433-8.

Furman M, F. A., Saxena M, Di Fabio JL, Cabello FC. (1994). "Salmonella typhi iron uptake mutants are attenuated in mice." Infect. Immun. 62(9): 4091-4.

George*, P. M. J. a. A. M. (2002). "Mechanism of ABC transporters: A molecular dynamics simulation of a well characterized nucleotide-binding subunit." Proc Natl Acad Sci 99(20): 12639-44.

Georgiou, F. B. a. G. (1991). "Construction and characterization of Escherichia coli strains deficient in multiple secreted proteases: protease III degrades high-molecular-weight substrates in vivo." J Bacteriol. 173(8): 2696-2703.

Giovanna Ferro-Luzzi Ames, C. P., and Sydner Kustu (1984). "Simple, Rapid, and Quantitative Release of Periplasmic Proteins by Chloroform." J. Bacteriol. 160(3): 1181-1183.

Glaser P, F. L., Buchrieser C, Rusniok C, Amend A, Baquero F, Berche P, Bloecker H, Brandt P, Chakraborty T, Charbit A, Chetouani F, Couve E, de Daruvar A, Dehoux P, Domann E, Dominguez-Bernal G, Duchaud E, Durant L, Dussurget O, Entian KD, Fsihi H, Garcia-del Portillo F, Garrido P, Gautier L, Goebel W, Gomez-Lopez N, Hain T, Hauf J, Jackson D, Jones LM, Kaerst U, Kreft J, Kuhn M, Kunst F, Kurapkat G, Madueno E, Maitournam A, Vicente JM, Ng E, Nedjari H, Nordsiek G, Novella S, de Pablos B, Perez-Diaz JC, Purcell R, Remmel B, Rose M, Schlueter T, Simoes N, Tierrez A, Vazquez-Boland JA, Voss H, Wehland J, Cossart P. (2001). "Comparative genomics of Listeria species." Science 294(5543): 849-52.

Gray-Owen SD, S. A. (1996). "Bacterial transferrin and lactoferrin receptors." Trends Microbiol.(4): 5.

Gre´gory Verdon1, S. V. A., Bauke W. Dijkstra1 and A. J. M. D. a. A.-M. W. H. Thunnissen1* (2003). "Crystal Structures of the ATPase Subunit of the Glucose ABC Transporter from Sulfolobus solfataricus: Nucleotide-free and Nucleotide-bound

Conformations." J. Mol. Biol. 330: 343-58.

Grossman SH, L. J. B., Mixon D. (1983). "A comparison of native and covalently crosslinked creatine kinases: denaturation and reassembly." Arch Biochem Biophys. 224(2): 449-55.

H. Anne Eisenhauer, S. S., Peter D. Pawelek, and James W. Coulton (2005). "siderophore Transport through Escherichia coli Outer Membrane Receptor FhuA with Disulfide-tethered Cork and Barrel Domains." J Biol Chem. 280(34): 30574-80.

H., N. (1992). "Porins and specific channels of bacterial outer membranes." Mol Microbiol. 6(4): 435-42.

Haag H, F. H., Meiwes J, Drechsel H, Jung G, Zahner H. (1994). "Isolation and biological characterization of staphyloferrin B, a compound with siderophore activity from staphylococci." FEMS Microbiol Lett. 115(2-3): 125-30.

Hanahan, D. (1983). "Studies on transformation of Escherichia coli with plasmids." J Mol Biol. 166(4): 557-80.

Hancock, R. W., and V. Braun. (1976). "nature of the energy requirement for the irreversible adsorption of bacteriophages T1 and Φ80 to Escherichia coli." J. Bacteriol. 125: 409-15.

Hashimoto-Gotoh T, F. F., Nordheim A, Timmis KN. (1981). "Specific-purpose plasmid cloning vectors. I. Low copy number, temperature-sensitive, mobilization-defective pSC101-derived containment vectors." Gene 1-3(227-35).

Hay, B. P. D., D. A. Vargas, R. Garza, J., and K. N. Raymond. (2001). "Structural criteria for the rational design of selective ligands. 3. Quantitative structure-stability relationship for iron(III) complexation by Tris-catecholamide siderophores." Inorg. Chem. 40: 3922-

3935.

Heidinger, S., V. Braun, V. L. Pecoraro, and K. N. Raymond. (1983). "Iron supply to Escherichia coli by synthetic analogs of enterochelin." J. Bacteriol. 153: 109-115.

Heinrichs JH, G. L., Kunsch C, Choi GH, Hanson MS. (1999). "Identification and characterization of SirA, an iron-regulated protein from Staphylococcus aureus." J Bacteriol. 181(5): 1436-43.

Held KG, P. K. (2002). "ExbB and ExbD do not function independently in TonB-dependent energy transduction." J Bacteriol. 184(18): 5170-3.

Higgs PI, L. R., Postle K. (2002). "Quantification of known components of the Escherichia coli TonB energy transduction system: TonB, ExbB, ExbD and FepA." Mol Microbiol. 44(1): 271-81.

Higgs PI, M. P., Postle K. (1998). "Interactions in the TonB-dependent energy transduction complex: ExbB and ExbD form homomultimers." J Bacteriol. 180(22): 6031-8.

Hilsenbeck JL, P. H., Chen G, Youn B, Postle K, Kang C. (2004). "Crystal structure of the cytotoxic bacterial protein colicin B at 2.5 A resolution." Mol Microbiol. 51(3): 711-20.

Hitchins, A. D. (1998). Listeria monocytogenes. In Food and Drug Administration Bacteriological Analytical Manual. R. L. Merker. Gaithersburg, MD, AOAC International. 10.

Hoffmann H, F. E., Kraut H, Braun V. (1986). "Preparation of the FhuA (TonA) receptor protein from cell envelopes of an overproducing strain of Escherichia coli K-12." J Bacteriol. 166(2): 404-11.

Hunt MD, P. G., McIntosh MA. (1994). "Promoter and operator determinants for fur-mediated iron regulation in the bidirectional fepA-fes control region of the Escherichia coli enterobactin gene system." J Bacteriol. 176(13): 3944-55.

Ichihara, S., N. Beppu, and S. Mizushima (1984). "Protease IV, a cytoplasmic membrane protein of Escherichia coli, has signal peptide peptidase activity." J. Biol. Chem. 259(9853-7).

Ichihara, S., T. Suzuki, M. Suzuki, and S. Mizushima (1986). "Molecular cloning and sequencing of the sppA gene and characterizaition of the encoded protease IV, a signal peptide peptidase, of Escherichia coli." J Biol Chem. 261(9405-11).

Jarosik GP, M. I., Hansen EJ. (1995). "Utilization of transferrin-bound iron by Haemophilus influenzae requires an intact tonB gene." Infect Immun. 63(2): 710-3.

Jin H, R. Z., Whitby PW, Morton DJ, Stull TL. (1999). "Characterization of hgpA, a gene encoding a haemoglobin/haemoglobin-haptoglobin-binding protein of Haemophilus influenzae." Microbiology. 145 (Pt 4): 905-14.

John E.Walker*, M. S., Michael J.Runswick, and and N. J.Gay (1982). "Distantly related sequences in the a- and f-subunits of ATP synthase, myosin, kinases and other ATP-requiring enzymes and a common nucleotide binding fold." The EMBO journal 1(8): 945-51.

Jon H. heinrichs, L. E. G., Charles Kunsch, Gil H. Choi, and Mark S. Hanson (1999). "Identification and Characterization of SirA, an Iron-Regulated Protein from Staphylococcus aureus." Journal of Bacteriology 181(5): 1436-43.

Jurado, R. L. (1997). "Iron, infections, and anemia of inflammation." Chin. Infec. Dis. 25: 888-895.

K., H. (1984). "Cloning of the repressor protein gene of iron-regulated systems in Escherichia coli K12." Mol Gen Genet. 197(2): 337-41.

K., H. (1990). "Dihydroxybenzoylserine--a siderophore for E. coli." FEMS Microbiol Lett. 55(1-2): 5-8.

Kammler M, S. C., Hantke K. (1993). "Characterization of the ferrous iron uptake system of Escherichia coli." J Bacteriol. 175(19): 6212-9.

Karl-Peter Hopfner, A. K., *, L. C. David S. Shin, * L. Matthew Arthur,†, et al. (2000). "Structural Biology of Rad50 ATPase: ATP-Driven Conformational Control in DNA Double-Strand Break Repair and the ABC-ATPase Superfamily." cell 101: 789-800.

Karlsson M, H. K., Higgins CF. (1993). "ExbB acts as a chaperone-like protein to stabilize TonB in the cytoplasm." Mol Microbiol. 8(2): 389-96.

Karpishin, T. B. D., Torin M.; Raymond, Kenneth N. (1993). "Coordination chemistry of microbial iron transport. 49. The vanadium(IV) enterobactin complex: structural, spectroscopic, and electrochemical characterization." J Am Chem Soc. 115(5): 1842-51.

Kim BH, A. C., Kreth J, Ulmke C, Schmid K, Benz R. (2002). "Site-directed mutagenesis within the central constriction site of ScrY (sucroseporin): effect on ion transport and comparison of maltooligosaccharide binding to LamB of Escherichia coli." J Membr Biol. 187(3): 239-53.

Klebba, P. E. (2003). "Three paradoxes of ferric enterobactin uptake." Front. Biosci. 8: 1422-1436.

Klebba, P. E., M. A. McIntosh, and J. B. Neilands. (1982). "Kinetics of biosynthesis of iron-regulated membrane proteins in Escherichia coli." J Bacteriol. 149: 880-888.

Klebba PE, N. S. (1998). "Mechanisms of solute transport through outer membrane porins: burning down the house." Curr Opin Microbiol 1(2): 238-47.

Klebba PE, N. S., Charbit A, Michel V, Perrin D, Hofnung M. (1997). "Further genetic analysis of the C-terminal external loop region in Escherichia coli maltoporin." Res Microbiol. 148(5): 375-87.

Kock J, O. T., Kamp RM, Braun V. (1987). "Primary structure of colicin M, an inhibitor of murein biosysnthesis." J Bacteriol. 169(7): 3358-61.

Konetschny-Rapp S, J. G., Meiwes J, Zahner H. (1990). "Staphyloferrin A: a structurally new siderophore from staphylococci." Eur J Biochem. 191(1): 65-74.

Konopka, K., and J. B. Neilands. (1984a). "Protein A reactivity with mouse immunoglobulins. Structural relationship between some mouse and human immunoglobulins." J. Immunol. 105: 1116-23.

Konopka, K., Neilands JB. (1984b). "Effect of serum albumin on siderophore-mediated utilization of transferrin iron." Biochemistry. 23(10): 2122-7.

Kreft J, V.-B. J., Altrock S, Dominguez-Bernal G, Goebel W. (2002). "Pathogenicity islands and other virulence elements in Listeria." Curr Top Microbiol Immunol. 264(2): 109-125.

Kronvall, G., H. M. Grey, and R. C. Williams, Jr. (1970). "Protein A reactivity with mouse immunoglobulins. Structural relationship between some mouse and human immunoglobulins." J. Immunol 105: 1116-23.

Kuan G, D. E., Saurin W, Hofnung M, Saier MH Jr. (1995). "Phylogenetic analyses of the ATP-binding constituents of bacterial extracytoplasmic receptor-dependent ABC-type nutrient uptake permeases." Res. Microbiol. 146(4): 271-278.

Kunkel TA, R. J., Zakour RA (1987). "Rapid and efficient site-specific mutagenesis without phenotypic selection." Methods Enzymol. 154: 367-82.

Larsen RA, F.-H. D., McIntosh MA, Postle K. (1997). "Regions of Escherichia coli TonB and FepA proteins essential for in vivo physical interactions." J Bacteriol. 179(10): 3213-21.

Larsen RA, L. T., Postle K. (2003). "In vivo evidence of TonB shuttling between the cytoplasmic and outer membrane in Escherichia coli." Mol Microbiol. 49(1): 211-8.

Larsen RA, T. M., Postle K. (1999). "Protonmotive force, ExbB and ligand-bound FepA drive conformational changes in TonB." Mol Microbiol. 31(6): 1809-24.

Larsen RA, W. G., Postle K. (1993). "The conserved proline-rich motif is not essential for energy transduction by Escherichia coli TonB protein." Mol Microbiol. 10(5): 943-53.

Lazdumski CJ, B. E., Rigal A, Journet L, Lloubes R, Benedetti H. (1998). "Colicin import into Escherichia coli cells." J Bacteriol. 180(19): 4993-5002.

Lei, M. L. a. B. (2005). "Heme Transfer from Streptococcal Cell Surface Protein Shp to HtsA of Transporter HtsABC." Infect Immun. 73(8): 5086-92.

Leong J, N. J. (1976). "Mechanisms of siderophore iron transport in enteric bacteria." J Bacteriol. 126(2): 823-30.

Leslie D. Cope, Z. H., and Eric J. Hansen (2000). "Detection of Phase Variation in Expression of Proteins Involved in Hemoglobin and Hemoglobin-Haptoglobin Binding by Nontypeable Haemophilus influenzae." Infect Immun. 68(7): 4092-101.

Letain TE, P. K. (1997). "TonB protein appears to transduce energy by shuttling between the cytoplasmic membrane and the outer membrane in Escherichia coli." Mol Microbiol.

24(2): 271-83.

Letellier L, L. K., Plancon L, Rosenbusch JP. (1997). "Modeling ligand-gated receptor activity. FhuA-mediated ferrichrome efflux from lipid vesicles triggered by phage T5." J Biol Chem. 272(3): 1448-51.

Letoffe S, W. K., Delepierre M, Delepelaire P, Wandersman C. (2005). "Activities of the Serratia marcescens heme receptor HasR and isolated plug and beta-barrel domains: the beta-barrel forms a heme-specific channel." J. Bacteriol. 187(13): 4637-45.

Lety MA, F. C., Dubail I, Beretti JL, Kayal S, Berche P, Charbit A. (2001). "Identification of a PEST-like motif in listeriolysin O required for phagosomal escape and for virulence in Listeria monocytogenes." Mol Microbiol. 39(5): 1124-1139.

Liu, J., Rutz, J. M., Klebba, P. E., and Feix, J. B. (1994). "A site-directed spin-labeling study of ligand-induced conformational change in the ferric enterobactin receptor, FepA." Biochemistry 33(45): 13274-83.

Locher KP, R. B., Koebnik R, Mitschler A, Moulinier L, Rosenbusch JP, Moras D. (1998). "Transmembrane signaling across the ligand-gated FhuA receptor: crystal structures of free and ferrichrome-bound states reveal allosteric changes." Cell 95(6): 771-8.

Luckey, M., J. R. Pollack, R. Wayne, B. N. Ames, and J. B. Neilands. (1972). "Iron uptake in Salmonella typhimurium: utilization of exogenous siderochromes as iron carriers." J. Bacteriol. 111: 731-738.

M Furman, A. F., M Saxena, JL Di Fabio and FC Cabello (1994). "Salmonella typhi iron uptake mutants are attenuated in mice." Infect Immun. 62(9): 4091-4.

M. Tom Sebulsky, C. D. S., Brian H. Shilton, David R. Edgell, and Savid E. Heinrichs

(2004). "FhuD1, a Ferric Hydroamate-binding Lipoprotein in Staphylococcus aureus." The Journal of Biological Chemistry 279(17): 53152-9.

M.E. Elish, J. R. P. a. C. F. E. (1988). "Biochemical analysis of Spontaneous fepA Mutants of Escherichia coli." Journal of General Microbiology 134: 1355-64.

Mark A. Mcintosh, S. S. C. a. C. F. E. (1979). "Genetic and Physiological Studies on the Relationship Between Colicin B Resistance and Ferrienterochlin Uptake in Escherichia coli K-12." Journal of Bacteriology 137(1): 653-7.

May, J. J. W., Thomas M.; Marahiel, Mohamed A. (2001). "The dhb operon of Bacillus subtilis encodes the biosynthetic template for the catecholic siderophore 2,3-dihydroxybenzoate-glycine-threonine trimeric ester bacillibactin." J Biol Chem. 276(10): 7209-17.

Mazmanian SK, S. E., Gaspar AH, Humayun M, Gornicki P, Jelenska J, Joachmiak A, Missiakas DM, Schneewind O. (2003). "Passage of heme-iron across the envelope of Staphylococcus aureus." Science. 299(5608): 906-909.

Mazmanian SK, T.-T. H., Su K, Schneewind O. (2002). "An iron-regulated sortase anchors a class of surface protein during Staphylococcus aureus pathogenesis." Proc Natl Acad Sci U S A 99(4): 2293-8.

McIntosh MA, C. S., Earhart CF. (1979). "Genetic and physiological studies on the relationship between colicin B resistance and ferrienterochelin uptake in Escherichia coli K-12." J Bacteriol. 137(1): 653-7.

Meerman H J, G. G. (1994). "Construction and characterization of a set of E. coli strains defective in all known loci effecting the proteolytic stability of secreted recombinant proteins." Biotechnology 12: 1107-1110.

Meiwes J, F. H., Haag H, Zahner H, Konetschny-Rapp S, Jung G. (1990). "Isolation and characterization of staphyloferrin A, a compound with siderophore activity from Staphylococcus hyicus DSM 20459." FEMS Microbiol Lett. 55(1-2): 201-5.

Messing, J. (1979). "A multipurpose cloning system based on the single-stranded DNA bacteriophage M13." DNA Tech. Bull. 3(2): 43-8.

Moeck GS, T. P., Xiang H, Ismail AA, Turnbull JL, Coulton JW. (1996). "Ligand-induced conformational change in the ferrichrome-iron receptor of Escherichia coli K-12." Mol Microbiol. 22(3): 459-71.

Morton DJ, S. T. (1999). "Distribution of a family of Haemophilus influenzae genes containing CCAA nucleotide repeating units." FEMS Microbiol Lett. 174(2): 303-9.

Mourino S, O. C., Lemos ML. (2004). "Characterization of heme uptake cluster genes in the fish pathogen Vibrio anguillarum." J Bacteriol. 186(18): 6159-67.

MP., S. (1997a). "Utilization of host iron sources by Corynebacterium diphtheriae: identification of a gene whose product is homologous to eukaryotic heme oxygenases and is required for acquisition of iron from heme and hemoglobin." J Bacteriol. 179(3): 838-45.

MP., S. (1997b). "Transcription of the Corynebacterium diphtheriae hmuO gene is regulated by iron and heme." Infect Immun. 65(11): 4634-41.

Murphy CK, K. V., Klebba PE. (1990). "Surface topology of the Escherichia coli K-12 ferric enterobactin receptor." J Bacteriol. 172(5): 2736-46.

Navarre WW, S. O. (1999). "Surface proteins of gram-positive bacteria and mechanisms of their targeting to the cell wall envelope." Microbiol Mol Biol Rev. 63(1): 174-229.

Neidhardt FC, B. P., Smith DF (1974). "Culture medium for enterobacteria." J Bacteriol. 119(3): 736-47.

Neilands, J. B. (1973). iron transport compounds (siderochromes). Inorganic Biochemistry. E. G.L. Eichhorn. New York. 1.

Neilands, J. B. (1974). Iron and its role in microbial physiology. Microbial iron metabolism: a comprehensive treatise. New York, Academic Press, Inc., New York. 1: 4-34.

Neilands, J. B. (1981). "Microbial iron compounds." Annu. Rev. Biochem. 50: 715-31.

Neilands, J. B. (1995). "Siderophores: structure and function of microbial iron transport compounds." J Biol Chem. 270(45): 26723-6.

Neilands JB, E. T., Rastetter WH. (1981). "Stereospecificity of the ferric enterobactin receptor of Escherichia coli K-12." J Biol Chem. 256(8): 3831-2.

Neilands, J. B., T. Peterson, and S. A. Leong (1980). High-affinity iron transport in microorganisms. Inorganic chemistry in biology and medicine. Washington, D.C., ACS Symposium Series. American Chemical Society. 140: 263-278.

Newton SM, A. J., Cao Z, Qi Z, Jiang X, Sprencel C, Igo JD, Foster SB, Payne MA, Klebba PE. (1997). "Double mutagenesis of a positive charge cluster in the ligand-binding site of the ferric enterobactin receptor, FepA." Proc Natl Acad Sci 94(9): 4560-5.

Newton SM, I. J., Scott DC, Klebba PE. (1999). "Effect of loop deletions on the binding and transport of ferric enterobactin by FepA." Mol Microbiol. 32(6): 1153-65.

Newton SM, K. P., Raynaud C, Shao Y, Jiang X, Dubail I, Archer C, Frehel C, Charbit A. (2005). "The svpA-srtB locus of Listeria monocytogenes: fur-mediated iron regulation

and effect on virulence." Mol Microbiol. 55(3): 927-940.

Nikaido H, N. T. (1979). "The outer membrane of Gram-negative bacteria." Adv Microb Physiol.(20): 163-250.

Nikaido H, V. M. (1985). "Molecular basis of bacterial outer membrane permeability." Microbiol Rev. 49(1): 1-32.

Occhino DA, W. E., Henderson DP, Wrona TJ, Payne SM. (1998). "Vibrio cholerae iron transport: haem transport genes are linked to one of two sets of tonB, exbB, exbD genes." Mol Microbiol. 29(6): 1493-507.

Olsen KN, L. M., Gahan CG, Kallipolitis B, Wolf XA, Rea R, Hill C, Ingmer H. (2005). "The Dps-like protein Fri of Listeria monocytogenes promotes stress tolerance and intracellular multiplication in macrophage-like cells." Microbiol 151(3): 925-33.

Orlik F, A. C., Benz R. (2002). "Site-directed mutagenesis of tyrosine 118 within the central constriction site of the LamB (Maltoporin) channel of Escherichia coli. I. Effect on ion transport." Biophys J. 82(5): 2466-75.

Orlik F, A. C., Benz R. (2002). "Site-directed mutagenesis of tyrosine 118 within the central constriction site of the LamB (maltoporin) channel of Escherichia coli. II. Effect on maltose and maltooligosaccharide binding kinetics." Biophys J. 83(1): 309-21.

Park RY, S. H., Choi MH, Bai YH, Shin SH. (2005). "Staphylococcus aureus siderophore-mediated iron-acquisition system plays a dominant and essential role in the utilization of transferrin-bound iron." J Microbiol. 43(2): 183-90.

Park, S. F., and G. S. Stewart. (1990). "High-efficiency transformation of Listeria monocytogenes by electroporation of penicillin-treated cells." Gene 94: 129-32

Pautsch A, S. G. (1998). "Structure of the outer membrane protein A transmembrane domain." Nat Struct Biol. 5(11): 1013-7.

Payne, M. A., J. D. Igo, Z. Cao, S. B. Foster, S. M. Newton, and P. E. Klebba (1997). "Biphasic binding kinetics between FepA and its ligands." J. Biol. Chem 272: 21950-21955.

Pettis GS, B. T., McIntosh MA. (1988). "Transcriptional mapping and nucleotide sequence of the Escherichia coli fepA-fes enterobactin region. Identification of a unique iron-regulated bidirectional promoter." J Biol Chem. 263(35): 18857-63.

Phan-Thanh L, G. T. (1997). "A chemically defined minimal medium for the optimal culture of Listeria." Int J Food Microbiol. 35(1): 91-5.

Pine L, M. G., Brooks JB, Daneshvar MI. (1989). "Physiological studies on the growth and utilization of sugars by Listeria species." Can J Microbiol. 35(2): 245-54.

Porter, R. R. (1959). "The hydrolysis of rabbit gamma-globulin and antibodies with crystalline papain." Biochem. J. 73: 119-26.

Portnoy DA, C. T., Goebel W, Cossart P. (1992). "Molecular determinants of Listeria monocytogenes pathogenesis." Infect. Immun. 60(4): 1263-1267.

Postle, K. (1993a). "TonB and the gram-negative dilemma." Mol. Microbiol. 4: 2019-2025.

Postle, K. (1993b). "TonB protein and energy transduction between membranes." J. Bioenerg. Biomembr. 25: 591-601.

Postle K, S. J. (1988). "Escherichia coli TonB protein is exported from the cytoplasm without proteolytic cleavage of its amino terminus." J Biol Chem. 263(22): 11000-7.

Postle, K. a. G., R.F. (1983). "DNA sequence of the Escherichia coli tonB gene." Proc Natl Acad Sci 80(17): 5235-9.

Poyart C, T.-C. P. (1997). "A broad-host-range mobilizable shuttle vector for the construction of transcriptional fusions to beta-galactosidase in gram-positive bacteria." FEMS Microbiol Lett. 156(2): 193-198.

Premaratne RJ, L. W., Johnson EA. (1991). "Development of an improved chemically defined minimal medium for Listeria monocytogenes." Appl Environ Microbiol. 57(10): 3046-8.

Pugsley AP, R. P. (1976). "Characterization of group B colicin-resistant mutants of Escherichia coli K-12: colicin resistance and the role of enterochelin." J Bacteriol. 127(1): 218-28.

Pugsley AP, R. P. (1977). "Uptake of ferrienterochelin by Escherichia coli: energy dependent stage of uptake." J Bacteriol. 130(1): 26-36.

Pugsley, A. P., W. Zimmerman, and W. Wehrli. (1987). "Highly efficient uptake of a rifamycin derivative via the FhuA-TonB-dependent uptake route in Escherichia coli." J. Gen. Microbiol. 133: 3505-3511.

Rajasekaran Annamalai, B. J., Zhenghua Cao, Salete M. C. Newton, and Phillip E. Klebba (2004). "Recognition of Ferric Catecholates by FepA." J Bacteriol. 186(11): 3578-89.

Randall-Hazelbauer L, S. M. (1973). "Isolation of the bacteriophage lambda receptor from Escherichia coli." J Bacteriol. 116(3): 1436-46.

Raveneau J, G. C., Beretti JL, Gaillard JL, Alouf JE, Berche P. (1992). "Reduced virulence of a Listeria monocytogenes phospholipase-deficient mutant obtained by

transposon insertion into the zinc metalloprotease gene." Infect Immun. 60(3): 916-921.

Raymond KN, C. C. (1979). "Coordination chemistry and microbial iron transport." Acc. Chem. Res. 12: 183-90.

Raymond, K. N., E. A. Dertz, and S. S. Kim. (2003). "Enterobactin: an archetype for microbial iron transport." Proc. Natl. Acad. Sci. 100: 3584-3588.

Rea RB, G. C., Hill C. (2004). "Disruption of putative regulatory loci in Listeria monocytogenes demonstrates a significant role for Fur and PerR in virulence." Infect Immun. 72(2): 717-27.

Reeves, M. W., L. Pine, J. B. Neilands, and A. Balows (1983). "Absence of siderophore activity in Legionella species grown in rion-deficient media." J. Bacteriol. 154: 324-9.

Ren Z, J. H., Morton DJ, Stull TL. (1998). "hgpB, a gene encoding a second Haemophilus influenzae hemoglobin- and hemoglobin-haptoglobin-binding protein." Infect Immun. 66(10): 4733-41.

Renauld-Mongenie G, P. D., Mignon M, Fraysse S, Chabanel C, Danve B, Krell T, Quentin-Millet MJ. (2004). "Role of transferrin receptor from a Neisseria meningitidis tbpB isotype II strain in human transferrin binding and virulence." Infect. Immun. 72(6): 3461-70.

Richardson AR, S. I. (1999). "HmbR, a hemoglobin-binding outer membrane protein of Neisseria meningitidis, undergoes phase variation." J Bacteriol. 181(7): 2067-74.

Robey M, C. N. (2002). "Legionella pneumophila feoAB promotes ferrous iron uptake and intracellular infection." Infect Immun. 70(10): 5659-69.

Rouault TA. (2004). "Microbiology. Pathogenic bacteria prefer heme." Science. 305(5690): 1577-8

Russell, L. M., S. J. Cryz, Jr., and R. K. Holmes. (1984). "Genetic and biochemical evidence for a siderophore-dependent iron transport system in Corynebacterium diphtheriae." Infect Immun. 45: 143-9.

Rutz, J. M., T. Abdullah, S. P. Singh, V. I. Kalve, and P. E. Klebba. (1991). "Evolution of the ferric enterobactin receptor in gram-negative bacteria." J.
Bacteriol. 173: 5964-5974.

Saier MH Jr, G. S., Maile RR, Moreno MS, Weyler W, Yang N, Paulsen IT. (2002). "Transport capabilities encoded within the Bacillus subtilis genome." J Mol Microbiol Biotechnol. 4(1): 37-67.

Sanders JD, C. L., Hansen EJ. (1994). "Identification of a locus involved in the utilization of iron by Haemophilus influenzae." Infect Immun. 62(10): 4515-25.

Sarkis K. Mazmanian, E. P. S., Andrew H. Gaspar, munir Humayun, Piotr Gornicki, Joanna Jelenska, Andrzej Joachmiak, Dominique M. Missiakas, Olaf Schneewind (2003). "Passage of Heme-Iron Across the Envelope of Staphylococcus aureus." Science 299: 906-9.

Schirmer T, K. T., Wang YF, Rosenbusch JP. (1996). "Structural basis for sugar translocation through maltoporin channels at 3.1 A resolution." Science 267(5197): 512-4.

Schmitt MP, D. E. (2001). "Construction and consequences of directed mutations affecting the hemin receptor in pathogenic Corynebacterium species." J Bacteriol. 183(4): 1476-81.

Schneider R, H. K. (1993). "Iron-hydroxamate uptake systems in Bacillus subtilis:

identification of a lipoprotein as part of a binding protein-dependent transport system." Mol Microbiol. 8(1): 111-121.

Schramm E, m. J., Braun V, Kamp RM. (1987). "Nucleotide sequence of the colicin B activity gene cba: consensus pentapeptide among TonB-dependent colicins and receptors." J Bacteriol. 169(7): 3350-7.

Schryvers AB, B. R., Yu RH, Wong H, Retzer M. (1998). "Bacterial lactoferrin receptors." Adv Exp Med Biol. 443: 123-33.

Schryvers AB, S. I. (1999). "Iron acquisition systems in the pathogenic Neisseria." Mol Microbiol. 32(6): 1117-23.

Scott DC, N. S., Klebba PE. (2002). "Surface loop motion in FepA." J Bacteriol. 184(17): 4906-11.

Scott, D. C., Z. Cao, Z. Qi, M. Bauler, J. D. Igo, S. M. Newton, and P. E. Klebba (2001). "Exchangeability of N termini in the ligand-gated porins of Escherichia coli." J. Biol. Chem 276: 13025-13033.

Sebulsky MT, H. D. (2001). "Identification and characterization of fhuD1 and fhuD2, two genes involved in iron-hydroxamate uptake in Staphylococcus aureus." J Bacteriol. 183(17): 4884-5000.

Sebulsky MT, H. D., Hunter MD, Heinrichs DE. (2000). "Identification and characterization of a membrane permease involved in iron-hydroxamate transport in Staphylococcus aureus." J Bacteriol. 182(16): 4394-400.

Sebulsky MT, S. B., Speziali CD, Heinrichs DE. (2003). "The role of FhuD2 in iron(III)-hydroxamate transport in Staphylococcus aureus. Demonstration that FhuD2 binds iron(III)-hydroxamates but with minimal conformational change and implication of mutations on transport." J Biol Chem. 278(50): 49890-900.

Sebulsky MT, S. C., Shilton BH, Edgell DR, Heinrichs DE. (2004). "FhuD1, a ferric hydroxamate-binding lipoprotein in Staphylococcus aureus: a case of gene duplication and lateral transfer." J Biol Chem. 279(51): 53152-9.

Shea CM, M. M. (1991). "Nucleotide sequence and genetic organization of the ferric enterobactin transport system: homology to other periplasmic binding protein-dependent systems in Escherichia coli." Mol Microbiol. 5(6): 1415-28.

Simon N, C. V., Andre P, Vidon DJ. (1995). "Utilization of exogenous siderophores and natural catechols by Listeria monocytogenes." Appl Environ Microbiol. 61(4): 1643-5.

SK., G. (1971). "Inhibition of colicin B by enterochelin." Biochim Biophys Acta. 44(5): 1149-55.

SK., G. (1973). "Colicin B: mode of actio and inhibition by enterochelin." J Bacteriol. 114(3): 1217-24.

Skaar EP, H. M., Bae T, DeBord KL, Schneewind O. (2004). "Iron-source preference of Staphylococcus aureus infections." Science. 305(5690): 1626-8.

Skare JT, R. S., Postle K. (1989). "A mutation in the amino terminus of a hybrid TrpC-TonB protein relieves overproduction lethality and results in cytoplasmic accumulation." J Bacteriol. 171(8): 4442-7.

Smith K, Y. P. (1992). "Use of a new integrational vector to investigate compartment-specific expression of the Bacillus subtilis spoIIM gene." Biochimie 74(7-8): 705-11.

Smith, Thomas J. (1993). "Purification of Mouse Antibodies and Fab Fragments." Methods in Cell Biology 37: 75-93

Snyder JA, H. B., Buckles EL, Lockatell CV, Johnson DE, Donnenberg MS, Welch RA, Mobley HL (2004). "Transcriptome of uropathogenic Escherichia coli during urinary tract infection." Infect Immun. 72(11): 6373-81.

Sonntag I, S. H., Hirota Y, Henning U. (1978). "Cell envelope and shape of Escherichia coli: multiple mutants missing the outer membrane lipoprotein and other major outer membrane proteins." J Bacteriol. 136(1): 280-5.

Sprencel C, C. Z., Qi Z, Scott DC, Montague MA, Ivanoff N, Xu J, Raymond KM, Newton SM, Klebba PE (2000). "Binding of ferric enterobactin by the Escherichia coli periplasmic protein FepB." J Bacteriol. 182(19): 5359-64.

Stack, T. D. P. H., Zhiguo; Raymond, Kenneth N. (1993). "Rational reduction of the conformational space of a siderophore analog through nonbonded interactions: the role of entropy in enterobactin." J Am Chem Soc. 115(14): 6466-7.

Stevens MK, P. S., Klesney-Tait J, Lumbley S, Thomas SE, Norgard MV, Radolf JD, Hansen EJ. (1996). "A hemoglobin-binding outer membrane protein is involved in virulence expression by Haemophilus ducreyi in an animal model." Infect Immun. 64(5): 1724-35.

Stojiljkovic I, S. N. (1997). "Neisseria meningitidis tonB, exbB, and exbD genes: Ton-dependent utilization of protein-bound iron in Neisseriae." J Bacteriol. 179(3): 805-12.

Stork M, D. L. M., Mourino S, Osorio CR, Lemos ML, Crosa JH. (2004). "Two tonB systems function in iron transport in Vibrio anguillarum, but only one is essential for virulence." Infet. Immun. 72(12): 7326-9.

Strauch, K. L., and J. Beckwith. (1988). "An Escherichia coli mutation preventing degradation of abnormal periplasmic proteins." Proc Natl Acad Sci 85(1576-80).

Strauch, K. L., K. Johnson, and J. Beckwith. (1989). "Characterization of degP, a gene required for proteolysis in the cell envelope and essential for growth of Escherichia coli at high temperatures." J Bacteriol. 171(2689-96).

Sudhakar Jha, N. K., Suman K, Dhar, Kasturi Mukhopadhayay, Suneet Shukla, Preeti Saini, Gauranga Mukhopadhayay, and Rajendra Prasad (2003). "Purification and Characterization of the N-Terminal Nucleotide Binding Domain of an ABC Drug Transporter of Candida albicans: Uncommon Cysteine 193 of Walker A Is Critical for ATP Hydrolysis." Biochemistry 42: 10822-32.

Sugawara E, N. H. (1992). "Pore-foming activity of OmpA protein of Escherichia coli." J Biol Chem. 267(4): 2507-11.

Sugimura, K., and T. Nishihara. (1988a). "Purification, characterization and primary structure of Escherichia coli protease VII with specificity for paired basic residues: identity of protease VII and OmpT." J Bacteriol. 170: 5625-32.

Sugimura K, H. N. (1988b). "A novel outer-membrane-associated protease in Escherichia coli." J Bacteriol. 170(8): 3650-4.

Sword, C. P. (1966). "Mechanisms of Pathogenesis in Listeria monocytogenes Infection. I. Influence of iron." Journal of Bacteriology 92(3): 536-42.

Szmelcman S, H. M. (1975). "Maltose transport in Escherichia coli K-12: involvement of the bacteriophage lambda receptor." J Bacteriol. 124(1): 112-8.

Tai SS, L. C., Winter RE (1993). "Hemin utilization is related to virulence of Streptococcus pneumoniae." Infect Immun. 61(12): 5401-5.

Tai SS, W. T., Lee CJ. (1997). "Characterization of hemin binding activity of Streptococcus pneumoniae." Infect Immun. 65(3): 1083-7.

Tarek Msadek, V. D., Frank Kunst, Marie-Laure Herbaud, Francois Denizot and Georges Rapoport. (1998). "ClpP of Bacillus subtilis is required for competence development, motility, degradative enzyme synthesis, growth at high temperature and soprulation." Molecular Microbiology 27(5): 899-914.

Thomas KL, L. I., Olsen B, Thomas CE, Cameron DW, Elkins C. (2001). "Cloning, overexpression, purification, and immunobiology of an 85-kilodalton outer membrane protein from Haemophilus ducreyi." Infect Immun. 69(7): 4438-46.

Thulasiraman, P., S. M. Newton, J. Xu, K. N. Raymond, C. Mai, A. Hall, M. A. Montague, and P. E. Klebba. (1998). "Selectivity of ferric enterobactin binding and cooperativity of transport in gram-negative bacteria." J. Bacteriol. 180(6689-6696).

Tidmarsh GF, K. P., Rosenberg LT. (1983). "Rapid release of iron from ferritin by siderophores." J Inorg Biochem. 18(2): 161-8.

Tsolis RM, B. A., Heffron F, Stojiljkovic I. (1996). "Contribution of TonB- and Feo-mediated iron uptake to growth of Salmonella typhimurium in the mouse." Infect Immun. 64(11): 4549-56.

Ulmke C, K. J., Lengeler JW, Welte W, Schmid K. (1999). "Site-directed mutagenesis of loop L3 of sucrose porin ScrY leads to changes in substrate selectivity." J Bacteriol. 181(6): 1920-3.

Une, T., and R. R. Brubaker (1984). "In vivo comparison of avirulent Vwa- and Pgm- or Pstr phenotypes of yersiniae." Infect. Immun. 43: 895-900.

Vakharia HL, P. K. (2002). "FepA with globular domain deletions lacks activity." J Bacteriol. 184(19): 5508-12.

Van der Helm, D. B., J. R.; Eng-Wilmot, D. L.; Hossain, M. B.; Loghry, R. A. (1980). "Crystal structure of ferrichrome and a comparison with the structure of ferrichrome A." J Am Chem Soc. 102(12): 4224-31.

Van Gelder P, D. F., Bartoldus I, Saint N, Prilipov A, Winterhalter M, Wang Y, Philippsen A, Rosenbusch JP, Schirmer T. (2002). "Sugar transport through maltoporin of Escherichia coli: role of the greasy slide." J Bacteriol. 184(11): 2994-9.

Vazquez-Boland JA, D.-B. G., Gonzalez-Zorn B, Kreft J, Goebel W. (2001). "Pathogenicity islands and virulence evolution in Listeria." Microbes Infect. 3(7): 571-584.

Velayudhan J, H. N., McColm AA, Bagshaw J, Clayton CL, Andrews SC, Kelly DJ. (2000). "Iron acquisition and virulence in Helicobacter pylori: a major role for FeoB, a high-affinity ferrous iron transporter." Mol Microbiol. 37(2): 274-86.

Wang YF, D. R., Rizkallah PJ, Rosenbusch JP, Schirmer T. (1997). "Channel specificity: structural basis for sugar discrimination and differential flux rates in maltoporin." J Mol Biol. 272(1): 56-63.

Wayne R, F. K., Neilands JB. (1976). "Siderophore protection against colicins M, B, V, and Ia in Escherichia coli." J Bacteriol. 126(1): 7-12.

Wayne R, N. J. (1975). "Evidence for common binding sites for ferrichrome compounds and bacteriophage phi 80 in the cell envelope of Escherichia coli." J Bacteriol. 121(2): 497-503.

WHITE, H. N. Y. A. J. R. (1982). "Iron Requirement in the Bactericidal Mechanism of

Streptonigrin." ANTIMICROBIAL AGENTS AND CHEMOTHERAPY 22(6): 961-968.

Wiener M, F. D., Ghosh P, Stroud RM. (1997). "Crystal structure of colicin Ia." Nature 386(6615): 461-4.

Wilks A, S. M. (1998). "Expression and characterization of a heme oxygenase (Hmu O) from Corynebacterium diphtheriae. Iron acquisition requires oxidative cleavage of the heme macrocycle." J Biol Chem. 273(2): 837-41.

Wyckoff EE, S. M., Wilks A, Payne SM. (2004). "HutZ is required for efficient heme utilization in Vibrio cholerae." J Bacteriol. 186(13): 4142-51.

Xiong A, S. V., Cabrera G, Jayaswal RK. (2000). "lecular characterization of the ferric-uptake regulator, fur, from Staphylococcus aureus." Microbiology 146(3): 659-68.

Yeowell HN, W. J. (1982). "Iron requirement in the bactericidal mechanism of streptonigrin." Antimicrob Agents Chemother 22(6): 961-8.

Zgurskaya HI, N. H. (1999). "AcrA is a highly asymmetric protein capable of spanning the periplasm." J Mol Biol. 285(1): 409-20.

Zhu W, H. D., Richardson AR, Stojiljkovic I. (2000). "Use of heme compounds as iron sources by pathogenic neisseriae requires the product of the hemO gene." J Bacteriol. 182(2): 439-47.